

Copyright
by
John Bertram Lantz
2004

**Determination of the Remaining Life of Rigid Airfield Pavement
through Super-Accelerated Pavement Testing**

by

John Bertram Lantz, B.S.C.E.

Thesis

Presented to the Faculty of the Graduate School of

The University of Texas at Austin

in Partial Fulfillment

of the Requirements

for the Degree of

Masters of Science in Engineering

The University of Texas at Austin

December 2004

Report Documentation Page				Form Approved OMB No. 0704-0188	
Public reporting burden for the collection of information is estimated to average 1 hour per response, including the time for reviewing instructions, searching existing data sources, gathering and maintaining the data needed, and completing and reviewing the collection of information. Send comments regarding this burden estimate or any other aspect of this collection of information, including suggestions for reducing this burden, to Washington Headquarters Services, Directorate for Information Operations and Reports, 1215 Jefferson Davis Highway, Suite 1204, Arlington VA 22202-4302. Respondents should be aware that notwithstanding any other provision of law, no person shall be subject to a penalty for failing to comply with a collection of information if it does not display a currently valid OMB control number.					
1. REPORT DATE 00 DEC 2004		2. REPORT TYPE N/A		3. DATES COVERED -	
4. TITLE AND SUBTITLE Determination of the Remaining Life of Rigid Airfield Pavement through Super-Accelerated Pavement Testing				5a. CONTRACT NUMBER	
				5b. GRANT NUMBER	
				5c. PROGRAM ELEMENT NUMBER	
6. AUTHOR(S)				5d. PROJECT NUMBER	
				5e. TASK NUMBER	
				5f. WORK UNIT NUMBER	
7. PERFORMING ORGANIZATION NAME(S) AND ADDRESS(ES) University of Texas at Austin				8. PERFORMING ORGANIZATION REPORT NUMBER	
9. SPONSORING/MONITORING AGENCY NAME(S) AND ADDRESS(ES)				10. SPONSOR/MONITOR'S ACRONYM(S)	
				11. SPONSOR/MONITOR'S REPORT NUMBER(S)	
12. DISTRIBUTION/AVAILABILITY STATEMENT Approved for public release, distribution unlimited					
13. SUPPLEMENTARY NOTES The original document contains color images.					
14. ABSTRACT					
15. SUBJECT TERMS					
16. SECURITY CLASSIFICATION OF:			17. LIMITATION OF ABSTRACT UU	18. NUMBER OF PAGES 263	19a. NAME OF RESPONSIBLE PERSON
a. REPORT unclassified	b. ABSTRACT unclassified	c. THIS PAGE unclassified			

**Determination of the Remaining Life of Rigid Airfield Pavement
through Super-Accelerated Pavement Testing**

**Approved by
Supervising Committee:**

Kenneth H. Stokoe, II

Jorge A. Prozzi

To my loving family

Acknowledgements

My sincere gratitude and thanks are extended to all of those who have helped me in this endeavor.

- My wonderful family for their love, support, and prayers.
- Dr. Kenneth H. Stokoe for advisement, guidance, project direction and technical expertise.
- Dr. Jorge A. Prozzi for advisement, guidance, and technical expertise.
- The Aviation Division at TxDOT, in particular Mr. Ed Oshinski for guidance, support, and more importantly for providing the opportunity to conduct this study.
- Mr. Jeffrey Lee for advisement, technical expertise, and data analysis.
- Mr. Boo Nam and Mr. Paul White for field assistance and tireless efforts during testing operations.
- Ms. Teresa Tice-Boggs for assistance and handling of logistical and administrative details.
- Mr. Ernest Henderson and the fine personnel at Fort Worth Meacham International Airport for support during field testing.
- Last and most importantly my love, for her never ending support and understanding.

Determination of the Remaining Life of Rigid Airfield Pavement through Super-Accelerated Pavement Testing

John Bertram Lantz, M.S.E.

The University of Texas at Austin, 2004

Supervisor: Kenneth H. Stokoe, II

Determination of remaining life of rigid airfield pavement generally involves a combination of engineering judgment and results of discrete test applications on the pavement and subgrade. Fatigue of pavement is almost never directly observed when examining long-term pavement performance of airfields. Observation and detection of distress and response can assist in assessing the remaining pavement life of in-service rigid pavements. In this study, accelerated pavement testing (APT) was employed to assess the remaining life of Runway 16/34 at Fort Worth Meacham International Airport in Fort Worth, Texas. A traffic model was established using reported Federal Aviation Administration aircraft operations. The pavement response, including the impact of fatigue, was observed under super-accelerated pavement (SAP) testing with input from the established traffic model. Investigation of the pavement consisted of two phases. The first phase involved continuous deflection profiles of the entire runway using the Rolling Dynamic Deflectometer (RDD). From the runway deflection profiles, candidate test locations were selected and tested to determine potential test locations outside of the main runway, as operational constraints prohibited testing of the main runway. A comparison of deflection responses was made between Runway 16/34 and the candidate

locations. Three test locations adjacent to Runway 16/34 were selected: Taxiway A6, the South Run-Up area, and the North Run-Up area. The second phase of this study consisted of evaluating the remaining life of the rigid airfield pavement using a reconfigured SAP testing application of the RDD, referred to as the Stationary Dynamic Deflectometer (SDD). Nearly 200,000 applications were applied to three independent test points (center, edge, and corner) at each selected test location. Deflection responses were measured and analyzed, resulting in two principal findings. First, visible crack development did not occur for the duration of SDD SAP testing and as a result no subsequent fatigue failure. Second, an acceptable deflection response of the airfield pavement, by three independent test slabs, supporting a relatively sufficient remaining pavement life. Variations occurred among the three test slabs, which are attributed to numerous observed conditions including environment, aircraft traffic, and construction composition. Based on the SDD SAP testing, aircraft traffic alone should not significantly degrade the pavement over the next 20-year period. However, the impact of other factors (environmental conditions, subgrade conditions, traffic growth, etc.), combined with aircraft traffic, have not been assessed in this study.

The views expressed in this study are those of the author and do not reflect the official policy or position of the United States Air Force, Department of Defense, or the United States Government.

Table of Contents

List of Tables	xii
List of Figures	xiii
Chapter 1 – Introduction	1
1.1 Introduction.....	1
1.2 Thesis Content and Research Objectives	2
1.3 Thesis Organization	3
Chapter 2 – Review of Accelerated Pavement Testing	5
2.1 Introduction.....	5
2.2 History of Accelerated Pavement Testing	5
2.3 Current State of APT	7
2.4 Recent Accelerated Pavement Testing Research on Airfields.....	10
2.4.1 Federal Aviation Administration National Airport Pavement Test Facility	10
2.4.2 A-380 Pavement Experimental Programme – Toulouse Blagnac Airport.....	13
2.4.3 Heavy Vehicle Simulator Related Research.....	14
2.5 Summary	17
Chapter 3 – Background on Rolling Dynamic Deflectometer and Stationary Dynamic Deflectometer Applications.....	19
3.1 Introduction.....	19
3.2 Development of the Rolling Dynamic Deflectometer	19
3.3 Methodology of the Rolling Dynamic Deflectometer	22
3.4 Continuous Profiling with the Rolling Dynamic Deflectometer	25
3.5 Development of the Stationary Dynamic Deflectometer.....	28
3.6 Methodology of the Stationary Dynamic Deflectometer.....	29
3.7 Super-Accelerated Pavement Testing with the Stationary Dynamic Deflectometer.....	31
3.8 Summary	34

Chapter 4 – Testing Site at Fort Worth Meacham International Airport.....	35
4.1 Introduction.....	35
4.2 History of Fort Worth Meacham International Airport	35
4.3 Fort Worth Meacham International Airport Usage Data	38
4.4 Geologic Setting of Airport	40
4.5 Airport Construction and As-Built Information	42
4.6 RDD Testing at Fort Worth Meacham International Airport in 2001 45	
4.7 Summary	50
Chapter 5 – Procedures for Airfield Pavement Assessment	51
5.1 Introduction.....	51
5.2 RDD Testing on Runway 16/34.....	51
5.3 Selection of SDD Test Locations.....	57
5.4 Load Frame Configuration.....	61
5.5 SDD Application.....	66
5.5.1 Test Pad Locations.....	66
5.5.2 Procedures for SDD SAP Testing Application.....	73
5.5 Summary	78
Chapter 6 – Development of Traffic Model	79
6.1 Introduction.....	79
6.2 Original Data.....	79
6.3 Data Reduction and Simplification.....	80
6.4 Rear Loading Determination and Configuration	81
6.5 Load Grouping Determination.....	82
6.6 Modeling Heavy Loads.....	88
6.7 Equipment Limitations.....	90
6.8 Assumptions Made in Developing the Traffic Model	91
6.9 Summary	92
Chapter 7 – Observations and Measurements During RDD Deflection Testing ...	93
7.1 Introduction.....	93

7.2	RDD Field Observations and Data Measurements	93
7.2.1	Testing Conditions and Observations	94
7.2.2	RDD Deflection Measurements	95
7.2.3	Comparison of 2004 and 2001 RDD Measurements	97
7.3	Summary	100
Chapter 8 – SDD SAP Testing at Meacham Airport – Field Measurements.....		101
8.1	Introduction.....	101
8.2	Observations and SDD Data	101
8.2.1	Testing Conditions and Observations	102
8.2.2	Raw SDD SAP Testing Data	103
8.3	Data Conversion.....	104
8.4	Presentation of Measurements	111
8.5	Summary	119
Chapter 9 – Analysis of SDD Field Measurements		121
9.1	Introduction.....	121
9.2	Analysis of Measured and Normalized Deflections	121
9.2.1	Analysis of Measured Deflections	122
9.2.2	Analysis of Normalized Deflections	129
9.3	Load Transfer Efficiency	140
9.4	Summary	156
Chapter 10 – Conclusions		157
10.1	Introduction.....	157
10.2	Final Assessment	157
10.2.1	Further Confirmation of SDD SAP Results.....	159
10.3	Future Testing and Research.....	162
10.4	Conclusions and Recommendations	165
10.5	Summary	166

Appendix A – Sample Meacham Airport Traffic Data.....	168
Appendix B – Summary of Analysis of Two-Wheel Versus Three-Wheel Load Frame Configuration.....	171
Appendix C – Reduction of Traffic History – January 1998 – May 2004	175
Appendix D – Modeling and Conversion of Heavy Load Group.....	179
Appendix E – Sample Induced-Stress Comparison Between Load Frame and Actual Aircraft Footprint	182
Appendix F – Determining Deflection from Accelerometer Voltage Output	185
Appendix G – Longitudinal Profiles from RDD Testing 5-8 July 2004.....	187
Appendix H – Sample Raw Data from SDD SAP Testing.....	191
Appendix I – Data Reduction and Summary for Each Test Point	194
Appendix J – Data Adjustment for Taxiway A6 Edge Loading Scenario.....	231
Appendix K – Normalized Deflection with Applications – Taxiway A6 and North Run-Up	234
Appendix L – PCASE Computer Program	238
References	239
Vita	244

List of Tables

Table 2.1 – United States APT Facilities (from Saeed and Hall, 2003)	8
Table 2.2 – A-380 Coverages on Flexible Test Pavement with Subbase of E=37,500 psi and CBR = 29 (from Joel, 2004).....	13
Table 5.1 – Comparison of RDD Deflection Measurements of Runway 16/34 and Selected Test Locations	73
Table 7.1 – Fort Worth Climatology Data for 2004 (USDOT 2004)	94
Table 7.2 – Fort Worth Climatology Data for 2001 (USDOT 2004)	99
Table 8.1 – Climatology Data in 2004 for Fort Worth (from USDOT 2004)	102
Table 8.2 – Sequence of SDD SAP Testing and Number Scheme	108
Table 9.1 – Linear Regression Relationships for Average Measured Deflection for Five-Years of Loading to Load Level	123
Table 9.2 – Comparison of Average Normalized Deflection in the Linear Range at the Center Load Point.....	139
Table 9.3 – Increase in Normalized Deflection Over Five-Year Increments at Edge Load Point	140
Table 9.4 – Decrease in Load Transfer over Duration of Testing	148
Table 10.1 – Deflection Data Comparison for BAe 146 (Edge Loading)	160
Table 10.2 – Comparison of Tested Load Repetitions to Allowable Passes	161

List of Figures

Figure 2.1 – LTPP Test Section Locations (from FHWA, 2004).....	9
Figure 2.2 – NAPTF Apparatus and Gear Assemblies (from FAA NAPTF, 2004)	11
Figure 2.3 – Test Pavement Construction at NAPTF (from FAA NAPTF, 2004)	12
Figure 2.4 – HVS Mark IV at USACE CRRL – Hanover, New Hampshire (from CRREL, 2004)	15
Figure 2.5 – Operational HVS-A Mark V (from Dynatest, 2004).....	15
Figure 2.6 – Sample Rut Development with Number of Passes (from Janoo et al., 2003)	17
Figure 3.1 – RDD at Fort Worth Meacham International Airport.....	21
Figure 3.2 – RDD and Key Components (from Bay and Stokoe, 1998)	21
Figure 3.3 – RDD Rolling Sensor.....	22
Figure 3.4 – Cross-Sectional View of the RDD Loading System (from Bay and Stokoe, 2000)	23
Figure 3.5 – Sensor and Towing Configuration (from Bay and Stokoe, 1998).....	24
Figure 3.6 – Sample Deflection at Joint Locations (Bay and Stokoe, 1998).....	26
Figure 3.7 – Sample Mid-Slab Deflections (from Bay and Stokoe, 1998).....	26
Figure 3.8 – SDD Configuration and Loading Frame (from Stokoe et al., 2000)	30
Figure 3.9 – SDD Loading Setup with Dimensions (from Chul et al., 2004)	31
Figure 3.10 – RDD and TxMLS Comparison of Permanent Deformation (from Stokoe et al., 2000).....	32
Figure 3.11 – Dynamic Displacement for Full-Scale Slabs (from Chul et al., 2004).....	33
Figure 4.1 – Location of Airport.....	36
Figure 4.2 – Aerial View of Runway 16/34 (from TxDOT, 2004).....	37
Figure 4.3 – Runway and Taxiway Layout (from AirNav, 2004)	38
Figure 4.4 – Total Operations from 1963-2000 (from TxDOT, 2001).....	39
Figure 4.5 – Geologic Setting of Meacham Airport (from Barnes, 1972).....	41
Figure 4.6 – Typical Cross-Section of Runway 16/34 (from TxDOT, 1975).....	43

Figure 4.7 – Close Up of Cross-Section of Runway 16/34 (from TxDOT, 1975)	44
Figure 4.8 – RDD Profiling Paths Along the Longitudinal Centerlines of Lane 1 and Lane 3 of Runway 16/34	46
Figure 4.9 – RDD Deflection Profile Runway 16/34 (from Lee et al 2003)	47
Figure 4.10 – Expanded RDD Deflection Profiles (from Lee et al., 2003)	49
Figure 5.1 – RDD Profiling Paths Along the Longitudinal Centerlines of All Six Lanes of the South End (34 End) of Runway 16/34.....	52
Figure 5.2 – Close-Up of Sensor Configuration for RDD Testing	54
Figure 5.3 – Dimensions of Sensor Array	54
Figure 5.4 – RDD Test Paths Used to Investigate Longitudinal Joints on North End (16 End) of Runway 16/34	55
Figure 5.5 – Loading Roller in Position to Test Longitudinal Joints.....	56
Figure 5.6 – Candidate Locations for SDD Testing	58
Figure 5.7 – Taxiway Cross Section (CBI, 1972).....	59
Figure 5.8 – Layer Dimensions for Final Candidate Test Locations.....	60
Figure 5.9 – Example Load Frame Arrangement for Dual-Wheel Footprint Representation for Testing Flexible Pavements (Stokoe et al., 2000)	62
Figure 5.10 – Schematic of Load Frame and Configuration of Loading Pads for Testing PCC Mid-Slab Regions (Suh et al., 2004).....	63
Figure 5.11 – Schematic of Altered Load Frame and Configuration of Loading Pads	65
Figure 5.12 – RDD Test Paths and SAP Testing Location at Taxiway A6.....	69
Figure 5.13 – RDD Deflection Response for Taxiway A6 Test Path.....	69
Figure 5.14 – RDD Test Paths and SAP Testing Location at South Run-Up (34 End).....	71
Figure 5.15 – RDD Deflection Response for South Run-Up Area Test Path.....	71
Figure 5.16 – RDD Test Paths and SAP Testing Location at North Run-Up (16 End).....	72
Figure 5.17 – RDD Deflection Response for North Run-Up Test Path.....	73
Figure 5.18 – Loading and Accelerometer Configurations	75
Figure 5.19 – Corner Loading Dimensions with Respect to Joint.....	75
Figure 5.20 – Typical Center-Loading Setup	77

Figure 5.21 – Corner Loading at North Run-Up – Supplemental Test Setup.....	77
Figure 6.1 – Three-Tiered Loading Representation Over 20-Year Pavement Life.....	83
Figure 6.2 – Typical Loadings Per Year at Meacham Airport	84
Figure 6.3 – Histogram of Yearly Occurrence of Rear Landing Gear Assembly Load	85
Figure 6.4 – Histogram of Average Aircraft Traffic Loads for Meacham Airport Over a Given 5-Year Period.....	87
Figure 7.1 – Complete Deflection Profile in 2004 for Lane #3, Runway 16/34 (Sensor #1).....	96
Figure 7.2 – Closer Examination of Deflection Profile in 2004 of Lane #3, Runway 16/34 Over the Distance of 6500 to 7500 Feet From the 34 End (Sensor #1).....	97
Figure 7.3 – Complete Deflection Profile in 2001 for Lane #3, Runway 16/34 (Sensor #1).....	98
Figure 7.4 – Comparison of RDD Deflection Data Measured in 2001 and 2004 Lane #3, Runway 16/34 (Sensor #1).....	98
Figure 7.5 – Comparison of 2001 and 2004 RDD Deflection Data Over the Distance of 2000 to 3500 Feet From the 34 End – Lane #3, Runway 16/34 (Sensor #1).....	100
Figure 8.1 – Loading and Accelerometer Configurations	103
Figure 8.2 – Load Cell Output for First Five-Year Increment at Taxiway A6 Edge	104
Figure 8.3 – Sampling Technique for Load and Deflection Readings Associated with the Different Load Groupings	106
Figure 8.4 – Testing Point Orientation with Load Frame Location and Accelerometer Arrangement on Test Slab.....	109
Figure 8.5 – Sample SDD SAP Data for Years 1-5 for Point #2 – Corner at Taxiway A6.....	110
Figure 8.6 – Measured Deflections over Complete Testing Period – North Run-Up – Center Load Point	112
Figure 8.7 – Measured Deflections over Complete Testing Period – North Run-Up – Edge Load Point.....	112
Figure 8.8 – Measured Deflections over Complete Testing Period – North Run-Up – Corner Load Point.....	113

Figure 8.9 – Measured Deflections over Complete Testing Period – South Run-Up – Center Load Point	113
Figure 8.10 – Measured Deflections over Complete Testing Period – South Run-Up – Edge Load Point	114
Figure 8.11 – Measured Deflections over Complete Testing Period – South Run-Up – Corner Load Point	114
Figure 8.12 – Measured Deflections over Complete Testing Period – Taxiway A6 – Center Load Point.....	115
Figure 8.13 – Measured Deflections over Complete Testing Period – Taxiway A6 – Edge Load Point	115
Figure 8.14 – Measured Deflections over Complete Testing Period – Taxiway A6 – Corner Load Point	116
Figure 8.15 – Supplemental Deflection Testing – North Run-Up – Corner	118
Figure 9.1 – Average Deflections Measured by Accelerometer #1 for Five- Year Load Period with Load Level: North Run-Up – Center Load Point.....	124
Figure 9.2 – Average Deflections Measured by Accelerometer #1 for Five- Year Loading Period with Load Level: North Run-Up – Edge Load Point.....	124
Figure 9.3 – Average Deflections Measured by Accelerometer for Five-Year Load Period with Load Level: North Run-Up – Corner Load Point	125
Figure 9.4 – Average Deflections Measured by Accelerometer #1 for Five- Year Load Period with Load Level: South Run-Up – Center Load Point.....	125
Figure 9.5 – Average Deflections Measured by Accelerometer #1 for Five- Year Load Period with Load Level: South Run-Up – Edge Load Point	126
Figure 9.6 – Average Deflections Measured by Accelerometer #1 for Five- Year Load Period with Load Level: South Run-Up – Corner Load Point.....	126
Figure 9.7 – Average Deflections Measured by Accelerometer #1 for Five- Year Load Period with Load Level: Taxiway A6 – Center Load Point	127
Figure 9.8 – Average Deflections Measured by Accelerometer #1 for Five- Year Load Period with Load Level: Taxiway A6 – Edge Load Point	127

Figure 9.9 – Average Deflections Measured by Accelerometer #1 for Five-Year Load Period with Load Level: Taxiway A6 – Corner Load Point	128
Figure 9.10 – Average Deflections Measured by Accelerometer #1 for Five-Year Load Period with Load Level: North Run-Up – Corner Load Point – Including Supplemental Testing	129
Figure 9.11 – Variation of Average Normalized Deflections with Number of Load Applications: South Run-Up – Center Load Point.....	131
Figure 9.12 – Variation of Average Normalized Deflections with Number of Load Applications: South Run-Up – Edge Load Point	131
Figure 9.13 – Variation of Average Normalized Deflections with Number of Load Applications: South Run-Up – Corner Load Point	132
Figure 9.14 – Variation of Average Normalized Deflections per Five-Year Load Period with Load Level: North Run-Up – Center Load Point.....	134
Figure 9.15 – Variation of Average Normalized Deflections per Five-Year Load Period with Load Level: North Run-Up – Edge Load Point	134
Figure 9.16 – Variation of Average Normalized Deflections per Five-Year Load Period with Load Level: North Run-Up – Corner Load Point.....	135
Figure 9.17 – Variation of Average Normalized Deflections per Five-Year Load Period with Load Level: South Run-Up – Center Load Point.....	135
Figure 9.18 – Variation of Average Normalized Deflections per Five-Year Load Period with Load Level: South Run-Up – Edge Load Point	136
Figure 9.19 – Variation of Average Normalized Deflections per Five-Year Load Period with Load Level: South Run-Up – Corner Load Point.....	136
Figure 9.20 – Variation of Average Normalized Deflections per Five-Year Load Period with Load Level: Taxiway A6 – Center Load Point.	137
Figure 9.21 – Variation of Average Normalized Deflections per Five-Year Load Period with Load Level: Taxiway A6 – Edge Load Point ...	137
Figure 9.22 – Variation of Average Normalized Deflections per Five-Year Load Period with Load Level: Taxiway A6 – Corner Load Point	138
Figure 9.23 – Load Transfer with Applications: North Run-Up – Center Load Point.....	142

Figure 9.24 – Load Transfer with Applications: North Run-Up – Edge Load Point.....	143
Figure 9.25 – Load Transfer with Applications: North Run-Up – Corner Load Point.....	143
Figure 9.26 – Load Transfer with Applications: South Run-Up – Center Load Point.....	144
Figure 9.27 – Load Transfer with Applications: South Run-Up – Edge Load Point.....	144
Figure 9.28 – Load Transfer with Applications: South Run-Up – Corner Load Point.....	145
Figure 9.29 – Load Transfer with Applications: Taxiway A6 – Center Load Point.....	145
Figure 9.30 – Load Transfer with Applications: Taxiway A6 – Edge Load Point.....	146
Figure 9.31 – Load Transfer with Applications: Taxiway A6 – Corner Load Point.....	146
Figure 9.32 – Supplemental Load Transfer Testing: North Run-Up – Corner Load Point	147
Figure 9.33 – Average Load Transfer Efficiency per Five-Year Load Period with Load Level: North Run-Up – Center Load Point	149
Figure 9.34 – Average Load Transfer Efficiency per Five-Year Load Period with Load Level: North Run-Up – Edge Load Point	150
Figure 9.35 – Average Load Transfer Efficiency per Five Year Load Period with Load Level: North Run-Up – Corner Load Point	150
Figure 9.36 – Average Load Transfer Efficiency per Five-Year Load Period with Load Level: South Run-Up – Center Load Point.....	151
Figure 9.37 – Average Load Transfer Efficiency per Five-Year Load Period with Load Level: South Run-Up – Edge Load Point	151
Figure 9.38 – Average Load Transfer Efficiency per Five-Year Load Period with Load Level: South Run-Up – Corner Load Point	152
Figure 9.39 – Average Load Transfer Efficiency per Five-Year Load Period with Load Level: Taxiway A6 – Center Load Point	152
Figure 9.40 – Average Load Transfer Efficiency per Five-Year Load Period with Load Level: Taxiway A6 – Edge Load Point.....	153
Figure 9.41 – Average Load Transfer Efficiency per Five-Year Load Period with Load Level: Taxiway A6 – Corner Load Point.....	153

Figure 9.42 – Average Load Transfer Efficiency per Five Years with Load Level: Longitudinal Joint at North Run-Up – Corner Load Point	155
Figure 9.43 – Average Load Transfer Efficiency per Five Years with Load Level: Supplemental Testing at North Run-Up – Corner Load Point.....	155

Chapter 1 – Introduction

1.1 INTRODUCTION

Pavements can be divided into three major categories based on composition: flexible, rigid, and composite. Flexible refers to pavements composed of bituminous and granular materials. Rigid refers to pavements composed of Portland cement concrete (PCC). Composite refers to a combination of the both flexible and rigid. The following study focuses on the behavior and performance of rigid pavements under loading, specifically addressing the deflection response and subsequent remaining life of an in-service airfield pavement.

In examining the response of pavements under loads, manifestations of distress compromise long-term pavement performance. Fatigue of concrete is a major concern in examining the long-term pavement performance of airfields, which often undergo heavy-wheel load applications. Early studies by the Illinois Division of Highways showed that flexural stress induced in concrete pavement under different loading scenarios could be endured indefinitely, provided the intensity never surpassed 50% of the modulus of rupture (Huang, 2004). These studies enabled empirical pavement performance to be applied to a theoretical design. Fatigue of concrete is typically manifested in the form of cracking and can be the result of secondary stresses like curling, where expansion and contraction result in a temperature gradient across the depth of a rigid slab. In general, cracking compromises the integrity of the pavement structure and results in reduction of performance. The phenomenon of pumping, which occurs when water and subbase are ejected along cracks, joints, and free pavement edges, is another common distress. Although common, this distress is often limited in rigid airfield pavements due to the significant thicknesses of both PCC pavement and subsequent base and subbase.

In analyzing in-service rigid pavements, determination of distress and response can assist in the investigation remaining pavement life. Methods of

accelerated pavement testing (APT) enable the rapid induction of loads and resulting manifestations of distress (Coetzee et al., 1999; Hugo and Epps-Martin, 2004; Saeed and Hall, 2003). The aforementioned manifestation of cracking is a potential visual consequence of fatigue distress. Other manifestations include an increase in deflections under loading, which can be a result of subgrade deformations and deterioration. An increase in deflections over time establishes a condition for the onset of deterioration of pavement performance. Typical deflection values produced on rigid pavements can range from trace up to 30 mils (Dong and Hayhoe, 2002). In addition, joints, while necessary for long-term rigid pavement performance and control of expansion and contraction, provide points of discontinuity where increased deflections occur which can degrade under active vehicular loading scenarios. This condition can expedite further development of manifestations of distress and overall reduction in pavement performance. Joint transfer efficiency enables quantification of joint response under loading. Observation of this pavement response enables APT results to be quantified and predictions on future pavement performance to be made.

1.2 THESIS CONTENT AND RESEARCH OBJECTIVES

At the request and funding of the Aviation Division of the Texas Department of Transportation (TxDOT), the University of Texas Austin, Department of Civil Engineering, Geotechnical Engineering Center conducted a series of pavement tests on Runway 16/34, the main runway at Fort Worth Meacham International Airport, Fort Worth, Texas in July and August 2004. The objective of this testing was to assess the remaining life of the main runway (Runway 16/34) by establishing a traffic model and observing pavement response under accelerated testing of the established traffic model. The initial testing phase involved performing continuous deflection profiles over the entire runway. This phase consisted of continuous deflection profiling along the midslab of each of the six slab-width lanes, using the Rolling Dynamic Deflectometer (RDD), a method of continuously profiling the pavement. The RDD can also be reconfigured to perform as a Stationary Dynamic Deflectometer

(SDD), with which a form of APT can be performed. The second phase of this study involved such testing at Fort Worth Meacham International Airport. Additional continuous deflection profiles were obtained along the longitudinal joints on the north end of the runway. This work was performed to investigate the relative response of all slabs and joints on the runway. The data from this July 2004 testing are also compared to deflection profiles produced by similar RDD testing conducted in May 2001 to investigate any changes with time.

The second phase of this project involved evaluating the remaining life of the rigid pavement at Fort Worth Meacham International Airport. This phase involved performing one type of APT. The APT performed consisted of using the SDD to perform super-accelerated pavement (SAP) testing in August 2004. Details of the SDD device and testing methodology are discussed at length in Chapter 3. The term “super-accelerated” pavement testing has been coined for any APT method which occurs over a very short time period and involves a high volume of load applications, on the order of 1,000,000 load applications in a single day of testing (Stokoe et al., 2000). This term is further explained in the presentation of SDD methodology in Chapter 3. The objective of this testing was to process the actual traffic history experienced by the runway, in order to develop and test a model for future traffic. Future traffic was forecasted for 20 years and then incrementally divided for application through SAP testing. Fatigue cracking and joint transfer efficiency was monitored closely to determine pavement response to loading.

1.3 THESIS ORGANIZATION

The following study introduces the methodology of APT (Chapter 2) and SAP testing (Chapter 3), where both RDD continuous deflection profiling and SDD SAP testing are presented. Information on the airport setting and usage (Chapter 4) is presented for situational familiarization. The remainder of the study focuses on procedure for assessment (Chapter 5), traffic model development (Chapter 6), testing (Chapter 7 and 8), and data analysis (Chapter 9) to facilitate determination of rigid

pavement response to the aforementioned SAP testing. With the results of the pavement response, conclusions are made regarding the determination of remaining life on the airfield and recommendations made for future development (Chapter 10).

Chapter 2 – Review of Accelerated Pavement Testing

2.1 INTRODUCTION

In this chapter, the history and development of accelerated pavement testing (APT) is discussed. APT dates back to the early 20th century. Moving forward from the development of early techniques, an examination of the current state of APT is presented. The current state includes applications on both flexible and rigid pavements at test tracks and controlled facilities. With the focus of this research directed on testing of airfield pavements, recent investigations conducted on airfields are presented with an examination of efforts made both in the United States and Europe.

2.2 HISTORY OF ACCELERATED PAVEMENT TESTING

The Transportation Research Board (TRB) and the National Cooperative Highway Research Program (NCHRP) defines accelerated pavement testing as “the controlled application of a prototype wheel loading, at or above the appropriate legal load limit, to a prototype or actual, layered, structural pavement system to determine pavement response and performance under a controlled, accelerated accumulation of damage in a compressed period” (Metcalf, 1996). Pavement response from APT applications has been used in determining design constraints and evaluations of in-service pavements. The earliest APT applications date back to 1919 with a test track in Arlington, Virginia. The circular track was loaded by a continuously moving truck. Results contributed to the early standards of concrete pavement design. The main advantage of APT is the expeditious nature of evaluating pavements through the ability to provide numerous loading cycles in a relatively compressed time period (Saeed and Hall, 2003). The writer notes that APT is sometimes referred to as accelerated load testing (ALT), particularly in Europe.

Since the early days, state departments of transportation and federal agencies, like the Federal Highway Administration (FHWA) and Federal Aviation Administration (FAA) have been heavily involved in APT research within the United States. Most notably, the AASHO (American Association of State Highway Officials) Road Test in 1950 provided the groundwork for design and construction practices still used today in the field of highway pavement engineering (TRB, 1962). This experiment involved extensive round-the-clock loading applications through six full-scale test loops. Different sections of the track were comprised of both flexible and rigid pavements with varying design parameters. Varying surface, base, and subgrade thicknesses were tested under similar environmental and loading conditions, providing a sensitivity analysis for various design constraints.

Over the past thirty years, worldwide activities have resulted in further advances in the field of APT, with Australia, Denmark, South Africa, France, Britain, and the Netherlands playing a significant role (Coetzee et al., 2000). According to a recent survey conducted by the NCHRP, there are 15 APT operational capabilities throughout the United States. Four of these operations are mobile, allowing in-service testing to be performed at varied locations, versus a fixed facility with a pavement specimen constructed strictly for testing (Saeed and Hall, 2003).

With regard to the focus of this research, APT on airfield pavements, limited work has been accomplished. The United States Army Corps of Engineers (USACE) Waterways Experiment Station (WES) has dominated APT research and testing in the field of airfield pavements, with the earliest airfield testing dating back to 1940 (Coetzee et al., 2000). The majority of the information generated at WES has been conducted on full-scale testing systems, performed primarily in controlled facilities on test pads constructed specifically for research. Limited APT research or testing has been accomplished on existing in-service airfield pavements.

In-service pavement testing methods conducted on airfields has been primarily limited to the falling weight deflectometer (FWD), the dynamic cone penetrometer (DCP), testing of cores, and pavement condition index (PCI)

assessments. These test methods allow various assessments of pavement quality and subgrade conditions to be made, but they are limited by the discrete nature of each test application. In addition, these tests do not incorporate long term, accelerated testing methods, which allow a high amount of loading to occur in a limited period of time. The following sections discuss the current state of APT and recent research conducted in the field of APT on airfield pavements.

2.3 CURRENT STATE OF APT

There are currently 28 active APT programs worldwide, with 15 of the programs based within the United States (Hugo and Epps-Martin, 2004). The bulk of these programs are being conducted at fixed facilities. The majority of APT, which has been carried out over the years, has been accomplished on flexible pavements commonly referred to as asphalt concrete (AC) pavements. Rigid pavements also known as Portland cement concrete (PCC) pavements have received limited attention. This is a by-product of the overall makeup of pavement types worldwide. The focus of APT research has been on improvement of design, performance, and maintenance of the network of roads worldwide. In the United States, the paved public road network totals over 2.5 million miles, of which less than 3% are rigid pavements (FHWA, 2002). Most test tracks have been comprised predominantly of AC test pads, with minimal representation of PCC test pads. Upon examination of pavement data from a recent FHWA study, only 5 of the 12 active facilities within the United States directly address and test rigid pavements, with the remainder focused on flexible pavements or composite pavements (Saeed and Hall, 2003). Table 2.1 presents a listing of most active and inactive facilities. Rutting has been a predominant source of failure in AC pavements and subsequently the focus of long-term effects within APT research.

Table 2.1 – United States APT Facilities (from Saeed and Hall, 2003)

Facility Name and Location	Facility Designation	Owner Agency
Advanced Transportation Research and Engineering Laboratory (ATREL); Rantoul, IL	ATREL	University of Illinois at Urbana-Champaign
Caltrans Accelerated Pavement Testing (CAL-APT) Heavy-Vehicle-Simulator (HVS) Program; Richmond, CA	CAL-APT	California Department of Transportation
U.S. Army Cold Regions Research and Engineering Laboratory (CRREL), Frost Effects Research Facility; Hanover, NH	CRREL-HVS	Cold Regions Research and Engineering Laboratory
FHWA Pavement Test Facility (PTF); McLean, VA	FHWA-PTF	Federal Highway Administration
Florida-Accelerated Pavement Testing and Research Facility ^a (APTRF); Gainesville, FL	FL-APTRF	Florida Department of Transportation
Indiana DOT/Purdue APT Facility; West Lafayette, IN	INDOT/Purdue	Indiana Department of Transportation
Kansas-Accelerated Pavement Testing (APT); Manhattan, KS	KS-APT	Kansas State University
Louisiana Transportation Research Center (LTRC) Pavement Research Facility (PRF); Port Allen, LA	LTRC-PRF	Louisiana Transportation Research Center
Minnesota Road Research Project (Mn/ROAD); Minneapolis, MN	Mn/ROAD	Minnesota Department of Transportation
National Center for Asphalt Technology (NCAT) Pavement Test Track (PTT); Auburn University, AL	NCAT-PTT	National Center for Asphalt Technology
Ohio-Accelerated Pavement Loading Facility (APLF); Lancaster, OH	OH-APLF	Ohio University/Ohio State University
Penn State (PS) Pavement Durability Facility ^b (PDF); College Park, PA	PS-PDF	Pennsylvania State University
Texas Mobile Load Simulator (TxMLS); Austin, TX	TxMLS	Texas Department of Transportation
U.S. Army Corps of Engineers Waterways Experiment Station (WES) HVS; Vicksburg, MS	WES-HVS	Engineers Research and Development Center
WesTrack ^c ; Reno, NV	WesTrack	Nevada Automotive Test Center

^a under construction, ^b inactive facility, ^c not in operation

Generally speaking, APT has been applied to either test roads or test tracks. Test roads refer to test road sections where loading is achieved by actual traffic or actual test vehicles. Test tracks refer to test sections where loading is achieved by specially designed mechanical systems (Coetzee et al, 2000). Test tracks have been constructed throughout the world, comprised of either linear or circular tracks. Test roads can include actual in-service experimental pavements, which are selected stretches of highway where performance and behavior are observed under a specified program. The FHWA established, under its Strategic Highway Research Program (SHRP), one such program called the Long-Term Pavement Performance (LTPP) studies. LTPP is a 20-year study that was started in 1987. In the LTPP study, 2,400

flexible and rigid highway segments located throughout the United States and Canada are being monitored and maintained at the local level (FHWA, 2004). Figure 2.1 illustrates the expanse of this study, encompassing extreme variations in climate and soil types.

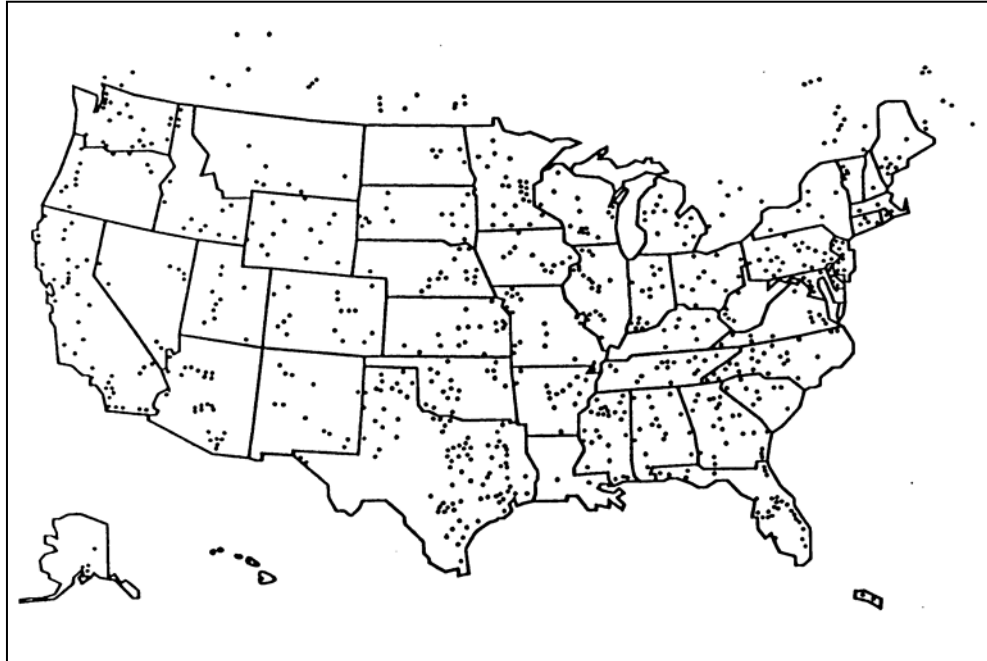


Figure 2.1 – LTTP Test Section Locations (from FHWA, 2004)

Both test roads and test tracks provide a capable approach to APT with some apparent limitations. Test roads provide evidence of pavement performance but are typically limited in environmental control. Test tracks provide a more controlled and restricted climate and environment and can be constructed in a linear or circular arrangement. Circular tracks are able to operate at high speeds, testing several independent sections; however, failure of one section can affect results of adjacent sections. Linear tracks are limited by both speed constraints and the two-way nature of loading, which can affect the pavement response and performance (Metcalf, 2001). This linear version of testing includes the mobile devices mentioned in Section 2.2.

The major limitation of in-service testing is that results are only applicable to the unique local characteristics associated with each respective test. Results are not always applicable from one location to another. With the research which will be discussed in later chapters, in-service testing is used to characterize response of an airfield, with the results representative of the pavement performance and response of the specific location.

2.4 RECENT ACCELERATED PAVEMENT TESTING RESEARCH ON AIRFIELDS

The present-day airport system in the United States is comprised of 6 billion square feet of rigid and flexible pavement, with a replacement value of approximately \$100 billion. As air traffic continues to grow and evolve, aircraft fleets will continue to increase in number, total load, gear configuration, and operating speed. Current operational airport pavements will require billions of dollars in capital improvements over the coming years (FAA NARP, 2000). Testing has been performed on airfield pavements both under research funded by the FAA and by the USACE WES to better understand the capability of today's pavement with tomorrow's aircraft. Studies have begun to determine pavement design standards to accommodate large-scale aircraft in excess of 1,000,000 pounds (FAA NARP, 2004).

2.4.1 Federal Aviation Administration National Airport Pavement Test Facility

Due to the proposed manufacturing of large-scale aircraft, the FAA has developed a full-scale testing capability at the National Airport Pavement Test Facility (NAPTF), located at the William J. Hughes Technical Center in Atlantic City, New Jersey. Commissioned in 1999, this testing center is designed to recreate landing gear loading configurations for full-scale testing for airfield pavements. The machine used in the APT testing at the facility is the largest APT apparatus in the world, capable of configuring two complete landing gear assemblies with up to 6 wheels on each (Coetzee et al., 2000). Figure 2.2 shows the NAPTF and the APT apparatus it employs. The results of testing will be used as input to future methods

for design, construction, and evaluation of airfield pavements. Testing and research is driven by the need for improved design methods, due to spatial changes and increasing loads associated with landing gear configurations.



Figure 2.2 – NAPTF Apparatus and Gear Assemblies (from FAA NAPTF, 2004)

The test facility includes nine independent test pavements constructed to specific tolerances. The test track is environmentally controlled by a covered facility and measures 900 ft in length and 60 ft in width. Figure 2.3 illustrates the sheer magnitude of the facility. Both rigid and flexible pavement structures can be tested with variance in subgrade design incorporated with unbound aggregate and stabilized base. Test speeds are limited to 2.5 to 5 mph with wandering incorporated for each pass, with an equivalent dummy gear load of up to two Boeing 747 or 777 landing gears. In recent testing scenarios, a cycle of 66 repetitions was used with embedded

sensors for sufficient determination of various pavement responses. Over 1,000 static and dynamic sensors have been incorporated to determine temperature, moisture, strain, and deflection in the pavement. Data has not been made public, but will be used in new pavement design standards in 2007 (FAA, 2004).



Figure 2.3 – Test Pavement Construction at NAPTF (from FAA NAPTF, 2004)

With the expected arrival of large-scale jumbo jets for commercial operation, multiple studies have been conducted at the NAPTF. An example of a recent study includes research to determine minimum requirements to widen existing standard 150-ft runway widths for flexible pavements under Airbus A-380 operations. The A-380 is classified as a Group VI aircraft, requiring 200-foot wide runways. Many airports in operation are only classified up to Group V aircraft with a standard 150-foot runway width. In a study conducted, considerable surface deformation was observed with each pass of the A-380 equivalent gear on the asphalt concrete

pavement (Joel, 2004). Different sections were tested with the dimensions of the AC surface and base remaining constant, while varying depth of subbase. Ultimate results provided allowable A-380 coverages given a specific subbase construction. Table 2.2 provides details of allowable A-380 coverages for the subbase tested. Subbase layer parameters were assumed to be: (1) elastic modulus (E) of 37,500 psi and (2) California bearing ratio (CBR) of 29. Aircraft coverage is a term which takes into account the fact that not every pass of every aircraft is considered a repetition in design practices. A single coverage is defined “when each point in the pavement within the limits of the traffic lane has experienced a maximum stress, assuming the stress is equal under the full tire print” (FAA, 2004). Due to the wandering associated with aircraft take-off, landing, and taxiing operations, several passes may be required to produce a single fatigue cycle.

Table 2.2 – A-380 Coverages on Flexible Test Pavement with Subbase of E=37,500 psi and CBR = 29 (from Joel, 2004)

Section	Surface	Base	Subbase	Allowable coverages
LFC1	5"	8"	16.0"	87
EB65	5"	8"	19.72"	241
LFC2	5"	8"	24"	622

2.4.2 A-380 Pavement Experimental Programme – Toulouse Blagnac Airport

APT on airfield pavements has seen limited attention internationally. Recently, the French Civil Aviation Administration and the French Roads and Bridges Laboratory in coordination with Airbus have contributed to testing on rigid pavements at Toulouse Blagnac Airport (Fabre et al., 2004). The A380 Pavement Experimental Programme (PEP) is a two-fold study to assist in the final landing gear configuration selection for the new widebody Airbus A-380 and to assist in comparing actual pavement response under new large-scale aircraft to finite element model predictions. Airbus S.A.S. developed a heavy aircraft landing gear simulator

for use during experimental testing. The results and analysis of this testing are still pending.

2.4.3 Heavy Vehicle Simulator Related Research

As well as APT conducted in test facilities, equipment has also been developed and used to assess and evaluate in-service pavements. A Heavy Vehicle Simulator (HVS) manufactured by Dynatest International has been used in many countries. The HVS is a mobile trailer, with a single or dual wheel assembly capable of testing uni-directionally or bi-directionally with loads ranging from 7 to 45 kips. Although mobile, the HVS is massive in size; it has dimensions of 75 feet in length, 12 feet in width, 13.5 feet in height, and a weight of 50 tons. The HVS is hydraulically-operated and fully-automated system which applies a load along a moving wheel load on a test beam over a distance of 6 meters (approximately 20 feet), with an automated capability for lateral wander. The system is capable of simulating 20 years of traffic in the period of three to six months (upwards of 4.5 million passes).

USACE has led the way in exclusively testing airfield pavements through the procurement of a specially built super-heavy HVS (HVS-A Mark V), capable of simulating wheel loads over a range of 10 to 100 kips over a linear testing area of 12.2 meters (approximately 40 feet) (Dynatest, 2004). The HVS-A Mark V is the world's largest portable device used for imposing accelerated traffic on pavements. Figure 2.4 shows the HVS Mark IV model in operation at the USACE Cold Regions Research Laboratory (CRRL) in New Hampshire. Figure 2.5 shows the HVS-A Mark V in operation at an active airfield. In November of 1998, the Geotechnical and Structures Laboratory at the Engineer Research and Development Center (ERDC) located at the USACE WES accepted delivery of this one-of-a-kind device. The device is being used for three different applications: high repetitions of heavy aircraft loads, low-volume roads, and trafficking on beach and soft soils. The device is

capable of applying loads at 8 mph, equating to 15,000 passes per 24 hour period of testing.



Figure 2.4 – HVS Mark IV at USACE CRRL – Hanover, New Hampshire (from CRREL, 2004)



Figure 2.5 – Operational HVS-A Mark V (from Dynatest, 2004)

The objective for the USACE WES application and testing with the HVS-A Mark V is primarily to determine pavement response and performance under high repetitions of heavy loading. Data from current testing is being used to calibrate and validate computational models being developed by the ERDC. The purpose of these models is to improve and refine design conservatism measures and to better predict pavement performance (WES ERDC, 2004).

In addition to the recent WES focus on testing airfield pavement response, the USACE Cold Regions Research and Engineering Laboratory (CRREL) in Hanover, New Hampshire has incorporated HVS testing into research on subgrade response. At the Frost Effects Research Facility (FERF), a controlled environment is used to conduct testing on freeze/thaw effects on pavement, soils, and other materials. Since CRREL procured an HVS in the late 1990's, it has focused its APT investigations on subgrade testing. Subsurface testing temperature capability ranges from -35° F to +120° F at FERG (USACE CRREL, 2004).

In general CRREL has focused its APT research on subgrade and bituminous pavements. Research has included effects of subgrade moisture contents on surface load carrying capacity (Darling, 2004). Other research investigation includes utilization of the HVS to support computer simulation results which has shown reduced truck tire pressure can significantly decrease damage to thin AC pavements and increase the life of the pavement. The HVS was applied to chip seal test sections with a frost depth of 4 ft (1.3m). Panels were trafficked during thawing sequence, using tire pressures of 100, 60, and 35 psi (689, 410, and 230 kPa), with considerably more deformation occurring at the higher tire pressure (Kestler, 1999).

Other work has focused on the phenomenon of rutting within flexible pavements. A study has been sponsored by the FHWA, in cooperation with CRREL and many leading international laboratories, to investigate the performance of subgrade materials in flexible pavement structures in order to improve and upgrade the failure design criteria used within current mechanistic design standards (Janoo et

al., 2003). Test slabs were created to simulate four different subgrade types under three varying moisture contents. Test slabs were then loaded using the HVS. Coaxial and coplanar coil gages were installed in the subgrade to determine permanent deformation from loading and resultant permanent strain. Vitel gages were used to determine moisture contents, with earth pressure cells installed to determine dynamic stresses in subgrade layers. Preliminary results have shown the rut development as function of the number of passes. A sample of this observed performance is presented in Figure 2.6. Additional information on the effects of subgrade conditions will be presented in future proceedings from the study (Janoo et al., 2003).

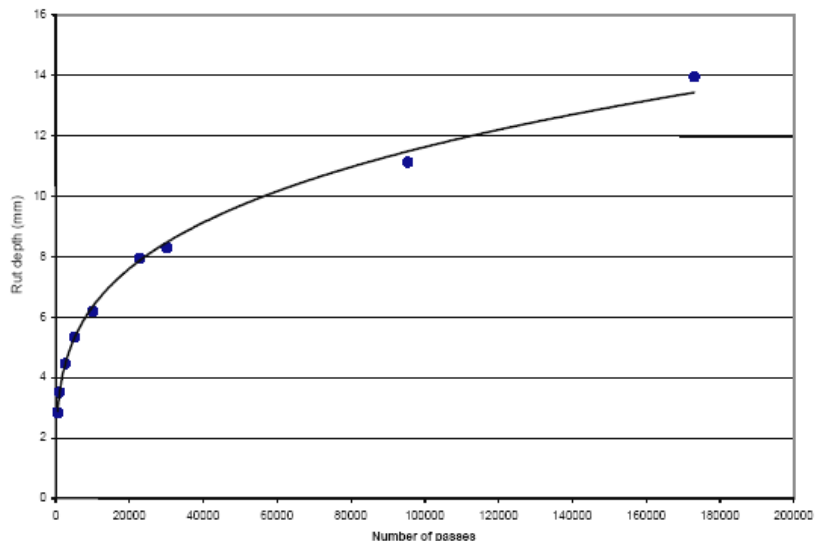


Figure 2.6 – Sample Rut Development with Number of Passes (from Janoo et al., 2003)

2.5 SUMMARY

A state-of-the-practice review of accelerated pavement testing is presented to illustrate the current allocation of resource initiatives within the field. APT has been a key resource in the development of design and performance standards for

pavements. As shown, the majority of the focus of APT research has been on flexible pavements, the largest need within the pavement industry. However, over the past decade, development of heavy load capable devices has enabled the field of APT to incorporate rigid airfield pavement testing. This incorporation is still in its infancy with the majority of the focus on subgrade and flexible pavement analysis.

Chapter 3 – Background on Rolling Dynamic Deflectometer and Stationary Dynamic Deflectometer Applications

3.1 INTRODUCTION

In this chapter, the development of the Rolling Dynamic Deflectometer (RDD) is presented to provide a better understanding of its origin and capabilities. An examination of the methodology of the RDD illustrates how the device and its systems operate. Recent research is presented to provide further background on the RDD testing capability. The RDD is capable of being adapted for use as the Stationary Dynamic Deflectometer (SDD). The development of this adaptation is also presented along with its methodology. The SDD is fairly new capability, and research and testing accomplished thus far is presented to familiarize the reader with the SDD capability.

3.2 DEVELOPMENT OF THE ROLLING DYNAMIC DEFLECTOMETER

The Rolling Dynamic Deflectometer (RDD) was developed at the University of Texas at Austin in 1996 by Dr. James Bay and Professor Kenneth H. Stokoe II (Bay, 1997). The idea for the device was generated by the need for a more comprehensive nondestructive testing method (NDT), for pavement evaluations. At the time, a large portion of the nation's pavement infrastructure had reached its effective design life and had begun to deteriorate. A need developed for an accurate nondestructive testing method to more thoroughly assess the changing conditions of pavements (Bay and Stokoe, 1998). Out of this need developed a continuous deflection measurement capability. This capability was the impetus for the development of the RDD. Prior to this development, deflection measurements were produced through discrete methods. Although effective, these methods enabled only a limited view of the response of the pavement. The development of the RDD brought about a capability of continuously testing over a given distance, while producing real-time continuous deflection data. This continuous measurement

capability enables a relative comparison of deflection measurements over extensive distances; thereby avoiding the inaccuracies inherent to discrete testing methods. The benefits of continuous pavement testing, enable improved infrastructure management and tracking of pavement condition, thereby improving utilization of rehabilitation, maintenance, and repair initiatives.

The inception of the RDD came about through modifications to a Vibroseis truck. A Vibroseis truck is used in the geophysical exploration industry for imparting a well-controlled (but adjustable) set of sinusoidal loading conditions to the ground surface. The electrohydraulic loading system of the Vibroseis was modified with specialized loading rollers that allowed large sinusoidal dynamic forces to be applied to the test pavement surface, while the truck is moving. Deflections induced in the pavement are measured by rolling sensors designed to minimize noise created by surface roughness of the pavement (Bay and Stokoe, 1998).

The RDD has a gross weight of approximately 49 kips. The servo hydraulic vibrator has a 7.5 kip weight; capable of inducing peak-to-peak dynamic forces of 2 to 70 kips. The frequency range of the system is 10 to 100 Hz. The hydraulic system is capable of producing a static load ranging from 2 to 40 kips. Deflection testing is performed while the device moves at speeds along the pavement of 1 to 2 fps (up to 1.5 mph). Figure 3.1 gives a present day view of the RDD. Figure 3.2 outlines the schematic of the device, noting the position of a typical sensor configuration with respect to the loading system and rollers. The sensor configuration can be modified to fit the requirements of specific tests (Bay and Stokoe, 2000). Figure 3.3 shows a typical rolling sensor used in RDD operations. There are a number of sensor configurations that are possible during deflection testing. The rolling sensor configuration with the sensor towing system is further discussed and illustrated in Section 3.3.



Figure 3.1 – RDD at Fort Worth Meacham International Airport

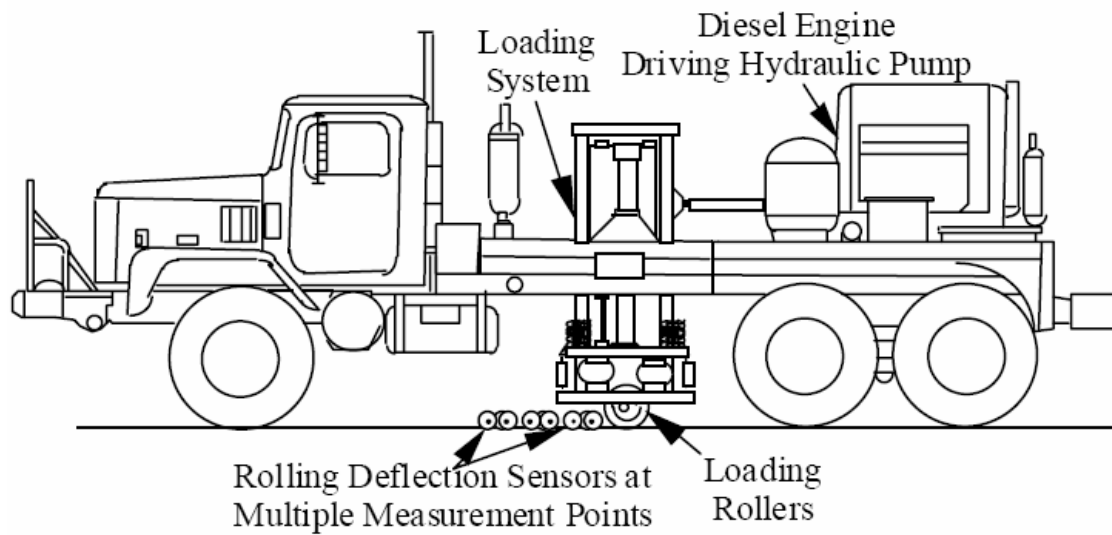


Figure 3.2 – RDD and Key Components (from Bay and Stokoe, 1998)

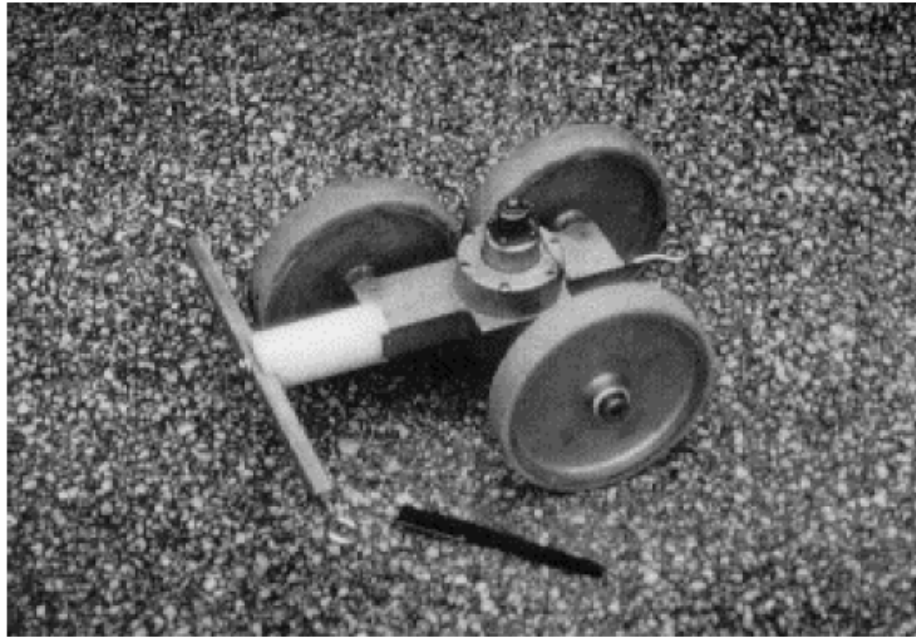


Figure 3.3 – RDD Rolling Sensor

3.3 METHODOLOGY OF THE ROLLING DYNAMIC DEFLECTOMETER

During testing, a hydraulic pump powered by a separate diesel engine on the rear of the vehicle applies combined static and dynamic loads to the pavement through two loading rollers. To generate the dynamic force, a reaction mass is forced up and down by hydraulic sinusoidal pressure, shown in Figure 3.4 which illustrates the complete RDD loading system. The hydraulic pressure is created by the cycling of hydraulic fluid within the chambers of the hydraulic actuator. The system is able to generate a peak force of 35 kips, which translates to a 70 kip peak-to-peak dynamic capability (Bay, 1997).

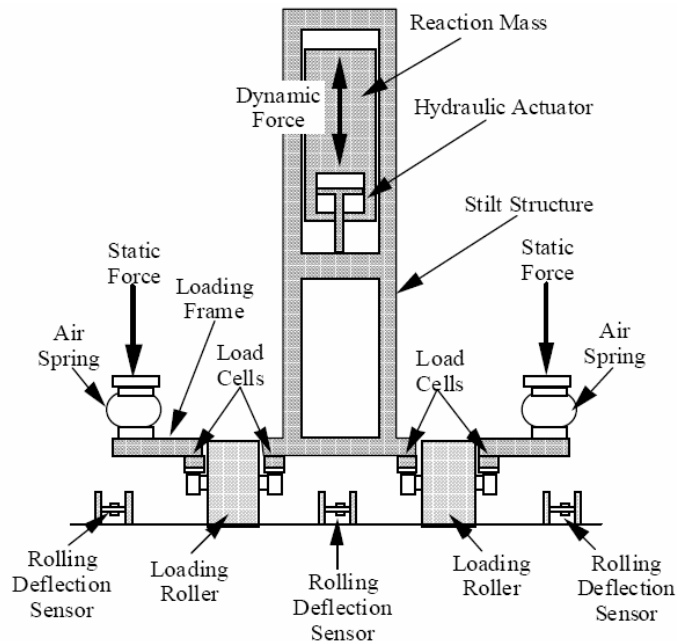


Figure 3.4 – Cross-Sectional View of the RDD Loading System (from Bay and Stokoe, 2000)

A static force is required to ensure the dynamic force does not render the device unstable or lift the RDD off the ground, in turn causing inaccuracies in the dynamic loading. The static loading system is comprised of the same hydraulic cylinder used to create the sinusoidal loading and a pair of air springs on both external sides of the dual loading roller platform. The air springs are intended to isolate the weight of the truck from the dynamic loading and to reduce vibratory effects of the testing on the truck itself (Bay and Stokoe, 2000).

The loading capability of the RDD is robust; capable of generating dynamic loads up to 70 kips. The main limitation of the RDD maximum loading capability is the combination of the static force capability and the gross weight of the entire system. The RDD is able to induce comparable loads for highway pavement testing, but is unable to replicate the full compliment of aircraft loading scenarios. For instance, aircraft loads can range from below 10,000 pounds to well in excess of

800,000 pounds. This equates to a single, rear-gear configuration loading range of up to 300,000 pounds. Typically during deflection testing, the goal is replicate the live load experienced in the field. With the extremely high loads produced by aircraft, the 70-kip capability of the RDD is surpassed. However, the severity of this limitation is minimized, since the relative nature of the RDD continuous deflection testing allows for comparisons to be made at the local level to identify regions of relatively high deflections within a sizeable pavement structure.

To model properly the pavement deflection profile, rolling deflection sensors can be arranged to meet the needs of the specific test situation. Figure 3.5 illustrates a typical rolling sensor configuration. A towing system is used to ensure sensor alignment and minimize wander. Additional sensors can be aligned along the exterior of either roller. This additional arrangement can be useful in determining deflection variations away from the loading points or comparing deflections on either side of a joint. These sensors provide a means for observing dynamic deflections induced by the applied force. An automated PC-based data acquisition system is used to monitor and record output from the load cells, deflection sensors, and the global positioning system (GPS) distance-measuring device.

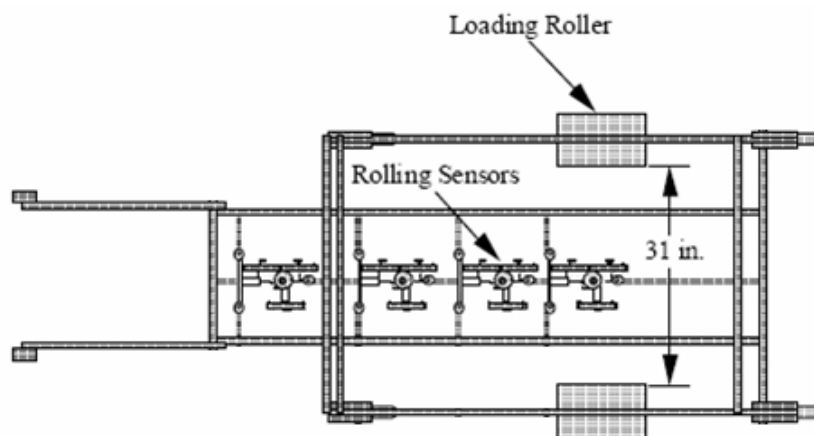


Figure 3.5 – Sensor and Towing Configuration (from Bay and Stokoe, 1998)

3.4 CONTINUOUS PROFILING WITH THE ROLLING DYNAMIC DEFLECTOMETER

There are five key parameters which affect the output and effectiveness of continuous RDD testing. These parameters are:

- (1) testing velocity along the pavement,
- (2) operating frequency,
- (3) applied force levels,
- (4) data sampling rate and filter settings, and
- (5) rolling sensor positions.

Selection of these parameters is necessary to properly set a given test condition. Specifics surrounding the parameters and procedures, incorporated into the field testing within this study, are described in Chapter 4.

The final result of RDD testing is a continuous deflection profile along a linear testing area. In prior testing, displacement peaks have been noted at joints and cracks. Figure 3.6 illustrates this phenomena differentiating between the higher deflections seen at dowelled construction joints versus sawn control joints. These data was collected during example comes from prior testing completed on Runway 16L-35R at Dallas-Fort Worth (DFW) International Airport. Relative joint transfer efficiency can be assessed over the course of a given testing area, as the effect of the joint is easily discerned from the profile, with larger deflections detected at the weaker joints. In addition, higher mid-slab deflections can generally be correlated to a number of common distress conditions including subgrade deterioration, weaker fill, and highly cracked slabs. Figure 3.7 illustrates variations in deflections measured over the extent of a testing area. In this figure, regions of high and low deflection are classified on a runway deflection profile from DFW International Airport. As mentioned before, regions that exhibit high overall deflections (not exclusively at the joints) signify areas of potential distress manifestations.

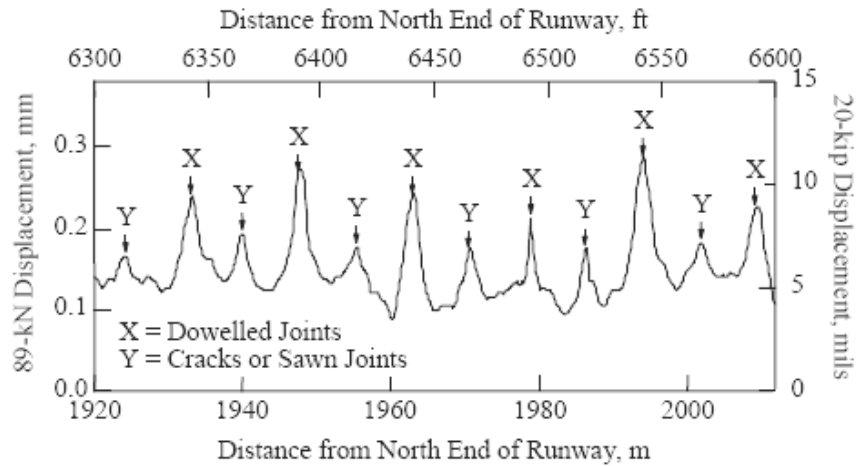


Figure 3.6 – Sample Deflection at Joint Locations (Bay and Stokoe, 1998)

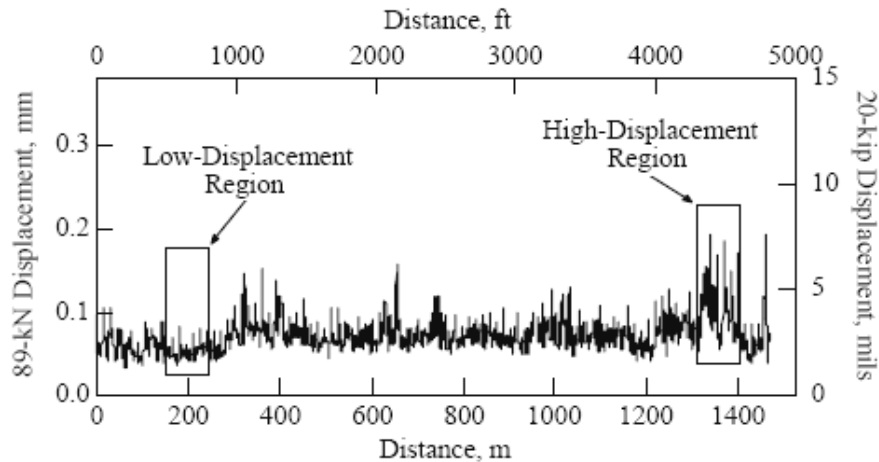


Figure 3.7 – Sample Mid-Slab Deflections (from Bay and Stokoe, 1998)

The RDD has been used in numerous research and support projects. These include continuous deflection profiles at: (1) Interstate Highway 10 at locations at Orange and Houston, Texas, and (2) runway and taxiway airport pavements at Dallas-Fort Worth International Airport (as seen in Figures 3.6 and 3.7), Fort Worth

Meacham International Airport, Seattle-Tacoma International Airport, and Atlanta Hartsfield Airport. Interstate highway applications have resulted in determination of highway pavement conditions and subsequent more efficient design of overlays (Bay and Stokoe, 1998). In airfield applications, both soft and stiff regions of the pavement have been identified while producing illustrations of distress in highly trafficked regions. Relative load transfer capability and joint efficiency can be assessed through examination of deflection profiles (Bay et al., 2000).

As additional research supports the development and progress of the RDD, applications in the matter of airfield structural evaluations will become more prominent. As mentioned previously, the RDD has been used extensively in airfield applications in the civilian sector at runways throughout the United States. There also exists the potential for direct military applications which often require rapid airfield assessment, evaluation, and recommendations. The capabilities of the RDD have far-reaching advantages in structural evaluation of pavements. Relative strengths can be correlated and assessed immediately following test completion, without a direct requirement for backcalculation of layer moduli. In addition, weaker areas of an airfield, such as those where voids may emerge, can be identified and differentiated from those areas with solid support. Currently the RDD is viewed as a “promising” technology by the military (Malvar and Cline, 2000). The U.S. Navy hopes to move toward this technology and further their pavement assessment and profiling capabilities with the objective of avoiding pavement failures. The U.S. Air Force and the offices at Air Force Civil Engineers Support Agency (AFCESA) support a movement toward this technology. In the future, airfield pavement evaluation teams may replace discrete testing methods, like the falling weight deflectometer (FWD) with continuous testing methods like the RDD.

It should be noted that other continuous deflection capabilities have been developed during the same period as the inception of the RDD. These devices include the Rolling Wheel Deflectometer (RWD) and the High Speed Deflectograph (HSD). The RWD is a project developed by Applied Research Associates, Inc. under

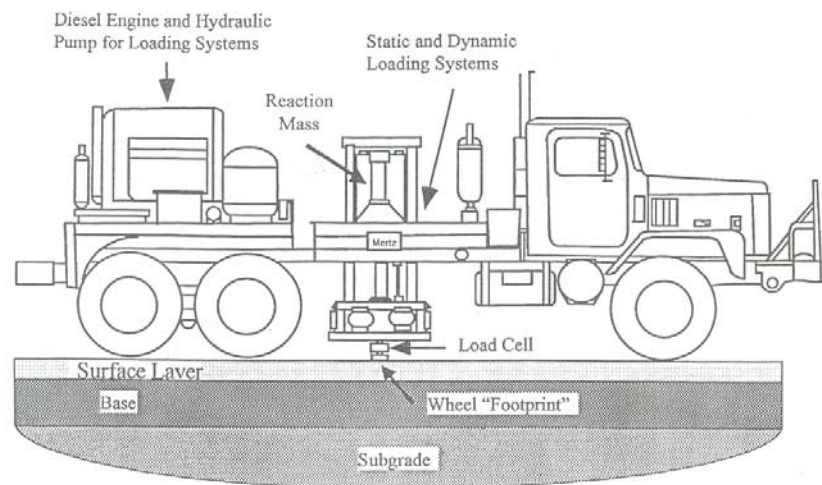
funding from the Federal Highway Administration. The purpose of the RWD is to develop a device which applies a moving truck load at typical highway speeds, while taking continuous deflection measurements (Herr et al., 1995). The RWD is based on spatial coincident methodology, where the difference in readings of four installed lasers, produces deflection measurements at high speeds (Hall, 1999). Similar to the RWD, the HSD also is capable of deflection measurements at standard highway speeds. The HSD has been developed by the Danish Road Institute in cooperation with the Danish Ministry of Business and Industry. The main difference between the RWD and HSD is that the HSD determines deflections by particle velocity measurements of the real-time deflections. In the HSD, laser Doppler sensors are mounted on a rigid beam attached to a semi-trailer. As the vehicle traverses the pavement, rays are emitted and the velocity of the deflection is registered by the sensors. Sudden changes in velocity can reveal discontinuities in the pavement system. Through data interpretation actual absolute deflection values can be obtained and moduli backcalculated from the deflection basin (Hildebrand et al., 1999).

3.5 DEVELOPMENT OF THE STATIONARY DYNAMIC DEFLECTOMETER

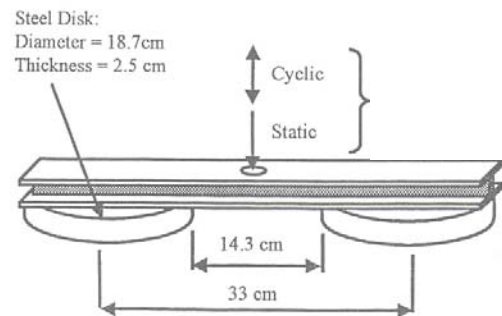
Recent research has brought an innovative and pioneering potential application of the RDD device, the stationary dynamic deflectometer (SDD). In this application, the RDD is used in a stationary mode in which its loading configuration is altered to impose harmonic loading to a wheel footprint on the pavement surface. Under this SDD application, load can be applied in the order of one million repetitions in a 24-hour period. Consequently, this capability is frequently referred to as super-accelerated pavement (SAP) testing. Results which once required weeks to months of testing can be acquired in the period of days. Potential benefits include the reduced time, less expense in testing, and the reduction in traffic loss and required workarounds for applications with in-service pavements (Stokoe et al., 2000).

3.6 METHODOLOGY OF THE STATIONARY DYNAMIC DEFLECTOMETER

In using the SDD in SAP testing, the loading area remains stationary and constant for the duration of the testing. The RDD applies a dynamic load in the same manner as previously described in Section 3.4. However in adapting the RDD, the load frame and attached loading rollers are raised, and a load cell is placed at a central loading point on the load frame. This load cell is then positioned over a preconfigured loading frame. Figure 3.8a illustrates a typical arrangement of the SDD for SAP testing. The loading frame can be designed to represent various wheel loads. An example of a two-point loading frame is shown in Figure 3.8b.



(a)



(b)

Figure 3.8 – SDD Configuration and Loading Frame (from Stokoe et al., 2000)

The main intent of SAP testing is to initiate and measure pavement deterioration during the accelerated load repetitions. Measured deterioration can be visible distress, permanent surface deformation, cross-sectional deformation (rutting in AC pavements), cracking, or joint transfer efficiency. A failure criterion is established for the applicable deterioration indicator for each testing scenario. Ultimate results are produced in terms of a selected distress measurement versus the

number of cycles applied. Many variables and assumptions are applied in correlating field performance to actual loads. This is discussed in further in Chapter 6, which presents the specific traffic modeled within this testing application. Figure 3.9 shows the dimensions of the device footprint with respect to the load point for a typical SDD loading scenario. Under this setup, the 49-kip static load of the device over its wheel footprint will affect measured deflection results. However, these results provide an excellent means of relative deflection comparison at multiple locations.

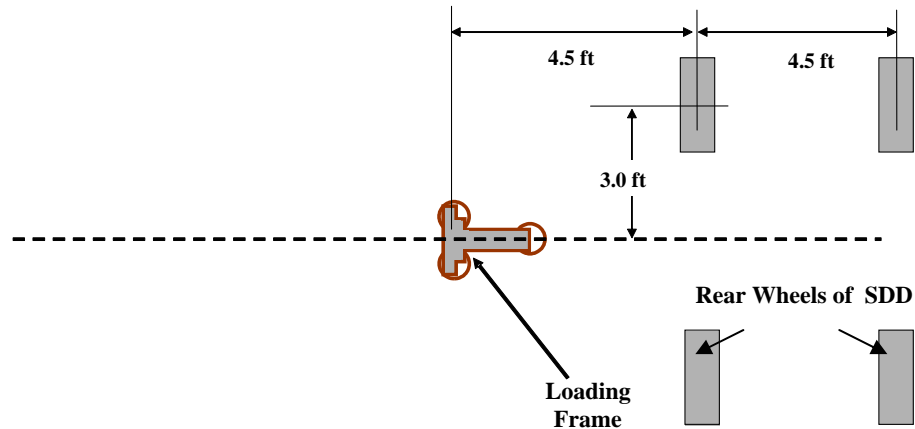


Figure 3.9 – SDD Loading Setup with Dimensions (from Chul et al., 2004)

3.7 SUPER-ACCELERATED PAVEMENT TESTING WITH THE STATIONARY DYNAMIC DEFLECTOMETER

There are three key parameters which affect the output, effectiveness, and duration of SDD SAP testing. These parameters are:

- (1) frequency of the harmonic load application,
- (2) maximum number of cycles for test completion, and
- (3) measurements used to characterized pavement deterioration and manifestation of distress.

Appropriate selection of these parameters is necessary to analyze properly a given set of pavement conditions (Bay and Stokoe, 1998). Specifics surrounding the procedure incorporated into the field testing in this study are present in Chapter 5.

Although the development of the SDD has been a recent addition, it has begun to be used in research and support projects. Areas of US-281 near Fort Worth have been tested in cooperation with Texas Department of Transportation. Results have shown the SDD application as a viable alternative in accelerated pavement testing applications. The SDD exhibits comparable results to more deliberate accelerated pavement testing methods, such as the Texas Mobile Load Simulator (TxMLS), which has been developed by Texas Department of Transportation in partnership with the Center for Transportation Research (CTR) of the University of Texas at Austin. This application focused on the rutting phenomenon with flexible pavements; therefore data was reduced into permanent settlement curves, produced over the cycling sequence (Stokoe et al., 2000). Figure 3.10 presents a comparison of the permanent settlement observed in this testing. Trends exhibit similarities between the RDD measurements and those measurements produced by the TxMLS.

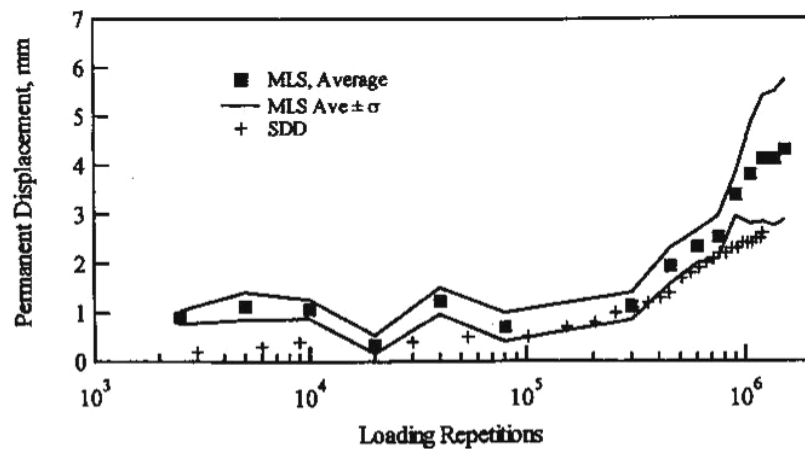


Figure 3.10 – RDD and TxMLS Comparison of Permanent Deformation (from Stokoe et al., 2000)

With regard to testing of rigid pavements, SDD has seen limited usage. Recent full-scale PCC slab testing at the Ferguson Research Laboratory at the University of Texas at Austin has shown promising results for rigid pavement applications. During this research accelerated fatigue tests were performed under a constant dynamic loading. Field results on full-scale slabs were compared to the fatigue relationship on laboratory beams, where results were fundamentally identical. Different from the beam fatigue behavior, the field slabs showed a stress redistribution phenomenon during the crack propagation period. The conclusive results showed that the SDD was found to be effective in SAP testing of a full-scale rigid pavement system (Chul et al., 2004). Figure 3.11 shows the typical results found in the field tests. Manifestation of cracking is seen by the sudden increase in measured deflections at point of occurrence.

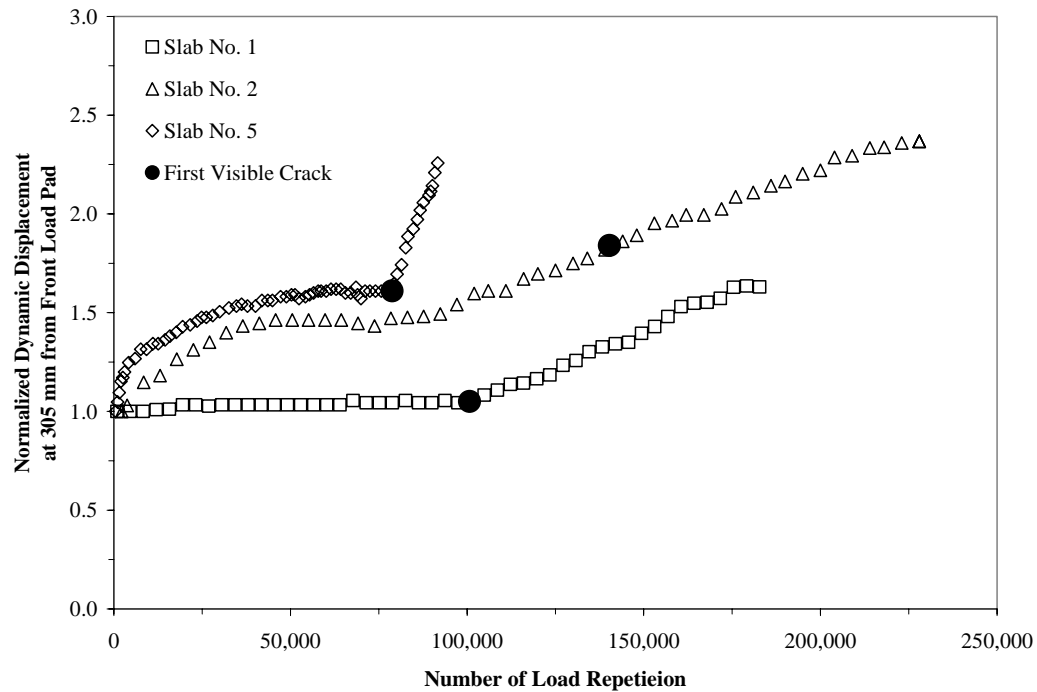


Figure 3.11 – Dynamic Displacement for Full-Scale Slabs (from Chul et al., 2004)

3.8 SUMMARY

In this chapter, a detailed background on both the RDD and SDD capability is presented. The development, methodology, and research conducted for each respective capability are discussed. Both methods play a vital role in the field testing presented in this study; use of the RDD enables continuous deflection profiling of the entire Runway 16/34 at Fort Worth Meacham International Airport, while the use of the SDD enables cyclic loading of test slabs to determine remaining life of a pavement. The chapters which follow further build upon the understanding of these two distinct methods of pavement testing and the capability each brings to this study.

Chapter 4 – Testing Site at Fort Worth Meacham International Airport

4.1 INTRODUCTION

As mentioned in Chapter 1, the purpose of this research was to determine the remaining life of Runway 16/34 at Fort Worth Meacham International Airport in Fort Worth, Texas. Prior to development of a load testing model and evaluation of the measured response of the pavement, it was important to understand the history, usage, and geologic setting of the airport. This background data enable a better understanding of applied loads, anticipated loads, and observed response of the pavement during testing. Information on construction of the airport along with as-built drawings enable explanations of the observed response. Three years ago, limited RDD deflection profiling was conducted at the airport. This preceding research also provides insight into expected response and enables direct comparison with current deflection measurements to better comprehend observed trends.

4.2 HISTORY OF FORT WORTH MEACHAM INTERNATIONAL AIRPORT

Fort Worth Meacham International Airport, which from this point is referred to as “Meacham Airport” (FAA identifier: FTW), is located five miles north of Fort Worth’s central business district at the intersection of Highway 287 and Interstate 820. The airport was originally constructed in 1925. Over its nearly 80-year existence, it has experienced many changes in both form (configuration) and function (operations). The present layout consists of two parallel runways and a single crosswind runway, with a parallel taxiway to the main runway, Runway 16/34. The two parallel runways have the designation Runway 16/34 (main runway) and Runway 17/35, while the crosswind runway is designated Runway 6/27. These designators represent the direction of approach from true north of the bidirectional runways. The far right zero in the degree heading is removed in the designation. For example Runway 16/34 approach is from either the 160° or 340° heading.

Runway 16/34 is comprised of reinforced PCC with a grooved surface. Runway 17/35 and Runway 6/27 are both AC overlays. Figure 4.1 shows the location of the airport. Figure 4.2 presents an aerial view over the main runway. Figure 4.3 is a schematic of Figure 4.2 with runway designations. American Airlines was originally based out of Meacham Airport, when it established its first hangar there in 1933. In 1953, all scheduled airline service was relocated to the nearby Greater Southwest International Airport. Since 1953, the airport has been associated with general aviation, corporate aviation, and student pilot activity (FTW, 2004).

Presently, the FAA reports a total of 219 aircraft based at Meacham Airport, of which nearly 60% are single-engine aircraft. The majority of these smaller aircraft utilize the shorter Runway 17/35. The crosswind runway rarely experiences any significant traffic as it is used predominantly in training operations and emergency landings.

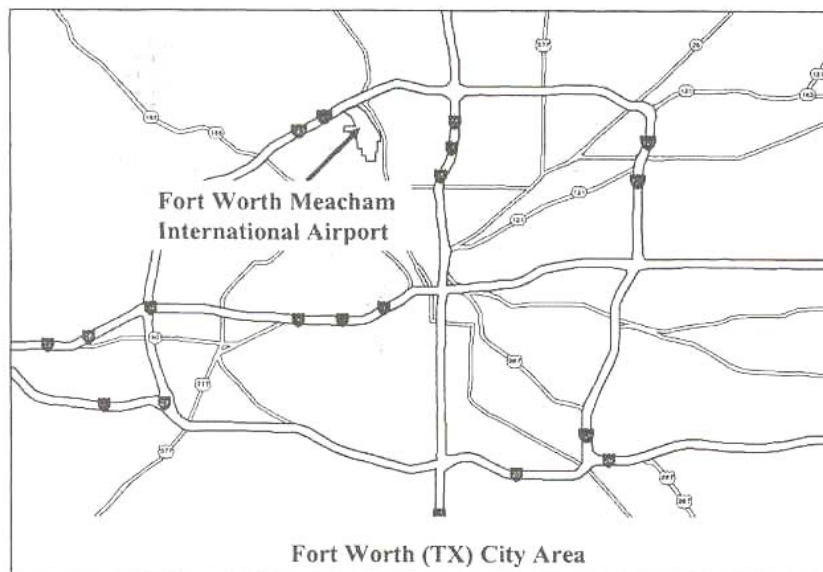


Figure 4.1 – Location of Airport



Figure 4.2 – Aerial View of Runway 16/34 (from TxDOT, 2004)

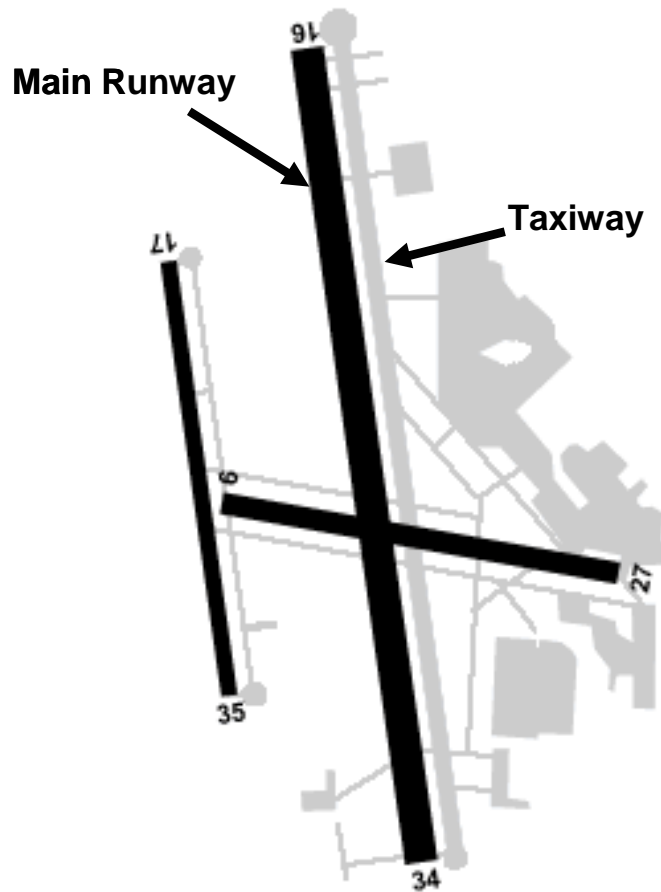


Figure 4.3 – Runway and Taxiway Layout (from AirNav, 2004)

4.3 FORT WORTH MEACHAM INTERNATIONAL AIRPORT USAGE DATA

From 1925 to 1953, Meacham Airport operations were focused on passenger travel and cargo transport, in particular airmail. At the time, air travel was still in its infancy and limited loadings and low repetitions were experienced by the airfield. Following this period, the airport has transitioned into the operational mode of general aviation, corporate aviation, and student pilot activity.

Airport usage data shows that Meacham Airport has not experienced the physical expansion and traffic increase, commiserate with standard growth models. Specific data has been obtained regarding total airport operations over the past 30

years. Figure 4.4 illustrates the distinct ebb and flow characteristic of the total airport operations over this period. Presently, the FAA reports an average 521 operations/day with over 50% of that being local generation, which is predominantly lighter single-engine aircraft. The total operations in Figure 4.4 differ noticeably in quantity from the officially reported data received from the FAA for determination of traffic model for testing. This data received from the FAA covered a period of 1998 through May 2004. However, the totals from the actual data still convey the ebb and flow characteristic seen in Figure 4.4. As can be seen from the trend in the figure, the period of 1998 through 2000 illustrates a portion of the peak and valley trend typical to the total airport operations over the life of the current runway pavement.



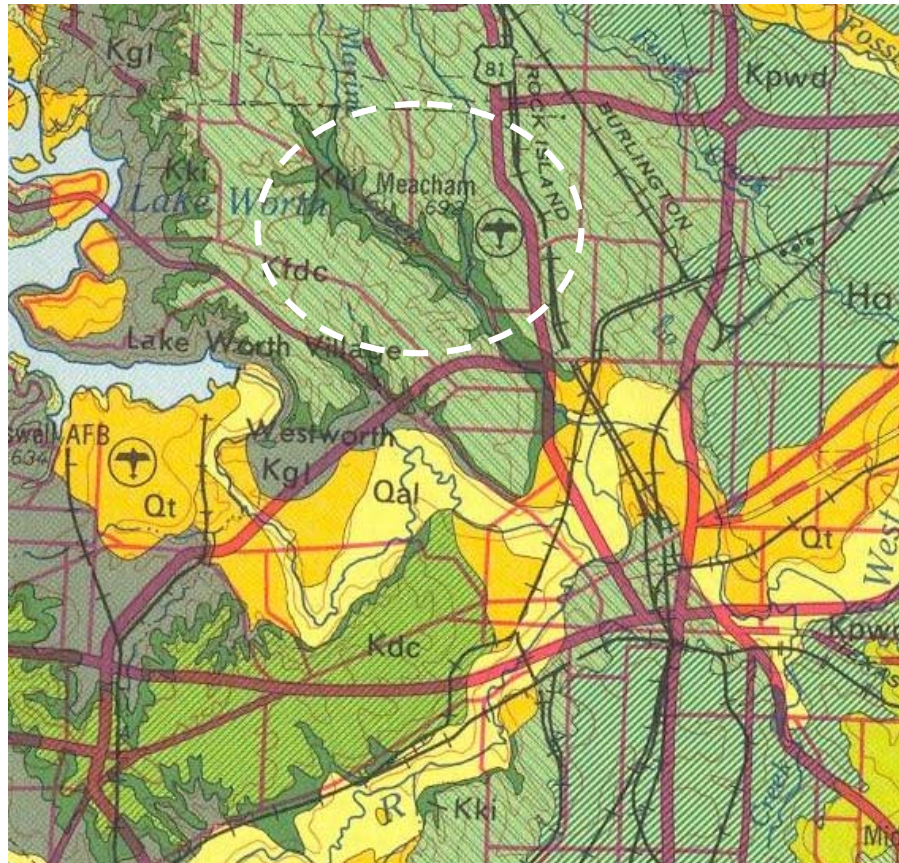
Figure 4.4 – Total Operations from 1963-2000 (from TxDOT, 2001)

An inclusive list of every single operation from January 1998 through May 2004 was obtained from the FAA and Meacham Airport Air Traffic Control. A representation of this data set is included in Appendix A (FAA, 2004). The

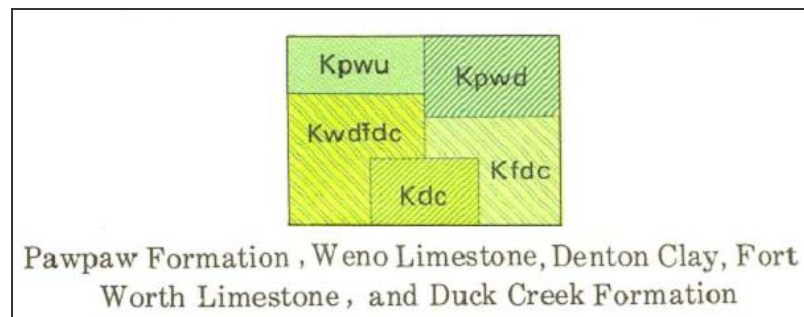
methodology used in reducing this window of traffic data into specific data used in determining the traffic data and loading scenario utilized in the SAP testing in this study is discussed in Chapter 6.

4.4 GEOLOGIC SETTING OF AIRPORT

A significant factor in examining the structural capability of an airfield is through examination of the existing soil composition and classification for that region. The soil formation which exists in the surrounding area of Meacham Airport can be classified as Lower Cretaceous; specifically the formation is referred to Denton Clay (Barnes, 1972). Figure 4.5a illustrates the geologic setting for the area surrounding Meacham Airport. A key outlining appropriate formations is included in Figure 4.5b.



a. Geologic Map of Meacham Airport



b. Soil Formation Key

Figure 4.5 – Geologic Setting of Meacham Airport (from Barnes, 1972)

Denton Clay is a combination of alternating clay, marl, and limestone beds. The clay is the predominant member of the formation, with the alternating units of clay having a thicknesses 5 to 10 times that of the thicknesses of the marl and limestone (Barnes, 1972). The clay is calcareous and known for its expansive characteristics, exhibiting considerable shrink/swell behavior. The North Central Texas Council of Governments (NCTCOG), Department of Environmental Resources reports a plasticity index (PI) range of 21 to 40% for the setting of Meacham Airport, with localized areas reaching as high as 50 (HAZMAP, 2003). This information is based on USDA-NRCS (United States Department of Agriculture – National Resources Conservation Services) Soil Survey Data. Swell potential is rated "very high" for any plasticity index over 35 % (Holtz and Gibbs, 1956).

4.5 AIRPORT CONSTRUCTION AND AS-BUILT INFORMATION

Runway 16/34, the main runway, was constructed in 1975. The runway is 7,500 ft (2,286 m) in length and 150 ft (45.7 m) in width, constructed on both cut and fill sections. Runway 16/34 is comprised of a layer of reinforced PCC pavement, arranged in slabs of 25 ft by 25 ft (7.6 m by 7.6 m). The main runway contained six “lanes” of single-slab widths. For ease of referencing, the lanes will be referred to as lane 1 through lane 6. Lane 1 is the far west lane when orientated to north, with successive lanes to the right. Pavement thickness ranges from 7 to 10 in (17.8 to 25.4 cm). The majority of the runway PCC pavement is 9 inches thick, with a thicker 10-inch pavement used on the north and south end of the runway where heavier loading is more frequent. The thickness of pavement tapers to 7 inches in areas where no direct aircraft loading is expected, particularly the slabs in lane 1 and lane 6. The subsurface pavement structure consists of 6 inches of cement-treated subbase and 5 inches of lime-treated subgrade. A typical cross-section of Runway 16/34 is shown in Figure 4.6. Figure 4.7 gives a closer look at the sections denoted in Figure 4.6. TxDOT Aviation Division supplied a complete set of as-builts. As-builts information

was assumed correct unless conflicted by information obtained from the present-day airfield visitations and surveys.

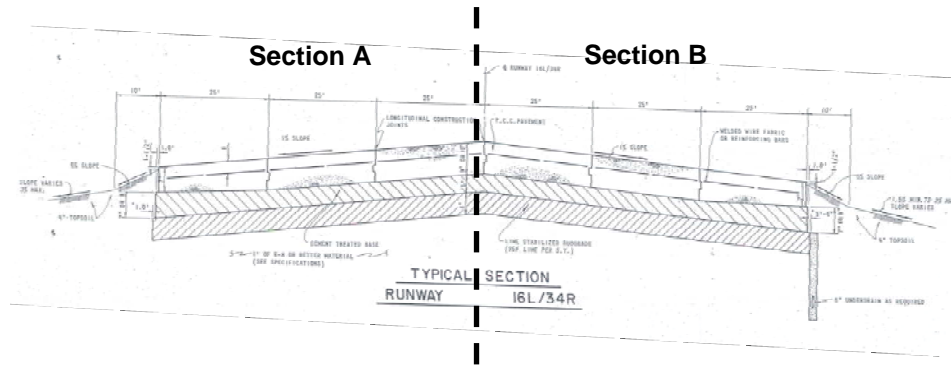
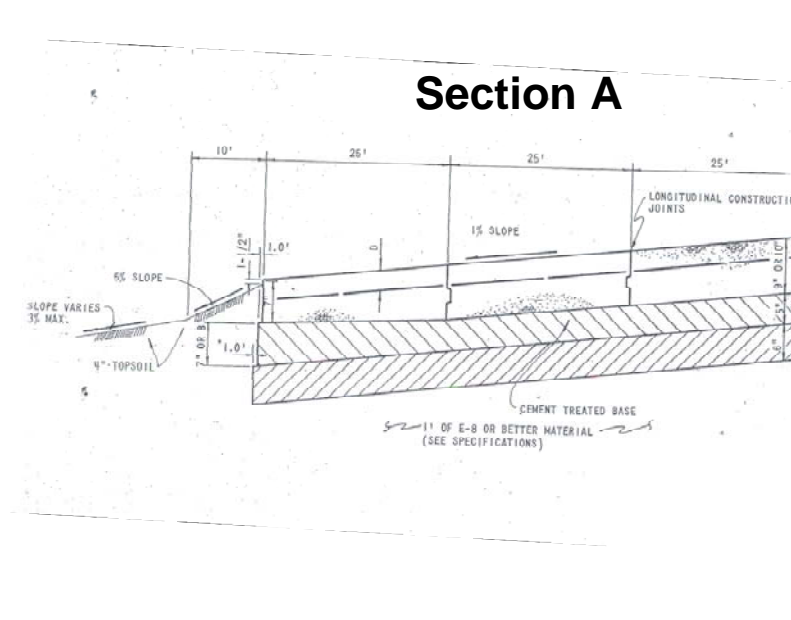
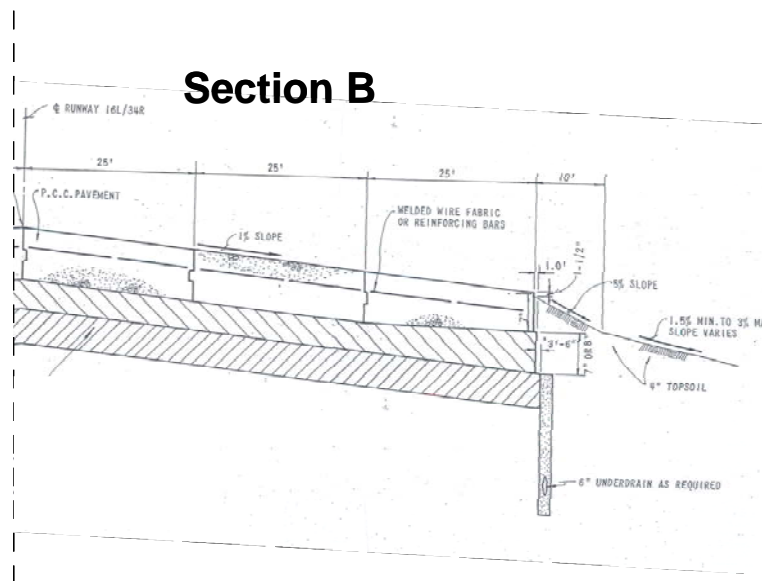


Figure 4.6 – Typical Cross-Section of Runway 16/34 (from TxDOT, 1975)



(a)



(b)

Figure 4.7 – Close Up of Cross-Section of Runway 16/34 (from TxDOT, 1975)

Over the past 29 years, Runway 16/34 has performed well, with typical routine maintenance performed periodically. An extensive drainage project was completed in 2002, which did not directly affect the continuity of Runway 16/34, but required a construction cut through the pavement of the neighboring south end run-up area. The most common distress from visual condition assessments was low severity longitudinal cracking. This cracking is contained primarily to the outside lanes of the main runway, concentrated between 1,200 and 2,200 ft (365.8 and 670.6 m) from the south end of the runway. It has been estimated that only 20% of the actual take-off and landing operations occur in this area (Lee et al., 2003), consequently direct response from aircraft loading can be eliminated as the predominant cause of distress.

4.6 RDD TESTING AT FORT WORTH MEACHAM INTERNATIONAL AIRPORT IN 2001

In May 2001, two longitudinal test paths were used in profiling Meacham Airport. In addition, five transverse test paths were also profiled at selected locations along the runway. The two longitudinal test paths were along the centerline of Lane 1 and Lane 3. Figure 4.8 illustrates the longitudinal test path orientation. All testing was conducted at night between the 10:00 PM and 6:00 AM, during scheduled non-flying hours.

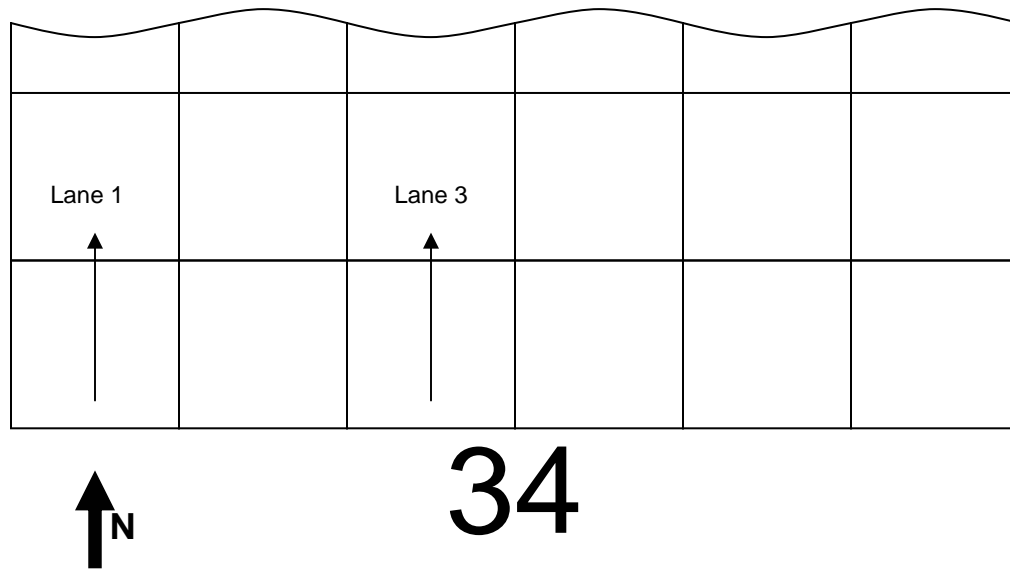
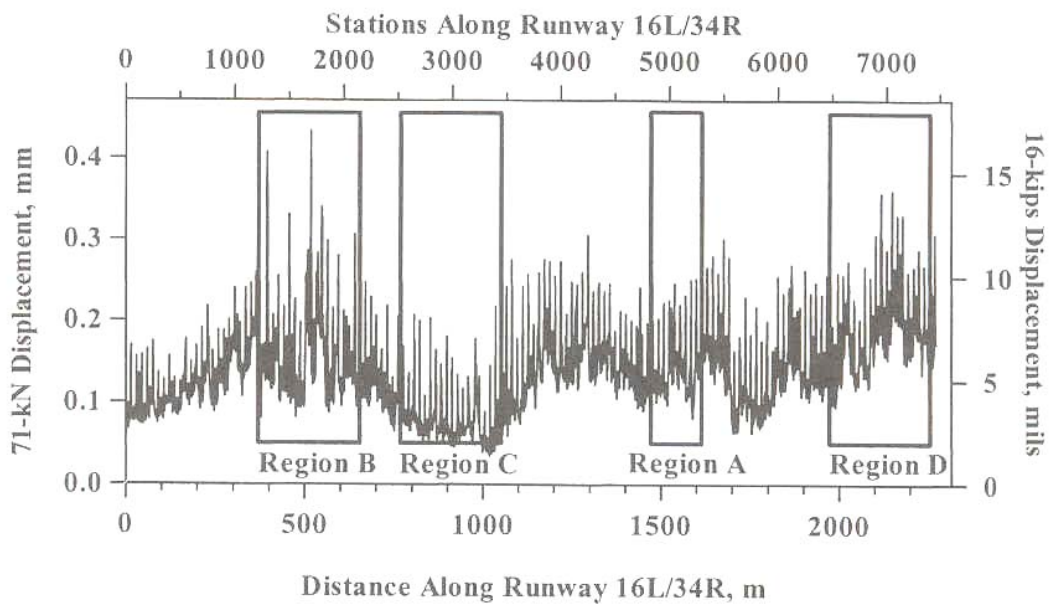
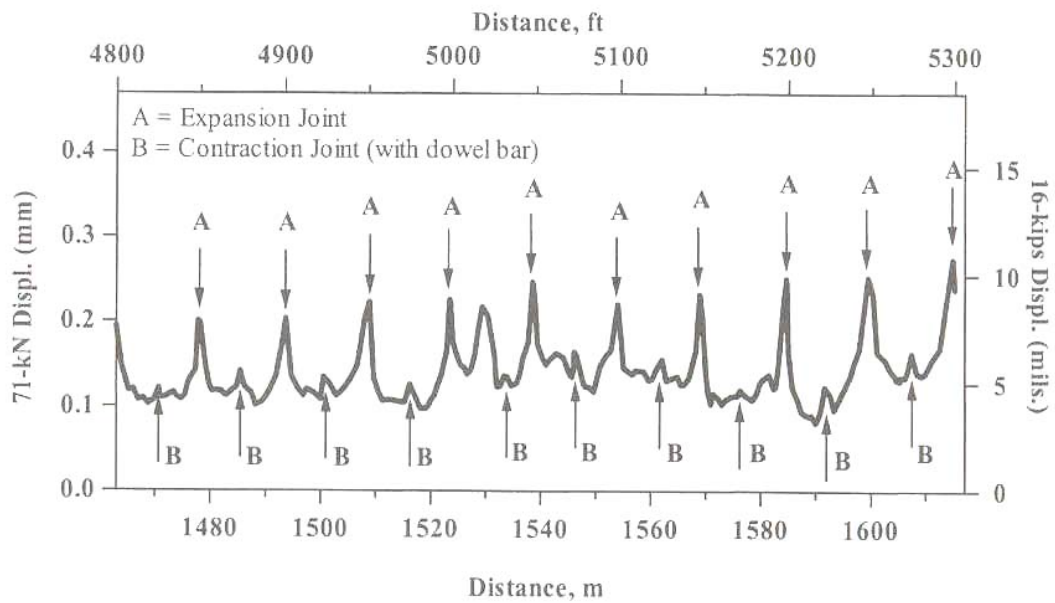


Figure 4.8 – RDD Profiling Paths Along the Longitudinal Centerlines of Lane 1 and Lane 3 of Runway 16/34

A general discussion on the methodology and test procedures involved with RDD testing are presented in Chapters 3 and 5. Results from the 2001 RDD testing included a general examination of the variability of the pavement structural condition along the length of the runway. Four specific regions were analyzed, with pavement deflection response and structural conditions being annotated. These four regions are illustrated on the complete runway deflection profile for Lane 3 shown in Figure 4.9a, Regions A, B, C, and D. The longitudinal test path along Lane 3 was used in the analysis, because this is the region of the runway which comes into contact with the majority of the traffic. From the overall pavement profile it is evident that there are two types of transverse joints within Runway 16/34, each type exhibited a unique response. The first type is an expansion joint, labeled as joints “A” in Figure 4.9b. These joints exhibited higher deflections than the other joint type (doweled contraction joints). Region A (Figure 4.9b) illustrates this phenomenon with expansion joints and contraction joints, labeled “A” and “B” respectively.



a) Continuous RDD Deflection Profile (Sensor #1) Along Path TL-a



b) Expanded RDD Deflection Profile for Region A (Sensor #1)

Figure 4.9 – RDD Deflection Profile Runway 16/34 (from Lee et al 2003)

In examining the runway longitudinally, the region between 1,200 and 2,200 ft from the south end of the runway exhibited the highest deflections. This area is represented by Region B in Figure 4.10a. Although this area experiences limited traffic, the higher deflection can be attributed to the concentration of longitudinal cracking. Region C (Figure 4.10b) represents the area between 2,500 and 3,500 ft from the south end of the runway. This area is located in a cut section of the subgrade and experiences limited and light traffic. Typically aircraft takeoff in the south direction along Runway 16/34, so fully-loaded aircraft experience significant lift by the time traffic reaches the region. Likewise, landing aircraft, lighter due to fuel consumption, pass over the area enroute to parking aprons. Region B experienced the lowest mid-slab deflections, inferring the highest pavement system integrity along the runway. Region D (Figure 4.10c) experienced the highest average deflections due to its high mid-slab deflections. This result is attributed to the collective effects of experiencing fully loaded aircraft take-off, aircraft landing, and the construction of Region D over fill material (Lee et al., 2004).

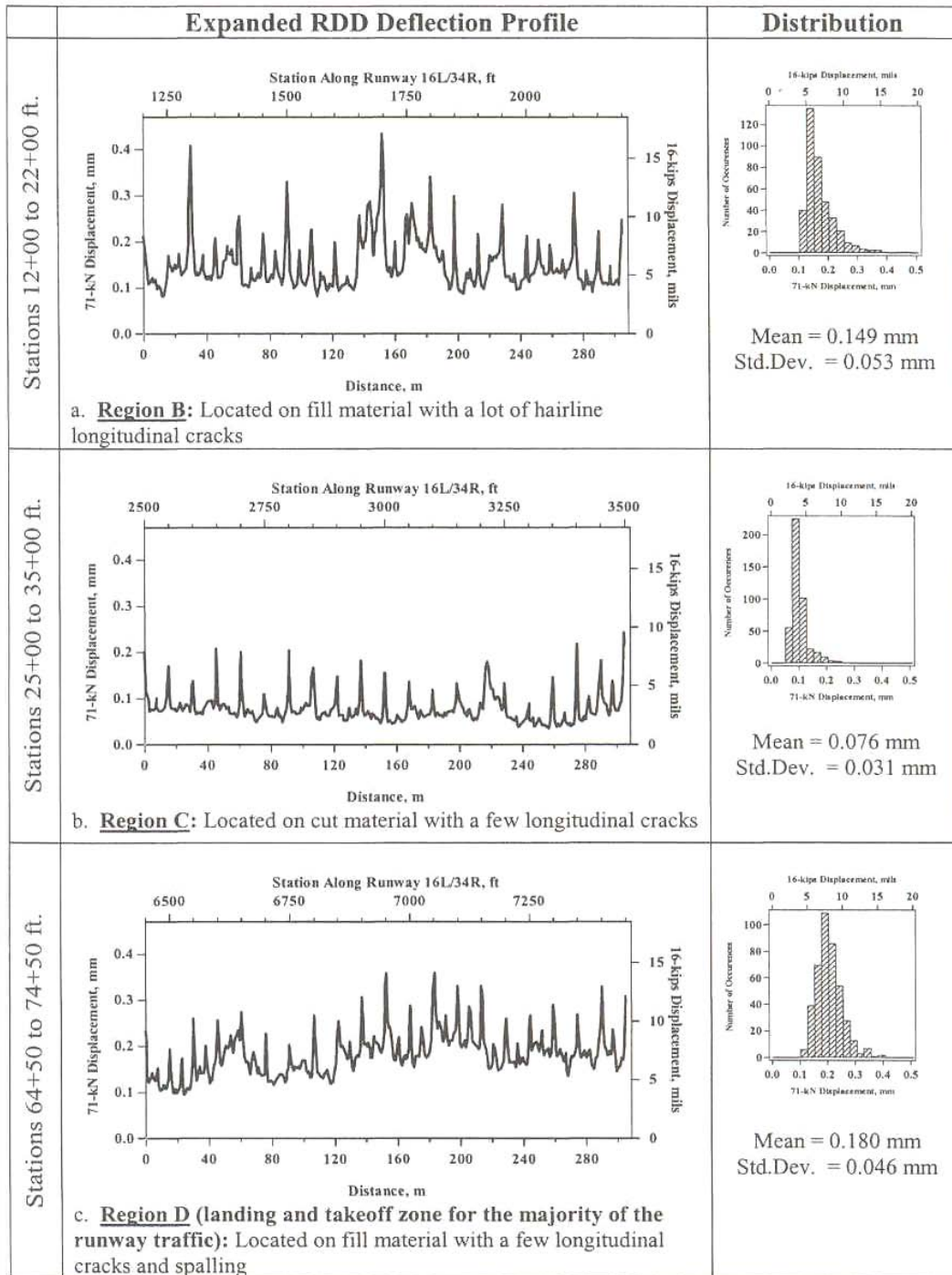


Figure 4.10 – Expanded RDD Deflection Profiles (from Lee et al., 2003)

One conclusion from the investigation showed a correlation between cut and fill material and higher deflections, with few exceptions. A second conclusion was that the effects of traffic also played a significant role, with the north end of the runway demonstrating higher average deflections. Once again, the only significant cracking distress was discovered in a region of low traffic and not in any of the highly trafficked areas. Chapters 5 and 7 address the more robust collection of continuous deflection profiles which occurred in this study. In Chapter 7, a comparison of present day data to the data collected in 2001 is made to observe changes in deflections with time, over a 3 year period of traffic and environmental effects.

4.7 SUMMARY

In this chapter, a framework of existing background conditions at the Fort Worth Meacham International Airport in Fort Worth, Texas is established. The information presented regarding history, usage, and geologic setting facilitates the development of an accurate load testing model, presented in Chapter 6. This information also supports the selected constraints applied to the testing within this study, including applied loads and anticipated loads. Observed response of the pavement during testing can be clarified through an understanding of the information contained in this chapter. Information on construction of the airport along with as-built drawings are presented along with the limited RDD deflection profiling performed in 2001. This information and the 2001 research provide further insight into expected deflection response of the runway and enable observation of any deflection response changes, which have occurred over the 3-year period between testing.

Chapter 5 – Procedures for Airfield Pavement Assessment

5.1 INTRODUCTION

The following chapter focuses on the procedures and measures taken to assess Runway 16/34 at Meacham Airport. The first step in preparing for the SDD SAP testing and airfield assessment was a complete RDD deflection profiling, conducted on each lane. The measured response from the main runway established a set of deflection data which could then be used in determining potential test locations outside the runway which yielded similar responses. The details surrounding the development of an appropriate load frame for use in testing are also discussed. Finally, specifics of the SDD SAP testing application are presented to detail the selection of the final three test slab locations and the procedures surrounding the SDD SAP testing application.

5.2 RDD TESTING ON RUNWAY 16/34

Previous RDD testing was conducted at Meacham Airport in June 2001. At that time, two of the six lanes of Runway 16/34, Lane 1 and Lane 3, were profiled longitudinally. As discussed in Section 4.6, the two primary findings included unique joint movements pertaining to joint type and the localized effects due to cut/fill or typical aircraft trafficking. Prior to beginning SAP testing with the SDD method, an in-depth investigation of the runway was performed. This investigation included profiling along all six lanes of the airfield as described below. A comparison of the results from present day deflection testing to data obtained in 2001 is presented in Chapter 7.

During the initial testing period in July 2004, a team from the Geotechnical Engineering Program in the Department of Civil Engineering, University of Texas at Austin, conducted a comprehensive RDD assessment of Runway 16/34 at Meacham Airport. The team, composed of three graduate students and one technician, initiated

each pass at the mid-slab point at the south end (34 end) of the runway, beginning at Lane 1 and continuing through Lane 6. Figure 4.1 shows the testing orientation for all six passes. Every 100 ft (every four slabs) in the longitudinal direction of the runway, a point mark was placed so that precise locations could be referenced during continuous RDD testing along the 7,500-foot long runway.

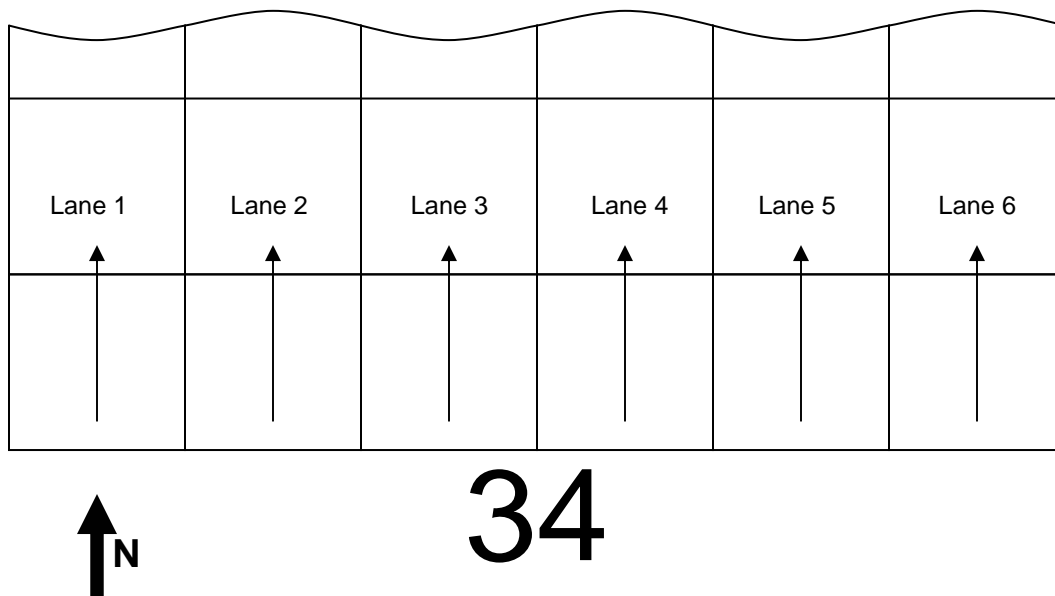


Figure 5.1 – RDD Profiling Paths Along the Longitudinal Centerlines of All Six Lanes of the South End (34 End) of Runway 16/34

In the same manner as in 2001, RDD testing took place during airport-designated, non-flying hours from 1000 to 0600 hours. Due to the challenges of nighttime operation, each member of the four-person team served a separate and important function during testing. A technician operated the RDD, ensuring location (along the centerline of the slabs) and testing speed (approximately 1.0 mph). A second team member acted as a “point man”, assisting the driver to ensure that the RDD stayed on a straight path during testing. An additional member stood at 100-foot markings to ensure marking data were recorded at the correct interval distances.

The final member managed the computer-interface, data-retrieval system, validating proper reading, retrieval, and logging of data.

Prior to RDD deflection testing, specific test-controlled parameters were established. For the loading, a static hold-down force of 18 kips was utilized with a 16-kip peak-to-peak force (maximum of 26-kip and minimum of 10-kip load). In all cases, a loading frequency of 35 Hz was used. These values are typical of test parameters used in RDD deflection testing. The 16-kip peak-to-peak dynamic force provided an ample load to produce a measurable deflection response. The slow test speed of approximately 1.0 mph and the loading frequency of 35 Hz (which equates to 35 load repetitions over 2.2 ft of test path), allowed development of a robust deflection profile. Sensor #1, Sensor #3, and Sensor #4 were used during data collection, Sensor #2 was out of service at the time of testing. Sensor #1 provided deflection data directly adjacent to the loading rollers. Figure 5.2 shows the RDD and the orientation of the sensors beneath the test vehicle. Note in this figure, the sensors are in the up position for vehicle movement to a given test location and will be lowered to pavement surface during testing operations. Figure 5.3 gives specific dimensions for the sensor array.



Figure 5.2 – Close-Up of Sensor Configuration for RDD Testing

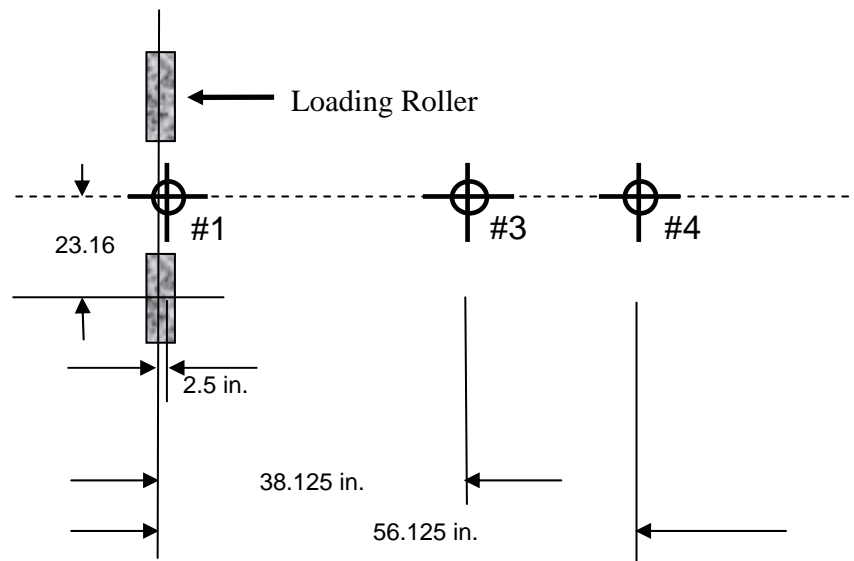


Figure 5.3 – Dimensions of Sensor Array

Following completion of testing along the centerline of each of the six runway lanes, additional RDD testing was conducted along three longitudinal joints on the north end (16 end) of the runway (see Figure 5.4). This area of the runway has been subjected to the most traffic, including fully-loaded aircraft taxiing prior to takeoffs, actual aircraft takeoff operations, and the majority of the touchdowns during landing operations. Tests were conducted with one loading roller positioned approximately 3 to 6 inches from the joint. A photograph showing the roller positioned prior to test execution is presented in Figure 5.5. Testing was conducted along the initial 1,000 ft (304.8 m) of the runway. The center longitudinal joint, between Lane 3 and Lane 4, was tested on both sides. In addition, the inside edge of the longitudinal joints between Lane 2 and Lane 3 and between Lane 4 and Lane 5 were also tested. Figure 5.4 illustrates these test paths.

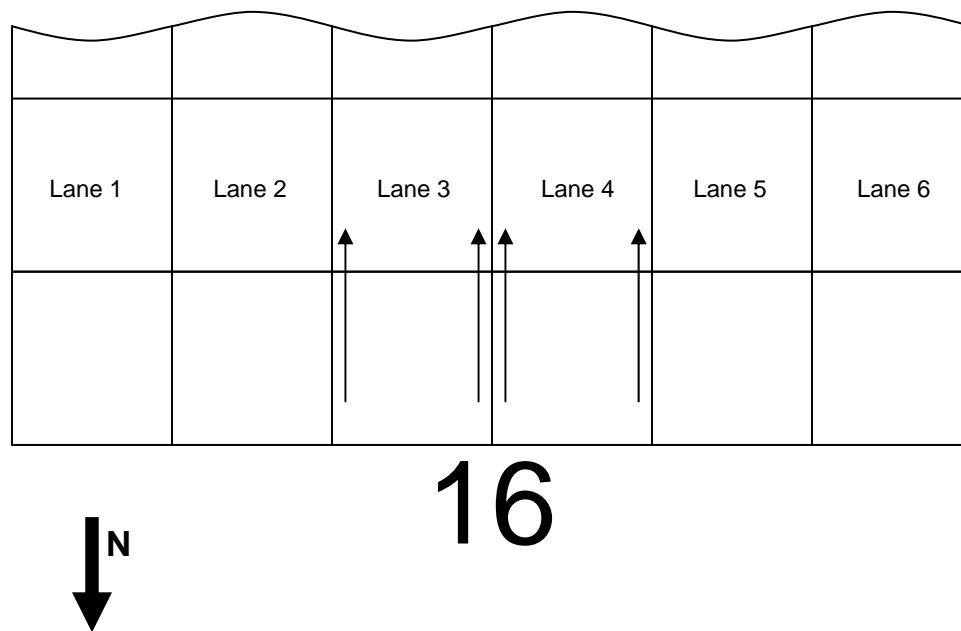


Figure 5.4 – RDD Test Paths Used to Investigate Longitudinal Joints on North End (16 End) of Runway 16/34

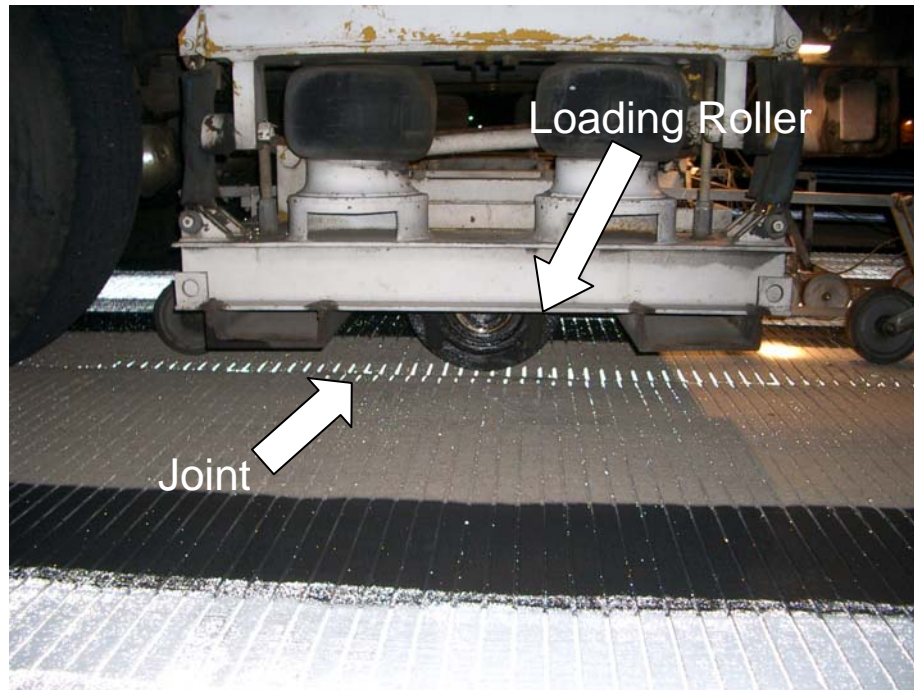


Figure 5.5 – Loading Roller in Position to Test Longitudinal Joints

Several assumptions and sources of error that should be noted are embedded in the RDD testing method. In general, RDD testing is not a true deflection measurement; rather it is a relative measurement. Due to the continuous nature of testing, an exact deflection response at an exact point with a specific load is not attainable (unless the RDD device is stationary which is possible if needed). In addition, the 49-kip load from the weight of the device, imposed on the pavement surface over the extent of the wheelbase, will effect deflection measurements. Since this deformation due to the weight of the RDD occurs over the continuous testing area, results are most conclusive when compared along the linear test area. As with most testing methods, the human element introduces possibilities of error. During testing, it is impossible to keep the rate of movement constant. The varying speed rate can cause some areas to endure additional loads per a given test length, causing the deflection response to

deviate slightly from a true equal-rate response. In addition, the test relies on human control for maintaining a linear test path. The natural wander in the steering controls of the RDD makes this impossible. Therefore, results can deviate from the assumed test path. Finally, the nighttime nature of operations for the RDD and human exhaustion and fatigue also play a role in the probability for error. Notwithstanding these potential sources of error, the RDD has proven to be an effective method for determining relative deflections and subsequently relative stiffnesses of a pavement structure over the extent of a testing area. Typical RDD test results and measurements performed in this study are presented in Chapter 7. The complete set of results, including additional deflection profiles of the longitudinal joints on the north end of Runway 16/34, will be presented in a companion study (Nam, 2005).

5.3 SELECTION OF SDD TEST LOCATIONS

SDD test locations were determined by conducting both visual field surveys and RDD profiling of potential locations. Any SAP testing that would be conducted on Runway 16/34 would have to be accomplished during hours of darkness (non-flying hours). Limitations of visual measurements and general testing operations associated with nighttime testing, coupled with the limited 8-hour test period resulted in a decision to locate the testing area on the taxiways and run-up areas. Figure 5.6 identifies each of the eight candidate SDD test areas on the taxiways or run-up areas. Note the North and South Run-Up areas are also referred to as the North and South End-Arounds.

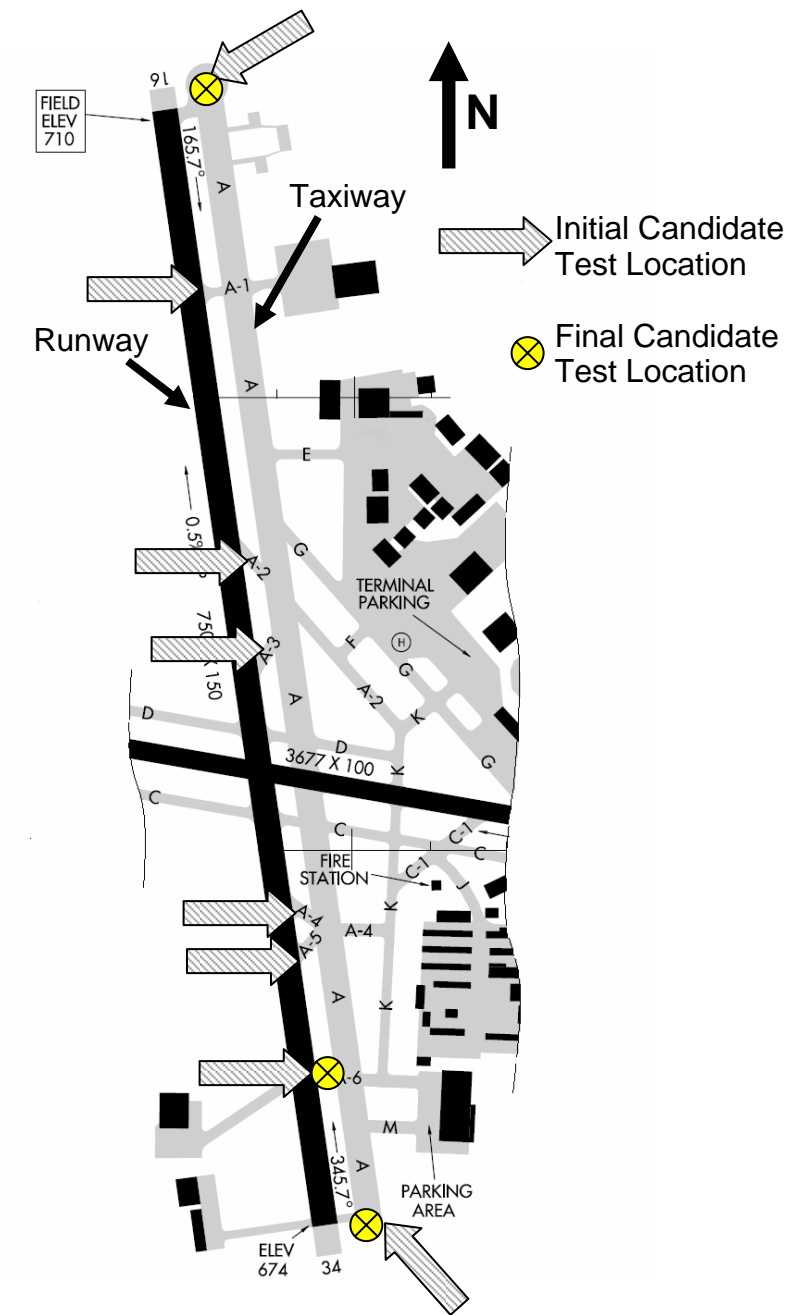


Figure 5.6 – Candidate Locations for SDD Testing

Prior to beginning the SAP testing portion of the study, an as-built review and visual survey was conducted of all candidate locations. The objective of this selection process was to find pavement test slabs at candidate test locations which matched the pavement on Runway 16/34. The pavement needed to be similar in composition, thickness of layers, cut or fill section, and visual appearance and condition. Not all six taxiway and two runway end-around locations produced viable prospective test locations. Taxiway A-5 only contained 6 in. of PCC, compared with the 9 and 10 in. of Runway 16/34. Taxiway A-2 has been resurfaced and now features the original 9 in. PCC with an AC overlay. A typical cross-section of original taxiway pavement has been included in Figure 5.7 to illustrate taxiway composition.

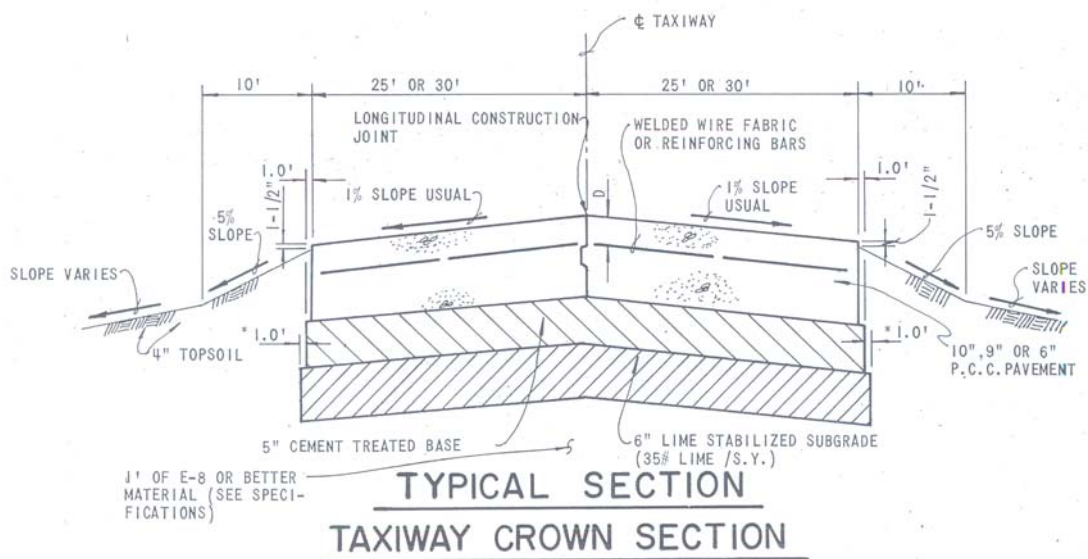


Figure 5.7 – Taxiway Cross Section (CBI, 1972)

Upon completion of the visual survey, three final candidate locations were selected: (1) Taxiway A-6, (2) South Run-Up area (34 end), and (3) North Run-Up

area (16 end). Taxiway A-6 is composed of a 9-inch thick PCC layer, similar to the thinner portions of the runway. The Taxiway A6 candidate location is indicated on Figure 5.6 with a cross-hair circle, the only symbol located on the taxiway between the main runway and parallel taxiway. Both run-up areas have a PCC thickness of 10 in., the same thickness as the first 1000 ft of both ends of the runway. These three candidate locations were selected due to the similar dimensions and visual condition to Runway 16/34. Figure 5.8 illustrates the typical section and composition of the three test locations along side a typical section of the Runway 16/34. Upon completion of the visual survey and correspondence of as-built information, RDD profiling was performed on the three candidate locations. The three final candidate test locations are denoted with crossed circles in Figure 5.6. In addition to matching the physical properties, the objective of RDD testing was to match the deflection profiles of the candidate location to that of problematic areas of the runway. Similar responses in the three areas would allow more accurate correlation of test location data to actual runway conditions.

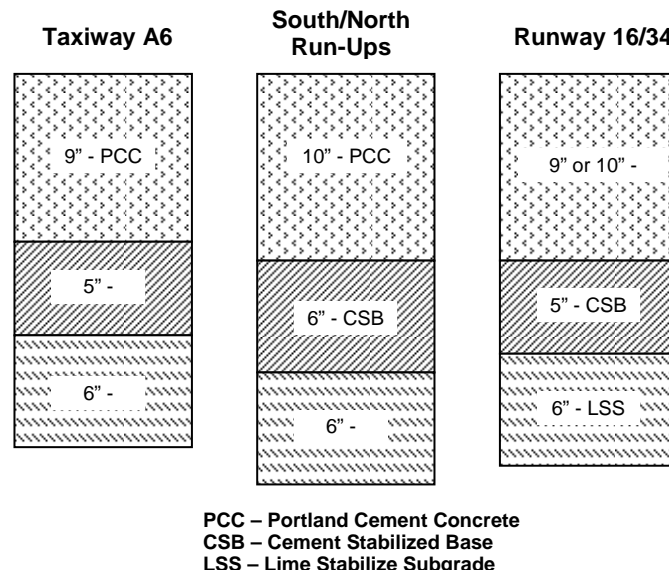


Figure 5.8 – Layer Dimensions for Final Candidate Test Locations

Once again, assumptions had to be made and sources of potential errors needed to be highlighted in the test location selection process. First, all as-built information was assumed correct. Visual surveys were conducted to highlight any changes and alterations to the pavement since construction in 1975. Key airport maintenance personnel were conferred with to ensure original concrete was assessed when the visual survey was questionable. It was also assumed that if the deflection profiles at the test locations were comparable to the profiles measured on Runway 16/34, then they could be assumed to be representative of the main runway. Even though the test locations were not part of the main runway, the test sections were found to be similar in age and condition. Apparent sources of error and variation include the fact that no two in-service concrete pavements are exactly the same, because subsurface conditions and concrete composition vary which may cause different situations to produce similar deflection responses. A more extensive round of testing encompassing a greater number test points could further enhance the findings of this study by providing additional data covering a larger range of testing locations.

5.4 LOAD FRAME CONFIGURATION

In order to load a pavement over a specific load footprint, a load frame needed to be configured and constructed. Various load frames have been used in the past, as previously mentioned in Section 3.6. The principal challenges with designing a load frame for SAP testing is the stability, contact locations, and contact pressure distribution with the pavement during dynamic load application. Previous configurations have been found unstable and a challenge in maintaining contact during dynamic loading. Rubber pads have been used to improve load distribution across contact areas with limited success. Previous SAP testing operations have found rubber pads to be ineffective; the super-accelerated nature of the testing has led to deterioration of these pads. Direct contact between the pavement surface and steel pads has proven to be successful and was used for all testing conducted herein.

Previous SDD SAP testing conducted on flexible pavements has included the use of a steel reference frame, in addition to a load frame. This reference frame provided a point of reference for vertical displacement transducers. The focus of the previous testing was the permanent deformation (rutting) of a flexible pavement, which required a reference point for deformation over time (Stokoe et al., 2000). Figure 5.9 shows a typical arrangement for dual-wheel loading used in previous testing applications. A different load frame was constructed for use on full-scale rigid pavement slabs (Suh et al., 2004). This load frame consisted of welded and braced steel I-beams with circular loading pads. The load frame configuration formed a T-shape with three circular loading pads. A schematic of this load frame is presented with associated dimensions in Figure 5.10.

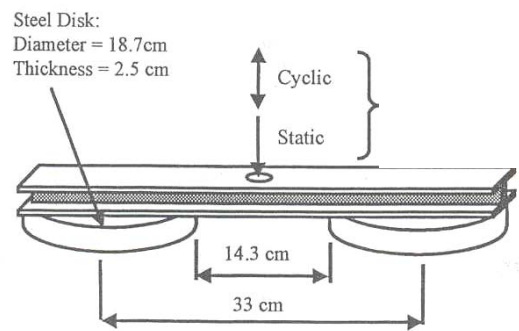


Figure 5.9 – Example Load Frame Arrangement for Dual-Wheel Footprint Representation for Testing Flexible Pavements (Stokoe et al., 2000)

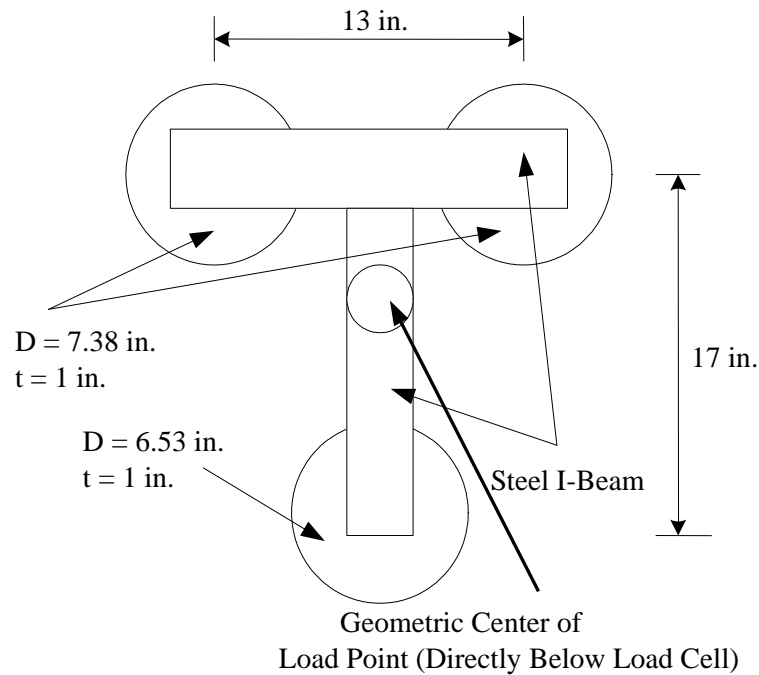


Figure 5.10 – Schematic of Load Frame and Configuration of Loading Pads for Testing PCC Mid-Slab Regions (Suh et al., 2004)

The existing load frame had a single load transfer point. To enable load transfer from the dynamic system to the pavement, a load point was employed which consisted of a 4 in. diameter steel round cut to form a disc with a thickness of 0.75 in. The disc was welded to the geometric center of the frame configuration and the loading pads. This set up effectively distributed 33.3% of the load onto each pad, as seen in Figure 5.10. For the SAP testing performed in this research, a dual-wheel load was desired. A dual wheel load configuration was desired since 46% of the traffic analyzed was either dual-wheel or dual tandem gears. Although the amount of single-wheel traffic was roughly the same, the dual-wheel traffic represented the majority of the total quantity of loading imparted on the airfield and therefore became the desired model for load configuration. The dimensions for the circular pad were already established under the previous research. The footprint created from the dual-

wheel configuration was on the order of 2.5 times the area of the highway design standard of 18-kip axle with dual wheels, making it acceptable for aircraft traffic modeling. Since this testing was conducted on rigid pavements, it is the total load rather than the contact stress that governed the pavement response and performance. Therefore tire pressure was not considered, but rather total load imparted by aircraft. The use of total load helped to further simplify the traffic data, since data from over 120 aircraft (with varying weights, tire pressures, and frequencies) were incorporated into the traffic model. A comparison of load frame induced stresses and deflection responses to actual aircraft footprints using a finite element model is discussed later in the chapter. It should be noted, that results of finite element analysis, further support load frame configuration as a viable representative of aircraft loading.

Adding a “third wheel”, to the dual-wheel footprint discussed above, would less accurately represent aircraft traffic loading conditions and dimensions. To ensure proper load application, an additional load point was welded to the center point between the top two wheel loads, effectively the center point of the cross bar of the “T” configuration. Figure 5.11 shows the same schematic as in Figure 5.10, but with the added load points. In addition to the load point for dual wheel load equivalence, a supplementary point was placed over the other end (base of the “T”) for single wheel load equivalence. This point was positioned for future research and applications; it was considered too unstable under the SDD loading performed in this study. Final determination between a two-wheel load configuration and a three-wheel load configuration was resolved during field operations at Meacham Airport. A decision prior to actual onsite testing was not attainable due to equipment scheduling and obligations, the SDD configuration of the RDD would not be installed until in the field, directly prior to the testing within this research, eliminating a chance to test the altered load frame.

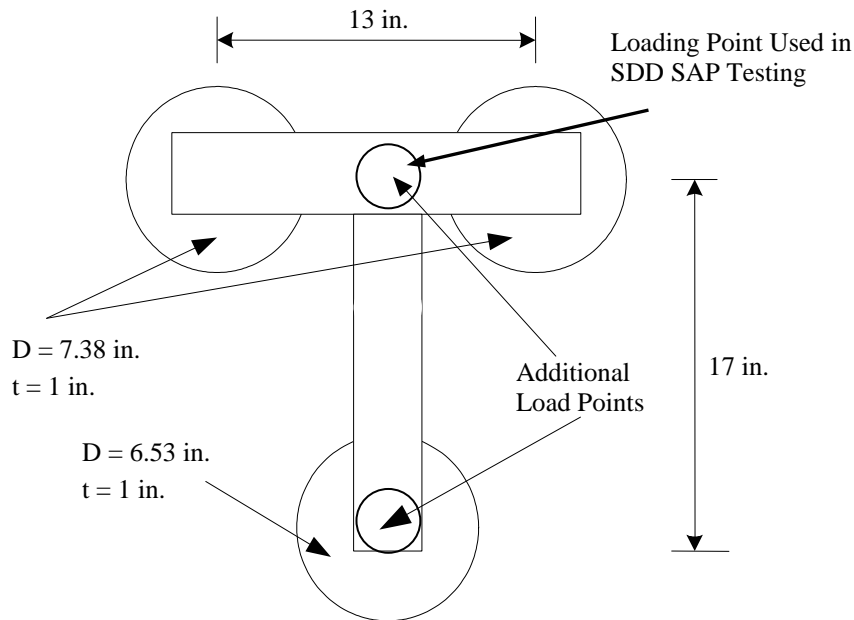


Figure 5.11 – Schematic of Altered Load Frame and Configuration of Loading Pads

In making the final selection to use a two-wheel loading frame configuration instead of a three-wheel load frame configuration, several assumptions had to be made. Prior to a field operations check to ensure the load frame was stable and to determine which configuration would be used during actual field testing, it was assumed that the two-wheel (dual wheel) loading scheme was preferred. Ultimately, the dual wheel configuration more accurately represents the majority of the traffic experienced by the airport. The “third wheel” provided no analytical advantage, only additional stability under dynamic loading. A sensitivity analysis was performed using EverFE finite element computer program. EverFE is a 3-D finite element analysis tool developed jointly by the University of Maine and the University of Washington, with funding by California and Washington State Departments of Transportation. The solver is a multi-grid, preconditioned conjugate gradient algorithm utilizing un-nested mesh sequences, with a maximum meshing sequence of

12 by 12 (Davids, 2004). This analysis has been included in Appendix B for examination and review. The analysis allowed a comparison of the stress induced in the pavement by a two-wheel loading scenario versus a three-wheel loading scenario for the same given load. Through sensitivity analysis a scalable factor was determined to apply to a three-wheel loading scenario to produce the same induced stresses as a given two-wheel loading scenario, for center, edge, and corner load points. Upon commencing field testing, it was determined that dual-wheel loading was a reasonable method to be utilized during testing. The scalable factors from the previous mentioned analysis were not required for this study, but have been included in Appendix B for use in future studies of the same load frame. An additional assumption was made that the two-wheel loading scenario enabled an equal 50/50 load distribution between the two circular loading pads. Although the frame configuration was rigid, it was assumed that the load produced on the “third wheel” would be negligible for the SAP testing conditions, given the load point directly between the two pads. To verify this assumption, future studies should include load cells in all three “wheels” of the load frame.

5.5 SDD APPLICATION

5.5.1 Test Pad Locations

Upon completion of preliminary RDD testing and selection of SAP testing locations, four extended days of testing began in August 2004. Prior to commencement of SAP testing, operation checks were performed on all equipment, including calibration of the load cell used as the contact point between the dynamic load system of the SDD and the load frame. Each selected slab was tested at three load locations typically used when examining stresses and deflections in rigid pavements: center of the slab, edge of the slab, and corner of the slab. The three load locations, on each slab, are further discussed within the SAD SAP testing procedures

in Section 5.5.2. Location, orientation of accelerometers, and dimensions for all three load locations are illustrated.

Due to the nature and orientation of the RDD testing during the first phase, longitudinal deflection profiles along the middle of each lane were measured on the runway. These data show the action of traffic crossing the transverse joints. For that reason, transverse joints with comparable deflections and load transfer relationships were selected and tested. At Meacham Airport, the transverse joints were comprised of three types: expansion (1 1/4-in. wide with neoprene sealant), contraction (7/16-in. wide with 1-in. diameter smooth dowel and neoprene sealant), and dummy (3/8-in. wide with neoprene sealant). As noted, only contraction joints contained a load transfer mechanism beyond aggregate interlock. Longitudinal joints were comprised of two types: construction joint with keyway (7/16-in.) and construction joint with tie bar (7/16-in. wide with #5 rebar). As-built drawings did not delineate specific joint type for a specific slab location (CBI, 1972). Visual surveys and field judgment were used to surmise conditions and type of joint at each test slab with the desire to test “the worst case”; hence, the 3/8-in. dummy joints without load transfer mechanism.

Under the SDD SAP testing performed, transverse joints were analyzed under edge and corner loadings. Transverse joints experience “true” load transfer conditions under traffic loading, where as mid-slab areas cycle between loaded and unloaded conditions with each pass. These joints experience a high volume of repetitions, are situated perpendicular to expected traffic, and rely solely on aggregate interlock at transverse dummy joints. Under a moving wheel load, one side would be fully loaded, whereas the other side would have no external load. After movement of the aircraft landing gear past the joint, the loading condition would reverse; this succession of loading and unloading leads to one of the prominent manifestations of distress in rigid pavements, pumping (Miller and Bellinger, 2003).

SAP Testing Location on Taxiway A6

Testing commenced with operations at the location on Taxiway A6. Taxiway A6 consisted of the thinner 9-in. PCC pavement. The test location was within the typical area of traffic movement. However, with six active taxiways on Meacham Airport, Taxiway A6 received a limited amount of traffic applications in comparison to Runway 16/34. The specific location of the selected slab is shown below in Figure 5.12, with the orientation of the RDD test paths denoted. To ensure the test slab tested was comparable to the runway pavement, deflection data were compared. The deflection data gathered on the mid-slab and joint slab were 4.0 and 7.1 mils respectively. These deflection values are comparable to the target deflection data from Runway 16/34. Figure 5.13 shows RDD deflection measurements from the test path with the test slab highlighted. Table 5.1, presented at the end of this section, summarizes all respective mid-slab and joint deflection data for all three test slab locations. Specific slab data is presented for the test locations, while a range is given for Runway 16/34. The range is obtained from data which is presented in detail in Section 7.2.2.

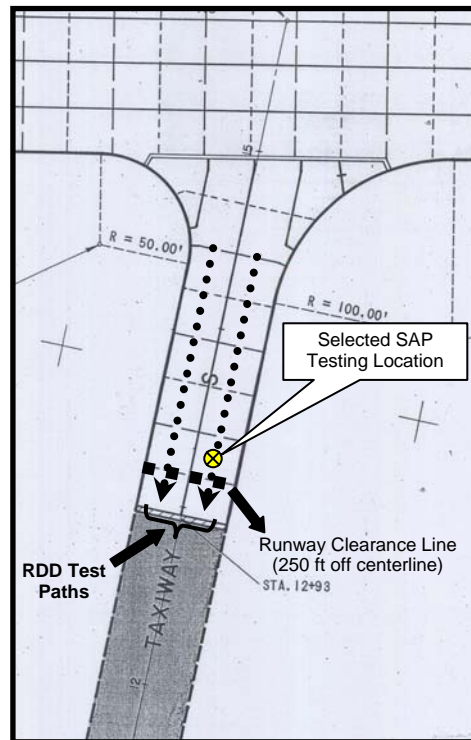


Figure 5.12 – RDD Test Paths and SAP Testing Location at Taxiway A6

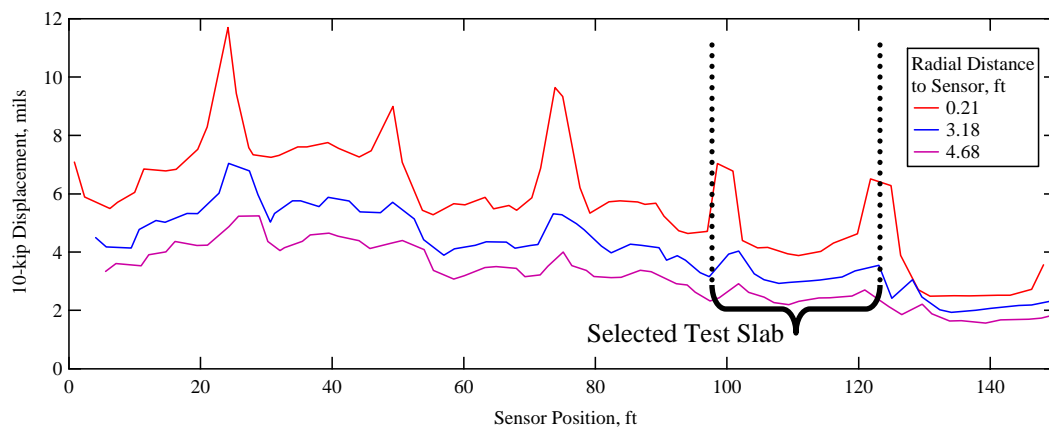


Figure 5.13 – RDD Deflection Response for Taxiway A6 Test Path

SAP Testing Location on South Run-Up

Following testing and data collection on Taxiway A6, the SDD equipment was relocated to the south end of the runway. At the South Run-Up area, another slab was tested. The south end run-up area was comprised of multiple-age PCC, constructed and repaired over periods of expansion and drainage reconstruction, since the original construction 29 years ago. The South Run-Up area consisted of a 10-inch thick PCC pavement. Testing was orientated on the slab as shown below in Figure 5.14. The test location was within the area of traffic movement, however the south end run-up area received limited traffic since the majority of taxing and take-off operations were generated at the north end. The deflection data gathered on the mid-slab and joint were 3.0 and 4.8 mils, respectively. These deflection data are comparable to the target deflection data from Runway 16/34. Figure 5.15 shows RDD deflection measurements from the test path with the test slab highlighted.

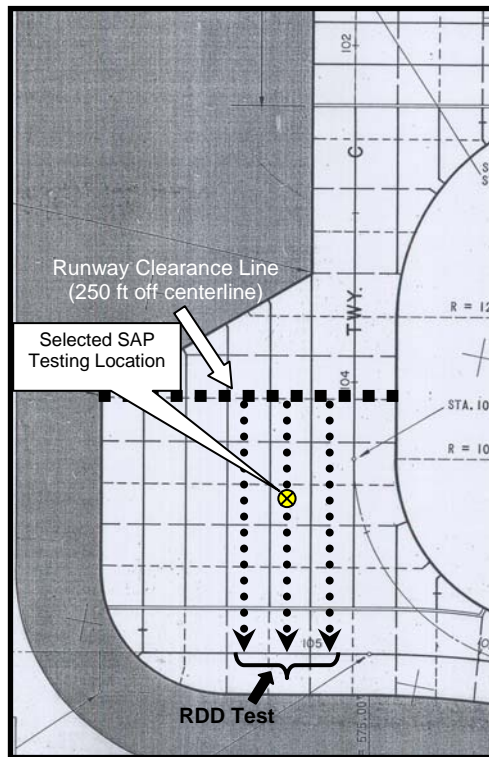


Figure 5.14 – RDD Test Paths and SAP Testing Location at South Run-Up (34 End)

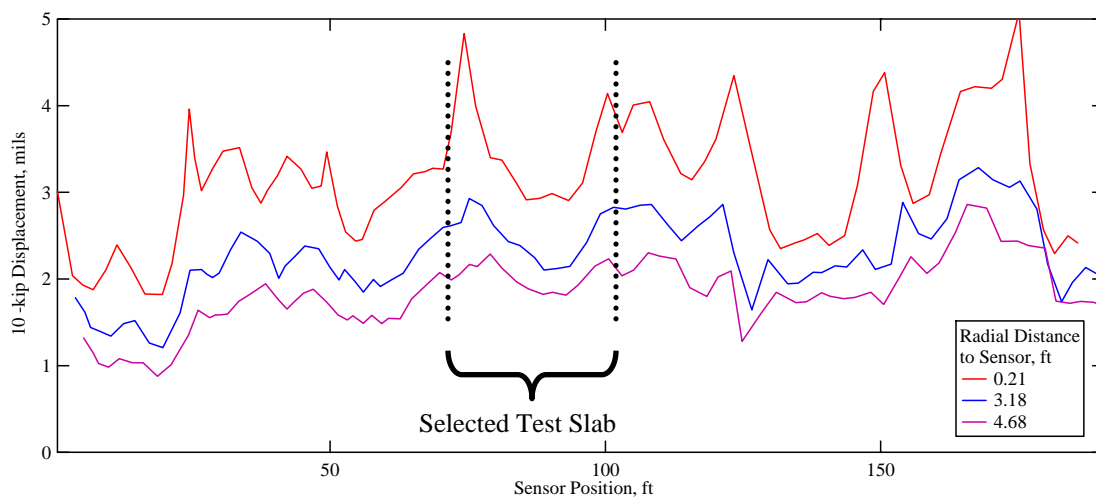


Figure 5.15 – RDD Deflection Response for South Run-Up Area Test Path

SAP Testing Location on North Run-Up

Following completion of the SAP testing at the South Run-Up, testing proceeded at the third and final location at the North Run-Up area. Like the South Run-Up, this testing location consisted of a 10-in. thick PCC pavement. The specific location of the test slab within the run-up area is shown in Figure 5.16. The test location was detached, outside the area of direct trafficking. The deflection data gathered on the mid-slab and joint tested were 2.1 and 2.8 mils, respectively. These values are marginally better than the target deflection data from Runway 16/34. Figure 5.17 shows RDD deflection measurements from the test path with the test slab highlighted.

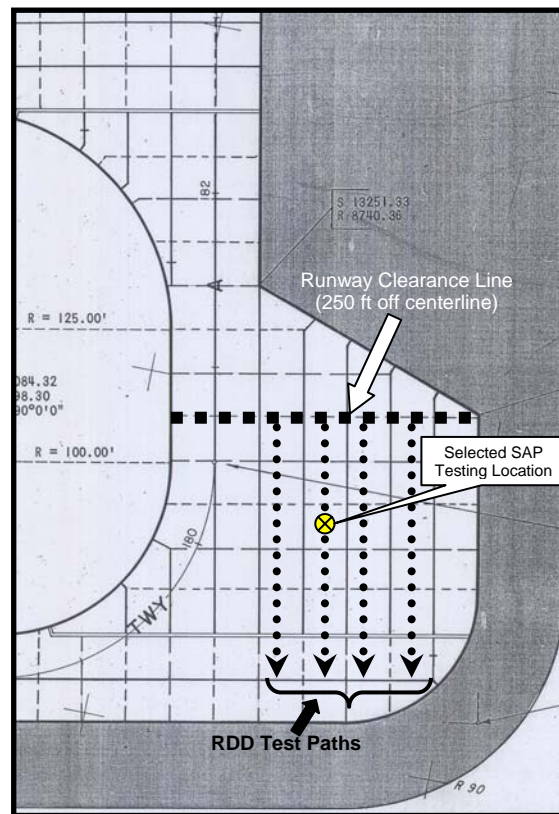


Figure 5.16 – RDD Test Paths and SAP Testing Location at North Run-Up (16 End)

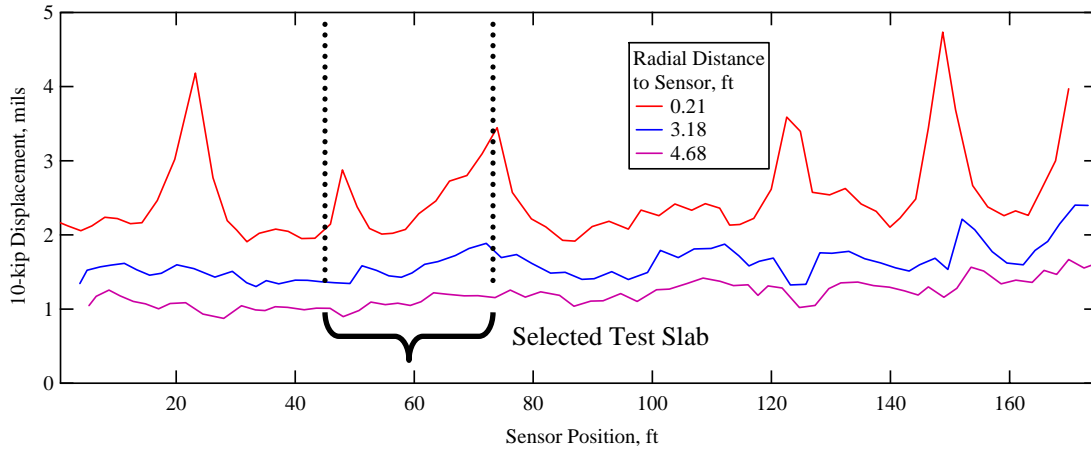


Figure 5.17 – RDD Deflection Response for North Run-Up Test Path

Table 5.1 – Comparison of RDD Deflection Measurements of Runway 16/34 and Selected Test Locations

Location	Typical Mid-Slab Deflection (mils)	Typical Joint Deflection (mils)
Runway 16/34	2.4 – 3.8	3.6 – 6.5
Taxiway A6 – Test Slab	4.0	7.1
South Run-Up – Test Slab	3.0	4.8
North Run-Up – Test Slab	2.1	2.8

5.5.2 Procedures for SDD SAP Testing Application

The SDD SAP test set up was similar at each of the three test points: center, edge, and corner. Orientation of loading and spacing of components remained constant for all three test points at each slab. Figure 5.17 illustrates the layout of the load point with respect to the accelerometer locations, with the spacings consistent at all three load points. The center loading scenario has been magnified in Figure 5.18

for clarity of dimensions. Generally speaking, three accelerometers were placed to detect pavement response. The first accelerometer was placed mid-way between the two circular load footprints, and 6 in. ahead (towards the joint) of the center point of loading footprint. For edge and corner loading, this equated to the center point of loading being placed 1 ft from the transverse joint. Therefore, the first accelerometer was placed midway between the load point and the joint, 6 in. from both. The second accelerometer was placed an additional foot from the first accelerometer (6 in. on the other side of joint for both edge and corner loadings), for a total of 1.5 ft from the center of the load footprint. The third accelerometer was placed an additional foot from the second accelerometer for a total of 2.5 ft from the center of the load footprint (1.5 ft on the other side of joint for both edge and corner loading).

As previously mentioned, all testing was conducted 1 ft from the slab transverse edge. In the case of corner testing, the center of load point was moved an additional 6.5 in. from the longitudinal joint (see Figure 5.18). The additional 6.5 in. represented half the distance between the two circular loading pad centers. This placement allowed the center of the left “wheel” to be one foot from both the transverse and longitudinal joint (see Figure 5.19). If the center point of the dual-wheel system had been used, then the left “wheel” would have been less than 2 in. from the joint, with the focus of the effect of loading on the longitudinal joint, not the transverse joint. This layout also enabled the supplemental testing to be conducted at the final corner loading at the North Run-Up, with two additional accelerometers placed 6 in. on both sides of the longitudinal joint.

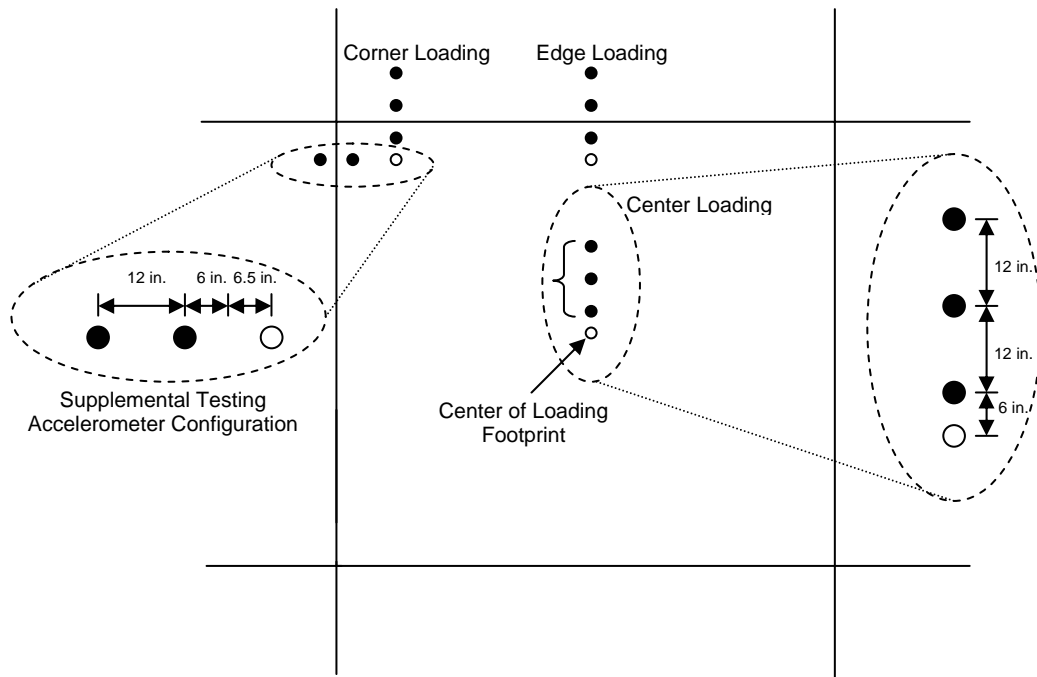


Figure 5.18 – Loading and Accelerometer Configurations

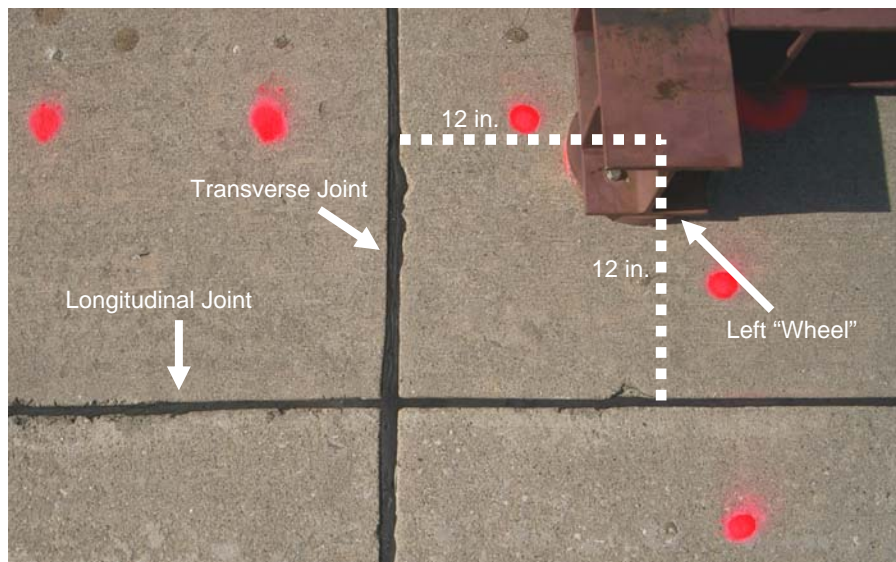


Figure 5.19 – Corner Loading Dimensions with Respect to Joint

Deviation from the above dimensions took place during the first edge test (only occurrence). The load point was placed an additional six inches from the edge and the first accelerometer. The overall layout regarding accelerometers and joint location remained the same. Only the load point moved this additional six inches. The reason for additional spacing was to insure any errant movement of the load frame, during dynamic load testing, would not interfere or potentially damage the nearest accelerometer. Once the test application was proved stable and unmoving, testing commenced with the aforementioned distances between the load frame and accelerometers. In the presentation of analysis of SDD field measurements in Section 9.2.1, this irregularity is addressed and an adjustment factor is determined to make the response analogous to the other test points.

Each accelerometer was connected to an accelerometer conditioner, which conditioned the measured signal into a calibrated output voltage. Figures 5.20 and Figure 5.21 are photographs which depict the overall test set-up for both typical center loading and the final corner loading (supplemental test with additional accelerometers). The accelerometer conditioners were then connected to an amplifier to boost the signal, prior to inputting their output into a computer interface and recording the voltage output versus time (a time-history of the output).

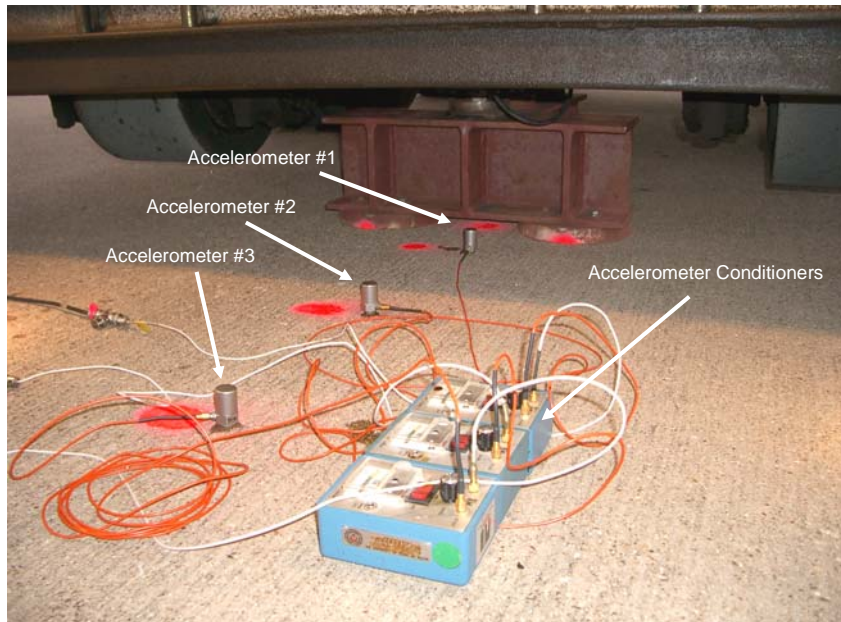


Figure 5.20 – Typical Center-Loading Setup

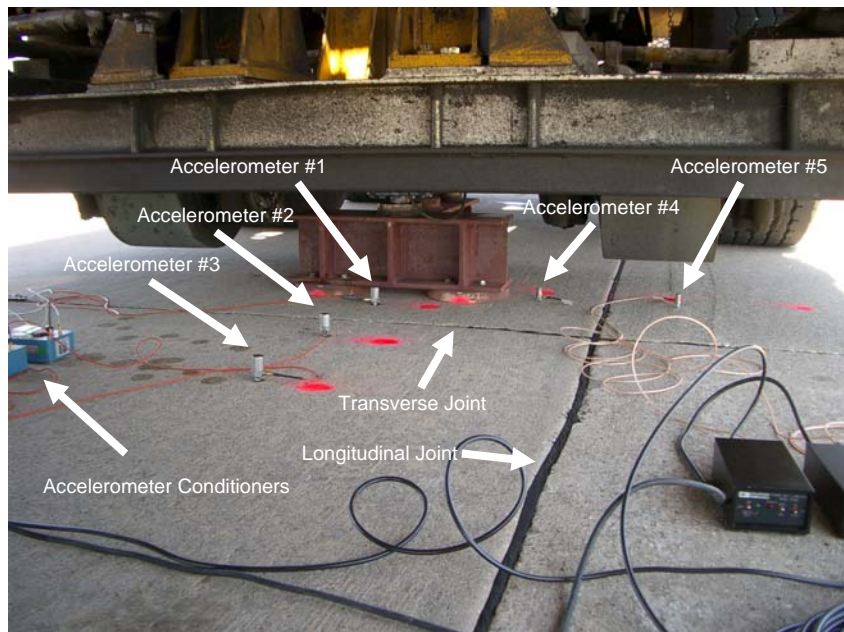


Figure 5.21 – Corner Loading at North Run-Up – Supplemental Test Setup

The frequency of loading was set at 20 Hz throughout all nine tests. Details of the loads levels (hence determination of the traffic model used in this testing) are provided in Chapter 6. The load cell measurements were recorded at a sampling rate of 200 readings per second. Due to time and test constraints, the same test slab was used for each set of three test scenarios: center, edge, and corner. Distances in excess of 10 ft between adjacent test points, limited any effects from one test to the next. As a standard for field testing procedures, if any discernable cracking was observed, a separate slab would have been selected if additional points were planned. However, no cracking was evident, as is discussed Chapter 9 and Chapter 10.

5.5 SUMMARY

In this chapter, the procedures and measures devised to assess the condition of the pavement of Runway 16/34 at Meacham Airport are discussed. A complete RDD deflection profile was conducted on the main runway, establishing a deflection response which was then compared to potential test locations on other pavement sections, outside the runway. These taxiway and run-up pavement sections were selected as to not disrupt airfield operations in the event of damage during testing. A comparable response enabled final selection of three candidate test locations. The SDD SAP testing application and procedures are presented along with an in-depth examination of the load frame development.

Chapter 6 – Development of Traffic Model

6.1 INTRODUCTION

The reason for developing a traffic model was to determine a loading scenario which would replicate the expected traffic at Meacham Airport. The traffic history containing all airport operations over the past 6.5 years was assembled. Several assumptions were made to take the known data and predict the future traffic. In this chapter, the development of the traffic model is presented, from data collection through final model determination. The final traffic model is composed of a three-tiered loading scenario, in which application of a given number of cycles of loads at three different load levels is used to represent 5-year periods. This series of applications is then repeated over a 20-year equivalent period of loading, as discussed below.

6.2 ORIGINAL DATA

The Aviation Division of TxDOT received a substantial set of data about traffic operations at Meacham Airport from the FAA. These data consisted of a listing of every operation, both take-offs and landings, which had occurred at Meacham International Airport from the period of January 1998 through May 2004. The end date was determined by the nearest complete month at the time of data retrieval. Data contained in-depth information of every operation occurring at the airport, down to the tail number of the specific aircraft. The alphanumeric four-digit International Civil Aviation Organization (ICAO) aircraft type designator enabled determination of the specific make, model, and type of aircraft for each operation.

The purpose of retrieving these data was to obtain an accurate history of the actual loads applied to the airport pavement, from which a future traffic model and loading scenario for SAP testing could be determined.

6.3 DATA REDUCTION AND SIMPLIFICATION

To reduce the large volume of data acquired from the FAA, significant simplifications were required to enable consumption, utilization, and processing of the massive record. Over 150,000 single line entries had to be reduced into a manageable and usable database. The Aviation Division of TxDOT led the task in reducing the extensive data into a useable set of information. First, the information was sorted by type designator (aircraft type) and by total operations per year of that aircraft type. Next, estimated weights and tire pressures were added for the known designators. Furthermore any exceptionally lightweight aircraft, with total weight under 10,000 pounds, were removed from the analysis. It was assumed that these lightweight aircraft would subject the pavement to negligible stresses, stress-levels which would not affect the pavement even if the total allowable passes were unlimited. In addition, the majority of lightweight aircraft utilized the adjacent parallel Runway 17/35. This greatly reduced the 150,000-plus line items into 143 different aircraft designators with a total number of operations of 55,885, during the nearly 6.5-year time period. It should be noted that there appears to be a large discrepancy between total number of operations during the 6.5-year time period as compared with the reported 521 average operations per day from Section 4.3. The listing received by the FAA as described in Section 6.2, refers only to aircraft who have submitted a FAA flight plan, either visual flight rules (VFR) or instrument flight rules (IFR). Meacham Airport supports a robust flight training operation, utilizing numerous single-engine aircraft which do not require FAA flight plans for all flights.

Once obtained from TxDOT, the data were further condensed and refined, grouping similar designators into a single line item. Often the aircraft type designator only differentiates a minor difference in a specific make and model aircraft. These similar designators were grouped into a single line item. This step further reduced the data to 121 line items.

Since the airfield under analysis is a rigid pavement, it was assumed that total load was a more important parameter for the aircraft line items, rather than tire

pressure. Although tire pressure is critical in determining the loading footprint, for simplification, gross load was examined since variance in the loaded area (tire footprint) was a limitation associated with using the footprint of the load frame. The database simplification was further carried out by the writer through determination of outstanding undetermined aircraft type designators and the estimation of maximum takeoff weight (MTOW) and maximum landing weight (MLW). This information was assembled from numerous sources, including aircraft manufacturer websites and certified internet databases like Sweden's Lulea University of Technology-sponsored *Airliners.net* and reference sections of other private websites like *Airodyssey.net*. Information was cross-referenced with as many sources as possible. The goal was the determination of specific aircraft MTOWs and MLWs. A copy of the final data sheet, with 121 line items, is included in Appendix C for completeness and examination.

6.4 REAR LOADING DETERMINATION AND CONFIGURATION

As mentioned above, total induced load was assumed to be the most important factor in characterizing the traffic loading scenario on this rigid pavement. If one assumes that the total aircraft operations had the same number of takeoffs as landings, by both transient and host aircrafts, an average loading value for each aircraft type is readily determined. A loading value was obtained for each aircraft type by summing and averaging the values obtained for MTOWs and MLWs. This load value represented the induced maximum loading by a given aircraft on a given operation.

In analyzing typical aircraft loading on pavements, it is imperative to examine a single, rear-gear load configuration. To determine the load on the rear gear of a given aircraft, typical load distributions had to be assumed. Load distributions vary from one aircraft type to another. Typically, the nose gear supports 5% to 8% of the total weight, and the two rear gear assemblies support the remaining 92% to 95% of the total weight (FAA, 2004). With over 120 different aircrafts to consider, assumptions were made to simplify the rear loading. The most typical value and conservative assumption was to use 95% of the total aircraft weight, being carried on

the rear gear assemblies. From this assumption, it can be rationalized that 47.5% of the aircraft weight is carried by each of the two rear landing gear assemblies. A rear landing gear assembly is defined as all components which comprise a single side, i.e. the portion of the landing gear which is situated under a given wing or side of fuselage. The majority of all aircraft have two sets of rear landing gear assemblies (one on each side of the aircraft), with the exceptions of highly specified aircraft used by military and industry,

In using this percentage of 47.5%, it was also assumed that each single gear assembly affects the pavement slab individually; that is to say that the loads induced in neighboring slabs or in those slabs even further away in the case of large frame aircraft can be considered negligible. A complete listing of all loads used and the associated aircraft can be found on the complete data sheets in Appendix C.

6.5 LOAD GROUPING DETERMINATION

To develop the methodology used in SAP testing, a rough concept and format were devised. To model the loadings, a structured loading scenario of adjusted loads was applied over designated time intervals. Each time interval was selected to contain enough load cycles to produce a sufficient loading time, during the SAP testing. With a frequency of 20 Hz, it was imperative that the time of loading at each load level was greater than some minimal time period so that the SDD applications were able to be controlled. Before the final determination of the load groups, the load applications for each load group, and the yearly intervals used in testing, a rough visual representation was devised. This rough visualization is illustrated in Figure 6.1.

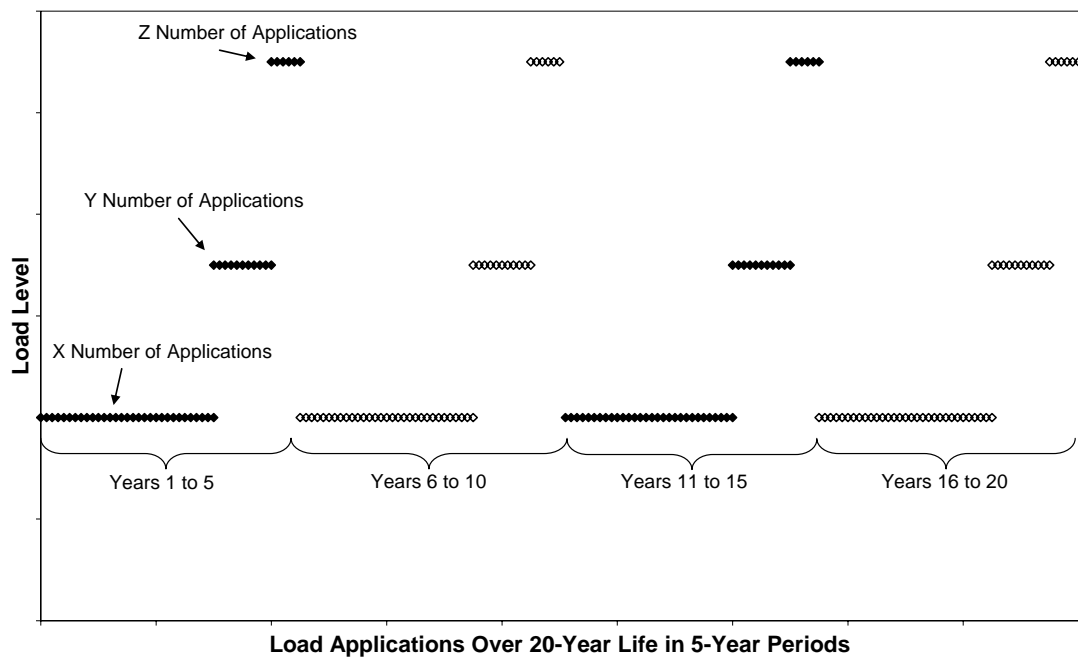


Figure 6.1 – Three-Tiered Loading Representation Over 20-Year Pavement Life

In Section 6.3, it is explained that the loading determined for each aircraft type was taken one step further in determining the load groupings for the SDD testing. Data for the rear gear load weight versus operations per year was plotted. One such plot is shown in Figure 6.2. This figure clearly illustrates the most prominent loads on Runway 16/34. The majority of the loads fell well under 50,000 pounds for a set of rear landing gears. In addition, those same loadings experience the most occurrences per year.

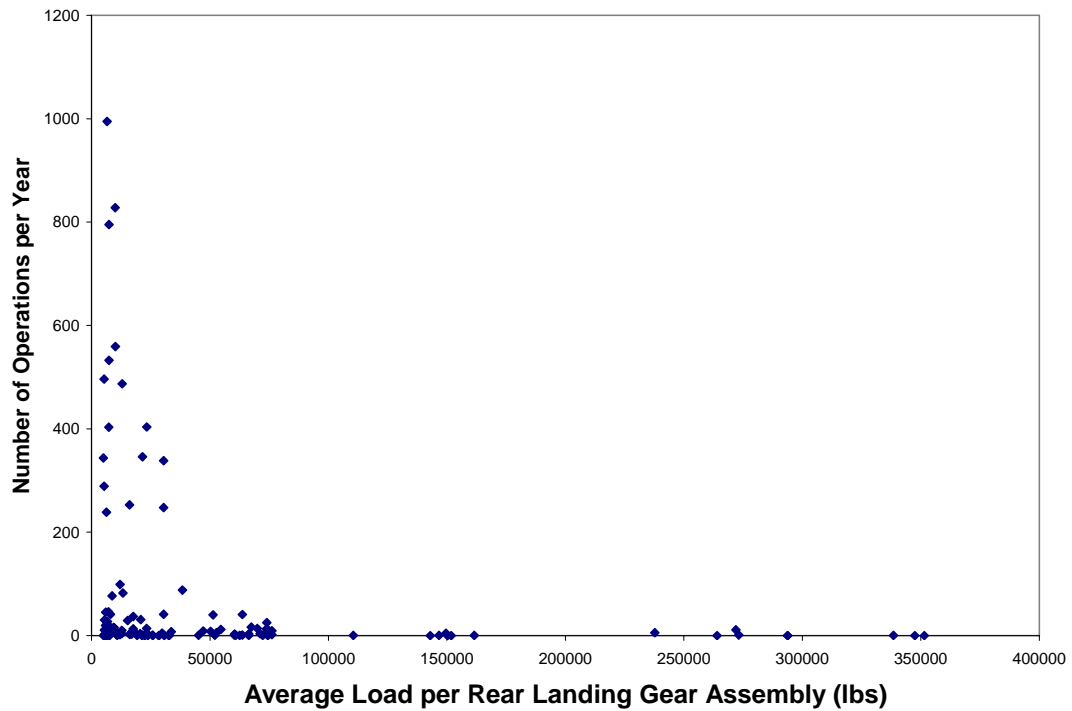


Figure 6.2 – Typical Loadings Per Year at Meacham Airport

A better visual representation of the data in Figure 6.2 can be portrayed in a histogram format. Such a histogram is presented in Figure 6.3. In this figure, the first step involves grouping similar loadings, specifically grouping the data that contain essentially the same load per rear gear. In other words, the data present in Figure 6.3 are used to simplify the data shown in Figure 6.2 by grouping data points and representing all operations which occurred at a specific load level.

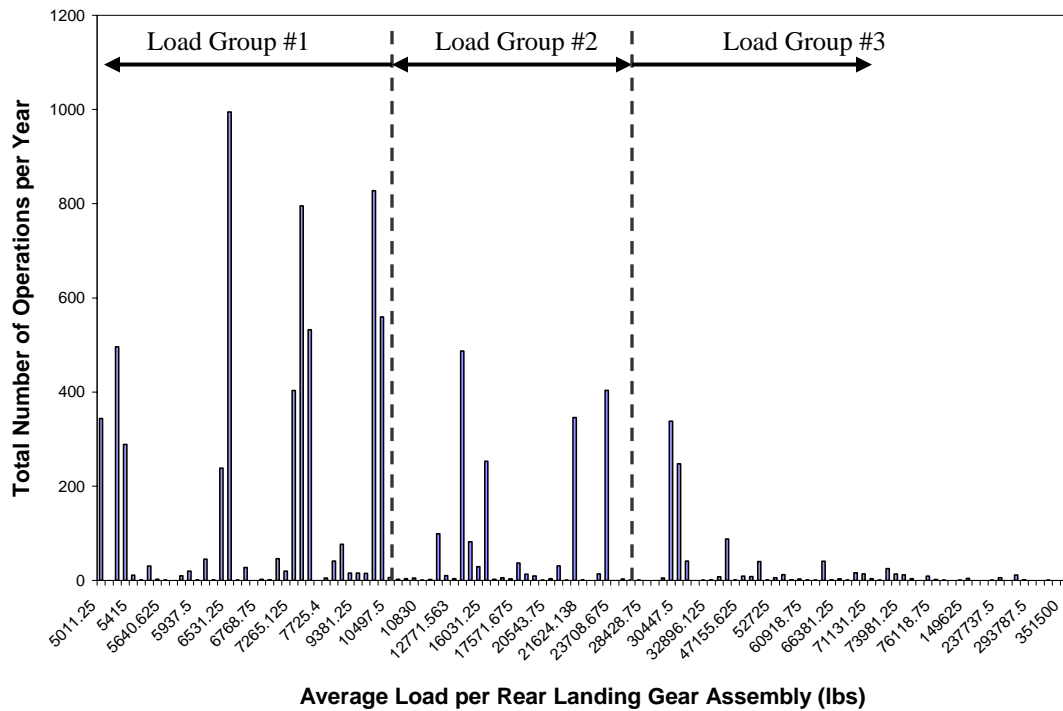


Figure 6.3 – Histogram of Yearly Occurrence of Rear Landing Gear Assembly Load

Once the data were better visualized with the assistance of Figures 6.2 and 6.3, a better understanding of the scope of loading and occurrences was achieved. Three load groups were selected arbitrarily, focusing the first group on the lower loads, the second group on mid-level loads, and the third group on the high-end loads, in the range of the maximum capability of the SDD. These load groups translated into the following three groupings:

- (1) Rear Gear Landing Assembly Load < 10 kips,
- (2) 10 kips < Rear Gear Landing Assembly Load < 25 kips, and
- (3) 25 kips < Rear Gear Landing Assembly Load < 50 kips.

Normalization of loads to operations was accomplished for each grouping, by multiplying the respective loads by operations per year and then dividing by the total number of operations. The normalized loadings are 7,114, 15,869, and 31,626 pounds respectively, for the three successive groupings. The normalized frequency of operation of each grouping is 5,309, 2,417, and 740 operations/year, respectively. The normalized loadings and frequencies were then used to define the final parameters used during SAP testing.

In addition to the three load groupings, there were additional low-frequency loadings with aircraft having extremely high loads, as seen on the far right side of Figures 6.2 and 6.3. These loadings fell outside the capability of the SDD loading system, capable of producing up to 70 kips. Similar to the three groupings discussed above, these excessive loads were divided into three groups as:

- (1) 50 kips < Rear Gear Landing Assembly Load < 100 kips,
- (2) 100 kips < Rear Gear Landing Assembly Load < 200 kips, and
- (3) 200 kips < Rear Gear Landing Assembly Load < 350 kips.

These loads groups were once again normalized into an equivalent single load with a specific frequency. In the ascending order presented above, the normalized loadings are 64,065, 147,372, and 265,203 pounds, respectively. The normalized frequency of operation for each load grouping are 217, 6, and 19 operations/year, respectively. Even though the occurrence intervals for these load groupings were extremely low, it was imperative to include these extremely heavy loads within the SAP testing. Figure 6.4 displays the three previously mentioned testable load groupings and three heavy load groupings, with occurrences over five years.

Fatigue cracking is a cumulative process, with load applications of lower frequency and higher weight often producing the most damage. Since these loadings fell outside the capability of the SDD, a method of conversion had to be adopted to account for these loads. This method is discussed in Section 6.6.

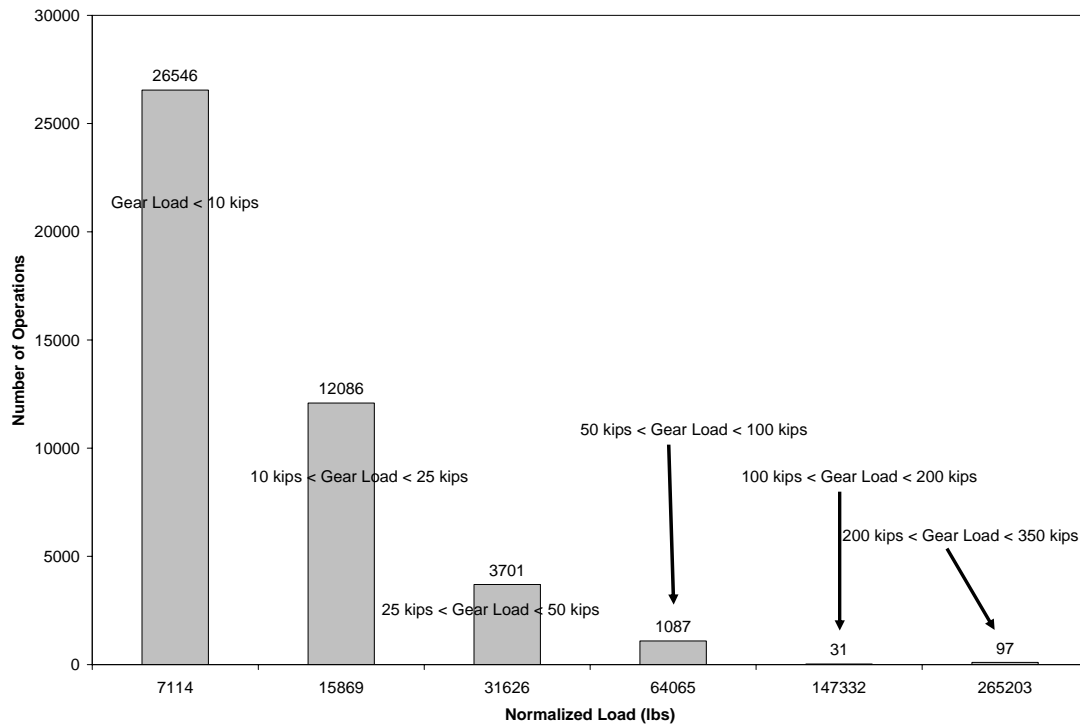


Figure 6.4 – Histogram of Average Aircraft Traffic Loads for Meacham Airport Over a Given 5-Year Period

The histogram of aircraft traffic loads in Figure 6.4 displays associated average operations for a given 5-year period for each loading. This 5-year estimate is based on actual traffic data from a typical period of traffic (1998 through mid-2004) during the existence of Runway 16/34. This period length was decided on by balancing two factors. First, the period had to be long enough to produce operation totals which would be conducive to SDD SAP testing, enabling load monitoring and adjustments to be made on-the-fly during the actual field testing. For example, a very small number of desired applications would limit the total test time for a given loading period. Due to the constraints and intricacies of the hydraulic loading system of the SDD, a desired load for cycling cannot be preset for testing. Instead, given a desired load, a voltage is entered to replicate this load magnitude, with adjustments being required as load cell measurements are monitored in real time. Second, the

period had to be short enough to reduce limitations of step loading over multiple years. In other words, all low level loads would be applied, after which the middle load levels would be applied followed by application of the highest load levels. This loading sequence differs from the random nature of airport pavement loading; therefore, the fewer the years in a loading period the more variance in the loading scenario. Traffic loading periods of three to seven years were considered. A five-year loading period was selected due to a significant number of operations per load grouping and the ease in modeling a future, 20-year period of pavement loading with four equal increments. Five-year periods also accounted for the limitations in time and scope of this research. Funding did not allow for an extensive and repetitive procedure. Five-year periods also minimized human induced error associated with continual adjustments. In general, 5-year periods were concluded to be a good balance of all previous mentioned factors.

6.6 MODELING HEAVY LOADS

As mentioned in the previous section, the three heavy load groups presented in Figure 6.4, Load Group #4, #5, and #6, needed to be converted into smaller loads to enable incorporation in the load application scenario. These loads were transformed into lighter loads through the use of Miner's Hypothesis and the fatigue cracking equation for concrete. Miner's Hypothesis states that stress induced distress on a pavement is cumulative and irrespective of loading order (Miner, 1945, and Huang, 2004). In addition, it enables heavy load application reduction; a higher application of a lighter load can be equivalent to a smaller number of applications of a heavier load. This equivalency is given by:

$$\frac{n_1}{N_{f1}} = \frac{n_2}{N_{f2}} \quad (6.1)$$

Equations 6.1 represents Miner's Hypothesis where: $N_{f1,2}$ is the total number of allowable applications for a specific load and $n_{1,2}$ represents the predicted (or actual) number of applications for that specific loading.

Equation 6.1 was used to transform the heavier load groupings, which were greater in magnitude than the loading capability of the equipment into the lighter-load groupings. The fatigue equation enabled determination of total load applications to failure, N_f . For a given load scenario, assumed damage is based on fatigue cracking. Darter and Barenberg (1977) recommended use of specific parameters as:

$$\log N_f = f_1 - f_2 \left(\frac{\sigma}{S_c} \right) \quad (6.2)$$

where f_1 and f_2 are empirically-based design constants:

$$f_1 = 17.61$$

$$f_2 = 17.61$$

Other fatigue cracking models have been developed including those recommended by the Portland Cement Association (PCA) (Packard and Tayabji, 1985). For the purpose of this research, only Equation 6.2 was utilized. The stress parameters involved with the PCA equation are:

$$\text{For } \sigma/S_c \geq 0.55: \quad \log N_f = 11.737 - 12.077 \left(\frac{\sigma}{S_c} \right) \quad (6.3a)$$

$$\text{For } 0.45 < \sigma/S_c < 0.55: \quad N_f = \left(\frac{4.2577}{\frac{\sigma}{S_c} - 0.4325} \right)^{3.268} \quad (6.3b)$$

$$\text{For } \sigma/S_c \leq 0.45: \quad N_f = \text{unlimited} \quad (6.3c)$$

The induced stress is assumed to be the direct load applied over the loading area and is represented by σ in Equation 6.2. S_c represents flexural strength of the concrete in the same units as σ . Equation 6.3a, 6.3b, and 6.3c were too broad for this scenario, returning a strength ratio (σ/S_c) higher than 0.45. Therefore there was an infinite number of allowable applications to failure for our given loading conditions.

With the knowledge of total number of applications to failure, N_f and the actual occurrences for a heavier load, these heavier loads were equated to equivalent loadings of Load Group #3. Once computed for each of the heavier loads, an additional 6,699 applications were added to Load Group #3 total applications for a five-year period. The final load scenario used in testing is given below:

- (1) Load Group #1 – 26,600 applications at 7.1 kips,
- (2) Load Group #2 – 12,100 applications at 15.9 kips, and
- (3) Load Group #3 – 10,400 applications at 31.6 kips.

Appendix D includes the detailed steps of the conversion for each of the heavier load groups. The resulting traffic model was used in the testing conducted on the nine test points on the three selected test pads, described in Section 8.2.

6.7 EQUIPMENT LIMITATIONS

In Sections 3.4 through 3.6, the SDD and its capabilities were discussed in depth. In testing airport pavements with the SDD, an important challenge is the replication of heavy aircraft loads. As seen in the previous sections of this chapter, the limitation of the SDD ability in applying loads is driven by its total weight and its stability. Higher dynamic loads require higher static forces to insure complete contact and stability. Due to the nature of the loading system and the SDD, dynamic loads are limited to a peak value of 35 to 40 kips. This limitation (along with some conservatism of the SDD operators) resulted in the application of a peak-to-peak load of 31.6 kips in Load Group #3.

In addition, all testing was conducted on the same load frame configuration and load footprint. This was driven by the scope and time allowed for this test. Use

of additional load frames would induce an additional variance in a testing application already embedded with a high level of variance due to the nature of in-service pavement testing. With the use of the load pads and the load frame configuration remaining constant, variance in tire pressure was ignored. This was considered reasonable given the rigid pavement. A sample sensitivity analysis was conducted in EverFE (as described in Section 5.4 and Appendix B) and in the aircraft-specific finite element program developed by the FAA: FEAFAA (Finite Element Analysis – FAA). This analysis ensured that stresses induced by the load frame were comparable to those induced by a specific aircraft footprint. The results of this portion are included in Appendix E.

6.8 ASSUMPTIONS MADE IN DEVELOPING THE TRAFFIC MODEL

Many assumptions were made during the development of the final traffic model. Miner’s hypothesis and the fatigue equation for concrete were used to correlate heavier loads to lighter loads in the test. In addition, a “worse case scenario” ideology was adopted in applying the traffic model. Thus, every load would be experienced at every test point, thereby ignoring any typical wander. Wander is typically accounted for in pass-to-coverage ratios. Pass-to-coverage ratios equate an aircraft-dependent coefficient which transfers actual aircraft passes on a runway to coverage on a specific slab (FAA, 1995). By ignoring this criterion, the testing models an absolute worse case scenario; a much safer assumption when examining remaining life of an in-service pavement.

Another major assumption was acceptance that a load produced on a stationary load frame was equivalent to a load induced by a moving wheel. Several studies have been conducted to investigate the correlation of these two different load scenarios. Flexible pavement testing requires heavy scrutiny on comparison of these two loading scenarios, as it experiences rutting and shoving due to movement of loads. The intrinsic nature of rigid pavements allows this assumption to be accepted without scrutiny. Rigid pavements are able to more effectively distribute the loading

than flexible pavements, minimizing any forces associated with a moving wheel load, which may occur oblique to the principal vertical axis. This is a function of the friction (skid resistance). Duration of load is a more important factor under these conditions.

6.9 SUMMARY

Interpretation and analysis of actual traffic history at Meacham Airport established the foundation upon which a traffic model was developed which replicates the expected traffic of the next 20 years. The collection of data, the formation assumptions, and establishment of model parameters all play an important role in the development of the model. The finalized traffic model incorporated a three-tiered loading scenario applied repeatedly over equivalent 5-year increments, until the extent of the 20-year equivalent period was achieved. The chapters which follow build upon this traffic model, moving the idea forward from theoretical concepts to experimental field application.

Chapter 7 – Observations and Measurements During RDD Deflection Testing

7.1 INTRODUCTION

Field testing took place over two separate testing periods in July and August 2004. The first period consisted of RDD deflection profiling of Runway 16/34, which took place 5 through 8 July 2004 at Meacham Airport. Many significant field observations were made during the RDD testing of Runway 16/34. Testing conditions were also noted for potential effects in SDD testing. In the following chapter, both the testing conditions and observations are presented. In addition, the RDD measurements are briefly presented. Previous RDD deflection testing, performed in May 2001, is presented for comparison purposes and assessment of any changes in conditions. These same RDD deflection results enabled comparison with candidate SDD test locations as mentioned in Section 5.3.

7.2 RDD FIELD OBSERVATIONS AND DATA MEASUREMENTS

Conditions and setting have historically played a significant role in the deflection response of pavements during RDD testing. For instance, at a previous RDD deflection test, conducted at Majors Field in Greenville, Texas in July 1998, two previously undetected subsurface conditions were revealed. The first was the presence of sleeper slabs, a common feature in pre-World War II construction which accounted for the unusually low deflections observed at joints, at a spacing of every 120 ft. Records were unable to produce original construction standards, but the results of continuous deflection testing enabled detection and confirmation. In addition, distress discovered in Taxiway E could be attributed to free water produced from test pit sampling (Lee et al., 2003). The following section focuses on pertinent observations found during RDD testing at Meacham Airport and the resulting data measurements which were gathered.

7.2.1 Testing Conditions and Observations

Due to the limited funding and time allocated for this study, additional test pits, soil sampling, and other subsurface investigation measures were not included in the scope of testing. Any detection of subsurface anomalies or areas of distress could not be directly addressed with additional tests for confirmation. However, information was collected on prevailing testing conditions to enable suggestions, explanations, and justifications in discussing the trends and any differences between the 2001 and 2004 RDD data. For the testing accomplished herein, RDD profiling took place over three nighttime operations in July 2004. The average overnight air temperature was 75.7 °F. Table 7.1 presents the pertinent climatology data from the testing period; no precipitation occurred during testing with only minor amounts during the daytime non-testing hours. Nonetheless, the previous month was the second wettest June on record, with 10.49 in. of rainfall. With the known expansive qualities of the primary local geologic formation, Denton Clay, water content in the subgrade could certainly be a dominant factor in producing the deflection response observed in the pavement, as discussed in Section 7.2.2.

Table 7.1 – Fort Worth Climatology Data for 2004 (USDOT 2004)

Date	High Temperature (°F)	Low Temperature (°F)	Precipitation (in.)
5 July	91	77	0
6 July	93	73	0.01
7 July	91	77	0.01
8 July	94	77	0

Along with the external conditions noted above, the final night of RDD testing produced concerns regarding the RDD loading mechanisms. During the final task of determining the deflection response along longitudinal joints on the first 1,000 ft of the primary approach and takeoff end (north end) of Runway 16/34, a technical problem was discovered with the RDD. The dynamic loading system was not

properly responding to the input sinusoidal waveform from the modulator. This problem caused the loading system to respond in a disorderly and uncontrollable manner. At this point a decision was made to cease operations, until an assessment of the system condition could be made. The problem went beyond the capability of a field repair and all further operations were aborted. These operations included a series of deflection profiling on potential SDD test locations, to allow for final selection of SDD test slab location. Due to these field difficulties, any and all RDD profiles on potential SDD SAP testing locations were delayed until the second period of field testing, requiring testing and selection to be completed one day prior to the actual SDD SAP testing. This change ultimately proved to be a better strategy, since conditions and observed response could change at any test slab location, during the time between the two field testing periods. Acquiring the most accurate deflection profiles of candidate test locations for direct comparison with the Runway 16/34 deflection profiles was of utmost importance.

7.2.2 RDD Deflection Measurements

Raw deflection data for Runway 16/34 was collected in accordance with the RDD methodology presented in Section 3.2 and the procedure presented in Section 5.2. After data were collected along the centerline of all six runway lanes and along the longitudinal joints on the North 16 end of the runway, voltage output from the sensor was converted into deflection readings. The transformation process of converting rolling sensor voltage output into deflection readings is included in Appendix F.

Deflection readings varied across the different lanes with general mid-slab deflections following a distinct pattern across the longitudinal extent of the runway. Data from Lane 3 were taken as representative and were further examined to determine deflection response patterns observed in a high trafficked area. The complete data set for profiles along all six lanes are included in Appendix G. The two center lanes, Lane 3 and Lane 4 received the highest traffic loading of any of the

lanes. Lane 3 was selected for further analysis because this same lane was sampled in the 2001 study conducted at Meacham Airport, enabling direct comparison of data. Deflection measurements from the testing in this study are presented for Lane 3 in Figure 7.1. The measurements are presented over the entire longitudinal extent of the runway in terms of mils per 10-kip load. The pattern of deflections over the length of Runway 16/34 is readily seen in Figure 7.1. The peaks in the plot represent higher deflections which occur at joint locations. A trend of higher overall deflections are observed on the north end of the runway (4000 to 7500 ft) where the majority of take-off and landing operations occur. The higher deflections experienced along the south end (1200 to 2100 ft) coincide with previously noted area of softer subgrade, drainage issues, and below grade culvert crossings under the runway.

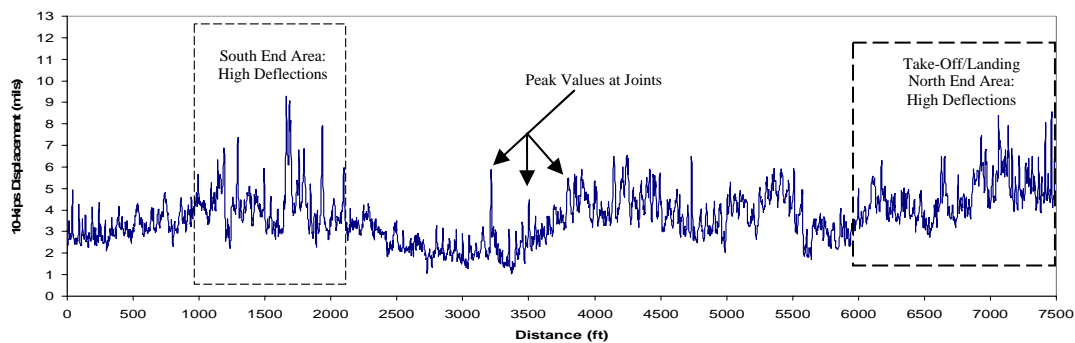


Figure 7.1 – Complete Deflection Profile in 2004 for Lane #3, Runway 16/34 (Sensor #1)

An expanded section of the continuous deflection profile in Figure 7.1 is presented in Figure 7.2. This expanded section is shown so that a closer examination of the deflection profile for Lane 3 can be done. The expanded continuous profile in Figure 7.2 shows that the peaks are wider, exhibiting a less pronounced deflection at joint locations. This general shape differs somewhat from the general trends observed in previous RDD deflection profiling of JRCP (Joint Reinforced Concrete Pavement) (Lee et al., 2003), as shown in Section 4.6 (Figures 4.9 and 4.10). The

exceptionally high volume of rain experienced during the month prior to testing, coupled with the expansive soils germane to the airport location could explain the lack of characteristic narrow peaking observed in the deflection measurements. Expansive soils with high water content can create large upward forces on the pavement, causing an apparent decrease in deflections at joints. In addition, the summer temperature which were observed during the daytime, kept the concrete temperature well above 80° F for the duration of testing. Joint movement is characteristically limited during this condition due to the temperature gradient, the expansion coefficient of concrete, and the subsequent upward curling effect.

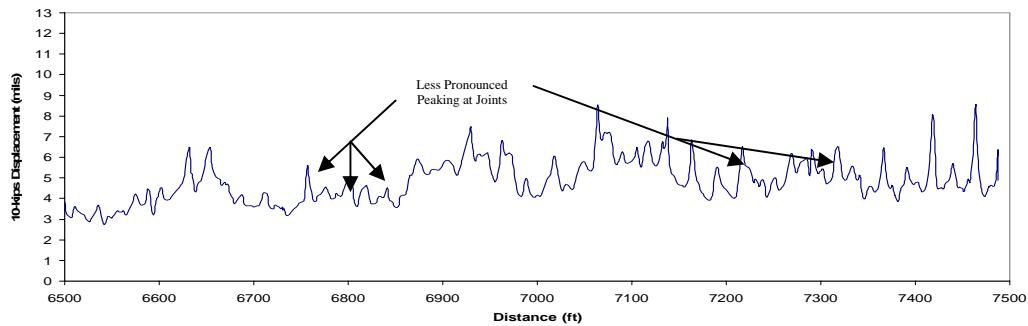


Figure 7.2 – Closer Examination of Deflection Profile in 2004 of Lane #3, Runway 16/34 Over the Distance of 6500 to 7500 Feet From the 34 End (Sensor #1)

7.2.3 Comparison of 2004 and 2001 RDD Measurements

In comparison with the measurements made in May of 2001, the RDD deflection data gathered in 2004 exhibited the same general trends. The deflection profile in 2004 is shown in Figure 7.1 and the same profile three years earlier in 2001 is shown in Figure 7.3. Figure 7.4 illustrates the similarity of the 2001 and 2004 data by superimposing the two sets of deflection data on the same plot. There are some areas of slight variation, but as can be seen in the figure, the overall trends and absolute deflections measured in 2001 are nearly the same as data measured in 2004.

The mean deflections are similar, with a slight increase occurring over the 3-year period in between testing. Aging of pavement system and changes in subgrade bearing capacity support the trend observed. On average the 10-kip displacement observed over the entire runway was 3.68 mils normalized to 10 kips. This is slightly higher than the average 10-kip deflection of 3.27 mils observed in 2001. However, climatic conditions and their impact on the pavement could explain most or all of this difference which is only approaches 12%.

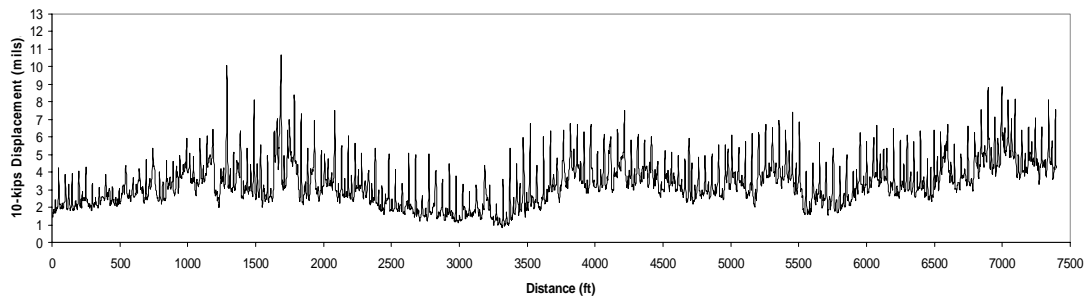


Figure 7.3 – Complete Deflection Profile in 2001 for Lane #3, Runway 16/34 (Sensor #1)

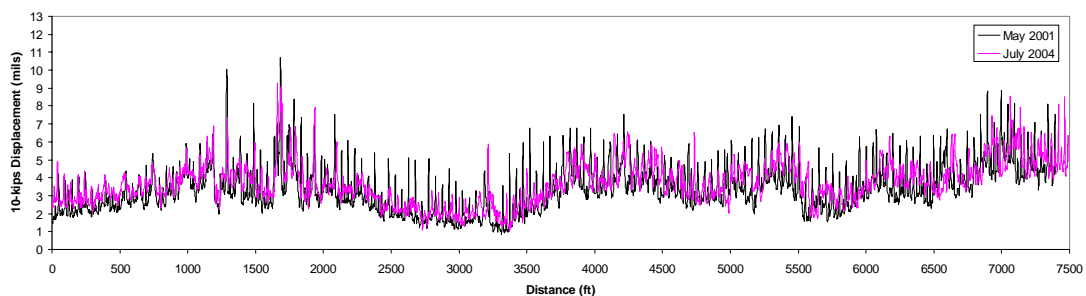


Figure 7.4 – Comparison of RDD Deflection Data Measured in 2001 and 2004 Lane #3, Runway 16/34 (Sensor #1)

Specific climate data for the month prior and the month during which 2001 RDD testing was performed are presented in Table 7.2. The month prior to RDD testing was the sixth driest on record for the month of April. This low level of precipitation resulting in a drier subgrade, combined with the cooler temperatures experienced relative to the recent 2004 testing could be responsible for the slightly larger deflections observed at the joints and the slightly smaller mid-slab deflections.

Table 7.2 – Fort Worth Climatology Data for 2001 (USDOC 2004)

Period	Average High Temperature (°F)	Average Low Temperature (°F)	Precipitation (in.)
April 2001	76.9	59.0	0.89
May 2001	83.9	64.5	5.58

A closer comparison of the joint deflections is illustrated in Figure 7.5, with deflection measurements displayed over a shorter total distance of Runway 16/34 (2000 to 3500 ft) to focus on the pavement response seen at the joints. With an increased resolution in the deflections, Figure 7.5 highlights the decrease in the peaking observed at joints and the overall higher mid-slab deflections in the 2004 deflection measurements compared to those measured in 2001.

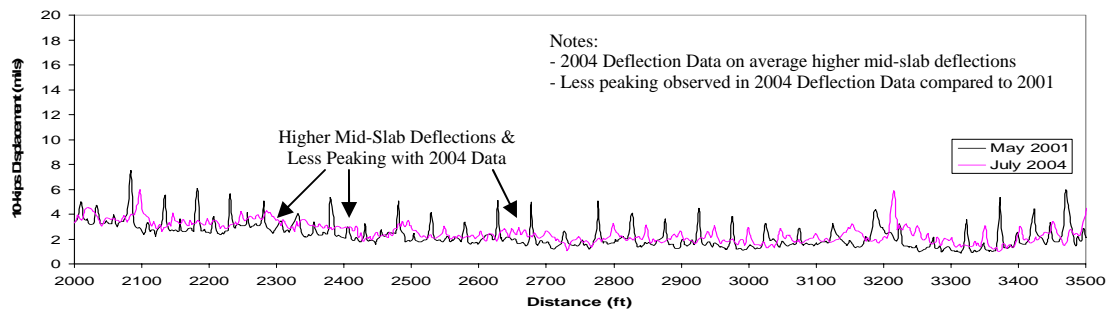


Figure 7.5 – Comparison of 2001 and 2004 RDD Deflection Data Over the Distance of 2000 to 3500 Feet From the 34 End – Lane #3, Runway 16/34 (Sensor #1)

7.3 SUMMARY

This chapter has examined the conditions which existed during the RDD deflection testing portion of this study. Specific conditions of higher temperatures and unusually high precipitation totals could have played an active and controlling role in the observed pavement response. RDD deflection testing measurements have been presented for both the current year and the prior 2001 testing to properly assess the current state of response of the pavement. This information on Runway 16/34 enabled the selection of specific test locations as explained in Section 5.3. A comparison was made between the 2004 deflection data and the deflections measured in the 2001 testing. Expected trends occurred within the 2004 data exhibiting higher overall deflection measurements than those of the 2001 data. The increase of overall deflections during this time period (averaging about 12%) is predominantly attributed to the environmental changes. Mid-slab deflections were considerable higher in 2004, with the increase saturation of the subgrade accounting for the overall increase in deflections. Joint movement was less pronounced in 2004, due to higher temperatures and slab expansion.

Chapter 8 – SDD SAP Testing at Meacham Airport – Field Measurements

8.1 INTRODUCTION

As mentioned in Chapter 7, field testing took place on two separate testing periods. The first period involved RDD testing as discussed in Chapters 5 and 7. The second test period consisted of SAP testing of selected test slabs. This testing took place on 22 through 26 August 2004 at Meacham Airport. As with the RDD deflection testing, many observations were made during the SAP testing, with conditions recorded for potential effects on testing. The following sections present both the testing observations and conditions along with an overview of the raw data produced during testing. An overview of the procedure for converting the raw data into a time-history of deflections is illustrated. Presentation of the final SDD SAP testing measurements is given in Section 8.4.

8.2 OBSERVATIONS AND SDD DATA

The SDD SAP testing procedure is a recent development, with its first field test conducted in November of 1998 (Stokoe et al., 2000). Since then, testing has been conducted under limited test conditions. SDD SAP procedures have been studied for possible inclusion within TxDOT's APT program for in-service flexible pavements (Stokoe et al., 2000). Limited work has been performed in the field of rigid pavements. As mentioned before, a test to failure was performed on a six controlled slabs at the University of Texas (Suh et al., 2004). The purpose of this research was to compare field results with laboratory fatigue tests. Results showed that the SDD proved to be an effective method for SAP testing on full-scale rigid pavements (see Section 3.7). The testing conducted in support of this study was the first such procedure accomplished on in-service rigid pavements. As mentioned in the Chapter 7, field conditions play a significant role in the deflection response of

pavements during RDD testing. Similarly, the same conditions can affect the deflection response of the test pavement during SDD SAP testing.

8.2.1 Testing Conditions and Observations

Once again, due to the limited nature of this study, investigations of subsurface anomalies or areas of distress could not be performed. Information was collected on prevailing conditions to assist in explaining and justifying testing trends and/or anomalies in the SDD measurements. SAP testing took part over a four-day period in August 2004. Testing began at approximately 0800 and concluded around 2130 (sundown). The average daytime high over that period was 94.0 °F. Table 8.1 presents the pertinent climatology data from this testing period. The only testing completed on 22 August was the RDD deflection profiles, enabling final determination of test slab locations for commencement of SAP testing on 23 August. No major precipitation occurred during the entire test period, with only minor amounts over the first two nights. Precipitation totals for the two previous months were 4.16 and 4.24 in. for July and August, respectively. These totals were not excessive but were both well above the monthly average of 2.12 and 2.03 in., respectively. However, as mentioned in Chapter 7, the second highest precipitation total ever for the month of June occurred in 2004, with 10.49 in. of rainfall on record. With the known expansive qualities and high plasticity index of the primary local geologic formation (Denton Clay), water content in the subgrade could certainly be a dominant factor in determining the higher deflection response of the pavement.

Table 8.1 – Climatology Data in 2004 for Fort Worth (from USDOC 2004)

Date	High Temperature (°F)	Low Temperature (°F)	Precipitation (in.)
22 August	90	71	0.03
23 August	91	74	0.04
24 August	94	78	0
25 August	95	78	0
26 August	96	80	0

The most significant observation from the SAP testing performed on the three test slabs was that no detectable cracking occurred. During testing, frequent visual observations were made, along with monitoring accelerometer output. Upon completion of testing at a specific slab, surface watering of the concrete slab was performed when necessary, as a technique for detection of any hairline stress cracks. None were detected.

8.2.2 Raw SDD SAP Testing Data

Raw SAP testing data were collected in accordance with the SDD methodology presented in Section 3.6 and the procedure presented in Section 5.5. Outputs from the three accelerometers and a single load cell (directly over the load point on the test frame) were collected. The three accelerometers were positioned in accordance with the layout presented in Figure 8.1.

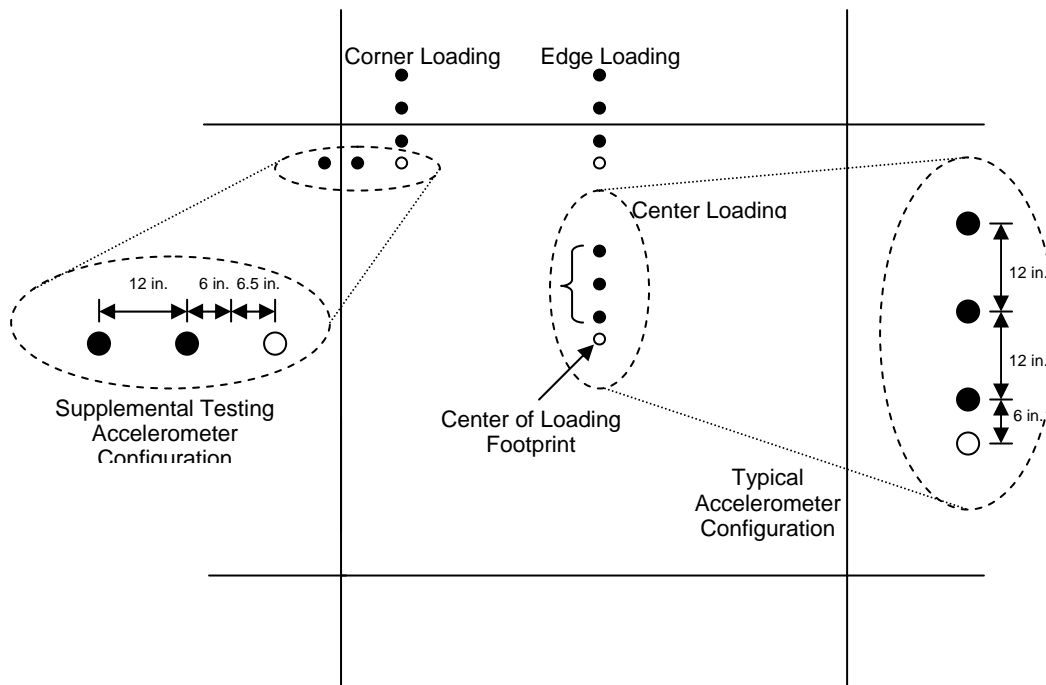


Figure 8.1 – Loading and Accelerometer Configurations

Continuous readings of each accelerometer and load cell were taken. The accelerometer output was in terms of voltage versus time, while the load cell output provided load readings in pounds. The accelerometers were connected to an accelerometer conditioner, which conditioned the measured signal into an equivalent readable output voltage. The instrument setup also included the use of a multi-channel analyzer and computer interface to convert the voltage-time output into a sample-history readout. The raw data provided load cell readings and accelerometer readings for each sample point. As mentioned before, a sampling rate of 200 samples per second allowed easy conversion into a time-history readout. Figure 8.2 is a sample raw data output from the load cell. Additional samples of the original raw data readout for both the load cell and an accelerometer are included in Appendix H.

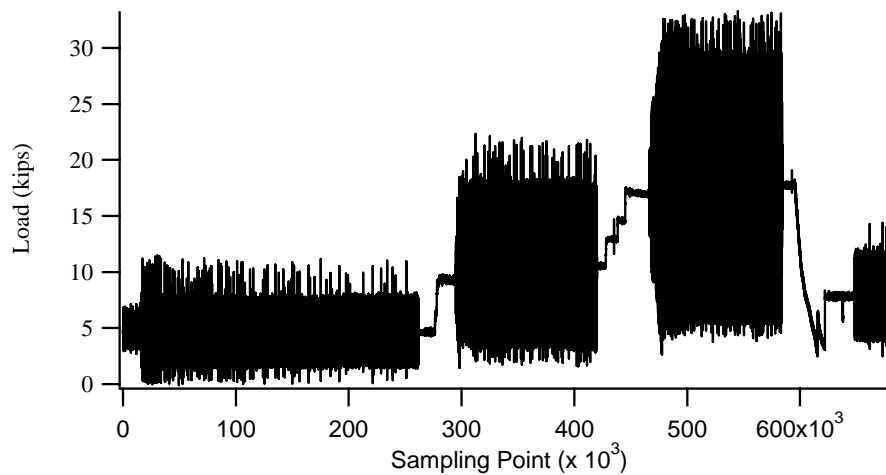


Figure 8.2 – Load Cell Output for First Five-Year Increment at Taxiway A6 Edge

8.3 DATA CONVERSION

From the original raw data, a series of procedures was carried out in order to take the raw output from the accelerometers and transform that output into deflection measurements versus time for analysis. The first step was to convert voltage readings

into acceleration readings in terms of the earth's gravitational field strength (g). The calibration for this output was 1 volt per g, for a simple one-to-one correlation. The readings could be converted and then presented in terms of mils per second squared, as:

$$a = \text{data reading (volts)} \cdot \frac{g}{\text{volts}} \cdot \frac{32.2 \frac{ft}{s^2}}{g} \cdot \frac{12 \text{ in.}}{1 \text{ ft}} \cdot \frac{1000 \text{ mil}}{1 \text{ in.}} \quad (8.1)$$

$$a = 386400 \cdot \text{data reading (volts)}$$

In using basic dynamic relationships, acceleration was established in terms of its relationship to angular frequency (ω) and distance (d) as:

$$a = \omega^2 d \quad (8.2)$$

where angular frequency (ω) is put in terms of frequency (f) is:

$$\omega = 2\pi f \quad (8.3)$$

Given a dynamic frequency of 20 Hz, a combination of Equations 8.1, 8.2, and 8.3 produced a conversion factor for translating raw data into deflection measurements as:

$$d = \frac{a}{\omega^2} = \frac{386400 \cdot \text{data reading}}{(2\pi f)^2} = \frac{386400 \cdot \text{data reading}}{(2\pi \cdot 20)^2} \quad (8.4)$$

$$d = 24.46906585 \cdot \text{data reading (volts)}$$

Once this conversion factor was determined, it was applied to all three accelerometer readings for each of the nine test points, as shown in Figure 8.1 (three center, three edge, and three corner). To enable further analysis, a LABVIEW program was created to allow more rapid and complete analysis of the raw data in

terms of deflection measurements. This program allowed average values of “peaks” and “valleys” to be determined for any sinusoidal load or deflection output, over any time segment. Overall average deflections were recorded for each of the three test load groups and then repeated for all five-year increments (Year 1-5, Year 6-10, Year 11-15, and Year 16-20). Within each of the respective load groups, averages were also taken over five separate random sample groups, typically 50 seconds (1,000 cycles) in length and spaced uniformly throughout the load period. This sampling technique downplayed any effects of errant deflection and load readings. The technique also facilitated documentation of any trends (increasing or decreasing) over the course of the loading period in each grouping. The entire period average was compared with the average of the five sample periods. Figure 8.3 illustrates the sampling procedure, building upon a tiered loading scenario (Figure 6.1), presented in Section 6.5.

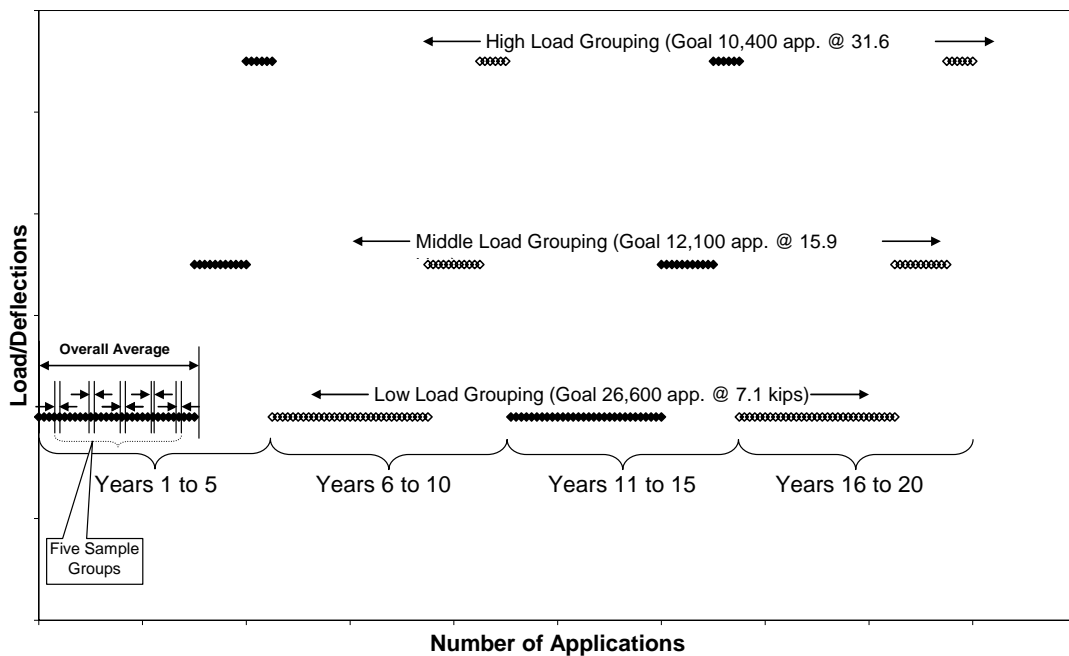


Figure 8.3 – Sampling Technique for Load and Deflection Readings Associated with the Different Load Groupings

These data were then used to determine average values for load and deflection measurements over the five sampling periods within each load grouping and over the entire load grouping, for comparison purposes. This step was then repeated for all three load groups within each five-year increment and then for each point tested. To enable a more detailed analysis, measured deflection readings were averaged for each sampling period and for the average over each entire loading period. Time readings were also converted into total applications to allow deflection measurement comparisons with number of applications, in addition to load levels. Both averaging the entire period and averaging the five sample periods produced comparable results, with no trends occurring across the course of a specific load grouping. Therefore, it was assumed the entire period average could be used in analysis (as exhibited in the data summary of each test point in Appendix I). Finally load transfer efficiency (LT_{US}) was determined as:

$$\text{Load Transfer Efficiency } (LT_{US}) = \frac{\text{Deflection at Accelerometer \#2}}{\text{Deflection at Accelerometer \#1}} \cdot 100 \quad (8.4)$$

The “US” in LT_{US} signifies upstream, which means using a ratio of the deflection on the far side of the joint (accelerometer #2) with respect to the deflection adjacent to the load point (accelerometer #1). Notice deflection readings determined within this study are affected by the heavy static load of 49 kips for the RDD/SDD device. This static load is in-place prior to the dynamic motion used in determining the load transfer efficiency. Due to the nature of the load point as oriented with respect to the vehicle and the joint at the edge and corner test points (see Figure 3.9 for point location relative to device footprint), the determined load transfer efficiency was not a true loaded-unloaded transfer scenario. Both sides of the joints experienced loading from the vehicle. However, since this vehicle positioning was consistent throughout all testing, these load transfer efficiencies can be compared to each other to observe any degradation or changes in response on a point-to-point relative level. In addition,

load transfer efficiency was also computed for center-point loading. Although this test section is not load transfer in the true sense, since no joints affected the deflection response, this location enabled a comparison to be made for slab response and degradation over distance from a given test point, from test location to test location.

The deflection measurements, testing time, and applications were loaded into a spreadsheet for further computation of averages and load transfer efficiency. Standard deviation and variance were computed for the five sample sets in each load group. Each test slab contained 3 test points, with the tests points labeled as Point #1 through Point #9 in order of completion. Table 8.2 gives the test locations and numbering sequence. Figure 5.6 in Section 5.3 shows a plan of the airport and the general test locations. Figure 8.4 gives the load point and accelerometer arrangement at each test location, illustrating the test point descriptions given in Table 8.2.

Table 8.2 – Sequence of SDD SAP Testing and Number Scheme

Location	Test Number	Test Point
Taxiway A6	#1	Edge
	#2	Corner
	#3	Center
South Run-Up	#4	Center
	#5	Corner
	#6	Edge
North Run-Up	#7	Center
	#8	Edge
	#9	Corner

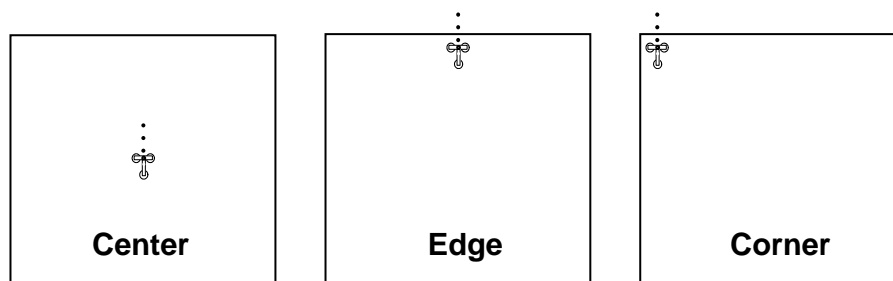


Figure 8.4 – Testing Point Orientation with Load Frame Location and Accelerometer Arrangement on Test Slab

Figure 8.5 is a sample of the data recorded and computed through the aid of the spreadsheet for years 1 to 5 for Point #2, the corner test point at Taxiway A6. Specifically, Figure 8.5 shows the sampling technique for load and deflection readings for Years 1-5, for testing at the corner loading on Taxiway A6. The first column of data presents the testing goals, with a comparison to the actual test time and number of applications. The next column illustrates the 5-period sampling technique and the times used for each period. Next, peak and valley loads are averaged over both the sampling periods and the entire test period for the respective load group. The highlighted rows bring attention to the average values generated for both the five sampling periods and the entire test periods. These values are highlighted for each loading scenario for each test point. A complete set of reduced data, illustrating all nine test points is included in Appendix I.

Point #2		A6 Corner	
0-5 Years		File "C1"	
Goal	Start (s)	Stop (s)	
26,600 app. (1330 s)	50	1400.0	
@ 7.1 kips	Test Time	1350.0	
	Total Apps./Period	27000	
	Total Apps./Overall	27000	
	Start (s)	Apps.	
	100	1000	
	300	5000	
	550	10000	
	800	15000	
	1050	20000	
	Avg Load	10.15	
	σ	0.45	
	Variance	0.20	
	Avg Reading for Entire Test Period	10.21	3.77
	Load	Peak	Valley
	9.99	3.94	
	9.89	4.02	
	9.94	4.08	
	9.96	4.04	
	10.95	3.01	
	Avg	4.62	
	σ	1.09	
	Variance	1.18	
	1.96	-2.18	4.14
Goal	Start (s)	Stop (s)	
12,100 app. (605 s)	1545	2152.0	
@ 15.9 kips	Test Time	607.0	
	Total Apps./Period	12140	
	Total Apps./Overall	39140	
	Start (s)	Apps.	
	1600	28100	
	1700	30100	
	1800	32100	
	1900	34100	
	2000	36100	
	Avg Load	15.99	
	σ	0.07	
	Variance	0.01	
	Avg Reading for Entire Test Period	15.96	3.23
	Load	Peak	Valley
	15.88	3.17	
	16.05	3.22	
	16.01	3.27	
	15.97	2.82	
	16.05	3.23	
	Avg	10.90	
	σ	0.11	
	Variance	0.01	
	4.14	-6.70	10.84
Goal	Start (s)	Stop (s)	
10,400 app. (520 s)	2440	2961.0	
@ 31.6 kips	Test Time	521.0	
	Total Apps./Period	10420	
	Total Apps./Overall	49560	
	Start (s)	Apps.	
	2500	40340	
	2600	42340	
	2700	44340	
	2800	46340	
	2900	48340	
	Avg Load	29.89	
	σ	0.08	
	Variance	0.01	
	Avg Reading for Entire Test Period	29.85	4.79
	Load	Peak	Valley
	29.82	4.64	
	29.96	4.87	
	29.94	4.82	
	29.92	4.81	
	29.79	4.97	
	Avg	20.44	
	σ	0.39	
	Variance	0.16	
	7.34	-13.05	20.39

Accelerometer #2	Peak	Valley	Defl.(mils)	Norm. Defl. (mils/pl)	LT us (%)
	1.37	-1.26	2.63	0.26	59.50
	1.32	-1.21	2.53	0.26	61.41
	1.27	-1.18	2.45	0.25	61.71
	1.29	-1.17	2.46	0.25	60.59
	1.77	-1.90	3.67	0.34	56.12
	Avg	2.78	0.27	60.09	
	σ	0.60	0.04		
	Variance	0.36	0.00		
	1.31	-1.21	2.52	0.25	
Accelerometer #3	Peak	Valley	Defl.(mils)	Norm. Defl. (mils/pl)	
	1.03	-0.93	1.96	0.20	
	0.99	-0.90	1.89	0.19	
	0.96	-0.86	1.82	0.18	
	0.97	-0.86	1.83	0.18	
	1.34	-1.42	2.76	0.25	
	Avg	2.05	0.20		
	σ	0.40	0.03		
	Variance	0.16	0.00		
	1.08	-1.01	2.09	0.20	
Accelerometer #2	Peak	Valley	Defl.(mils)	Norm. Defl. (mils/pl)	LT us (%)
	2.94	-3.83	6.77	0.43	61.88
	3.02	-3.97	6.99	0.44	63.26
	2.98	-3.96	6.94	0.43	63.90
	2.93	-3.94	6.87	0.43	63.91
	3.01	-4.01	7.02	0.44	64.34
	Avg	6.92	0.43	63.46	
	σ	0.10	0.00		
	Variance	0.01	0.00		
	2.97	-3.89	6.86	0.43	
Accelerometer #3	Peak	Valley	Defl.(mils)	Norm. Defl. (mils/pl)	
	2.23	-2.95	5.18	0.33	
	2.26	-3.06	5.32	0.33	
	2.26	-3.07	5.33	0.33	
	2.24	-3.05	5.29	0.33	
	2.72	-3.12	5.84	0.36	
	Avg	5.39	0.34		
	σ	0.26	0.02		
	Variance	0.07	0.00		
	2.25	-3.01	5.26	0.33	
Accelerometer #2	Peak	Valley	Defl.(mils)	Norm. Defl. (mils/pl)	LT us (%)
	5.21	-8.09	13.30	0.45	66.27
	5.28	-8.11	13.39	0.45	66.52
	5.27	-8.19	13.46	0.45	66.34
	5.38	-8.43	13.81	0.46	65.95
	5.35	-8.39	13.74	0.46	66.12
	Avg	13.54	0.45	66.24	
	σ	0.22	0.01		
	Variance	0.05	0.00		
	5.27	-8.22	13.49	0.45	
Average LT		63.26			
Accelerometer #3	Peak	Valley	Defl.(mils)	Norm. Defl. (mils/pl)	
	3.95	-6.29	10.24	0.34	
	4.03	-6.32	10.35	0.35	
	4.02	-6.37	10.39	0.35	
	4.09	-6.55	10.64	0.36	
	4.07	-6.92	10.99	0.37	
	Avg	10.52	0.35		
	σ	0.30	0.01		
	Variance	0.09	0.00		
	4.01	-6.89	10.90	0.37	

Figure 8.5 – Sample SDD SAP Data for Years 1-5 for Point #2 – Corner at Taxiway A6

8.4 PRESENTATION OF MEASUREMENTS

Plots were produced for all test points to illustrate the relationship of measured deflections versus load applications. The term measured deflections refers simply to the dynamic deflections that were measured at each point and is used to differentiate between the normalized deflections, which are presented in detail in the analysis portion in Chapter 9. Figures 8.6 through 8.14 illustrate this relationship for each test point. All deflection measurements shown in Figures 8.6 through 8.14 were measured by accelerometer #1 reading for each location (accelerometer closest to the load point). Expected trends of increasing absolute deflection with increasing load were observed for all nine points. In addition, larger deflection trends were noted at corner test points in comparison to edge test points. Likewise, edge points exhibited larger deflection trends than center points. Less scatter in data was observed at center points in comparison to corner and edge points. Proximity to joint and inherent variability associated with the joints and the subgrade beneath substantiate these findings. Any adverse subgrade condition will be more pronounced at joint locations.

Note that all measurement and analysis plots presented within this report include a small depiction of load/accelerometer configuration for reader orientation. Each configuration is located in the upper right corner of each plot, above the key. These depictions are miniature scaled versions of the three different loading scenarios presented in Figure 8.4.

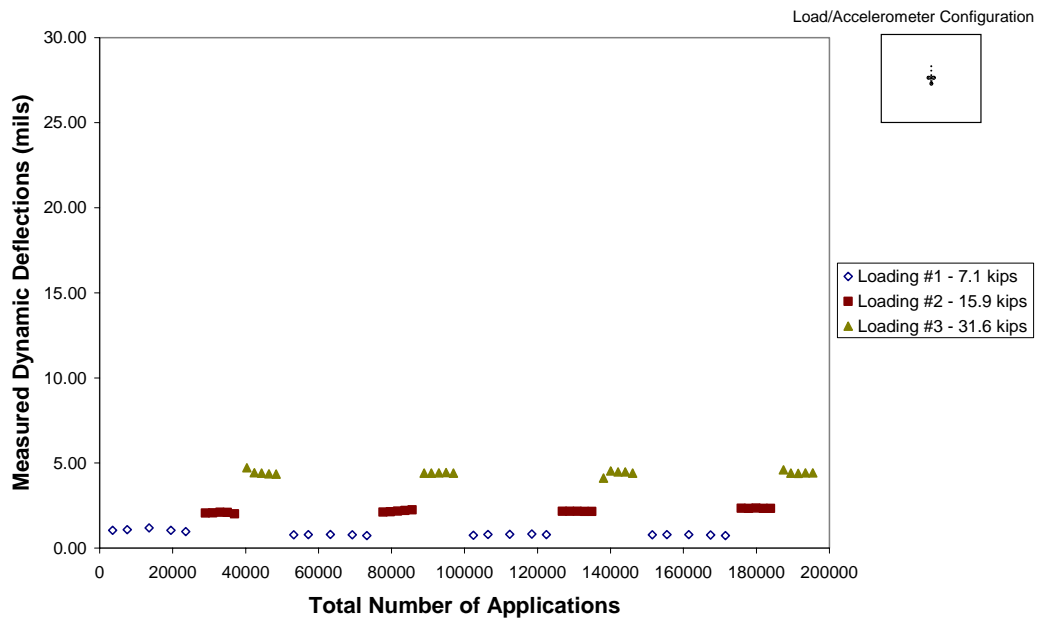


Figure 8.6 – Measured Deflections over Complete Testing Period – North Run-Up – Center Load Point

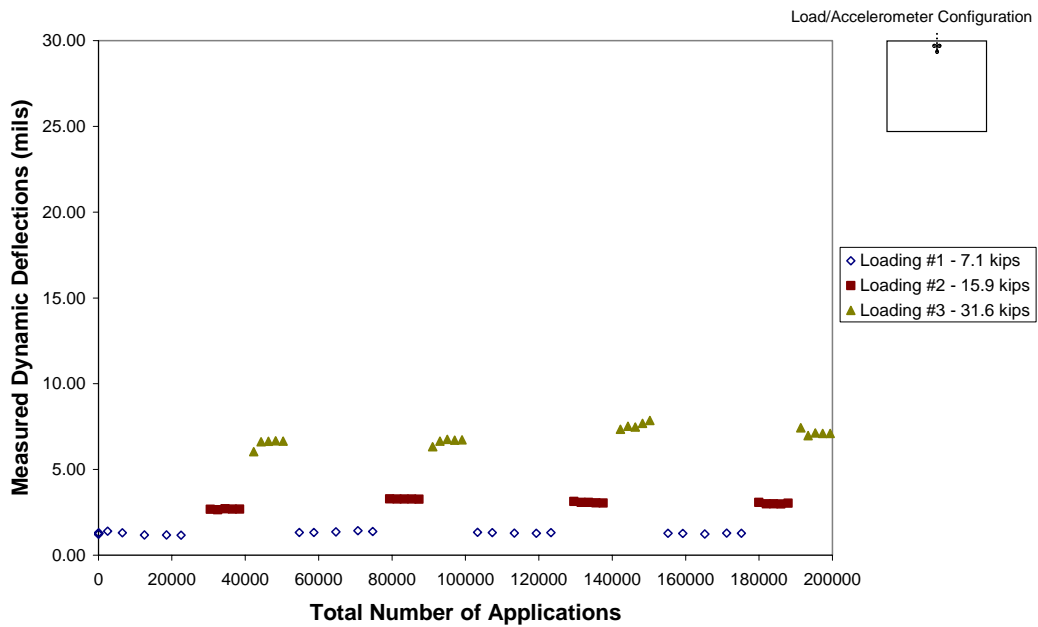


Figure 8.7 – Measured Deflections over Complete Testing Period – North Run-Up – Edge Load Point

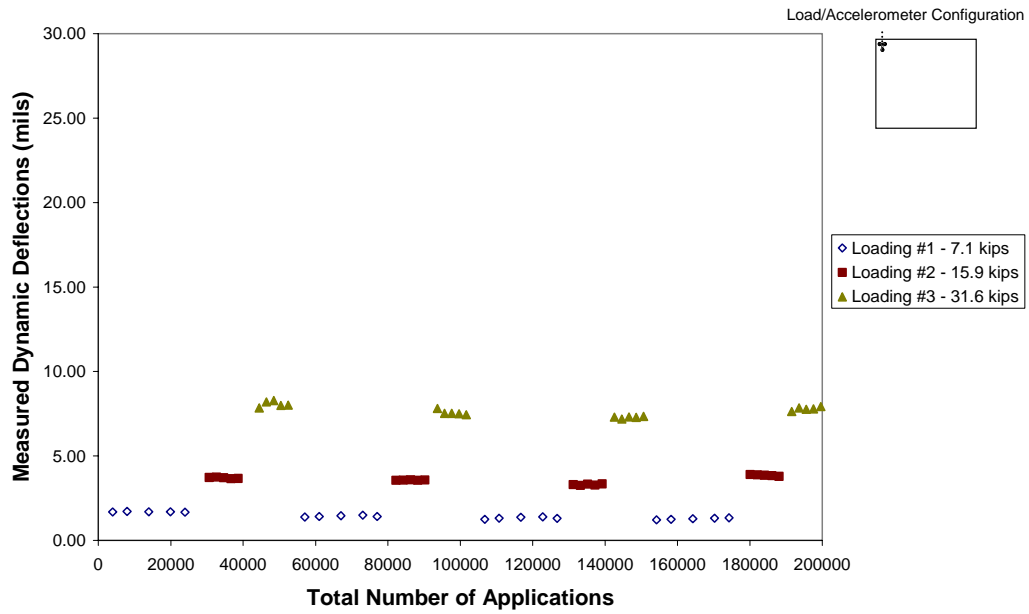


Figure 8.8 – Measured Deflections over Complete Testing Period – North Run-Up – Corner Load Point

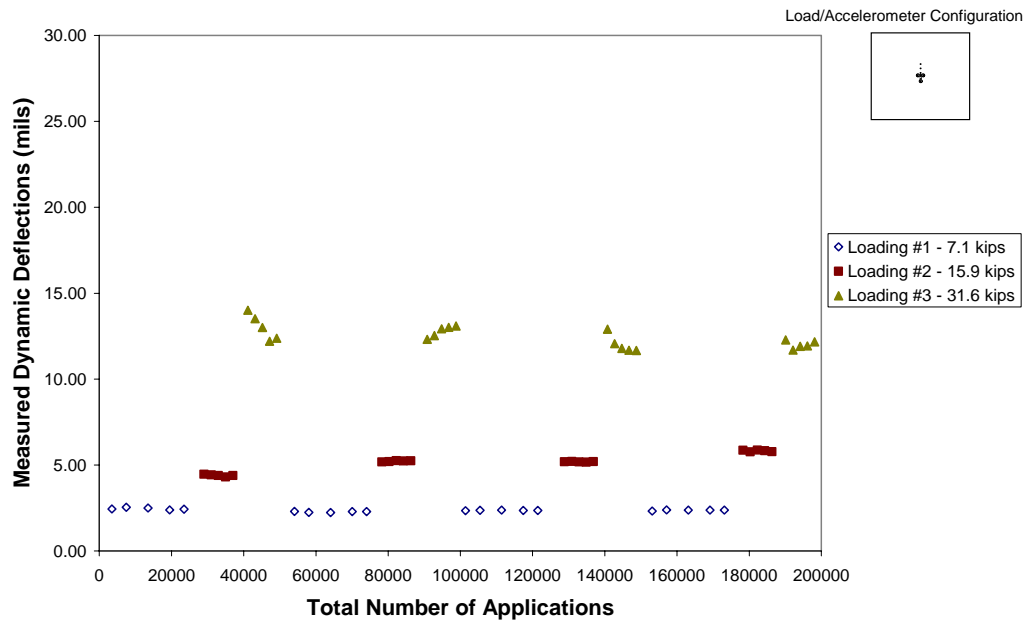


Figure 8.9 – Measured Deflections over Complete Testing Period – South Run-Up – Center Load Point

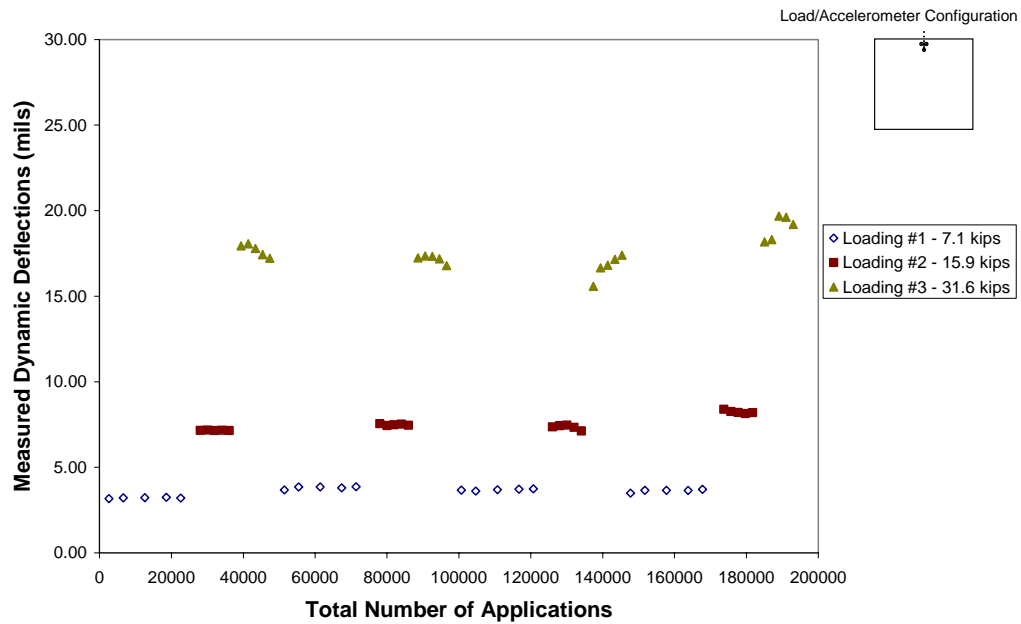


Figure 8.10 – Measured Deflections over Complete Testing Period – South Run-Up – Edge Load Point

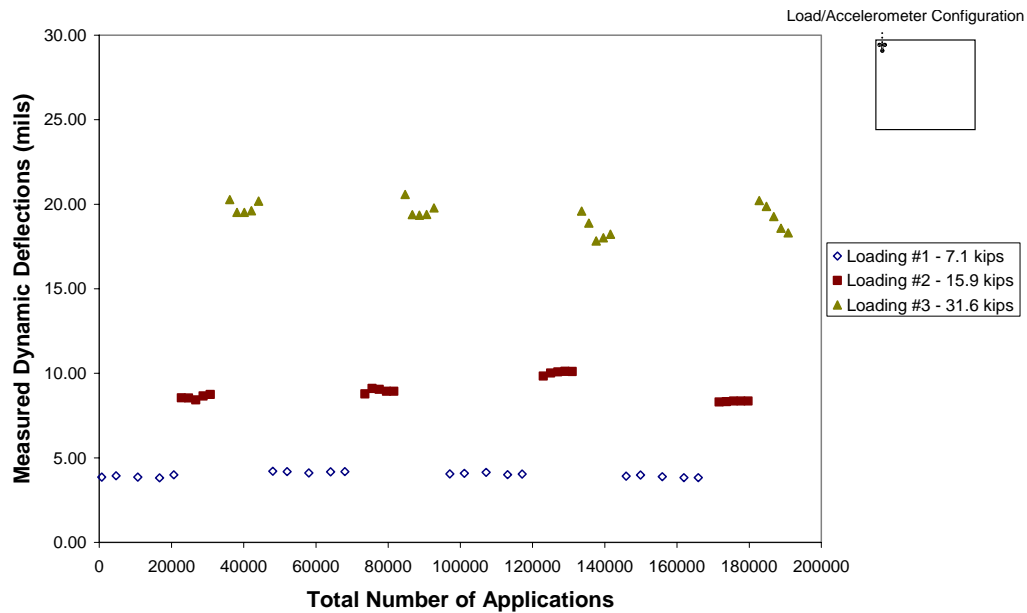


Figure 8.11 – Measured Deflections over Complete Testing Period – South Run-Up – Corner Load Point

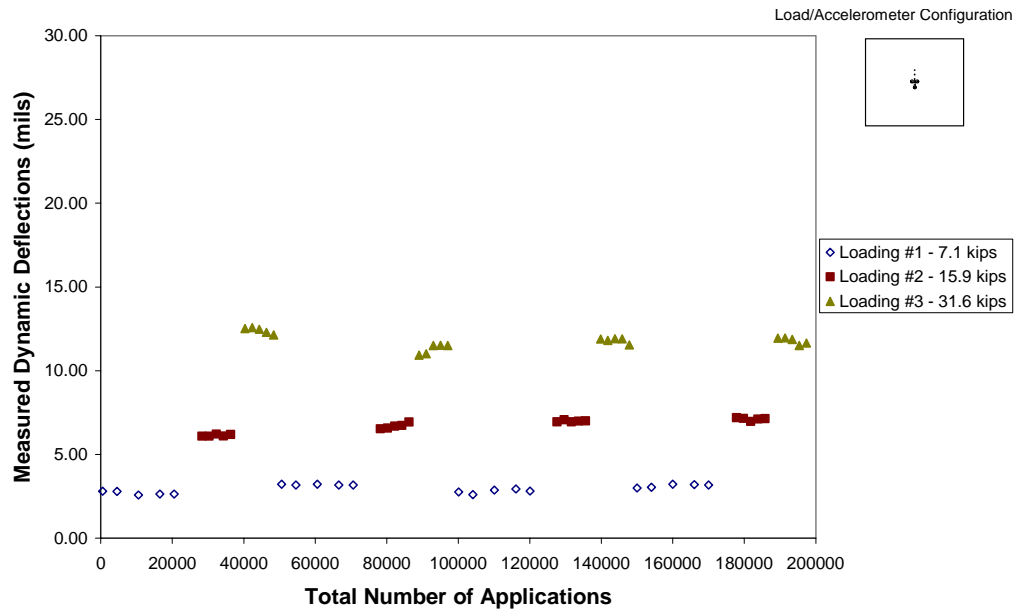


Figure 8.12 – Measured Deflections over Complete Testing Period – Taxiway A6 – Center Load Point

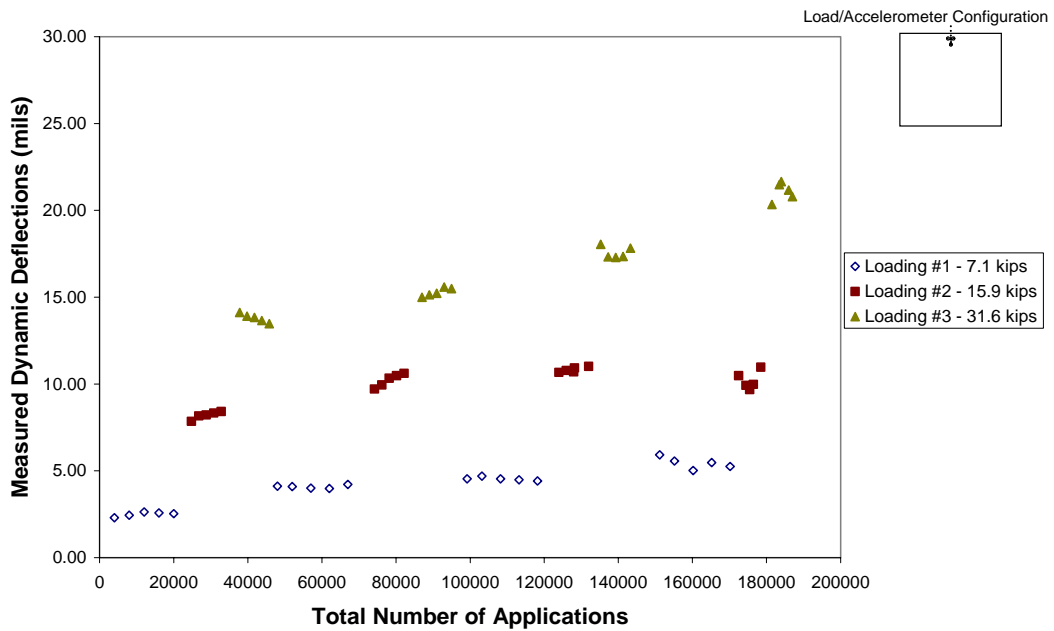


Figure 8.13 – Measured Deflections over Complete Testing Period – Taxiway A6 – Edge Load Point

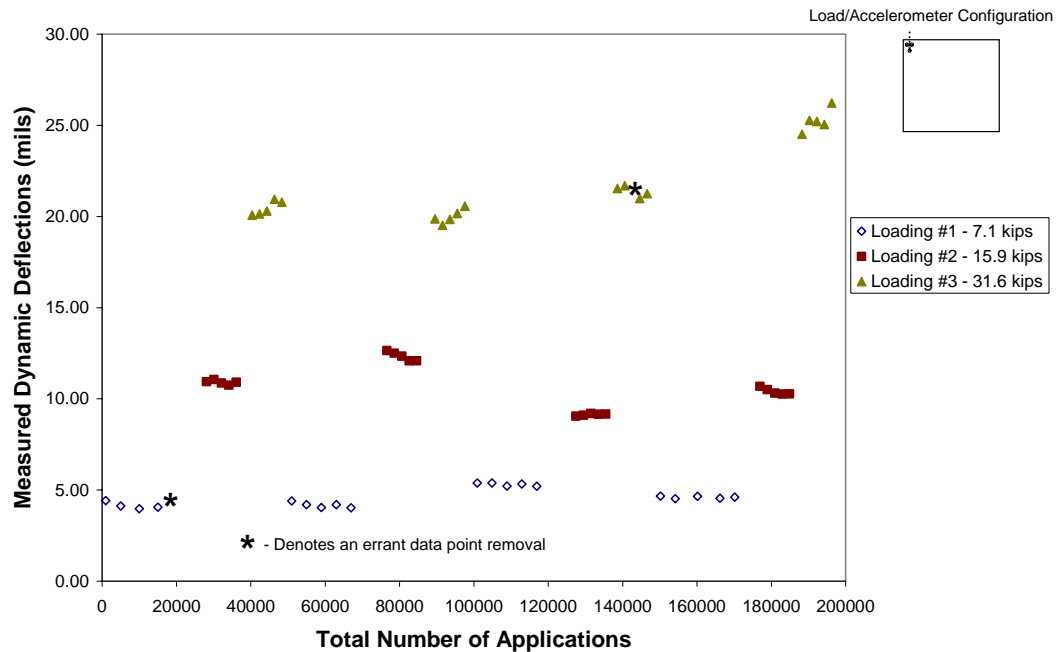


Figure 8.14 – Measured Deflections over Complete Testing Period – Taxiway A6 – Corner Load Point

In general, variations in data points occur at the highest load level at each test point. Variations may be the result of complications in the testing methods, possibly the accelerometer seating affecting the results. This variation is contrary to anticipated response (decrease in deflection with applications), and may be the result of subgrade action. A decreasing pattern is seen particularly in the first period of applications of the highest load level, possibly the result of settling of subgrade during continuous dynamic application.

By looking at Figures 8.6 through 8.14, observations can be made regarding the site conditions at each testing location. The test points at the South Run-Up and Taxiway A6 locations exhibited much greater deflections than at the North Run-Up location. By examining the center test-point locations at the three general locations (Figures 8.6, 8.9, and 8.12), the highest deflection measurements are on the order of three times greater at the South Run-Up and Taxiway A6 locations than the North

Run-Up location. It can be concluded that the stiffness of the pavement structure at the North Run-Up location is significantly greater than the other two.

An examination of the original construction cut/fill profile from the airfield construction plans was conducted to determine if the response of cut or fill sections coincided with this observed differences in the deflection response. Expected cut/fill locations did not correspond with the anticipated deflection response. As a general rule, typically cut areas exhibit higher stiffnesses in the subgrade profile as determined from lower deflection response, whereas compacted fill areas typically exhibit lower stiffnesses as inferred from a higher deflection response. Fill and compaction techniques are unable to equal the original in situ stiffness, likely due to the subgrade disturbance associated with the filling process. In the case of this study, an estimated two to four feet of fill was used during construction of Taxiway A6 as determined from the cut/fill profile, while the South Run-Up was constructed with little to no fill at the existing elevation. These areas exhibited greater deflections than the North Run-Up area, which was constructed on approximately 2.5 feet of fill. Since the subgrade construction did not support the observed trends, the disparity in deflections was attributed to test slab location with respect to anticipated trafficking patterns. The North Run-Up area fell outside of direct loading by aircraft passes. Although situated in areas experiencing less aircraft passes than the North Run-Up area, Taxiway A6 and the South Run-Up area were both located in the line of direct traffic loading.

In addition to the aforementioned testing scenario comprised of the tiered loading scenario representative of five-year increments, an additional supplemental test (with the objective of reaching failure) was devised for the last corner test location at the North Run-Up area. The purpose of this test was to exert additional loads above and beyond the 20-year expected cycle (nearly 200,000 equivalent load applications), in the event that distress failure or cracking was not achieved within the equivalent 20-year period of testing. This increased load applications would provide an additional set of data to better understand the response of the pavement beyond the

equivalent 20-year cycle. The corner loading scenario was selected since this loading scenario exhibits the highest deflections compared to edge and center loading points, effectively testing the worse case scenario. Figure 8.15 shows the same data that was presented in Figure 8.8, with the additional supplementary loading added for comparison. Note, the supplemental testing was completed with a dynamic load of approximately 40 kips for a duration of just over one hour. At a frequency of loading of 20 Hz, this supplemental loading was equivalent to an additional 74,400 applications at a load level above the previous high level; an increase of over 25% of the 20-year expected repetitions and an increase of 30% over the highest load group within the original testing model (31.6 kips). Sample sets over the course of the hour of test data were averaged to determine if any trends occurred over the duration. This averaging was done in the same manner as the method describe in Section 8.3 and Figure 8.1. Due to the longer nature of the testing period, a total of seven sample sets were analyzed.

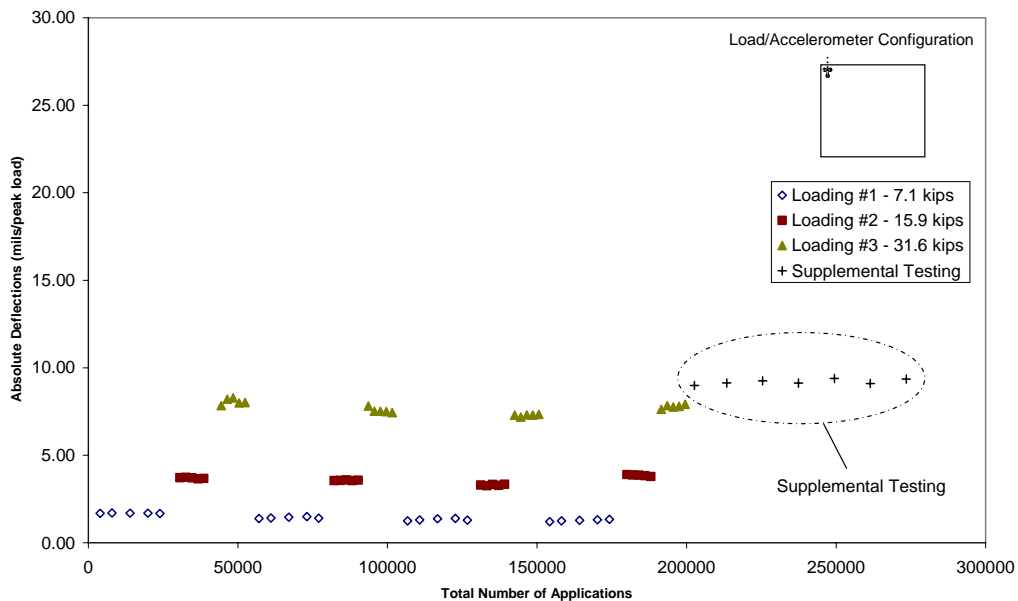


Figure 8.15 – Supplemental Deflection Testing – North Run-Up – Corner

A minimal increase in deflections was observed over the extensive heavy loading sequence of the supplemental test period. The results in Figure 8.15 showed a minimal increase of 4% in deflection from the average of the first sample set compared to the average of the last sample set. In the end, no manifestation of cracking occurred during the period of supplemental testing.

It should be noted that in hindsight, supplemental testing should have been performed at the corner of the Taxiway A6 location. This location exhibited the largest deflections, inferring the least stiff subgrade and as a result the most likely to fail.

It should also be noted that an additional two accelerometers were installed during the testing of the final corner at the North Run-Up location. The additional accelerometers enabled detection of deflection and joint transfer across the longitudinal joint (see Figure 8.1). All other corner tests focused solely on loading across the transverse joint. Transverse joints experience direct loading more often than longitudinal joints, hence the focus of testing on the transverse joints. According to as-builts, transverse joints are supported with No. 6 rebar at 16 inches on center, whereas the longitudinal joints are keyed for load transfer between slabs and additional support at the joint. The measurements of this additional deflection testing is presented in Section 9.2 for comparison with other load transfer efficiency data.

8.5 SUMMARY

In this chapter, the conditions which prevailed during the SDD SAP testing portion of this research are examined. Specific conditions of higher temperatures and precipitation totals support and substantiate the observed pavement response. Deflection measurements resulting from the SDD SAP testing have been presented in order to properly assess the current state of response of the pavement. Differences existed between test points and test locations. As expected for test points, center loading exhibited the lowest deflections with deflections increasing at edge loading, and increasing even further at the corner loading. For example, the average

deflections at the final load grouping at each location (for all three load scenarios, respectively) exhibited an increase of approximately 61% to 79% from center to edge, and 2% to 28% from edge to corner. In examining test locations, the North Run-Up exhibited approximately 1/3 the measured deflections of the Taxiway A6 and South Run-Up locations, a possible result of the relatively untrafficked condition existing at the North Run-Up. With the same layer dimensions for the North and South Run-Up, the larger deflections at the South Run-Up can be attributed to trafficking and local condition effects (subgrade, drainage, etc.). With respect to deflections over the course of 20-year equivalent loading cycle, very little increase was observed over time. Taxiway A6 exhibited the most significant trend, with observable increases occurring over the course of the equivalent loading periods. Although the three test locations provide data specific to the area which were tested, the similarity in composition, age, and construction standards of the selected test locations make the test measurements applicable as an assessment of concrete typical to Runway 16/34.

Chapter 9 – Analysis of SDD Field Measurements

9.1 INTRODUCTION

Conversion of the raw data into viable deflection measurements is presented in Chapter 8. These measurements are presented in Section 8.3 and Figures I1 through I36 in Appendix I. Analysis and comparison of deflection measurements is presented in this chapter. The magnitude of the deflections and the load transfer, evaluated at the different test points, are studied as a function of both number of applications and load level. This analysis allows observation of distinct relationships and further deductions to be made on the condition of Runway 16/34. The deflection responses exhibited by the three different loading points (center, edge, corner) at the three general test locations (Taxiway A6, South Run-Up, North Run-Up) are also studied.

9.2 ANALYSIS OF MEASURED AND NORMALIZED DEFLECTIONS

In the following section, the SDD deflection measurements presented in Chapter 8 are studied in greater depth. As shown in Section 8.4, the relationship of measured deflection with number of load applications provides insight into the behavior of the pavement at each test point at each test location. Additional comparison of the deflection relationships with load level also reveals different relationships, at different test points and locations. In addition to measured deflections, normalized deflections provide an additional means of comparing the deflection responses. Normalized deflections are defined in this study as the measured deflection divided by the applied load during the time of measurement. Normalizing deflections takes into account any variability in the load level which was applied during the SDD SAP testing process. The following subsections address both measured and normalized deflection relationships which were determined by further analysis of the testing measurements.

9.2.1 Analysis of Measured Deflections

The measurements presented in Section 8.4 focus on the change in measured deflections with respect to the total number of load applications. As discussed in Section 8.4, there was no apparent trend found in the deflection measurements among each load grouping, within a five-year increment at each test point. Therefore, the average measured deflection was used to produce the plots of average deflection versus load. These plots enable the relationship to be established between average deflection per five years of loading and load level. For the following data analysis, the readings produced by accelerometer #1 (closest to load point) were used in producing deflection data for comparison.

Figures 9.1 through 9.9 illustrate the relationship of average measured deflections per five-year load period to load level. All figures are plotted using the same scales on the x and y axes. Figures 9.1 through 9.3 show the measured deflections relationships at the North Run-Up location. All three load test points (center, edge, and corner) exhibit a linear relationship as averaged measured deflection increases with increasing load. Equations for the linear regression trend lines have been added to all figures. Figures 9.4 through 9.6 show the measured deflections relationships at the South Run-Up location. In this case, a linear relationship for the first two load groups is exhibited, after which a slight nonlinearity is seen at the third load group at all three load points. Figures 9.7 through 9.9 show the average measured deflections relationships at the Taxiway A6 location. A linear relationship is seen at the center load point (Figure 9.7). However the edge and corner load points exhibit the most scatter and the most nonlinearity of any of the test locations. In general, Figures 9.4 through 9.9 can be considered to be linear as a first-order effect, with any nonlinearity appearing as a second order effect. Figures 9.4 through 9.6 highlight the typical observed nonlinearity at the third load level of the South Run-Up location.

Overall, a nearly linear relationship was found for all data. Regression lines were fit to all nine plots. These regression lines are presented in Table 9.1. By

comparing the slopes of each of these trend lines, the findings from the relationship between measured deflections and load applications is confirmed. For each test location, center-edge-corner is the order of increasing deflection as noted by increasing slope values for the respective trend lines. The first plot (Figure 9.1) highlights the different load grouping data. Once again this relationship demonstrated the stiffer nature of the North Run-Up area in comparison with Taxiway A6 and the South Run-Up area.

Table 9.1 – Linear Regression Relationships for Average Measured Deflection for Five-Years of Loading to Load Level

Figure No.	Location	Slope (mils/kip)	R²
9.1	North Run-Up Center	0.1357	0.9897
9.2	North Run-Up Edge	0.2076	0.9711
9.3	North Run-Up Corner	0.2359	0.9882
9.4	South Run-Up Center	0.3880	0.9705
9.5	South Run-Up Edge	0.5539	0.9761
9.6	South Run-Up Corner	0.6070	0.9888
9.7	Taxiway A6 Center	0.3933	0.9906
9.8	Taxiway A6 Edge	0.5576	0.9464
9.9	Taxiway A6 Corner	0.6837	0.9411

$$y = A * x$$

where x = load level in kips, y = deflection in mils,

A = the slope of the line in mils/kip, and R^2 = the % variation of the data explained by the fitted regression line.

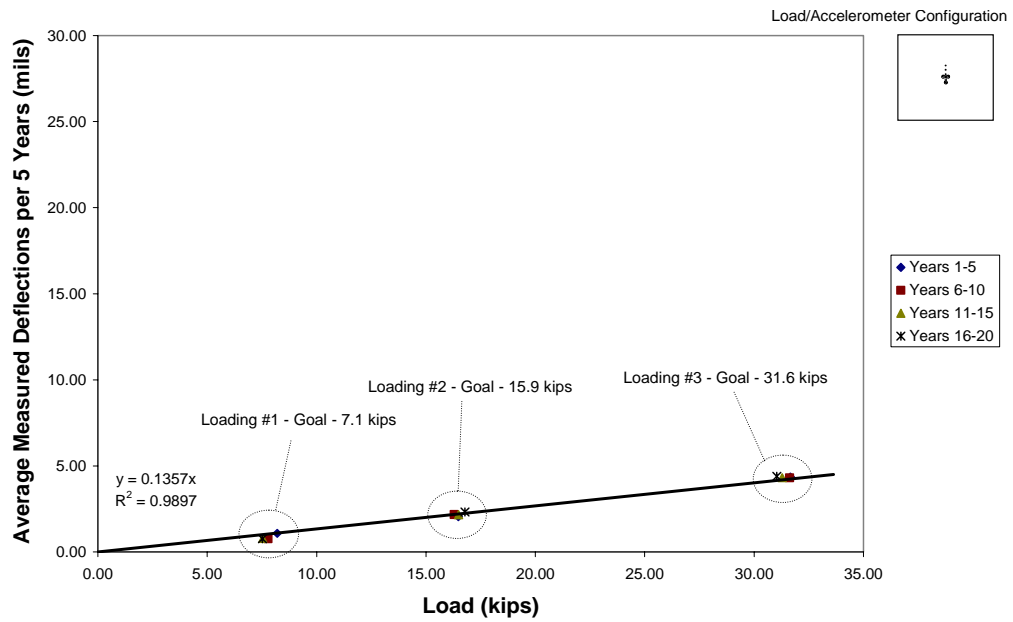


Figure 9.1 – Average Deflections Measured by Accelerometer #1 for Five-Year Load Period with Load Level: North Run-Up – Center Load Point

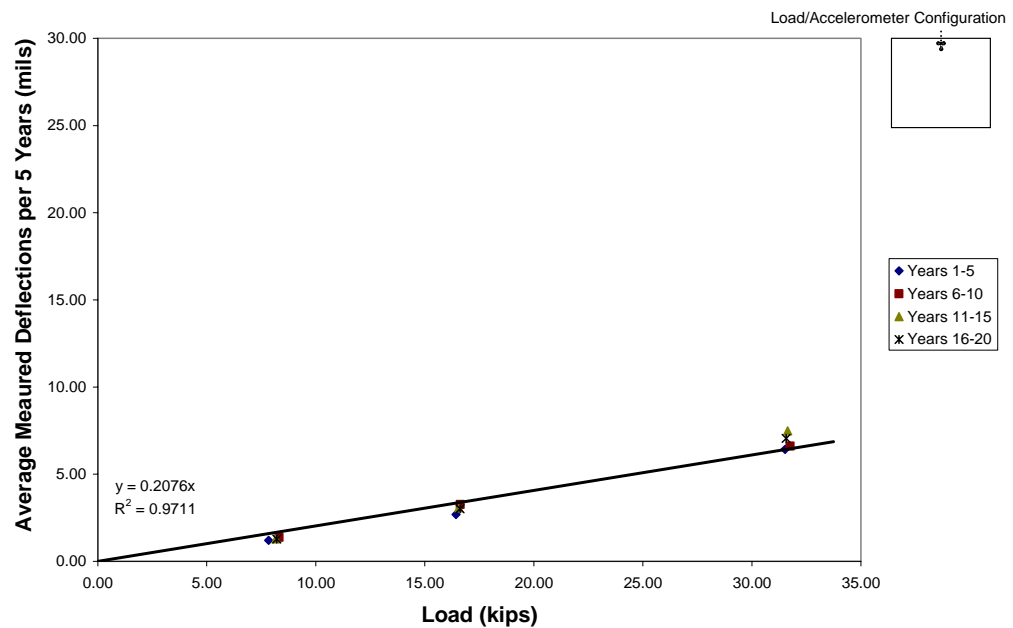


Figure 9.2 – Average Deflections Measured by Accelerometer #1 for Five-Year Loading Period with Load Level: North Run-Up – Edge Load Point

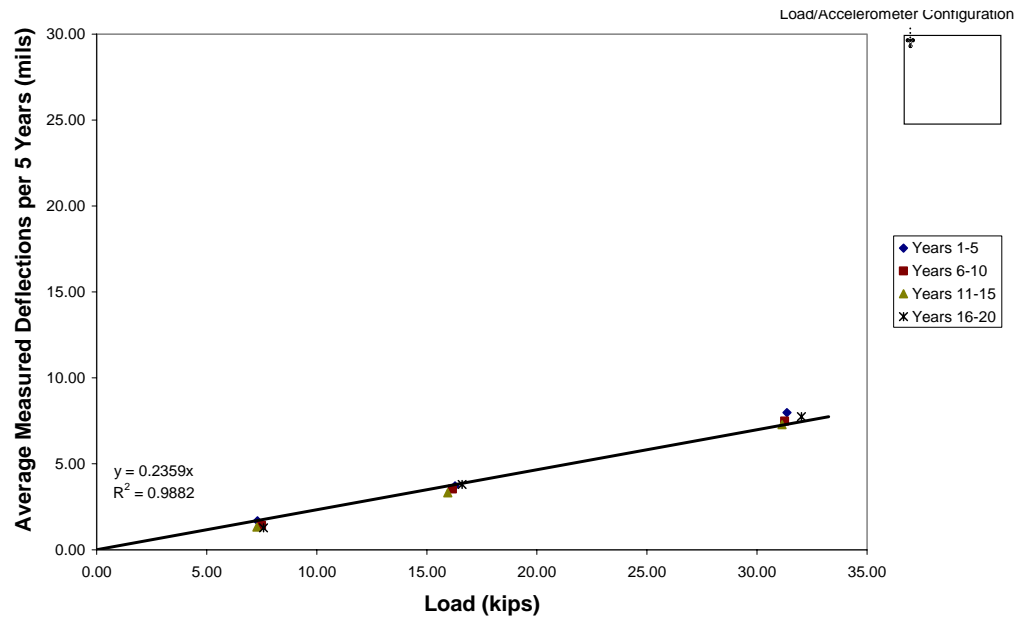


Figure 9.3 – Average Deflections Measured by Accelerometer for Five-Year Load Period with Load Level: North Run-Up – Corner Load Point

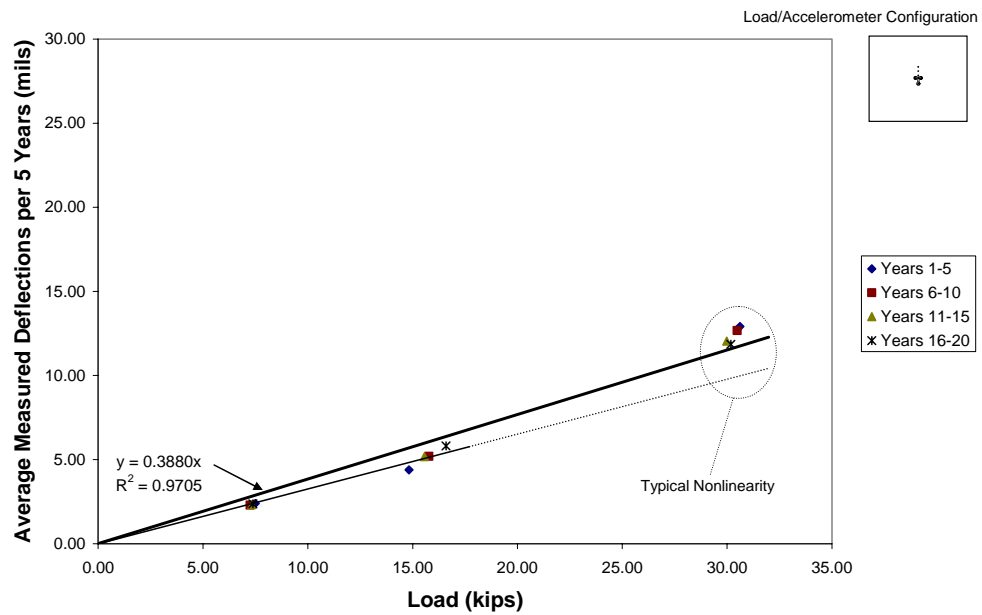


Figure 9.4 – Average Deflections Measured by Accelerometer #1 for Five-Year Load Period with Load Level: South Run-Up – Center Load Point

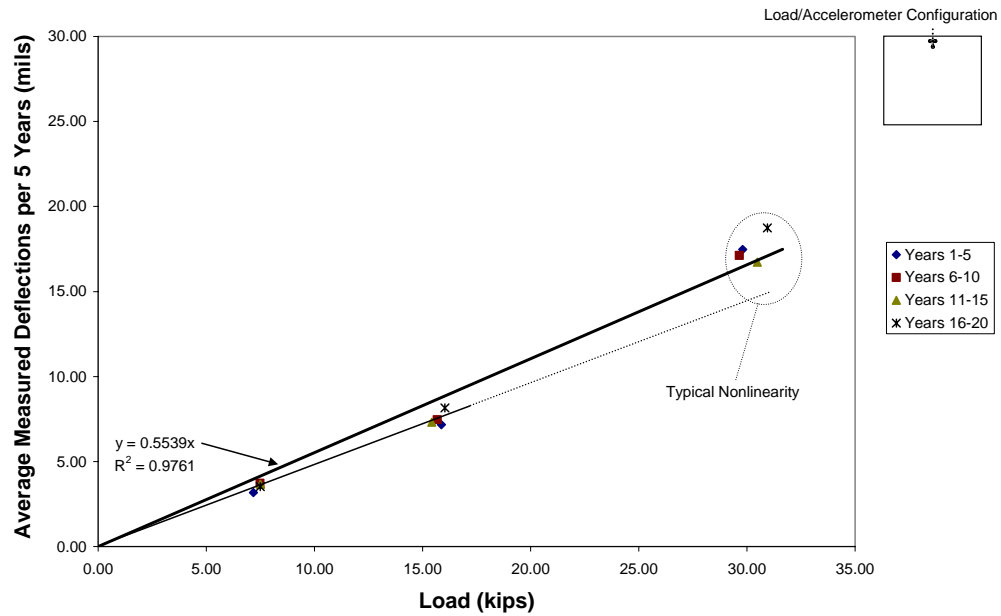


Figure 9.5 – Average Deflections Measured by Accelerometer #1 for Five-Year Load Period with Load Level: South Run-Up – Edge Load Point

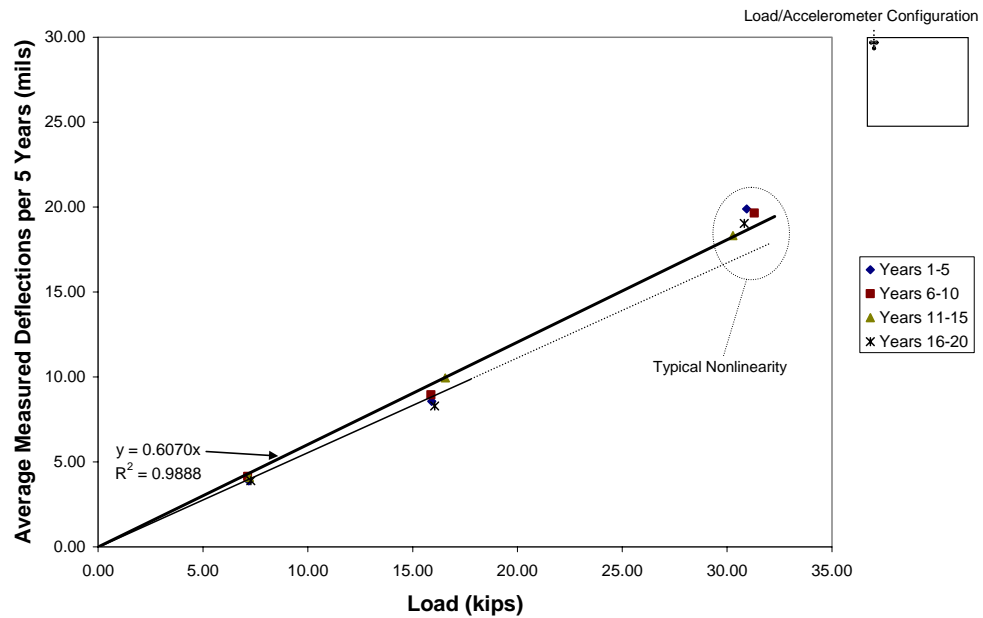


Figure 9.6 – Average Deflections Measured by Accelerometer #1 for Five-Year Load Period with Load Level: South Run-Up – Corner Load Point

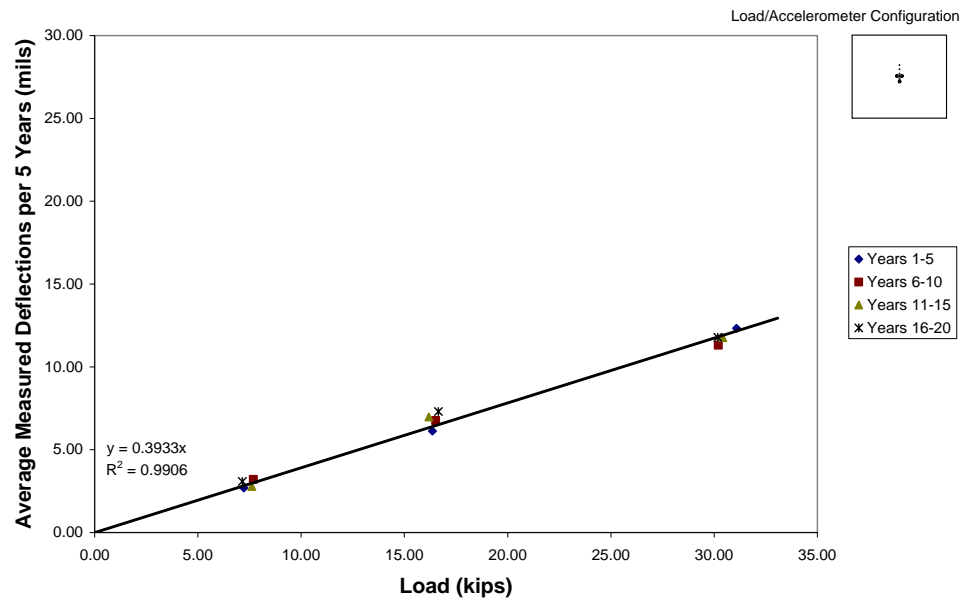


Figure 9.7 – Average Deflections Measured by Accelerometer #1 for Five-Year Load Period with Load Level: Taxiway A6 – Center Load Point

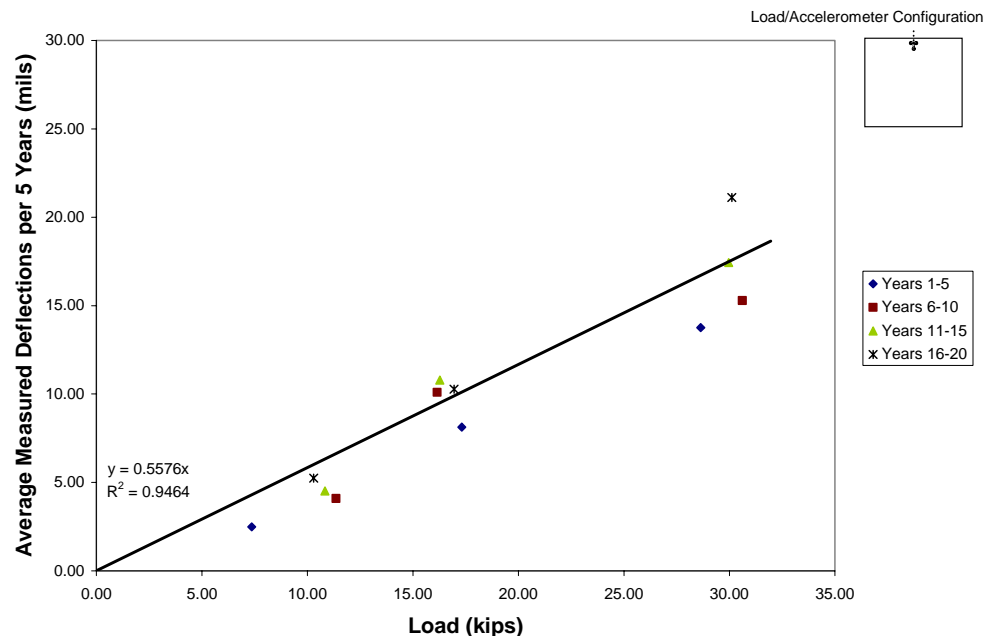


Figure 9.8 – Average Deflections Measured by Accelerometer #1 for Five-Year Load Period with Load Level: Taxiway A6 – Edge Load Point

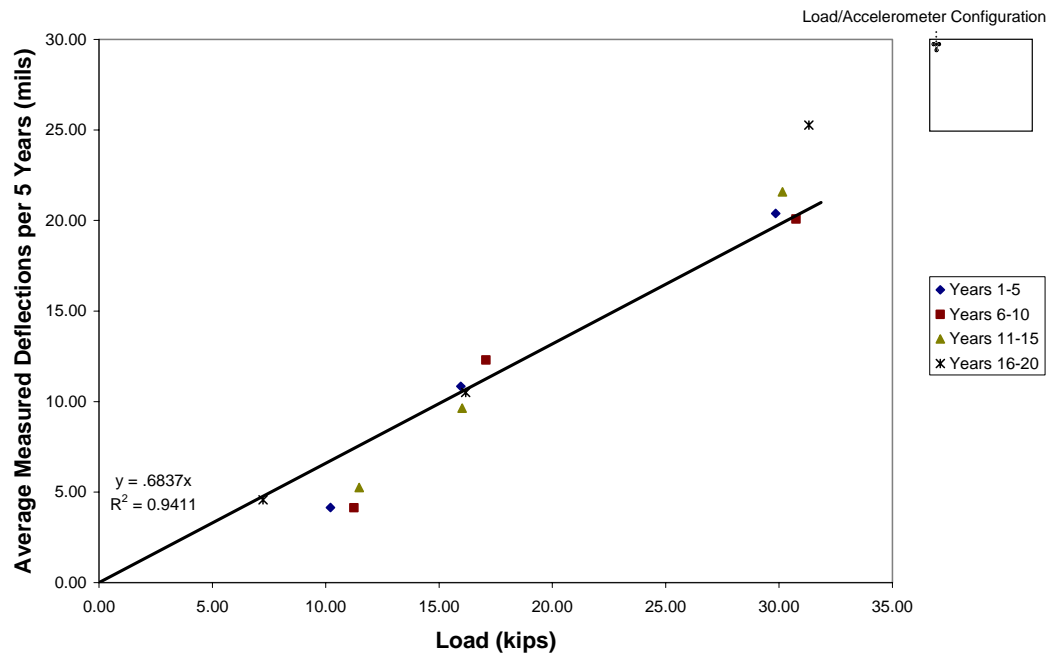


Figure 9.9 – Average Deflections Measured by Accelerometer #1 for Five-Year Load Period with Load Level: Taxiway A6 – Corner Load Point

By using the approximate linear trend in the deflection-load level relationship, the adjustment for loading position of the Taxiway A6 edge loading data could be made. As mentioned in Section 5.5.2, this was the first point tested, where the load was placed an additional 6 in. from the first accelerometer, with the purpose to test the stability of the load frame under dynamic loads. However, this additional distance of 6 in., lowered the deflection response determined for this test point. Comparisons and percentage increases were calculated for each location, comparing the slope of the line for each loading scenario at all three locations. A factor was determined which was applied to the Taxiway A6 edge location deflection data. A more detailed overview of the concept for data adjustment is presented in Appendix J.

In addition to the presentation of the nine test points, Figure 9.10 is included to show the results of the supplemental testing conducted at the North Run-Up corner, following completion of the equivalent 20-year loading. Figure 9.10 includes the data

from the plot from the North Run-Up corner, shown in Figure 9.3. This average measured deflection value under the supplemental test load falls directly on the observed trend line, further substantiating the linear trend observed this test location.

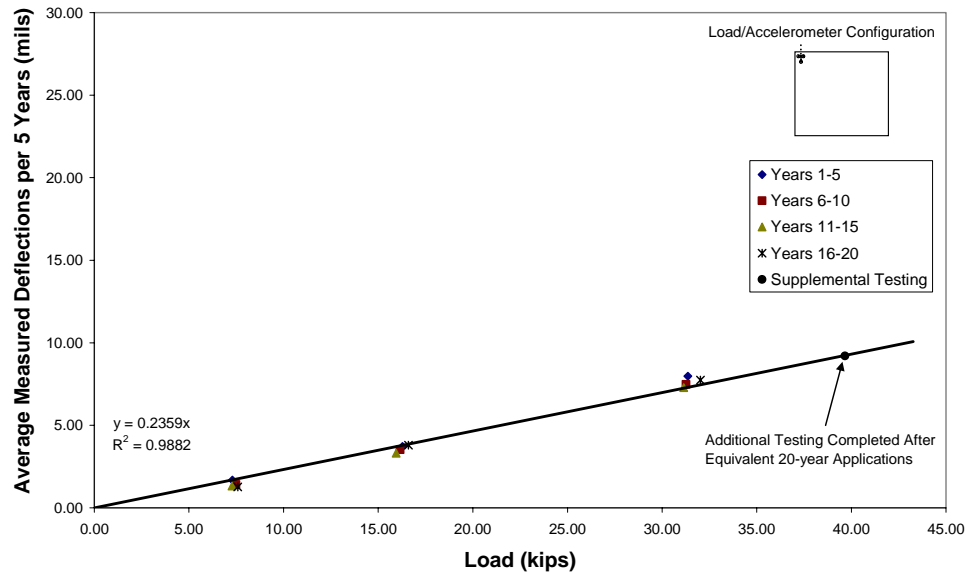


Figure 9.10 – Average Deflections Measured by Accelerometer #1 for Five-Year Load Period with Load Level: North Run-Up – Corner Load Point – Including Supplemental Testing

9.2.2 Analysis of Normalized Deflections

Variation of Average Normalized Deflections with Number of Load Applications

Along with the analysis of the average measured deflections per five-year loading periods, normalized deflections per five-year loading periods were also examined to enable further comparison of the responses between the different locations and different load levels. Normalization of the average deflection was accomplished by dividing average measured deflections by the respective average peak load which caused the deflection. This process decreased the pronounced difference between load groups. Examples of these data are shown in Figures 9.11, 9.12, and 9.13. These figures comprise all three test points at the South Run-Up

location and are presented as a sample set for this relationship. Higher load levels caused increased normalized deflections for the center, edge, and corner load points of the South Run-Up locations. The remaining two test locations are included in Appendix K. Note, the y-axis scale for Figures 9.11, 9.12, and 9.13 has been kept consistent with figures in Appendix K for ease in correlating the trends.

Examination of the normalized deflections versus total load applications demonstrates two points. The first point is that the normalized deflections at each load level remain essentially constant and independent of number of load applications. The second point is that the largest load level causes slightly larger equivalent deflections (mils per peak load), even after normalization. Load Group #1 and #2 (labeled Loading #1 and #2 in Figures 9.11, 9.12, and 9.13) are linear. The increase at the third load level, once again demonstrates the slight nonlinearity found in the data in Section 9.2.1. It is important to note that if the response were linear across all load groups, then the normalization would result in all normalized deflections being equal in value, at a given test point. There would not be an increase in value at the third load group as seen in Figures 9.11, 9.12, and 9.13. The Taxiway A6 location did experience some apparent degradation (as seen in Appendix K) with normalized deflections increasing with number of applications.

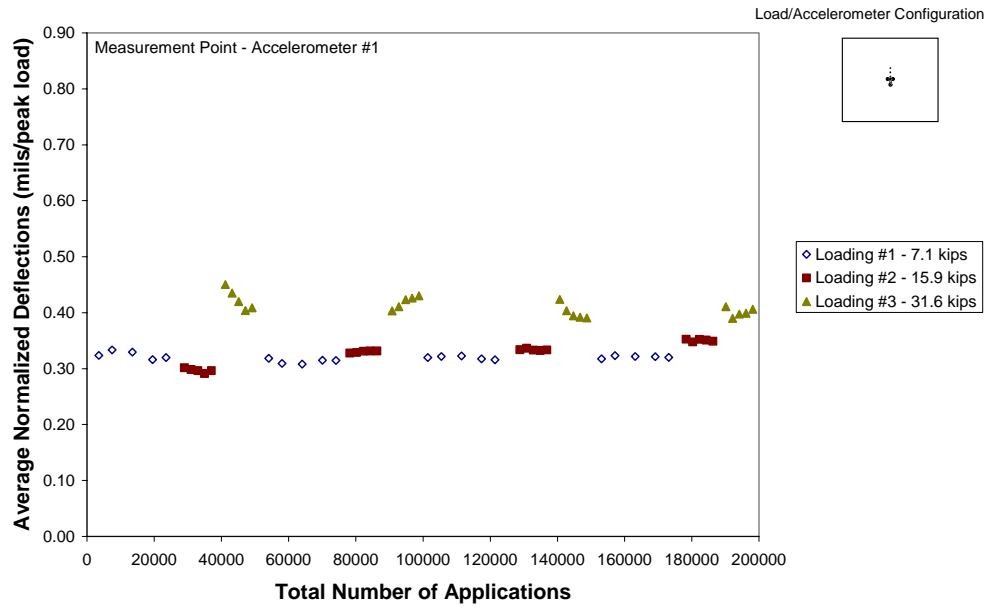


Figure 9.11 – Variation of Average Normalized Deflections with Number of Load Applications: South Run-Up – Center Load Point

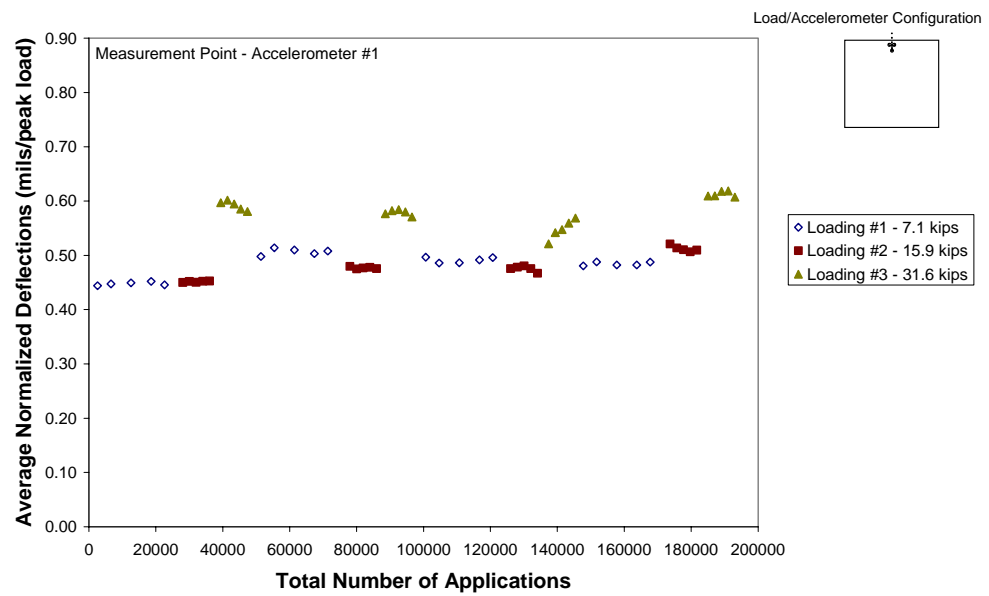


Figure 9.12 – Variation of Average Normalized Deflections with Number of Load Applications: South Run-Up – Edge Load Point

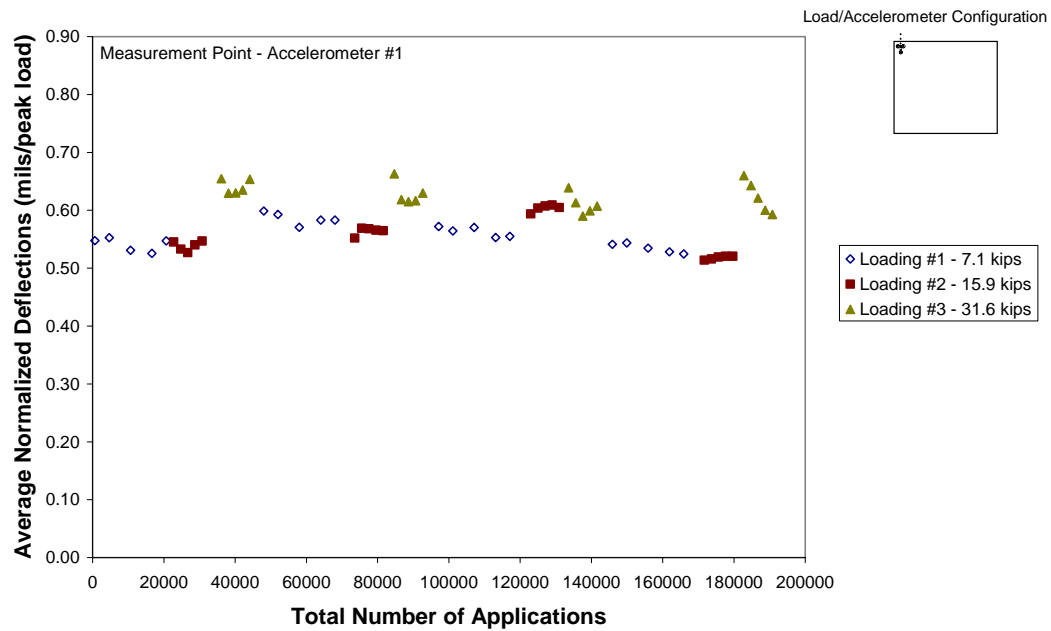


Figure 9.13 – Variation of Average Normalized Deflections with Number of Load Applications: South Run-Up – Corner Load Point

Variation of Average Normalized Deflections with Load

As noted in Section 9.2.1 in the discussion of the average measured deflections per five-year load periods versus load level, the relationship between deflection and actual load provides valuable insight into the response of the pavement. Figures 9.14 through 9.22 build upon this relationship, presenting the average normalized deflections per five-year load period with load level. Once again, normalization of the deflections highlights the previously observed trend in examining measured deflections versus load level, discussed in Section 9.2.1. The linear trend between measured deflections and load level should plot as a horizontal line in the normalization of deflections. Minor variations in the horizontal line would be attributed to slight nonlinearity. A nearly true horizontal line among the three load groups for given five-year load periods would infer a linear relationship between deflections and load. Figures 9.14, 9.15, and 9.16 for the North Run-Up location can be approximated by a horizontal line. However, even in this case there is some

nonlinearity shown in the behavior at the highest load level. Scatter of data and variability associated with the testing can likely account for some of the slight divergence in these three plots.

Plots of the variation in average normalized deflections versus load level for the South Run-Up and Taxiway A6 load points are shown in Figures 9.17 through 9.22. Once again, these results illustrate the nonlinearity was a second order effect in all tests, except the tests at the edge and corner load points on Taxiway A6. The divergence from the horizontal line with the third load group level is shown again at the South Run-Up location. Figures 9.17 and 9.18 highlight this nonlinearity. The plots from this location also enable a visual comparison with previously presented normalized deflection versus application plots (Figures 9.11, 9.12, and 9.13). The only locations which did not show this slight nonlinearity are the North Run-Up and Taxiway A6 locations (Figures 9.14 and 9.20).

The edge and corner load points of Taxiway A6 (Figures 9.21 and 9.22) show considerable scatter and nonlinearity of data. Part of this may be a result of familiarization of field personnel with test procedures, these two locations were the first two tests performed in the field. Load levels varied considerably more from the desired target (Load Group #1 – 7.1 kips, Load Group #2 – 15.9 kips, Load Group #3 – 31.6 kips) than during other test points. The trend lines have been added to Figure 9.21 and 9.22 emphasizing the increase in normalized deflection seen from the first load period to the last load period, illustrating the higher level of degradation occurring at Taxiway A6. Local effects at this location could have contributed to the increase in normalized deflections, including adjacent drainage and subgrade condition.

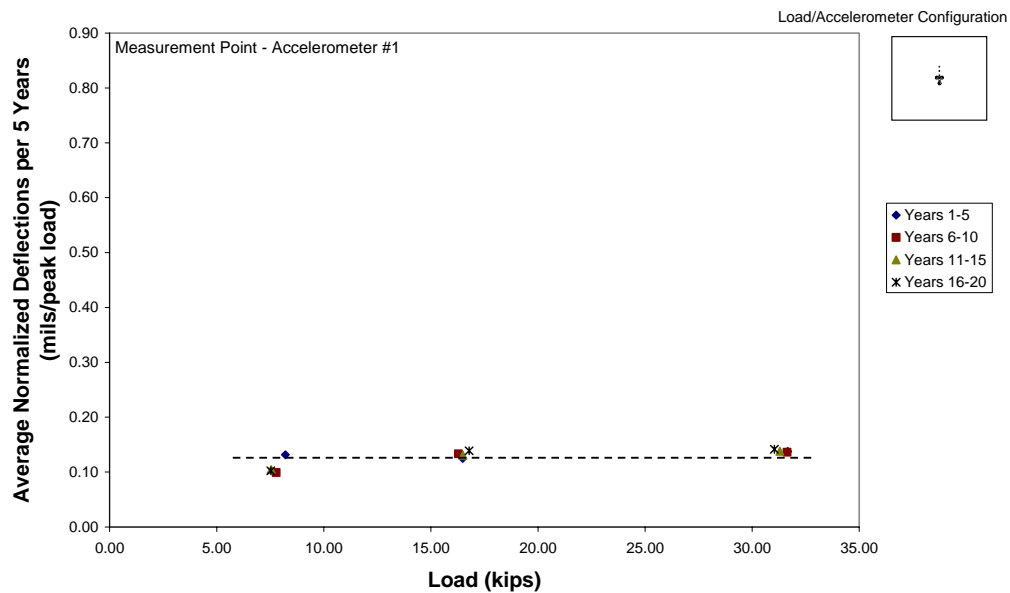


Figure 9.14 – Variation of Average Normalized Deflections per Five-Year Load Period with Load Level: North Run-Up – Center Load Point

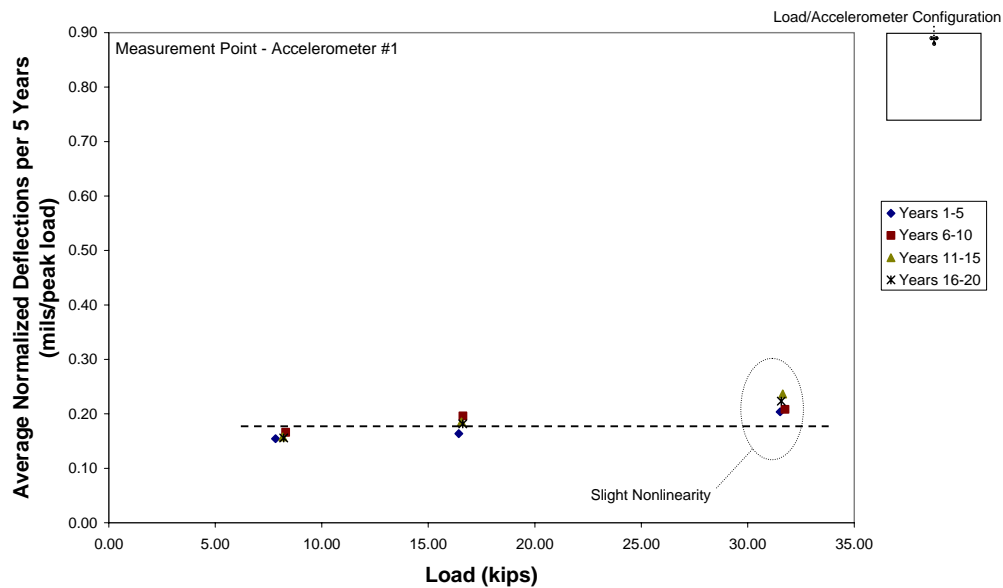


Figure 9.15 – Variation of Average Normalized Deflections per Five-Year Load Period with Load Level: North Run-Up – Edge Load Point

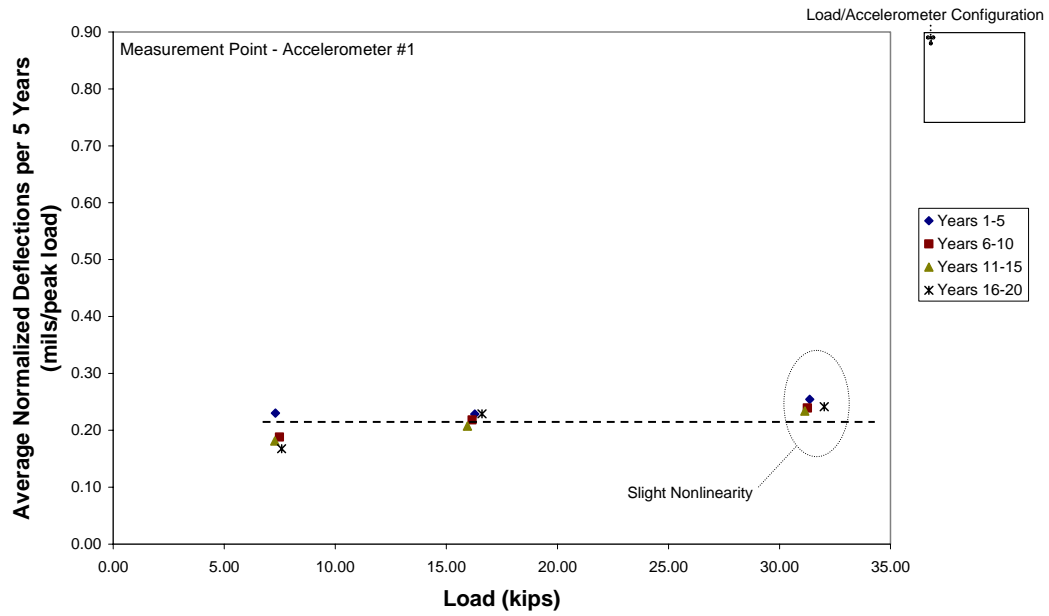


Figure 9.16 – Variation of Average Normalized Deflections per Five-Year Load Period with Load Level: North Run-Up – Corner Load Point

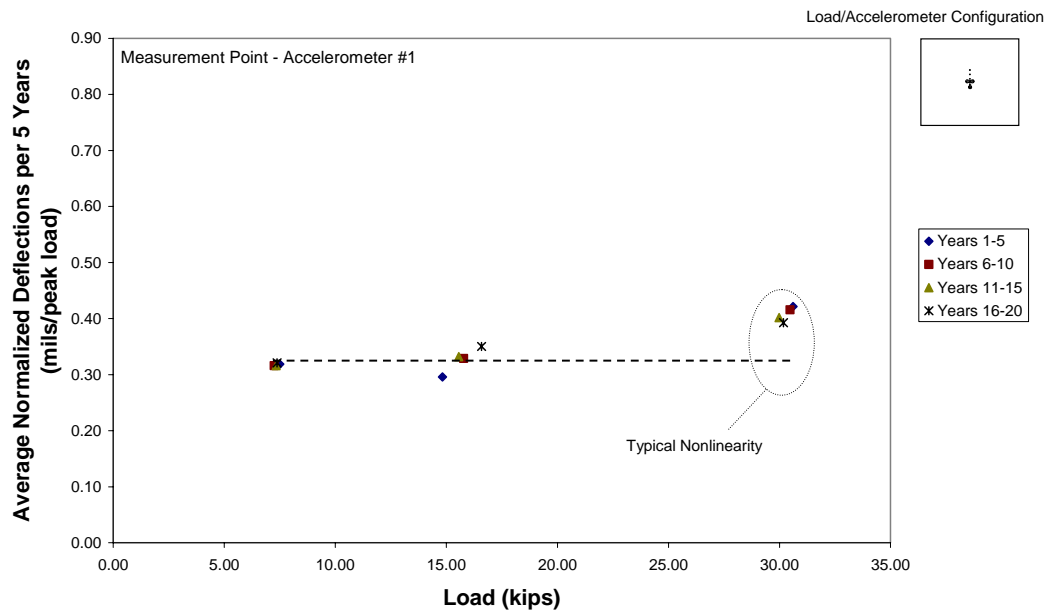


Figure 9.17 – Variation of Average Normalized Deflections per Five-Year Load Period with Load Level: South Run-Up – Center Load Point

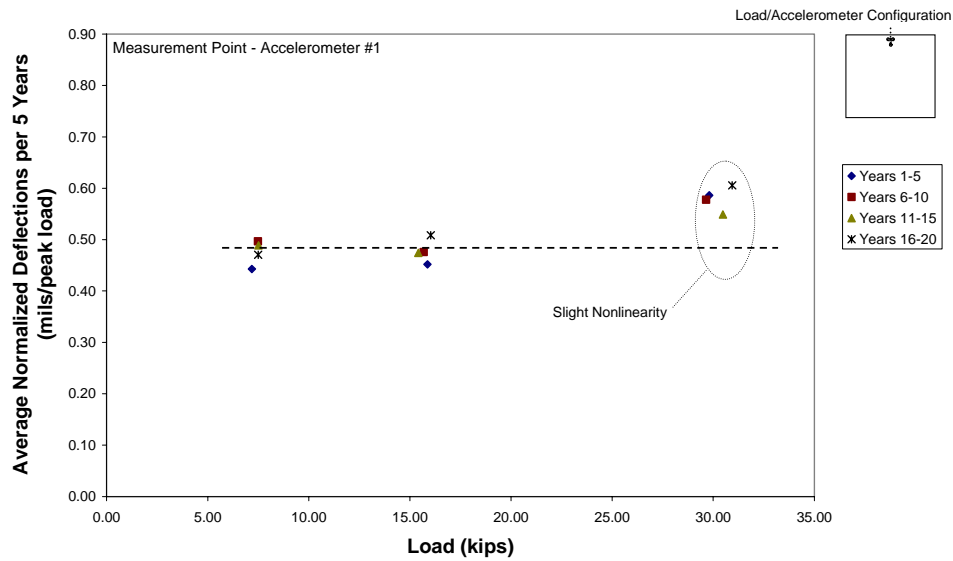


Figure 9.18 – Variation of Average Normalized Deflections per Five-Year Load Period with Load Level: South Run-Up – Edge Load Point

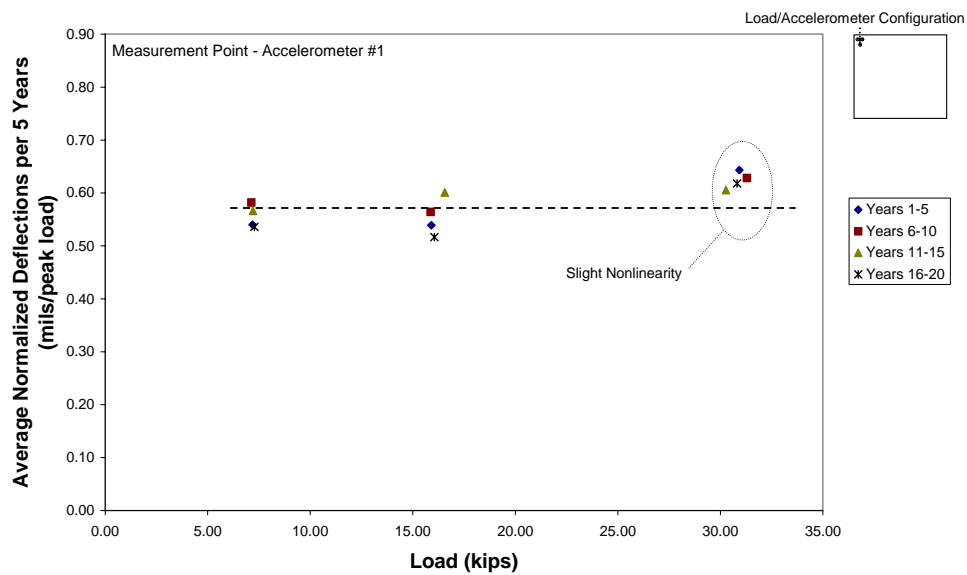


Figure 9.19 – Variation of Average Normalized Deflections per Five-Year Load Period with Load Level: South Run-Up – Corner Load Point

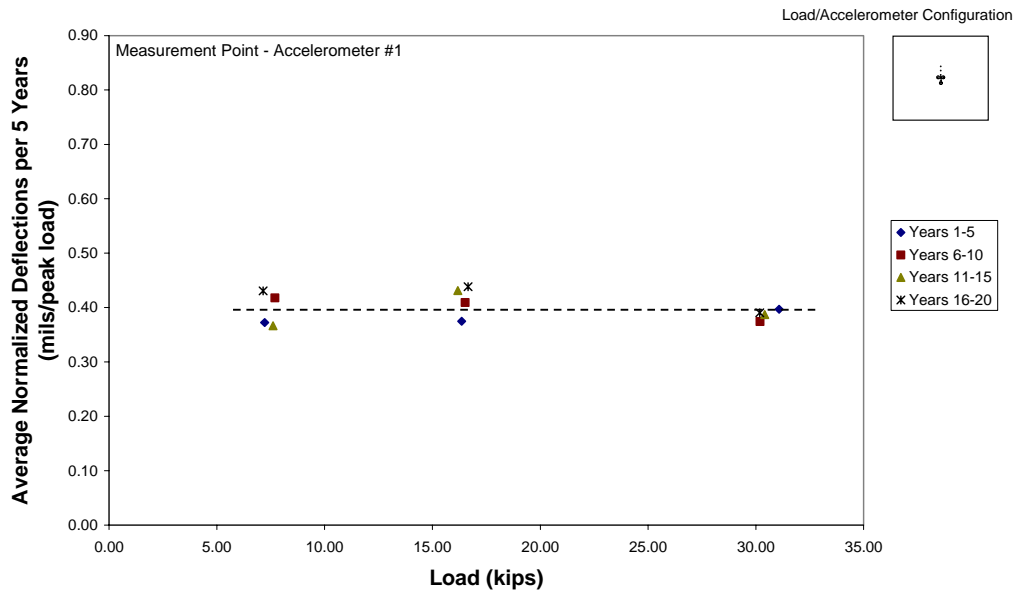


Figure 9.20 – Variation of Average Normalized Deflections per Five-Year Load Period with Load Level: Taxiway A6 – Center Load Point

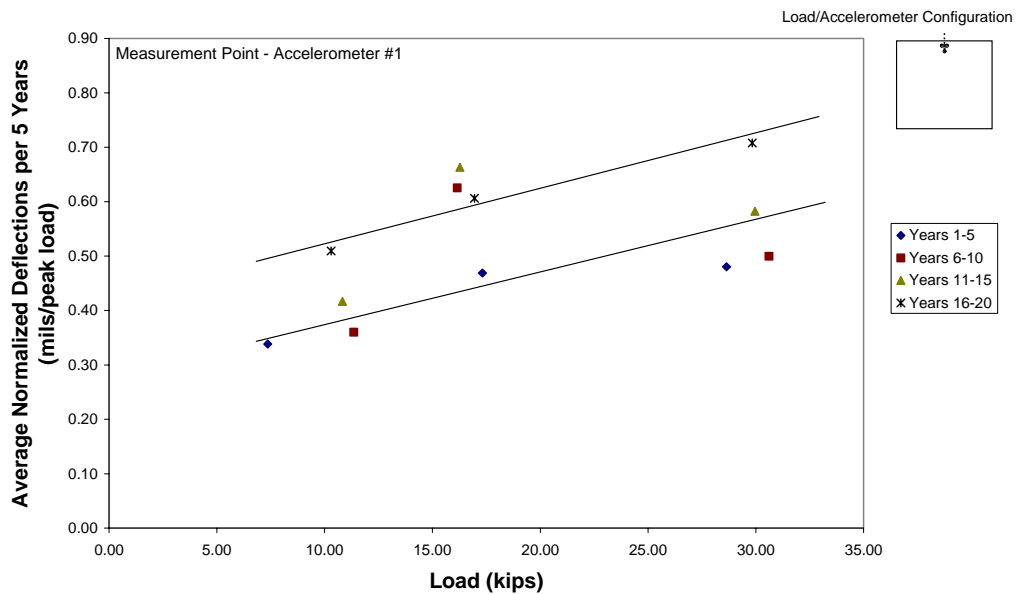


Figure 9.21 – Variation of Average Normalized Deflections per Five-Year Load Period with Load Level: Taxiway A6 – Edge Load Point

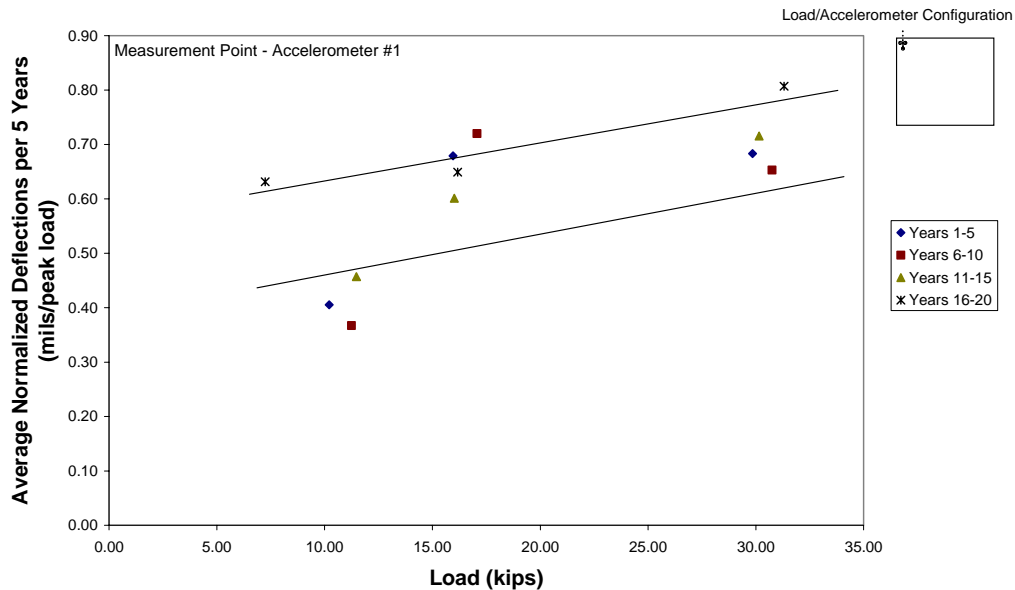


Figure 9.22 – Variation of Average Normalized Deflections per Five-Year Load Period with Load Level: Taxiway A6 – Corner Load Point

Using Figures 9.14, 9.17, and 9.20, the center load point at each location, a comparison of normalized deflections provides a good indication of typical mid-slab pavement response. The average of the normalized deflections per five-year load period, in the linear range at the center of the slab provides a characteristic parameter of the pavement system (essentially the bending of the slab), where a larger average normalized deflection indicates less support within a pavement system at a given location. For example, an average of the normalized deflections for the middle load group at each of the center loading scenarios revealed the previously exhibited trend among test locations. The largest deflections were exhibited at Taxiway A6 and the smallest deflections at the North Run-Up area. Table 9.2 lists the average normalized deflections for each location, supporting this trend. Once again all values are generated from the accelerometer closest to the load point (accelerometer #1).

Table 9.2 – Comparison of Average Normalized Deflection in the Linear Range at the Center Load Point

Location	Average Normalized Deflection (mils/peak load)
Taxiway A6	0.40
South Run-Up	0.35
North Run-Up	0.13

The relationship between average normalized deflections and load level also showed a slight increase of normalized deflections over the course of the testing, hence increasing with load period. When comparing deflections caused by each respective load groups, during the first five-year equivalent increment and the last five-year equivalent load increment, an increase was observed at the edge loading point. The edge point was selected due to the critical nature of edge loading in concrete performance. Table 9.3 illustrates this trend, presenting the percentage increase from normalized deflection during the first five-year increment to the final five-year increment, for the edge load point at each of the three locations. This is an anticipated trend as a given load group deflection is expected to increase from the first five-year increment on through the testing cycles. The much higher increases experienced at Taxiway A6 could be a result of a site-specific subgrade conditions. As mentioned and revealed before in other relationships, this location demonstrates the greatest deflections and tendency for increased deflections.

Table 9.3 – Increase in Normalized Deflection Over Five-Year Increments at Edge Load Point

Location	Percent Increase From Equivalent Years 1-5 to Years 16-20		
	Lowest Load Grouping	Middle Load Grouping	Highest Load Grouping
Taxiway A6	56	28	46
South Run-Up	8	13	4
North Run-Up	-3	11	9

9.3 LOAD TRANSFER EFFICIENCY

Variation of Load Transfer Efficiency with Number of Applications

In addition to the measured and normalized deflections which have been the focus of the analysis thus far, it is also important to analyze the potential degradation of load transfer efficiency from one slab to another. In the following section, the SDD measurements are studied in terms of the parameter of load transfer efficiency. Determination of load transfer efficiency is discussed in Section 8.3. It is a vital parameter in determining how a rigid pavement system reacts under given loads. Investigating the load transfer efficiency over time (with load applications) at a specific test point provides insight into the behavior of the pavement structure and its respective setting. Additional comparison of the relationship of load transfer efficiency with load level reveals the reaction at a joint under increasing load levels. As mentioned previously, testing at the load points in this study does not represent the way load transfer is typically defined. Load transfer is typically defined under conditions tested with standard pavement testing equipment, like the falling weight deflectometer (FWD). In this case, there is no “preload” on the joint. However, with the weight of the RDD/SDD device already causing initial stress and deflection conditions (hence a “preload”), load transfer values produced in this study are higher than expected under an unloaded (no “preload”) condition. On the other hand, the values presented in this study are effective in comparing transfer efficiency in a

relative sense. The real merit of SDD SAP testing, as conducted in this study, is the opportunity to compare multiple test locations loaded over accelerated applications in a relatively limited time period. With this approach, any degradation trends are easily observed.

Figure 9.23 through 9.31 illustrate load transfer over the entire test application period for each test location and for all three test points. As mentioned in Section 8.3, the center loading scenarios are clearly not representative of a “true” load transfer. Nevertheless, this load condition provides a look at the bending mechanism in the slab and supporting base/subgrade. As expected, the center testing exhibited the highest LT_{US} value (as defined in Section 8.3) for each location. All three locations exhibited similar magnitudes for the center testing with overall average values of 86%, 94%, and 92% for the North Run-Up, South Run-Up, and Taxiway A6, respectively (Figures 9.23, 9.26, and 9.29). It can be assumed all three slabs experienced similar bending and deflection dissipation across the extent of the slab based on these results. Also note, insignificant degradation was measured at the center load points.

In examining load transfer efficiency with respect to number of load applications, a minor decrease is generally observed in the load transfer efficiency over the duration of the testing for edge and corner load points. Only the corner load point at the South Run-Up location (Figure 9.28) and the edge load point at the Taxiway A6 location differed, exhibiting significant downward trends. These observations coincide with previous observations of a lower stiffness profile at both the Taxiway A6 and South Run-Up locations. Local effects due to variations in the pavement system (particularly supporting subgrade) may have played a role, with these two points degrading more significantly than the other test points at their respective location.

Figures 9.23 and 9.28 are the only plots with obvious errant data points which were removed. Figure 9.23 illustrates the center load point for the North Run-Up, where the first loading group for Years 1-5 contain significant scatter as compared to

any other load groupings. This skewed the load transfer efficiency measurements which are a result of the second accelerometer readings. Figure 8.9 illustrates that the first accelerometer gave reasonable values for measured deflections. These outlying data points may be attributed to a system error in accelerometer readings. The error was rectified as seen by consistent data produced over the remaining 160,000-plus applications. Figure 9.28 illustrates the corner load point for the South Run-Up. This plot contained a single errant data point, the first point of the third load group in the last five-year increment. Since this single point occurred at the onset of the third load group application, this error can be attributed to fluctuations in the load cell during the beginning of the last load level. Variations are more likely to occur with equipment directly following a load level increase.

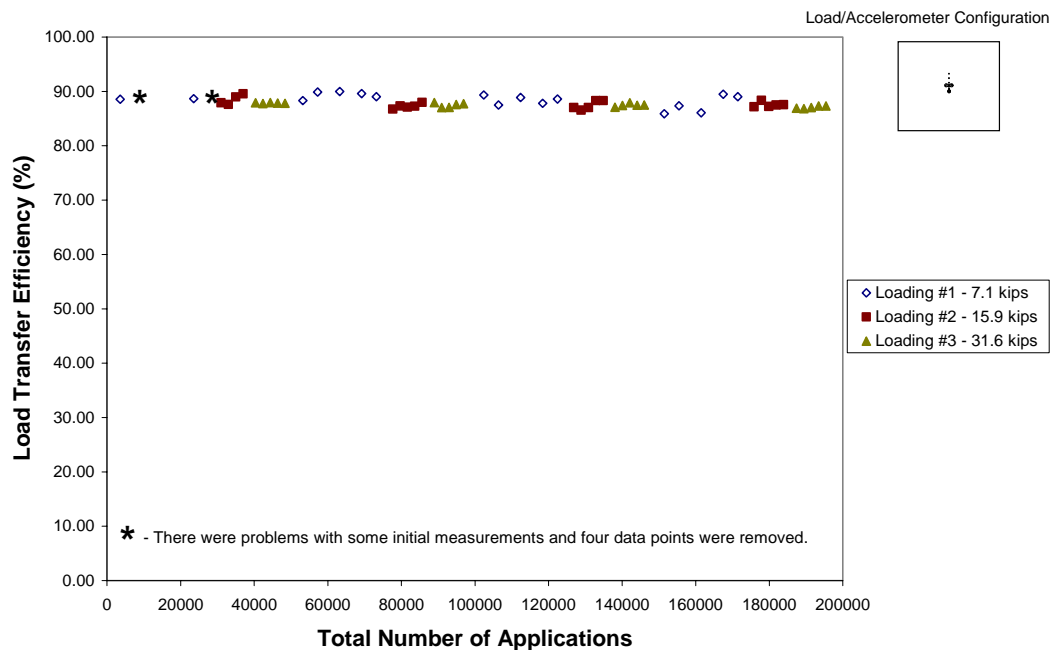


Figure 9.23 – Load Transfer with Applications: North Run-Up – Center Load Point

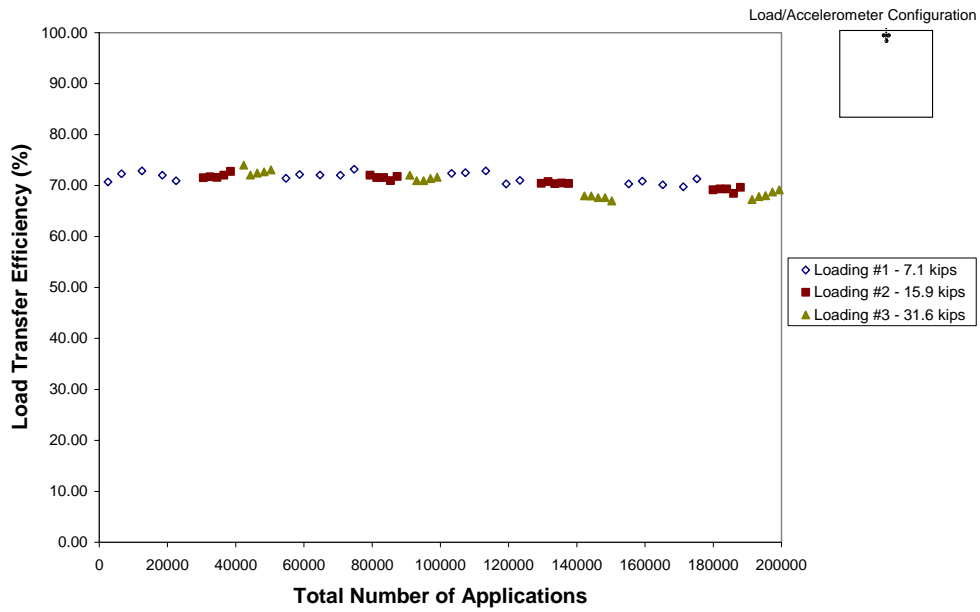


Figure 9.24 – Load Transfer with Applications: North Run-Up – Edge Load Point

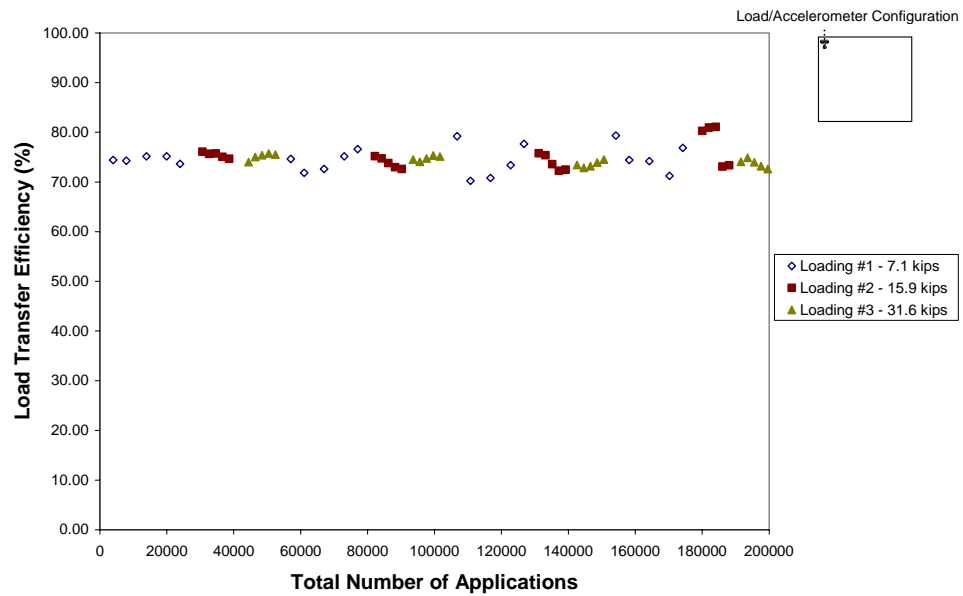


Figure 9.25 – Load Transfer with Applications: North Run-Up – Corner Load Point

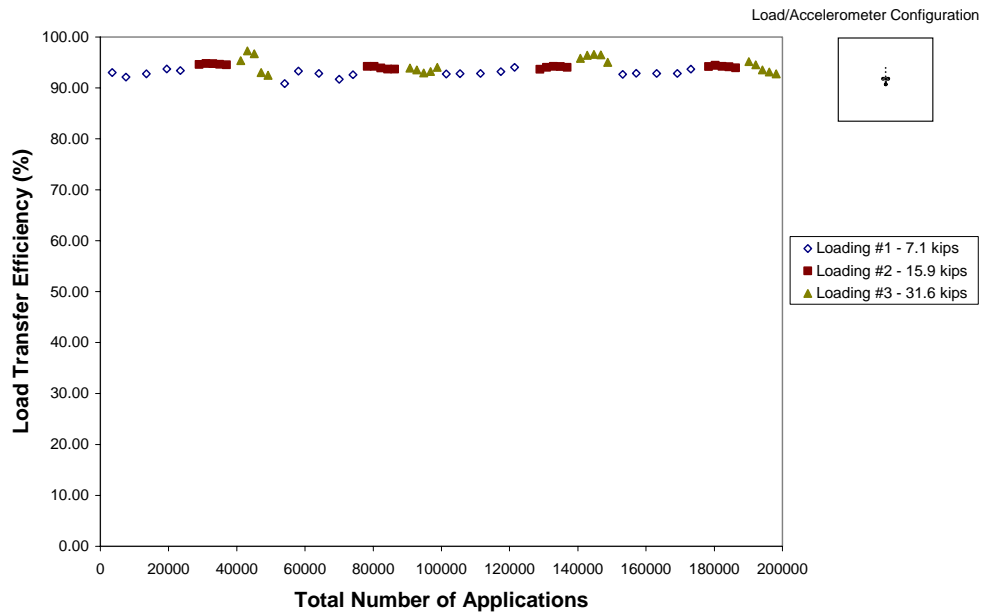


Figure 9.26 – Load Transfer with Applications: South Run-Up – Center Load Point

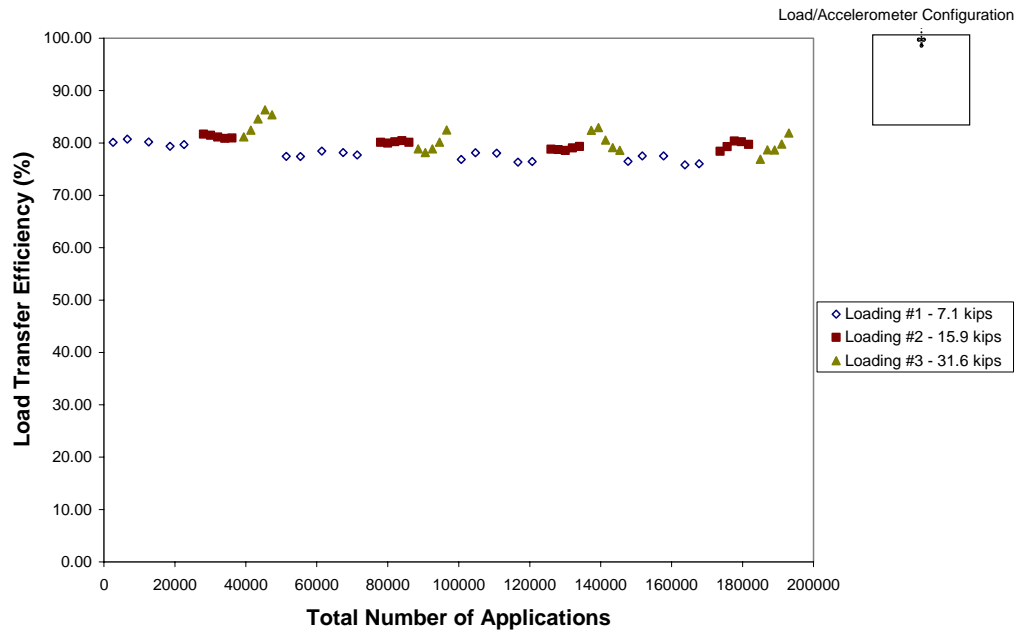


Figure 9.27 – Load Transfer with Applications: South Run-Up – Edge Load Point

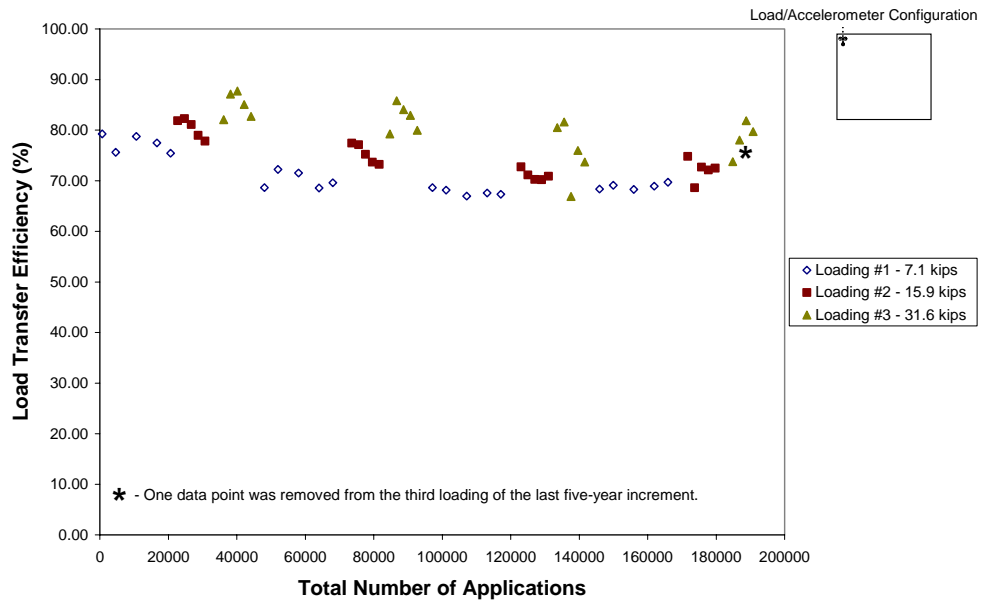


Figure 9.28 – Load Transfer with Applications: South Run-Up – Corner Load Point

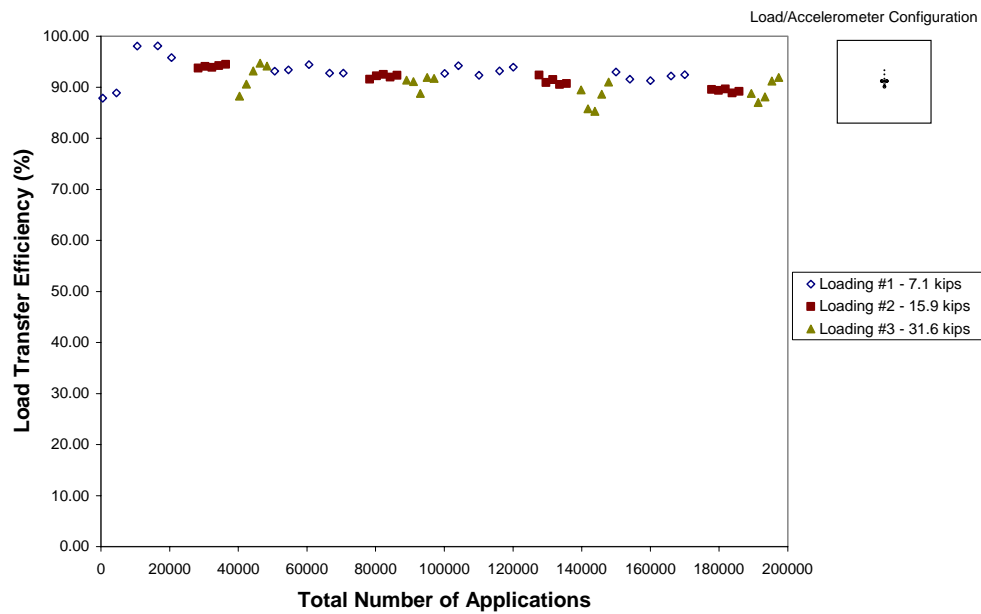


Figure 9.29 – Load Transfer with Applications: Taxiway A6 – Center Load Point

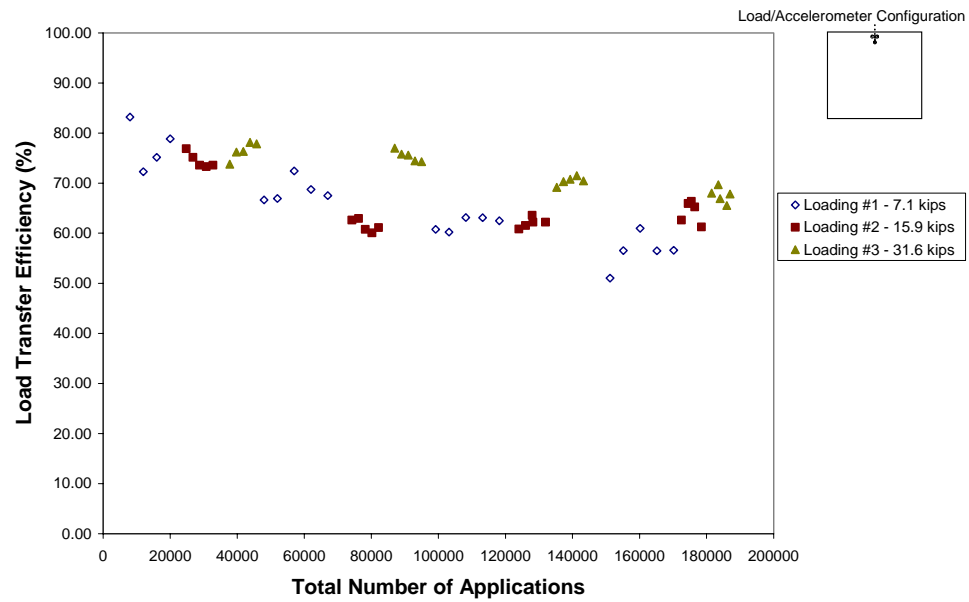


Figure 9.30 – Load Transfer with Applications: Taxiway A6 – Edge Load Point

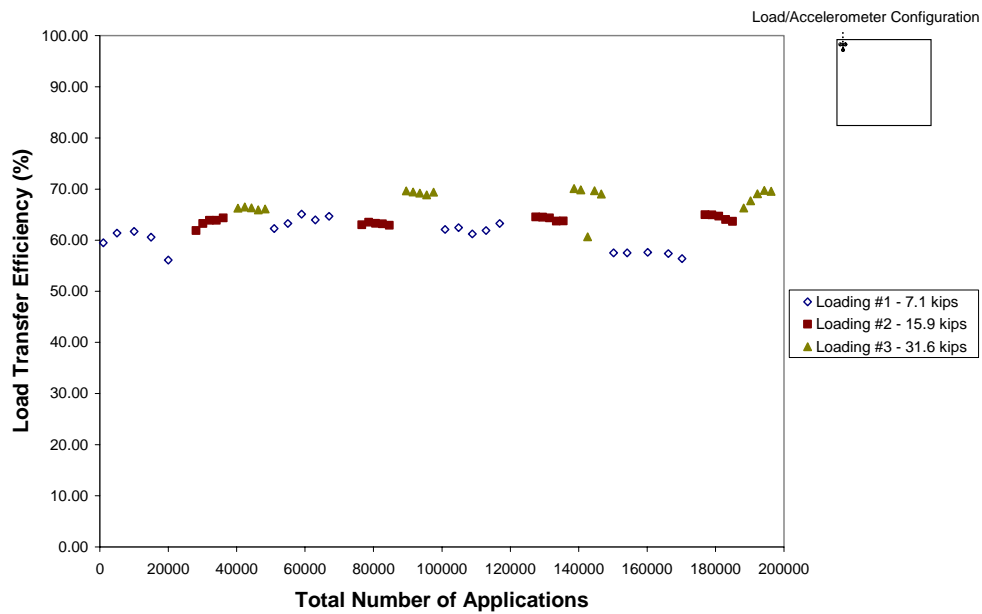


Figure 9.31 – Load Transfer with Applications: Taxiway A6 – Corner Load Point

The observed increase in load transfer efficiency with load level seen predominantly in the South Run-Up and Taxiway A6 locations, is believed to be caused a subsurface mechanism at the joint. The larger deflections imparted by these larger load levels engaged the load transfer mechanism more efficiently. That is to say, there is an apparent movement which is generated at lower load levels at these locations. Once the heavier load is applied, this “free movement” is surpassed causing engagement of a load transfer mechanism. Since this is seen at only the South Run-Up and Taxiway A6 locations, this phenomenon may be attributed to areas with weaker support within the pavement system.

Figure 9.32 pertains to the supplemental testing performed at the final test point (North Run-Up corner loading). It has been included to illustrate the minor trend of slight degradation of load transfer over the course of loading. As seen in the figure, load transfer efficiency continues to degrade at a deliberate pace. This trend, although expected, is extremely minor over the 20-year equivalent cycle and is not indicative of problematic pavement response.

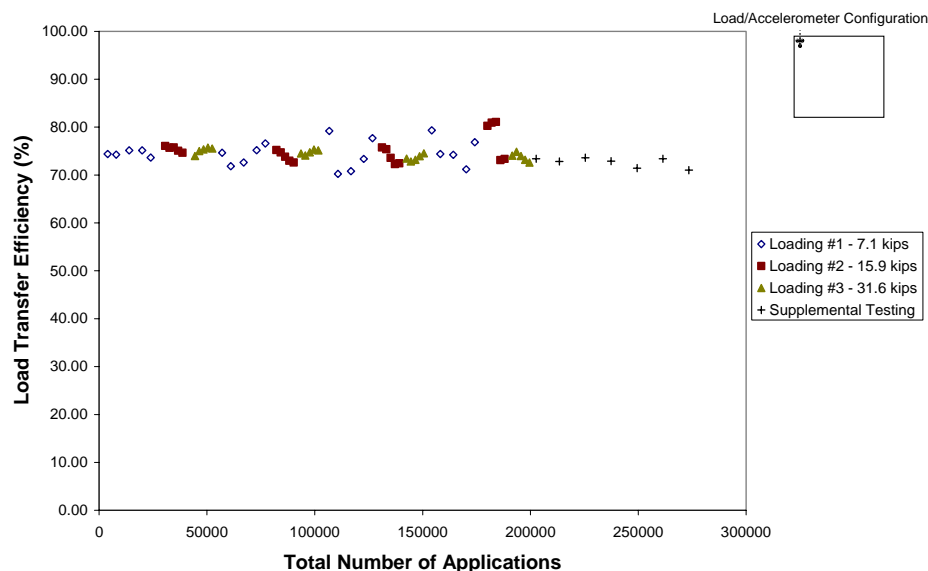


Figure 9.32 – Supplemental Load Transfer Testing: North Run-Up – Corner Load Point

In focusing on the edge load point, a comparison of the overall decrease in load transfer at each location is presented in Figures 9.24, 9.27, and 9.30. As mentioned before, this is the critical loading scenario in examining fatigue under stress in rigid pavements due to the direct loading/unloading caused by the aircraft traffic. The decrease in load transfer was determined by averaging values for load transfer during the first (Years 1-5) and last (Years 16-20) equivalent test increments. Table 9.4 presents these average values, illustrating a slight decrease at the South and North Run-Up with Taxiway A6 once again experiencing a more significant decrease.

Table 9.4 – Decrease in Load Transfer over Duration of Testing

Location	Average Load Transfer Efficiency (%)	
	Years 1-5	Years 16-20
Taxiway A6	76	62
South Run-Up	81	78
North Run-Up	71	69

Variation of Load Transfer Efficiency with Load Level

Figures 9.33 through 9.41 illustrate average load transfer efficiency per five-year loading period with respect to load for each load point. In general terms, load transfer efficiency is nearly independent of load level except for the corner data for the South Run-Up (Figure 9.38) and the edge and corner data for Taxiway A6 (Figure 9.40 and Figure 9.41). As mentioned before, an internal mechanism within the joint may have allowed for degradation in deflection (less load transfer) to occur under lighter loads, while engaging under heavier loads giving the appearance of improved load transfer efficiency with load level. No significant degradation was observed over the course of the five-year loading increments for a given load at the North Run-Up (Figures 9.33 through 9.35). However, the South Run-Up corner load point (Figure 9.38) and Taxiway A6 edge load point (Figure 9.40) exhibited measurable degradation for a

given load. Particularly the Figures 9.38 and 9.40 exhibit a significant decrease over load transfer efficiency when analyzing the data across the five-year incremental testing, at a given load level. An outlying data point was removed from Figure 9.33. This is a result of errant readings from accelerometer #2, the same occurrence as described previously for Figure 9.23.

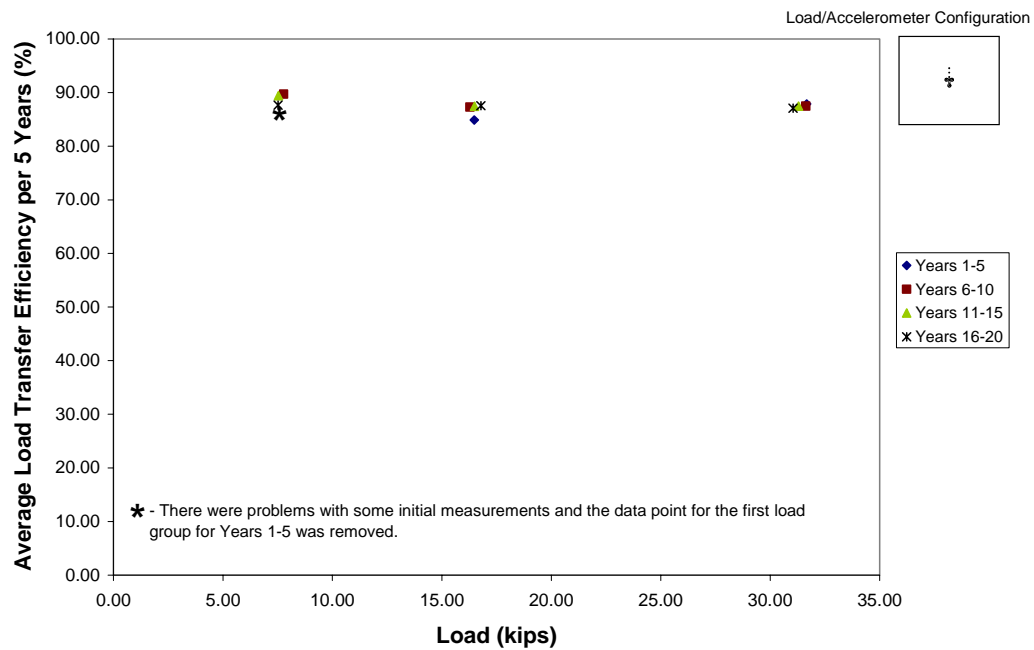


Figure 9.33 – Average Load Transfer Efficiency per Five-Year Load Period with Load Level: North Run-Up – Center Load Point

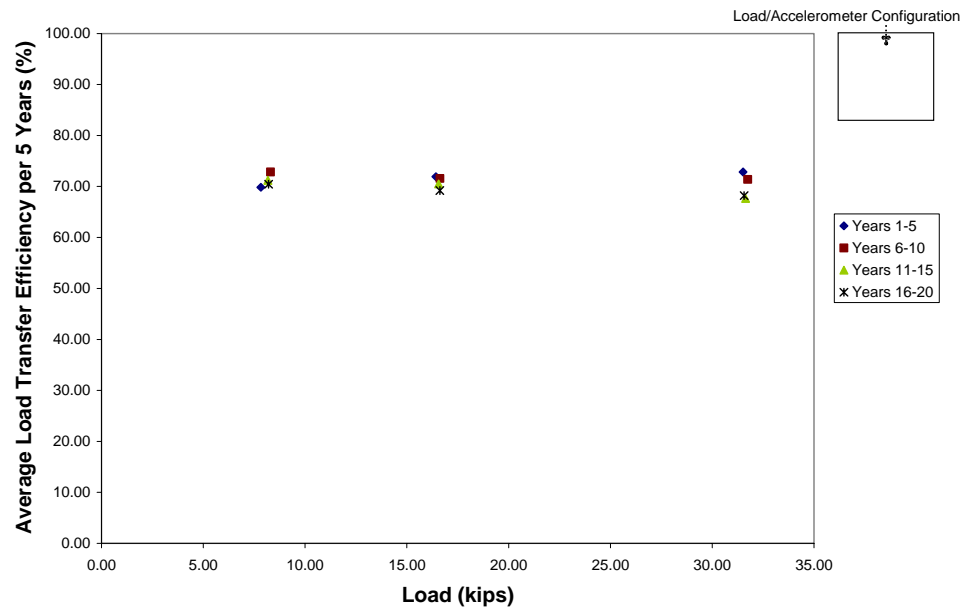


Figure 9.34 – Average Load Transfer Efficiency per Five-Year Load Period with Load Level: North Run-Up – Edge Load Point

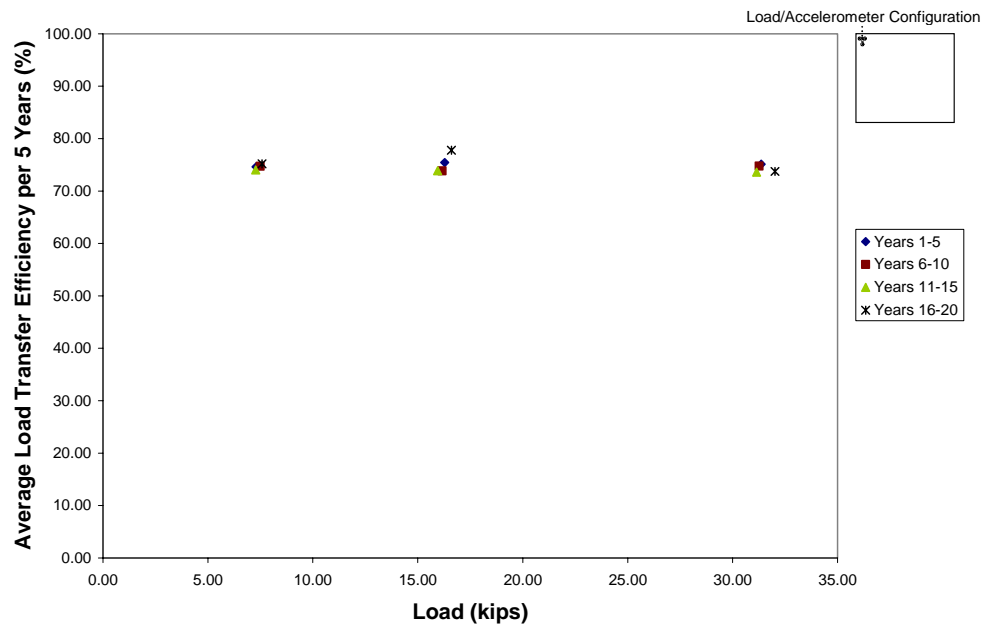


Figure 9.35 – Average Load Transfer Efficiency per Five Year Load Period with Load Level: North Run-Up – Corner Load Point

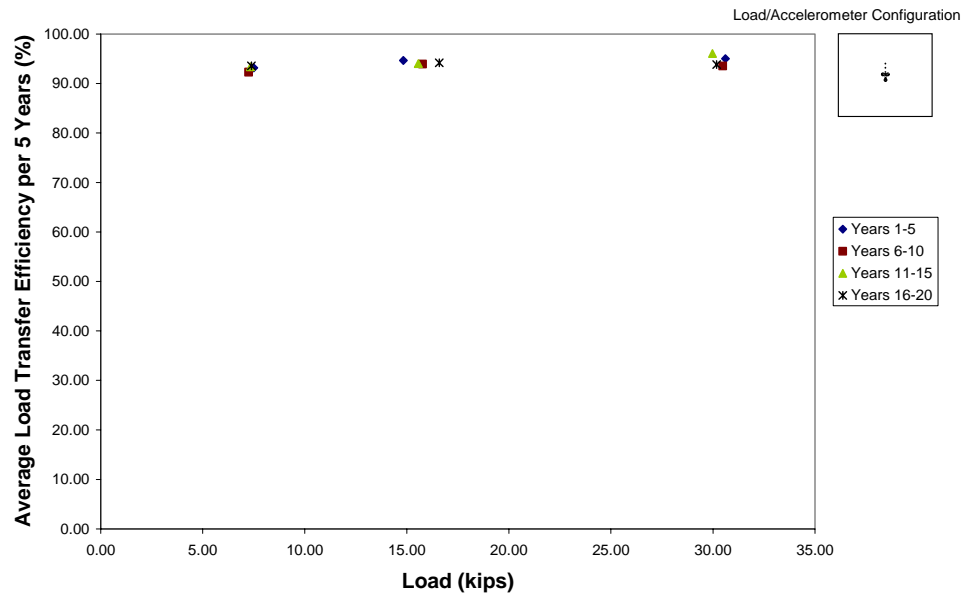


Figure 9.36 – Average Load Transfer Efficiency per Five-Year Load Period with Load Level: South Run-Up – Center Load Point

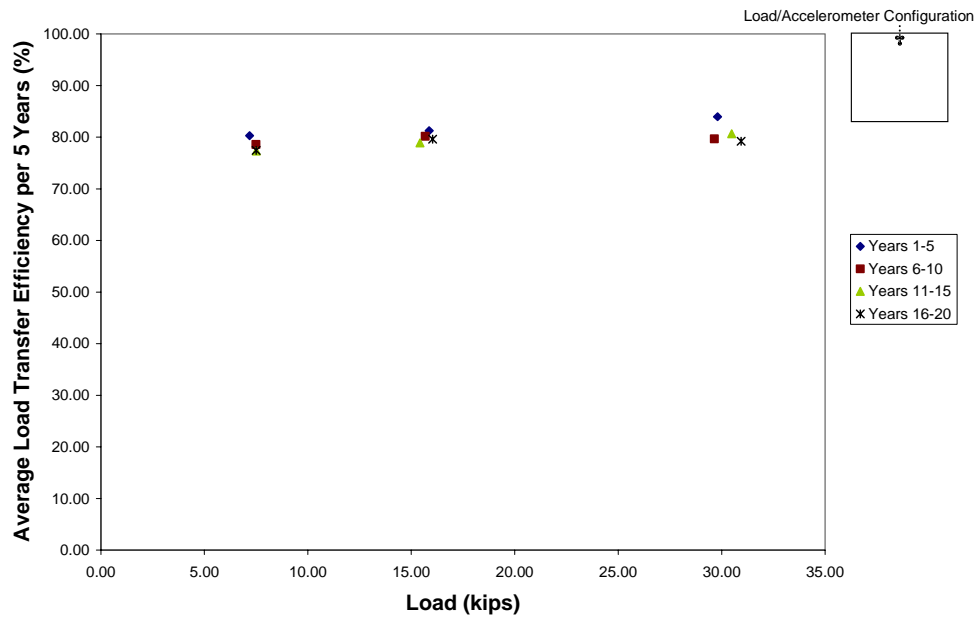


Figure 9.37 – Average Load Transfer Efficiency per Five-Year Load Period with Load Level: South Run-Up – Edge Load Point

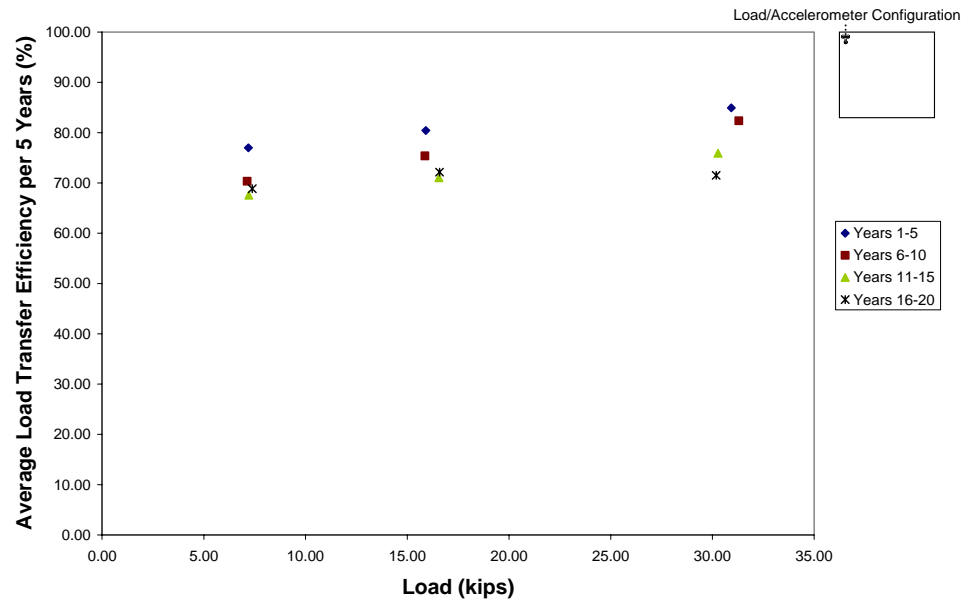


Figure 9.38 – Average Load Transfer Efficiency per Five-Year Load Period with Load Level: South Run-Up – Corner Load Point

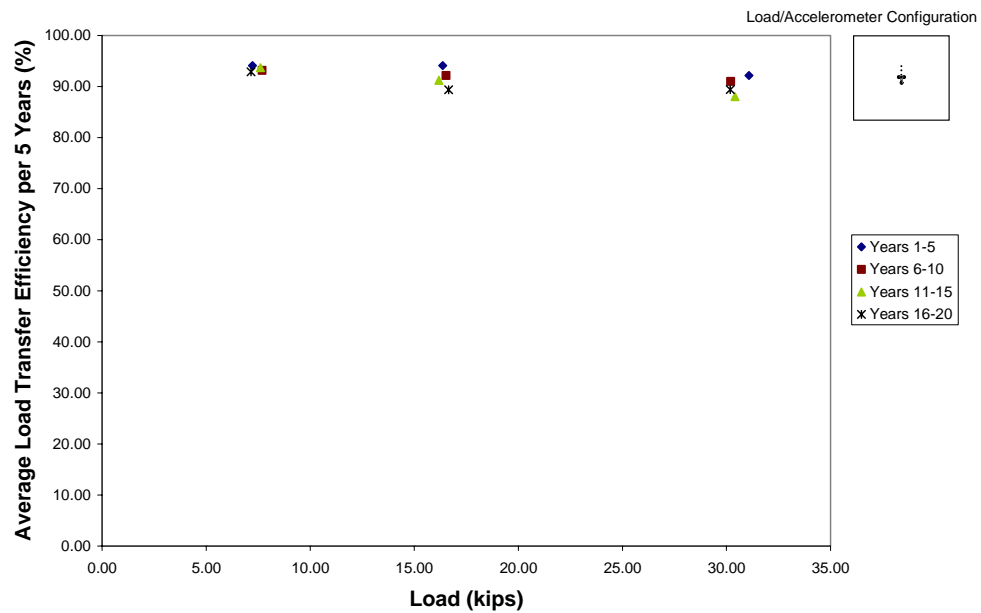


Figure 9.39 – Average Load Transfer Efficiency per Five-Year Load Period with Load Level: Taxiway A6 – Center Load Point

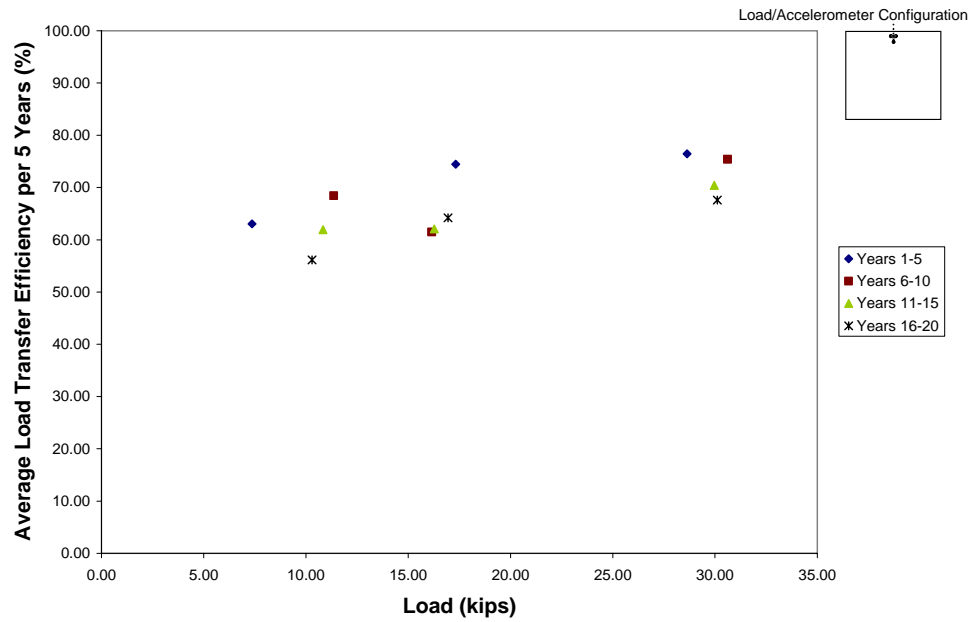


Figure 9.40 – Average Load Transfer Efficiency per Five-Year Load Period with Load Level: Taxiway A6 – Edge Load Point

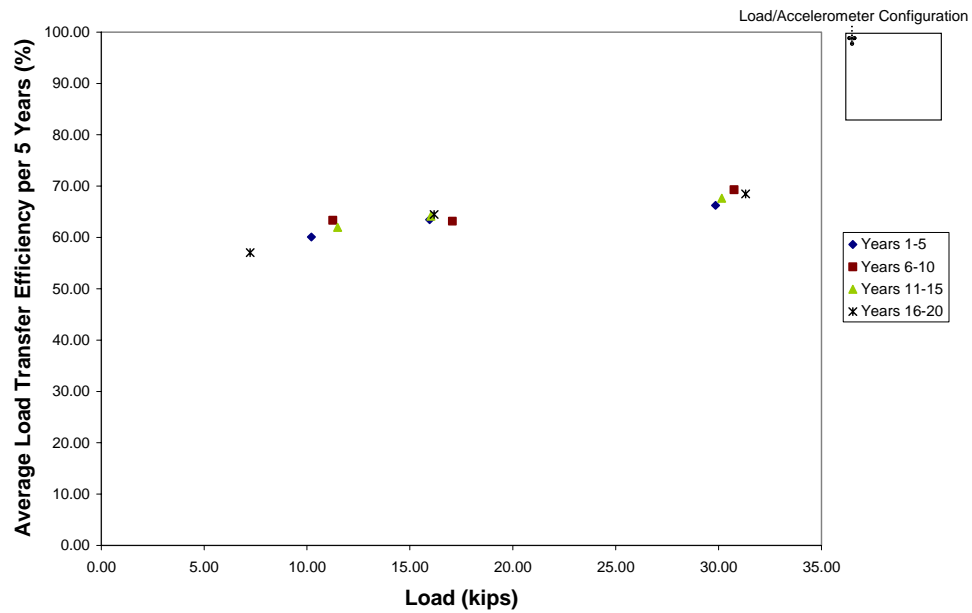


Figure 9.41 – Average Load Transfer Efficiency per Five-Year Load Period with Load Level: Taxiway A6 – Corner Load Point

In addition to examining the average load transfer efficiency with load level at the nine test points, two supplementary cases are presented for further analysis. As mentioned in Section 8.3, two additional accelerometers were installed over the longitudinal joint on the final test point at the North Run-Up corner loading. Section 8.2.2 and Figure 8.1 specifically illustrates the location and dimensions of the accelerometer, joint, load point, and load frame configurations. As with all plots presented thus far, a smaller version of the load/accelerometer configuration has been included in Figure 9.42 for reader orientation. This setup enabled data collection for load transfer efficiency for the longitudinal and transverse joint. In comparing Figure 9.35 with Figure 9.42, the observation is made that the longitudinal joint performed much better yielding load transfer efficiency on the order of 10% greater. From the as-builts, this longitudinal joint is shown to be keyed or tied, whereas the transverse joint was believed to be a dummy joint (no load transfer mechanism). The load transfer efficiency values produced support the expected performance of the two joints.

Data from the supplemental test period at the final location at the corner load point of the North Run-Up is presented to examine load transfer efficiency at the higher supplemental loading. Figure 9.43 illustrates the supplemental loading, adding the average load transfer efficiency data point to the data from the North Run-Up corner load point (Figure 9.35). A slight decrease, on the order of 2%, is observed in comparison with the load transfer efficiency from the third load group. This marginal decrease may be a result of the culmination of degradation over the course of the entire test at the corner point.

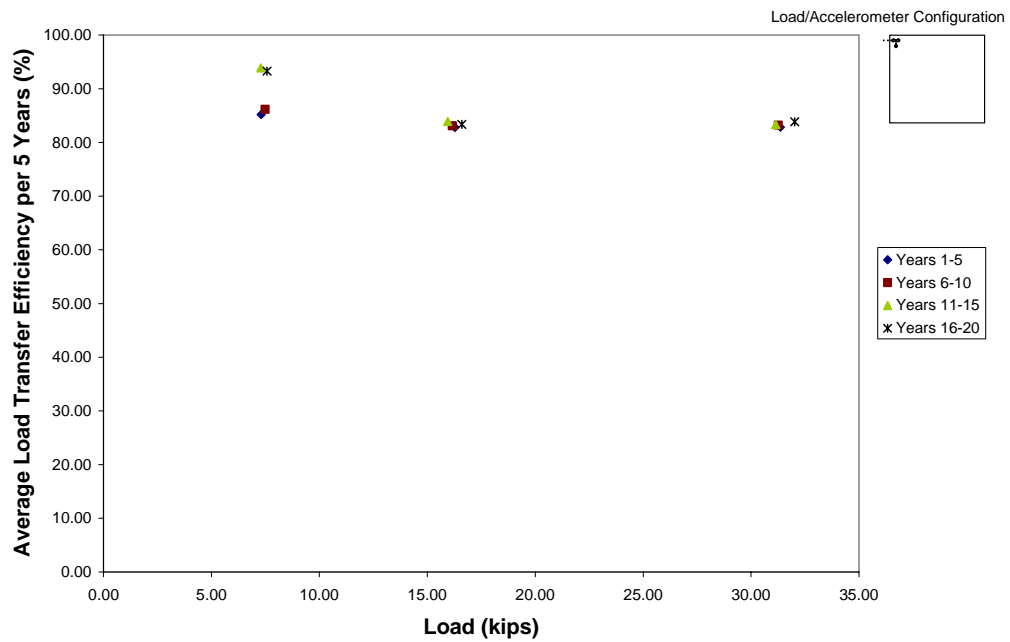


Figure 9.42 – Average Load Transfer Efficiency per Five Years with Load Level: Longitudinal Joint at North Run-Up – Corner Load Point

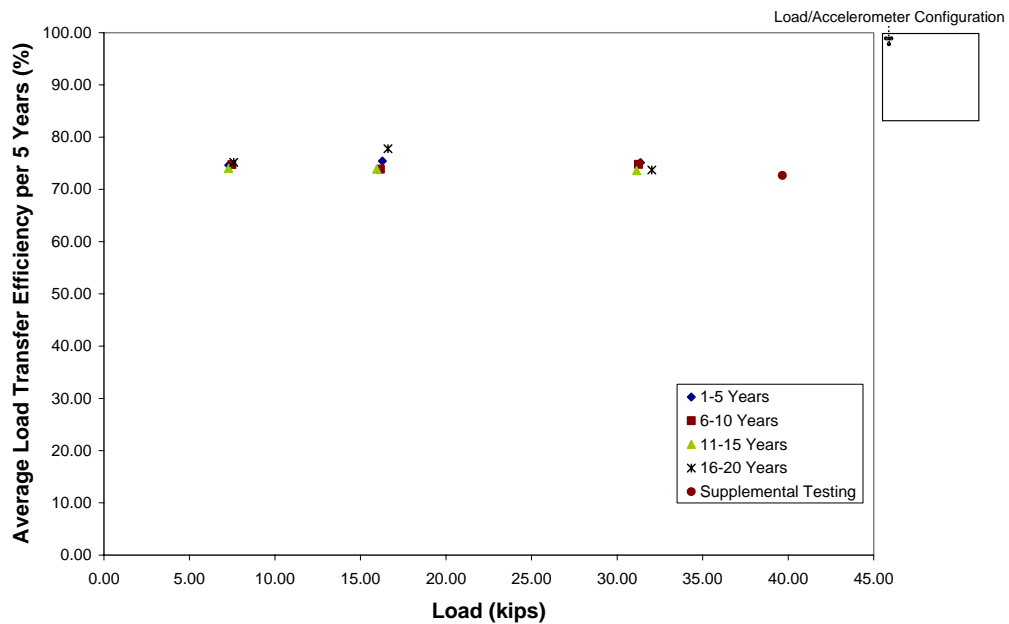


Figure 9.43 – Average Load Transfer Efficiency per Five Years with Load Level: Supplemental Testing at North Run-Up – Corner Load Point

9.4 SUMMARY

In this chapter, further analysis of the observed trends in SDD SAP field measurements are presented. The test results support the consequential roles both external conditions (temperatures and precipitation) and internal conditions (pavement composition and subgrade) have played in the observed pavement response. Temperature (expansion and curling of slabs) and precipitation (expansive clay in subgrade) may have played a significant role in the response at the joints, increasing the observed load transfer efficiency by counteracting any degradation of load transfer, with the total number of load applications that the pavement may have experienced. Both deflection measurements and load transfer efficiencies resulting from the SDD SAP testing have been presented to assess the current state of response of the pavement. Measured deflections with increasing load levels exhibited an approximate linear trend, with nonlinearity being a second order effect. The nonlinear effect was more readily seen when deflections were normalized and viewed with both load level and number of load applications. An increase was observed for average normalized deflections over time for all locations with Taxiway A6 exhibiting the highest increase; as normalized deflection for a specific load grouping increased from the first five-year increment to the last five-year increment. A slight decrease in load transfer efficiency was noted with number of load applications. Higher load levels exhibited higher load transfer efficiency, inferring free movement until a load transfer mechanism took effect. Degradation in the load transfer efficiency was particularly noted at the South Run-Up corner load point and Taxiway A6 edge load point. In general, these trends supported the previous findings in Chapter 8 stating that the North Run-Up exhibited a higher stiffness of the pavement system than South Run-Up and Taxiway A6. Once more, although the investigated locations provided data specific to the area tested, the similarity in composition, age, and construction standards of the selected test locations make observed measurements, conclusions, and assessments applicable to the rigid airfield pavement system, typical to Runway 16/34.

Chapter 10 – Conclusions

10.1 INTRODUCTION

This study involves the field of super-accelerated pavement (SAP) testing. It is the first of its kind to be conducted on an in-service rigid airfield pavement. The majority of APT to date has been performed on controlled pavement test sections. This is the first usage of SDD SAP testing to perform full-scale rigid pavement analysis of an in-service pavement. The following chapter analyzes the results of this testing process and makes a final assessment on the remaining life of Runway 16/34 at Meacham Airport. Future testing and research is discussed, along with its significance, and final recommendations are formulated.

10.2 FINAL ASSESSMENT

The principle goal at the outset of this research was to provide a means of testing Runway 16/34 in order to make an assessment on the remaining life of the rigid airfield pavement. Actual airport traffic data was provided by the FAA to facilitate development of a traffic model. This model enabled determination of a testing scenario which imparted an equivalent of 20 years of future traffic applications over the duration of a short testing period. SDD SAP testing was selected due to its capability to perform a large number of applications over a relatively short period of time, which resulted in less than three hours of actual equipment operation time per test point.

The test pavements performed well, with no manifestations of cracking observed over the course of the entire test program, including the nine separate test points on three different test slabs. Prior to test completion, the research team had anticipated the occurrence of visible signs of distress or the detection of a distinct failure mechanism at a given point in time. This point in time would reflect failure at an equivalent year and ultimately the remaining life of the pavement. In the end, neither a visible sign of failure nor a distinct failure trend within the field

measurements occurred. The pavement structure exhibited typical deflection trends and limited pavement system degradation, even after experiencing very large deflections on the order of 20 to 25 mils. The pavement endured the entire loading scenario, making the results of this research favorable in terms of an expected remaining life, which is predicted to be considerably longer than the 20-year equivalent loading period (assuming all critical loading conditions were properly accounted for in these SAP results).

General trends were observed for both deflection measurements and load transfer efficiency computations. Deflections increased with increased load levels. An approximate linear relationship was observed for deflections with load level. This relationship supports previous findings by Dong and Hayhoe (2002), which were produced at an FAA instrumented test site at Denver International Airport (DIA). Through testing with a Heavy Weight Deflectometer (the heavier version of the FWD), the same linear relationship was seen over varying load levels at both interior (center) and edge loading scenarios. HWD testing was conducted at varying loads up to 55.5 kips, with deflections varying from 6.0 to 6.2 mils at the center of the slab and 9.1 to 13.0 mils at the edge. These data exhibited the same trends produced by SDD SAP testing and are comparable to the SDD SAP results, given the more robust pavement system at DIA. The advantage of SDD SAP testing over HWD testing is the capability of evaluating fatigue over a period of time. The HWD is a discrete test method, capable of delivering only a limited number of load repetitions.

Load transfer efficiency demonstrated a decreasing trend over the total number of applications. Trends noticed between center, edge, and corner test scenarios fell within the expectations, with edge and corner testing experiencing greater deflections. Taxiway A6 and the South Run-Up exhibited a less stiff pavement system response than the North Run-Up location.

The overall observed performance of the pavement system was anticipated, given the predicted traffic loads experienced by each of the three test slab locations. Although comparisons between the RDD deflection profiles of Runway 16/34 and the

candidate test slab were used to select the test locations, in general, the less trafficked test locations exhibited smaller deflections and less load transfer degradation than the more trafficked locations. At this point, a direct comparison can only be based on RDD profiling data. Most likely, the actual runway exhibits somewhat greater trends than those of the outside test locations (i.e. increased deflection and decreased load transfer efficiency). Given the more than adequate response of the pavement system at the test points, the anticipated field performance of the actual runway would still be within an acceptable limit, likewise demonstrating a significant remaining life. This supposition is based solely on similarity in distress conditions and deflection profile between the test points and actual Runway 16/34.

10.2.1 Further Confirmation of SDD SAP Results

In order to further validate the reported findings, a number of finite element programs were employed to determine expected deflections and allowable load repetitions given conditions similar to the field. Prior iterations conducted in EverFE (see Section 5.4) were reexamined for additional information on estimated deflections. A simulation of a sample aircraft, the British Aerospace (BAe) 146 with a single rear gear load of approximately 38.4 kips, was applied via a two-wheel load frame configuration to a similar pavement system. The original purpose of the simulation was to ensure comparable stresses induced by both an actual aircraft gear configuration and the load of that aircraft applied over the load frame, as described in Appendix E. As well as providing stress distribution over the slab, EverFE also calculates maximum deflection under loading. A comparison of field deflections to those forecasted by EverFE could further support the measured results. In addition to EverFE, an alternate computer simulation, Finite Element Analysis FAA (FEAFAA), was employed using the same analysis presented in Appendix E. FEAFAA produced expected deflections for the same aircraft model, the BAe 146. Table 10.1 summarizes deflection data for an edge loading equivalent to a BAe 146. Field

testing equivalent deflection values were obtained through extrapolation of the edge loading scenarios presented in Section 9.2.1 (Figures 9.2, 9.5, and 9.8).

Table 10.1 – Deflection Data Comparison for BAe 146 (Edge Loading)

	Computer Simulations		Field Testing (Extrapolated)		
	EverFE	FEAFAA	Taxiway A6	South Run-Up	North Run-Up
Load	40 kips (BAe 146)	BAe 146	38.4 kips (BAe 146)	38.4 kips (BAe 146)	38.4 kips (BAe 146)
Deflection	23.0 mils	18.6 mils	21.4 mils	21.3 mils	8.0 mils

Table 10.1 illustrates the similar deflections between what was measured in the field and what was expected via simulation. Any difference in the deflection values observed in Table 10.1 could be attributed to the nature of the finite element program and the material parameters assumed for the simulation. As mentioned before, finite element programs have inherent limitations associated with meshing techniques and assumed parameters. The considerably low values for the North Run-Up location correspond to the stiffer pavement profile observed, and could be result of subgrade conditions. The light traffic experienced at the North Run-Up not likely the cause, since finite element programs do not account for fatigue accumulation and therefore a simulated slab is considered newly constructed (no prior traffic).

In addition to comparison of actual field values with expected deflection values, a comparison of actual number of loads induced with estimated allowable loads could further support the field observations and subsequent conclusions regarding pavement life. Pavement-Transportation Computer Assisted Structural Engineering (PCASE) is a robust program developed as a tri-service effort of the United States Army, Air Force, and Navy. The process of utilizing this tool for analysis and associated program assumptions are presented in Appendix L. Table 10.2 summarizes the findings of the analysis. Selected aircraft representative of the three-tiered loading scenario are presented below with allowable passes. An

additional aircraft (Boeing 747) loading was selected to model infrequent heavy loads on Runway 16/34. Although these loads are represented in the testing by additional repetitions in the third load group, analysis of the actual loading of pavement and subsequent allowable passes further validated the testing process.

Table 10.2 – Comparison of Tested Load Repetitions to Allowable Passes

Aircraft Model	Load Group Equivalent	Tested Repetitions (20-Year Period)	Allowable Passes
BAe Jetstream T MK3	No. 1 (7.1 kips)	106,400	Unlimited
DHC Dash 7	No. 2 (15.9 kips)	48,400	54,787,614
BAe 146	No. 3 (31.6 kips)	41,600	70,905
Boeing 747-400	- - none - -	- - none - -	1,114

Calculated allowable passes support the favorable results noted with regard to remaining life of Runway 16/34. The analysis conducted in PCASE does not account for previous loads on the runway, other than through assumptions of material parameters equivalent to actual field conditions. Notwithstanding this fact, the allowable passes were far in excess of the sum of traffic experienced over the past 20 years and traffic expected over the next 20 years. The only exception is the equivalent third group loading (BAe 146), which shows that the allowable passes will be compromised at some time towards the end of the next 20 years, assuming the actual traffic pattern remains consistent with the estimated traffic pattern. It should be noted that the calculated allowable passes takes into account pass-to-coverage ratio, which equates number of operations to actual loading experienced at a given point. In addition, calculation of allowable passes is stochastically based and therefore should be heavily scrutinized when applied to a specific in-service pavement.

10.3 FUTURE TESTING AND RESEARCH

The scope and size of this project placed limitations on the scale of the study conducted at Meacham Airport. Three slabs were tested at each of three load points for a total of nine test points. This testing provided an extensive amount of information on the response to loading of the three tested slabs. Ideally, additional test points could be selected and tested in the future to build a more robust set of data pertaining to the airfield. There is extensive variability associated with a pavement system, including the variance in mixture and construction techniques in constructing the concrete pavement, the variability and potential irregularities associated with the subgrade (compaction, settlement, water content), and the variability in realized loads and usage at a potential test point. By increasing the amount of test points and potential data, a corresponding decrease in data variability will occur.

Increasing the data set for SDD SAP testing conducted under this research would also assist in localizing trends. Additional test slabs selected at different locations would help to develop a deflection trend pattern for the entire airfield area, determining whether certain trends are localized to specific areas or establish prominence over the entire airfield. A broader study could also assist in determining the extent of localization of trends and in corroborating or refuting evidence discovered within this study, such as expected traffic patterns and its governance on determining deflection trends.

Additional testing could also benefit load transfer and joint analysis. Load transfer was strictly examined from the upstream orientation for all cases. Conducting additional edge load testing on the adjacent slab to determine load transfer over the original slab, often referred to as downstream, would help to corroborate or refute load transfer trends. Often, crack propagation under a control joint will not propagate directly to the subgrade. This non-verticality of cracking causes one side to support the other more than the subsequent reverse condition. As a result one slab essentially rests on the other. If the under cutting slab is loaded, joint transfer is less effective; conversely if the superseding slab is loaded additional

support may provide the appearance of a more effective load transfer condition. The end result is an asymmetrical load transfer condition. Additional edge testing could determine if any asymmetrical conditions existed at the test locations.

In addition to the variability mentioned earlier in this section, a parametric field study could be accomplished by adjusting for various environmental conditions. The period of time under which this research was conducted was relatively high in precipitation, extremely warm, with testing conducted during the daylight hours. The concrete was under a large temperature gradient with the surface experiencing extremely high temperatures. This condition could have created a positive curling effect which could play an important role in the observed deflection response, establishing additional tensile stresses on the bottom of the concrete slab. The precipitation certainly affected the highly expansive Denton Clay subgrade. The thermal expansion could have played a role in the load transfer efficiency observed. To better understand and comprehend the controlling mechanisms within this testing, varying these parameters and completing additional test points would be constructive and beneficial. The most straightforward adaptation in testing would be to repeat the previous testing on the same test slabs during cold winter months. The drastically lower temperatures will play a significant role in load transfer and potentially provide downward curling conditions, establishing additional tensile stresses on the top of the concrete slab. Other tests have noted the contraction experienced by concrete under cooler temperatures with pavement systems exhibiting much lower load transfer during the winter months (Dong and Hayhoe, 2002).

Testing directly after a period of low precipitation would also be advantageous, enabling a better understanding of the expansive qualities of the geologic setting of the airfield. Unfortunately, controlling this parameter is extremely difficult if not impractical. Test conditions are often reliant on the time period (season) under which the study is funded and the specific time period under which field testing can be scheduled, as was the case with support originating from end-of-year funds for this study, which required immediate allocation and expenditure.

Again, SDD SAP testing is a new capability for the RDD/SDD vehicle. Due to the newness of the technique and the necessity to observe testing for visual signs of distress, nighttime operations are not recommended at this time. As methods are improved and personnel become more experienced, nighttime operations could be introduced to better understand changes in response which may occur to the airfield within a 24-hour period.

At the end of the SDD SAP testing conducted at Meacham Airport, a supplemental test period commenced for one hour. As mentioned in Section 8.4, this period of testing was an attempt to push the load limit to the highest attainable and equipment-capable load. The testing resulted in a 40-kip peak-to-peak maximum dynamic load. Future tests should attempt to surpass the maximum load tested under this study. In addition, selection of the additional test locations would enable a worse-case scenario selection, which was not attained in this work. If failure is reached in future tests, computations can be made to determine equivalent traffic loading to cause failure, effectively determining remaining life of pavement system and maximum allowable loads.

Along with variations in testing, further investigations of field conditions and pavement structure could be completed for comparative analysis. A soil survey has yet to be conducted since the advent of RDD deflection profiling and SDD SAP testing at Meacham Airport. A complete analysis of the in situ soil conditions and laboratory tests could bring additional validity and support to prior studies. In addition, pulling concrete cores for a full-scale laboratory analysis would provide specific strength data for the PCC in the runway pavement system. It would also enable quantification of load repetitions to failure from laboratory stress ratio determinations.

With supplemental testing and more extensive investigations at Meacham Airport, further examination and analysis of existing data could provide added insight into the current status and future response of the airfield. Due to the current limited scope of this research, a more earnest investigation through future allocation of

manpower for analysis could pay dividends in not only determining status of the Runway 16/34 at Meacham Airport, but also in fully realizing the capabilities of the SDD SAP testing method and analysis. Further in-depth analysis of the linear relationship of deflection with loading could provide insight into the specific parameters and properties of the rigid pavement system. A complete assessment of in situ constraints and parameters of in-service pavements have never been achieved solely through SAP testing. Numerous versions of pavement design and analysis software exist that produce expected deflections under given loads. Through development of a backcalculation capability, either manual backcalculation or program rewrite, parameters that are normally defined or assumed could be determined from measured deflection data. This would enable a more accurate determination of in-service pavement properties never before attainable. It will be important to scrutinize the methodology of any program employed to determine the validity of the backcalculation approach. A program is often limited to the stochastic and/or mechanical foundation upon which it established.

10.4 CONCLUSIONS AND RECOMMENDATIONS

The goal at the outset of this research project was to produce a practical and reliable prediction of remaining life of the pavement on Runway 16/34 at Fort Worth Meacham International Airport. Since an ultimate failure was not observed, a correlation to a quantifiable length in time of remaining life was unattainable. However, given the excellent response of all three test slabs to the 20-year loading equivalence, some broad conclusions can be made. Concerns had existed on whether the current condition of Runway 16/34 would support multiple future years of traffic. This study showed that the pavement sustained the next 20 years of equivalent loading without failure. Given the performance of the three independent test slabs of comparable composition to Runway 16/34 (with varying subgrade conditions), it can be assumed that Runway 16/34 would perform similarly over the next 20 years of

load applications, notwithstanding the effects of time (deterioration) and all other parameters remaining constant (environmental conditions and traffic). Given these constraints, the results of the analysis, and unpredictable future environmental conditions, a reevaluation should be made at a designated time in the future (on the order of five years). Once again, it should be noted that the testing presented herein only supports findings on fatigue distress and load transfer in concrete. A full-scale runway is a superstructure that must be monitored frequently to determine all areas of potential concern. The research presented did not include a full-scale survey and analysis of current runway conditions. Additional causes of distress and potential compromise of pavement integrity need to be addressed separately, such as surface distress and surface roughness. Conclusions have not addressed these potential causes of distress and their respective effect on remaining life.

As mentioned in the previous section, there are many potential opportunities for future testing and research in the development of SDD SAP testing. As opportunities arise, the capability and viability of the SDD SAP testing method will continue to advance the field of APT. It is important that the future testing build on the trends and response discovered in this analysis. As future research endeavors allow, additional testing at Meacham Airport will build on this foundation. It is important that the large volume of data produced under this research not fall to the wayside. Through allocation of future resources, a more in-depth analysis and deeper examination into the response of this pavement could be achieved.

10.5 SUMMARY

This chapter has addressed the final assessment and fundamental conclusions of this research. Two principal findings were produced in this study. First, a lack of crack propagation or ultimate failure was observed for the duration of the SDD SAP testing. Second, an overall excellent response to SDD SAP testing, by three independent test slabs, supported a relatively sufficient remaining life. The variable nature of pavement systems coupled with the indeterminate future effects of outside

sources of distress makes quantifying a specific remaining life impractical. Future testing and research opportunities have been presented for further development of this research and the SDD SAP method.

Appendix A – Sample Meacham Airport Traffic Data

TxDOT Aviation Division obtained a complete set of traffic data for the 6.5 years prior to the testing and analysis conducted herein. These data included every takeoff and landing operation conducted at Meacham Airport from the date starting 1 January 1998 and ending 31 May 2004. This information includes aircraft type, class, and model. In addition, precise takeoff and landing information included departure/arrival time and location. Figure A1 and Figure A2 provide a sample of the traffic data used to develop the traffic model representative of the next 20-year period of operations.

DATE	ACID	FLIGHT PHYSICAL CLASS	AIRCRAFT TYPE	AIRCRAFT NAME	AIRCRAFT COMPANY	AIRCRAFT MAXIMUM WEIGHT	DEPARTURE AIRPORT CODE	DEPARTURE AIRPORT NAME	DEPARTURE TIME	ARRIVAL TIME	ARRIVAL AIRPORT CODE	ARRIVAL AIRPORT NAME	ARRIVAL TIME
1-Jan-98	ASH2002	85600 Jlt	CL65	Regional Jet	Canadair Bombardier	24 FTW	FOU	FORT WORTH MEACHAM	15:43:00	15:43:00	HOU	WILLIAM P HOBBY	16:34:00
1-Jan-98	ASH2003	95707 Jlt	CL65	Regional Jet	Canadair Bombardier	24 FTW	WIL	WILLIAM P HOBBY	16:55:00	16:55:00	FTW	FORT WORTH MEACHAM	17:41:00
1-Jan-98	ASH2004	76917 Jlt	CL65	Regional Jet	Canadair Bombardier	24 FTW	WIL	WILLIAM P HOBBY	18:22:00	18:22:00	HOU	WILLIAM P HOBBY	19:02:00
1-Jan-98	ASH2005	90063 Jlt	CL65	Regional Jet	Canadair Bombardier	24 FTW	WIL	WILLIAM P HOBBY	19:26:00	19:26:00	FTW	FORT WORTH MEACHAM	20:10:00
1-Jan-98	ASH2006	97010 Jlt	CL65	Regional Jet	Canadair Bombardier	24 FTW	WIL	WILLIAM P HOBBY	20:40:00	20:40:00	FTW	FORT WORTH MEACHAM	21:19:00
1-Jan-98	ASH2007	79151 Jlt	CL65	Regional Jet	Canadair Bombardier	24 FTW	WIL	WILLIAM P HOBBY	21:51:00	21:51:00	HOU	WILLIAM P HOBBY	22:36:00
1-Jan-98	ASH2008	79411 Jlt	CL65	Regional Jet	Canadair Bombardier	24 FTW	WIL	WILLIAM P HOBBY	22:00:00	22:00:00	HOU	WILLIAM P HOBBY	22:45:00
1-Jan-98	ASH2009	89480 Jlt	CL65	Regional Jet	Canadair Bombardier	24 FTW	WIL	WILLIAM P HOBBY	04:46:00	04:46:00	FTW	FORT WORTH MEACHAM	1:32:00
1-Jan-98	ASH2102	81790 Jlt	CL65	Regional Jet	Canadair Bombardier	24 FTW	WIL	WILLIAM P HOBBY	15:28:00	15:28:00	SAT	SAN ANTONIO INTL	16:12:00
1-Jan-98	ASH2103	92243 Jlt	CL65	Regional Jet	Canadair Bombardier	24 SAT	SAN	SAN ANTONIO INTL	15:46:00	15:46:00	FTW	FORT WORTH MEACHAM	17:43:00
1-Jan-98	ASH2104	69460 Jlt	CL65	Regional Jet	Canadair Bombardier	24 FTW	WIL	WILLIAM P HOBBY	17:54:00	17:54:00	SAT	SAN ANTONIO INTL	18:38:00
1-Jan-98	ASH2105	86703 Jlt	CL65	Regional Jet	Canadair Bombardier	24 SAT	SAN	SAN ANTONIO INTL	19:02:00	19:02:00	FTW	FORT WORTH MEACHAM	19:59:00
1-Jan-98	ASH2106	87496 Jlt	CL65	Regional Jet	Canadair Bombardier	24 SAT	SAN	SAN ANTONIO INTL	20:00:00	20:00:00	FTW	FORT WORTH MEACHAM	20:45:00
1-Jan-98	ASH2107	67496 Jlt	CL65	Regional Jet	Canadair Bombardier	24 SAT	SAN	SAN ANTONIO INTL	21:32:00	21:32:00	FTW	FORT WORTH MEACHAM	22:25:00
1-Jan-98	ASH2108	72009 Jlt	CL65	Regional Jet	Canadair Bombardier	24 FTW	WIL	WILLIAM P HOBBY	22:42:00	22:42:00	SAT	SAN ANTONIO INTL	23:28:00
1-Jan-98	ASH2402	71807 Jlt	CL65	Regional Jet	Canadair Bombardier	24 FTW	WIL	WILLIAM P HOBBY	14:20:00	14:20:00	AUS	ROBERT MUELLER MUNI	14:53:00
1-Jan-98	ASH2403	84660 Jlt	CL65	Regional Jet	Canadair Bombardier	24 AUS	ROB	ROBERT MUELLER MUNI	15:27:00	15:27:00	FTW	FORT WORTH MEACHAM	16:15:00
1-Jan-98	ASH2404	92857 Jlt	CL65	Regional Jet	Canadair Bombardier	24 FTW	WIL	WILLIAM P HOBBY	15:28:00	15:28:00	AUS	ROBERT MUELLER MUNI	17:03:00
1-Jan-98	ASH2405	84147 Jlt	CL65	Regional Jet	Canadair Bombardier	24 FTW	WIL	WILLIAM P HOBBY	15:38:00	15:38:00	AUS	ROBERT MUELLER MUNI	17:12:00
1-Jan-98	ASH2406	84147 Jlt	CL65	Regional Jet	Canadair Bombardier	24 FTW	WIL	WILLIAM P HOBBY	18:38:00	18:38:00	AUS	ROBERT MUELLER MUNI	19:12:00
1-Jan-98	ASH2407	93910 Jlt	CL65	Regional Jet	Canadair Bombardier	24 AUS	ROB	ROBERT MUELLER MUNI	20:01:00	20:01:00	FTW	FORT WORTH MEACHAM	20:51:00
1-Jan-98	ASH2408	66512 Jlt	CL65	Regional Jet	Canadair Bombardier	24 FTW	WIL	WILLIAM P HOBBY	21:12:00	21:12:00	AUS	ROBERT MUELLER MUNI	21:50:00
1-Jan-98	ASH2409	72585 Jlt	CL65	Regional Jet	Canadair Bombardier	24 AUS	ROB	ROBERT MUELLER MUNI	22:36:00	22:36:00	FTW	FORT WORTH MEACHAM	23:25:00
1-Jan-98	ASH2410	76964 Jlt	CL65	Regional Jet	Canadair Bombardier	24 FTW	WIL	WILLIAM P HOBBY	23:36:00	23:36:00	AUS	ROBERT MUELLER MUNI	0:08:00
1-Jan-98	ASH2433	135962 Turbo	C309	Jetstar	Cessna Aircraft	5 T1A	TUL	TULSA INTL	14:38:00	14:38:00	FTW	FORT WORTH MEACHAM	15:25:00
1-Jan-98	M11273	108611 Jlt	L329	Jetstar	Lockhead Corp	21 FTW	WIL	FORT WORTH MEACHAM	23:48:00	23:48:00	MIA	MIAMI INTL	4:15:00
1-Jan-98	M11273	121411 Jlt	L329	Jetstar	Lockhead Corp	21 PHK	PHN	PHOENIX SKY MABOR INTL	5:11:00	5:11:00	FTW	FORT WORTH MEACHAM	6:56:00
1-Jan-98	M1699	103489 Jlt	G2	Gulfstream II	Gulfstream American	52 FTW	WIL	WILLIAM P HOBBY	21:32:00	21:32:00	BFI	BOEING FIELD/KING COUNTY INTL	1:24:00
1-Jan-98	M1699	111625 Jlt	GUJF	Aero Star	Gunnman	17 JAK	JAC	JACKSONVILLE INTL	18:38:00	18:38:00	FTW	FORT WORTH MEACHAM	20:59:00
1-Jan-98	M2655	107955 Piston	CL52	Boeing Stearman	Piper Aircraft	1 FTW	WIL	FORT WORTH MEACHAM	19:07:00	19:07:00	CHP	CHRYSLER FIELD	3:58:00
1-Jan-98	M3164M	110265 Piston	BE76	Ducless 76	Boeing Stearman	2 RVS	RIC	RICHARD LLOYD JONES JR	21:40:00	21:40:00	FTW	FORT WORTH MEACHAM	22:30:00
1-Jan-98	M5164M	124777 Piston	BE76	Ducless 76	Boeing Stearman	2 RVS	RIC	RICHARD LLOYD JONES JR	14:06:00	14:06:00	FTW	FORT WORTH MEACHAM	16:31:00
1-Jan-98	M53AM	111042 Turbo	P31T	Cherokee	Boeing Stearman	5 E38	APN	ALPINE-CASPARIS MUNICIPAL	15:50:00	15:50:00	RVS	RICHARD LLOYD JONES JR	18:08:00
1-Jan-98	M53AM	123832 Turbo	P31T	Cherokee	Piper Aircraft	5 FTW	APN	ALPINE-CASPARIS MUNICIPAL	17:00:00	17:00:00	FTW	FORT WORTH MEACHAM	18:42:00
1-Jan-98	M53880	146702 Piston	P428	Cherokee	Piper Aircraft	5 FTW	WIL	WILLIAM P HOBBY	13:54:00	13:54:00	E38	ALPINE-CASPARIS MUNICIPAL	15:35:00
1-Jan-98	M53880	146702 Piston	P428	Cherokee	Piper Aircraft	5 FTW	WIL	WILLIAM P HOBBY	15:55:00	15:55:00	MWL	MINERAL WELLS	16:20:00
1-Jan-98	M67437	100235 Piston	C310	M65 Rocket/Turbo	Piper Aircraft	3 NEW	LAK	LAKEFRONT	20:53:00	20:53:00	MKT	MURFREESBORO MUNI	23:57:00
1-Jan-98	M67437	110034 Piston	C310	M65 Rocket/Turbo	Piper Aircraft	3 NEW	LAK	LAKEFRONT	15:58:00	15:58:00	FTW	FORT WORTH MEACHAM	18:34:00
1-Jan-98	M7009P	112084 Not Determined	TBM7	TBM TB-700	Aerospatale/France	3 ELP	EL	EL PASO INTL	18:19:00	18:19:00	FTW	FORT WORTH MEACHAM	20:06:00
1-Jan-98	M766M4	101795 Jlt	C650	Citation 3/6/7	Cessna Aircraft	11 HOU	WIL	WILLIAM P HOBBY	20:14:00	20:14:00	FTW	FORT WORTH MEACHAM	21:01:00
1-Jan-98	M766M4	111605 Jlt	C650	Citation 3/6/7	Cessna Aircraft	11 GUC	GUN	GUNNISON COUNTY	17:14:00	17:14:00	FTW	FORT WORTH MEACHAM	18:42:00
1-Jan-98	M840P	119911 Jlt	B410	Boeing Stearman	Boeing Stearman	14 FTW	WIL	WILLIAM P HOBBY	17:10:00	17:10:00	EDG	EDWARDS AIRFIELD	18:42:00
1-Jan-98	M840P	129911 Jlt	B410	Boeing Stearman	Boeing Stearman	14 FTW	WIL	WILLIAM P HOBBY	17:10:00	17:10:00	EDG	EDWARDS AIRFIELD	19:15:00
1-Jan-98	M852R8	98844 Piston	BE55	Baron S5/Cherokee	Boeing Stearman	3 FTW	WIL	WILLIAM P HOBBY	16:36:00	16:36:00	DWH	DAVID WAYNE HOOKS MEMORIAL, TX	17:54:00
1-Jan-98	M94AM	127567 Turbo	BE50	King Air 90	Boeing Stearman	5 CLL	EAS	EASTERNWOOD FIELD	16:29:00	16:29:00	FTW	FORT WORTH MEACHAM	17:21:00
1-Jan-98	M960FA	129150 Jlt	WV24	Westwind 1124	Boeing Stearman	11 FTW	WIL	WILLIAM P HOBBY	15:05:00	15:05:00	ASE	ASPEN-PITKIN CO/SARDY FIELD	17:56:00
1-Jan-98	ASH2000	3224 Jlt	CL65	Regional Jet	Canadair Bombardier	24 FTW	WIL	WILLIAM P HOBBY	13:14:00	13:14:00	HOU	WILLIAM P HOBBY	13:55:00
1-Jan-98	ASH2001	3224 Jlt	CL65	Regional Jet	Canadair Bombardier	24 FTW	WIL	WILLIAM P HOBBY	13:14:00	13:14:00	HOU	WILLIAM P HOBBY	13:55:00
1-Jan-98	ASH2002	12990 Jlt	CL65	Regional Jet	Canadair Bombardier	24 FTW	WIL	WILLIAM P HOBBY	15:42:00	15:42:00	HOU	WILLIAM P HOBBY	16:30:00
1-Jan-98	ASH2003	31672 Jlt	CL65	Regional Jet	Canadair Bombardier	24 FTW	WIL	WILLIAM P HOBBY	15:56:00	15:56:00	FTW	FORT WORTH MEACHAM	17:46:00
1-Jan-98	ASH2004	14823 Jlt	CL65	Regional Jet	Canadair Bombardier	24 FTW	WIL	WILLIAM P HOBBY	18:29:00	18:29:00	HOU	WILLIAM P HOBBY	19:07:00
1-Jan-98	ASH2005	188002 Jlt	CL65	Regional Jet	Canadair Bombardier	24 FTW	WIL	WILLIAM P HOBBY	19:41:00	19:41:00	FTW	FORT WORTH MEACHAM	20:29:00
1-Jan-98	ASH2006	21997 Jlt	CL65	Regional Jet	Canadair Bombardier	24 FTW	WIL	WILLIAM P HOBBY	21:06:00	21:06:00	FTW	FORT WORTH MEACHAM	21:50:00
1-Jan-98	ASH2007	20923 Jlt	CL65	Regional Jet	Canadair Bombardier	24 HOU	WIL	WILLIAM P HOBBY	22:28:00	22:28:00	FTW	FORT WORTH MEACHAM	23:20:00
1-Jan-98	ASH2008	13820 Jlt	CL65	Regional Jet	Canadair Bombardier	24 HOU	WIL	WILLIAM P HOBBY	02:26:00	02:26:00	FTW	FORT WORTH MEACHAM	11:11:00
1-Jan-98	ASH2009	13820 Jlt	CL65	Regional Jet	Canadair Bombardier	24 HOU	WIL	WILLIAM P HOBBY	02:26:00	02:26:00	FTW	FORT WORTH MEACHAM	11:11:00
1-Jan-98	ASH2100	1460 Jlt	CL65	Regional Jet	Canadair Bombardier	24 FTW	WIL	WILLIAM P HOBBY	12:40:00	12:40:00	SAT	SAN ANTONIO INTL	13:24:00
1-Jan-98	ASH2101	5488 Jlt	CL65	Regional Jet	Canadair Bombardier	24 SAT	SAN	SAN ANTONIO INTL	13:50:00	13:50:00	FTW	FORT WORTH MEACHAM	14:33:00
1-Jan-98	ASH2102	10575 Jlt	CL65	Regional Jet	Canadair Bombardier	24 FTW	WIL	WILLIAM P HOBBY	15:06:00	15:06:00	SAT	SAN ANTONIO INTL	14:33:00
1-Jan-98	ASH2103	26937 Jlt	CL65	Regional Jet	Canadair Bombardier	24 SAT	SAN	SAN ANTONIO INTL	15:21:00	15:21:00	FTW	FORT WORTH MEACHAM	15:49:00
1-Jan-98	ASH2104	10575 Jlt	CL65	Regional Jet	Canadair Bombardier	24 SAT	SAN	SAN ANTONIO INTL	15:21:00	15:21:00	FTW	FORT WORTH MEACHAM	15:49:00
1-Jan-98	ASH2105	17255 Jlt	CL65	Regional Jet	Canadair Bombardier	24 SAT	SAN	SAN ANTONIO INTL	15:52:00	15:52:00	FTW	FORT WORTH MEACHAM	16:39:00

Figure A1 – Sample Traffic – January 1998

Appendix B – Summary of Analysis of Two-Wheel Versus Three-Wheel Load Frame Configuration

The 3D finite element analysis tool, EverFE, was employed to determine stresses induced by either a two-wheel or three-wheel configuration. Since a dry run test of the different load frame configurations could not be carried out until field work commenced, it was imperative to determine load grouping equivalents for both two-wheel and three-wheel cases to be prepared for use of either configuration. As mentioned in Section 5.4, the two-wheel configuration was the preferred method, since it was a closer representation of the predominant dual-wheel loading, experienced by Runway 16/34. However, the three-wheel configuration would be used if deemed necessary, due to stability issues during operations.

EverFE is designed for highway applications with limitations on thickness of layers. Runway analysis is limited with this program because of a maximum pavement thickness of 12 in., however due to the relatively thin pavement thickness (9 or 10 in.) of Runway 16/34 this program provided a reasonable approximation. Depths were set at the predominant construction tolerances for the runway: 9 in. for the PCC, 5 in. for the base, and 6 in. for the subbase. Elastic moduli and Poisson's ratio were left at the typical values provided by the program: 4,000 ksi and 0.20 for PCC, 750 ksi and 0.20 for base, and 25 ksi and 0.20 for subbase. An analysis was run for a series of different loadings (18, 24, and 30 kips) for both two-wheel and three-wheel configurations on a three-by-three slab representation. The field slab dimensions of 25 ft in length and width was used. The advantage of utilizing EverFE was ease of use, minimal computation time required, and the ability to model any loading footprint desired. Exact dimensions of the footprint for two-wheel and three-wheel configurations were reproduced. Once again, it was assumed that the load was distributed equally in both load configurations. Table A1 presents the compressive

stress, tensile stress, and deflections determined for each scenario. As expected, the two-wheel configuration produced higher stresses in the slab.

Table A1 – EverFE Analysis of Two-Wheel and Three-Wheel Configurations

Load (kips)	Load Configuration	Load Scenario	Compressive Stress, σ (ksi) @ PCC Surface	Tensile Stress, σ (ksi) @ Bottom of PCC Layer	Deflection, δ (in.) @ PCC Surface
18.0	Two-Wheel	Center	-0.228	0.185	0.019
		Edge	-0.210	0.173	0.023
		Corner	-0.204	0.132	0.024
18.0	Three-Wheel	Center	-0.194	0.157	0.019
		Edge	-0.183	0.150	0.022
		Corner	-0.161	0.104	0.023
24.0	Two-Wheel	Center	-0.305	0.247	0.023
		Edge	-0.269	0.215	0.027
		Corner	-0.264	0.151	0.029
24.0	Three-Wheel	Center	-0.259	0.209	0.023
		Edge	-0.250	0.205	0.026
		Corner	-0.207	0.119	0.028
36.0	Two-Wheel	Center	-0.343	0.277	0.025
		Edge	-0.336	0.268	0.032
		Corner	-0.329	0.188	0.035
36.0	Three-Wheel	Center	-0.324	0.261	0.026
		Edge	-0.300	0.240	0.031
		Corner	-0.247	0.136	0.031

After further research and determination of the characteristics of typical runway pavement (PCA, 2004), the aforementioned parameters of the pavement system were altered to better represent field conditions (cemented base, lime-treated subbase). Elastic moduli and Poisson's ratio for each layer changed respectively: 4,000 ksi and 0.15 for PCC, 2000 ksi and 0.20 for base, and 1000 ksi and 0.20 for subbase. A sensitivity analysis was re-accomplished in EverFE to determine changes to induced stress with the more representative, stiffer model. Compressive stress at the surface decreased 61% to 62% and the tensile stress at the bottom of the PCC layer decreased 37% to 45%, under these more accurate parameters. Since the percentage drop was consistent across the different loads and loading configurations, the relationships presented in Table 1 could be utilized. With tensile stress being the controlling stress in concrete, an analysis was conducted to determine the percentage increase required to have a three-wheel load represent a two-wheel load. Sensitivity analysis was performed for center, edge, and corner loading scenario. Results of percentage increase proved to be consistent for each loading scenario as seen in Table A2.

Table A2 – Relating Three-Wheel to Two-Wheel Load Frame Configuration

Loading Scenario	Percentage of Two-Wheel Induced Tensile Stress by a Three-Wheel for the Same Given Load	Increase Factor Required for Three-Wheel Scenario
Three-Wheel - Center	88	1.1
Three-Wheel - Edge	90	1.1
Three-Wheel - Corner	77	1.3

For the purpose of this research, the two-wheel load frame configuration proved stable and effective. Had the three-wheel load frame configuration been required for stability, a process similar to that presented for modeling heavy loads would have been incorporated using Miner's hypothesis (See Section 6.5). This data

has been included for possible use in future research requirements which may incorporate varying load configurations.

Appendix C – Reduction of Traffic History – January 1998 – May 2004

The raw traffic data provided by the FAA was initially compiled by the TxDOT Aviation Division, as presented in Appendix A. After reducing the more than 150,000 operations, the TxDOT Aviation Division assimilated the single operations by type of aircraft and included pertinent data, specific to each type of aircraft. The author received this reduced raw data, and through analysis and merging of operations, of similar aircraft with equivalent weights, extensive reduction was achieved into 121 aircraft line items. Along with reducing the data, the writer continued determination of parameters of each aircraft type. The final aircraft line items, with associated limits used in traffic model determination, are presented in Figures C1, C2, and C3. Aircraft types are listed in order of least to greatest single rear gear assembly loading.

Aircraft Model			Model - Series										Type Designator	1988-2004 Ops										Total Ops Jan 1998 to May 2004	Gear Config.	Max Takeoff Weight (lbs)	Max Landing Weight (lbs)	Avg. Load (MTOW + MLW)/2	Load/Rear Assembly	Load/Tire	Avg Ops/FY	% of traffic > 10,000 lb	Number & Type of Engines / Weight Class	Additional Comments																																																																																																																																																																																																																																																																																																																																																																																																																																																																																																																																																								
100 King Air (U-21F Ute) Guststream Aerospace 5000 Citation, Citation 1 501 Citation TSP Mitsubishi Fokker Piper PA-42-720 Cheyenne 3 PA-42-1000 Cheyenne 400 DHC-6 Twin Otter, UV-18, CC-138 Fokker 10 Merlin 2 Lejeal 24 EMB-110/111 Bandeirante (C-95, Citation 11) F-86 Sabre 300 Super King Air 200/1300 Super King Air, (C-12,T101,Huron) Fairchild 328 Lejeal 25 Lejeal 28, 29 Lejeal 23 BAC-3100 Jetstream 31 (T Mk 3) MU-300 Diamond Lejeal 31 400 Beechjet (T-1 Jayhawk, T-400) 560 Citation5/Ultra/Ultra Encore(UC-35,OT-citation V 550, S550, 552 Citation 2/S2/Bravo (T-47, U-s550 citation11 C-26 Metroliner Beech 1900 35, 36 (C-21, RC-35, RC-36, U-36) Dassault Falcon 10 Lejeal 55 Lejeal 60 1123 Westwind 650 Citation 3/6/7 1124 Westwind Israeli Asra 1125 Westwind ASTR 1125 330, Sherpa (C-23), SD3-30 Rockwell Sabreliner 65 BAC-3200 Jetstream Super 31			1988 Ops	1989 Ops	1990 Ops	2000 Ops	2001 Ops	2002 Ops	2003 Ops	2004 Jan-Ops	Ops	2004 May-Ops	2004 Total	2004 Jan-May	2004 Ops	2004 Total	2004 Jan-May	2004 Ops	2004 Total	2004 Jan-May	2004 Ops	2004 Total	2004 Jan-May	2004 Ops	2004 Total	2004 Jan-May	2004 Ops	2004 Total	2004 Jan-May	2004 Ops	2004 Total	2004 Jan-May	2004 Ops	2004 Total	2004 Jan-May	2004 Ops	2004 Total	2004 Jan-May	2004 Ops	2004 Total	2004 Jan-May	2004 Ops	2004 Total	2004 Jan-May	2004 Ops	2004 Total	2004 Jan-May	2004 Ops	2004 Total	2004 Jan-May	2004 Ops	2004 Total	2004 Jan-May	2004 Ops	2004 Total	2004 Jan-May	2004 Ops	2004 Total	2004 Jan-May	2004 Ops	2004 Total	2004 Jan-May	2004 Ops	2004 Total	2004 Jan-May	2004 Ops	2004 Total	2004 Jan-May	2004 Ops	2004 Total	2004 Jan-May	2004 Ops	2004 Total	2004 Jan-May	2004 Ops	2004 Total	2004 Jan-May	2004 Ops	2004 Total	2004 Jan-May	2004 Ops	2004 Total	2004 Jan-May	2004 Ops	2004 Total	2004 Jan-May	2004 Ops	2004 Total	2004 Jan-May	2004 Ops	2004 Total	2004 Jan-May	2004 Ops	2004 Total	2004 Jan-May	2004 Ops	2004 Total	2004 Jan-May	2004 Ops	2004 Total	2004 Jan-May	2004 Ops	2004 Total	2004 Jan-May	2004 Ops	2004 Total	2004 Jan-May	2004 Ops	2004 Total	2004 Jan-May	2004 Ops	2004 Total	2004 Jan-May	2004 Ops	2004 Total	2004 Jan-May	2004 Ops	2004 Total	2004 Jan-May	2004 Ops	2004 Total	2004 Jan-May	2004 Ops	2004 Total	2004 Jan-May	2004 Ops	2004 Total	2004 Jan-May	2004 Ops	2004 Total	2004 Jan-May	2004 Ops	2004 Total	2004 Jan-May	2004 Ops	2004 Total	2004 Jan-May	2004 Ops	2004 Total	2004 Jan-May	2004 Ops	2004 Total	2004 Jan-May	2004 Ops	2004 Total	2004 Jan-May	2004 Ops	2004 Total	2004 Jan-May	2004 Ops	2004 Total	2004 Jan-May	2004 Ops	2004 Total	2004 Jan-May	2004 Ops	2004 Total	2004 Jan-May	2004 Ops	2004 Total	2004 Jan-May	2004 Ops	2004 Total	2004 Jan-May	2004 Ops	2004 Total	2004 Jan-May	2004 Ops	2004 Total	2004 Jan-May	2004 Ops	2004 Total	2004 Jan-May	2004 Ops	2004 Total	2004 Jan-May	2004 Ops	2004 Total	2004 Jan-May	2004 Ops	2004 Total	2004 Jan-May	2004 Ops	2004 Total	2004 Jan-May	2004 Ops	2004 Total	2004 Jan-May	2004 Ops	2004 Total	2004 Jan-May	2004 Ops	2004 Total	2004 Jan-May	2004 Ops	2004 Total	2004 Jan-May	2004 Ops	2004 Total	2004 Jan-May	2004 Ops	2004 Total	2004 Jan-May	2004 Ops	2004 Total	2004 Jan-May	2004 Ops	2004 Total	2004 Jan-May	2004 Ops	2004 Total	2004 Jan-May	2004 Ops	2004 Total	2004 Jan-May	2004 Ops	2004 Total	2004 Jan-May	2004 Ops	2004 Total	2004 Jan-May	2004 Ops	2004 Total	2004 Jan-May	2004 Ops	2004 Total	2004 Jan-May	2004 Ops	2004 Total	2004 Jan-May	2004 Ops	2004 Total	2004 Jan-May	2004 Ops	2004 Total	2004 Jan-May	2004 Ops	2004 Total	2004 Jan-May	2004 Ops	2004 Total	2004 Jan-May	2004 Ops	2004 Total	2004 Jan-May	2004 Ops	2004 Total	2004 Jan-May	2004 Ops	2004 Total	2004 Jan-May	2004 Ops	2004 Total	2004 Jan-May	2004 Ops	2004 Total	2004 Jan-May	2004 Ops	2004 Total	2004 Jan-May	2004 Ops	2004 Total	2004 Jan-May	2004 Ops	2004 Total	2004 Jan-May	2004 Ops	2004 Total	2004 Jan-May	2004 Ops	2004 Total	2004 Jan-May	2004 Ops	2004 Total	2004 Jan-May	2004 Ops	2004 Total	2004 Jan-May	2004 Ops	2004 Total	2004 Jan-May	2004 Ops	2004 Total	2004 Jan-May	2004 Ops	2004 Total	2004 Jan-May	2004 Ops	2004 Total	2004 Jan-May	2004 Ops	2004 Total	2004 Jan-May	2004 Ops	2004 Total	2004 Jan-May	2004 Ops	2004 Total	2004 Jan-May	2004 Ops	2004 Total	2004 Jan-May	2004 Ops	2004 Total	2004 Jan-May	2004 Ops	2004 Total	2004 Jan-May	2004 Ops	2004 Total	2004 Jan-May	2004 Ops	2004 Total	2004 Jan-May	2004 Ops	2004 Total	2004 Jan-May	2004 Ops	2004 Total	2004 Jan-May	2004 Ops	2004 Total	2004 Jan-May	2004 Ops	2004 Total	2004 Jan-May	2004 Ops	2004 Total	2004 Jan-May	2004 Ops	2004 Total	2004 Jan-May	2004 Ops	2004 Total	2004 Jan-May	2004 Ops	2004 Total	2004 Jan-May	2004 Ops	2004 Total	2004 Jan-May	2004 Ops	2004 Total	2004 Jan-May	2004 Ops	2004 Total	2004 Jan-May	2004 Ops	2004 Total	2004 Jan-May	2004 Ops	2004 Total	2004 Jan-May	2004 Ops	2004 Total	2004 Jan-May	2004 Ops	2004 Total	2004 Jan-May	2004 Ops	2004 Total	2004 Jan-May	2004 Ops	2004 Total	2004 Jan-May	2004 Ops	2004 Total	2004 Jan-May	2004 Ops	2004 Total	2004 Jan-May	2004 Ops	2004 Total	2004 Jan-May	2004 Ops	2004 Total	2004 Jan-May	2004 Ops	2004 Total	2004 Jan-May	2004 Ops	2004 Total	2004 Jan-May	2004 Ops	2004 Total	2004 Jan-May	2004 Ops	2004 Total	2004 Jan-May	2004 Ops	2004 Total	2004 Jan-May	2004 Ops	2004 Total	2004 Jan-May	2004 Ops	2004 Total	2004 Jan-May	2004 Ops	2004 Total	2004 Jan-May	2004 Ops	2004 Total	2004 Jan-May	2004 Ops	2004 Total	2004 Jan-May	2004 Ops	2004 Total	2004 Jan-May	2004 Ops	2004 Total	2004 Jan-May	2004 Ops	2004 Total	2004 Jan-May	2004 Ops	2004 Total	2004 Jan-May	2004 Ops	2004 Total	2004 Jan-May	2004 Ops	2004 Total	2004 Jan-May	2004 Ops	2004 Total	2004 Jan-May	2004 Ops	2004 Total	2004 Jan-May	2004 Ops	2004 Total	2004 Jan-May	2004 Ops	2004 Total	2004 Jan-May	2004 Ops	2004 Total	2004 Jan-May	2004 Ops	2004 Total	2004 Jan-May	2004 Ops	2004 Total	2004 Jan-May	2004 Ops	2004 Total	2004 Jan-May	2004 Ops	2004 Total	2004 Jan-May	2004 Ops	2004 Total	2004 Jan-May	2004 Ops	2004 Total	2004 Jan-May	2004 Ops	2004 Total	2004 Jan-May	2004 Ops	2004 Total	2004 Jan-May	2004 Ops	2004 Total	2004 Jan-May	2004 Ops	2004 Total	2004 Jan-May	2004 Ops	2004 Total	2004 Jan-May	2004 Ops	2004 Total	2004 Jan-May	2004 Ops	2004 Total	2004 Jan-May	2004 Ops	2004 Total	2004 Jan-May	2004 Ops	2004 Total	2004 Jan-May	2004 Ops	2004 Total	2004 Jan-May	2004 Ops	2004 Total	2004 Jan-May	2004 Ops	2004 Total	2004 Jan-May	2004 Ops	2004 Total	2004 Jan-May	2004 Ops	2004 Total	2004 Jan-May	2004 Ops	2004 Total	2004 Jan-May	2004 Ops	2004 Total	2004 Jan-May	2004 Ops	2004 Total	2004 Jan-May	2004 Ops	2004 Total	2004 Jan-May	2004 Ops	2004 Total	2004 Jan-May	2004 Ops	2004 Total	2004 Jan-May	2004 Ops	2004 Total	2004 Jan-May	2004 Ops	2004 Total	2004 Jan-May	2004 Ops	2004 Total	2004 Jan-May	2004 Ops	2004 Total	2004 Jan-May	2004 Ops	2004 Total	2004 Jan-May	2004 Ops	2004 Total	2004 Jan-May	2004 Ops	2004 Total	2004 Jan-May	2004 Ops	2004 Total	2004 Jan-May	2004 Ops	2004 Total	2004 Jan-May	2004 Ops	2004 Total	2004 Jan-May	2004 Ops	2004 Total	2004 Jan-May	2004 Ops	2004 Total	2004 Jan-May	2004 Ops	2004 Total	2004 Jan-May	2004 Ops	2004 Total	2004 Jan-May	2004 Ops	2004 Total	2004 Jan-May	2004 Ops	2004 Total	2004 Jan-May	2004 Ops	2004 Total	2004 Jan-May	2004

Figure C1 – Aircraft Traffic Summary – Loads ≤ 10,830 lbs

Aircraft Model	Model - Series	Type Designator	1998 Ops	1999 Ops	2000 Ops	2001 Ops	2002 Ops	2003 Ops	2004 Jan-May Ops	Total Ops Jan-May 1998 to May 2004	Gear Config.	Max Takeoff Weight (lbs)	Max Landing Weight (lbs)	Avg. Load MLW120 + Assembly	Load/ Rear Gear	Load/Tire	Avg Ops/FY	% of Traffic > 10,000 lb	Number & Type Engines / Weight Class	Additional Comments
Skytrain (C-47, C-53, C-117, R4D, DC-3)		DC3	2	6	1	2	1			12	S	25200	25200	25200	11970	11970	1,870,129	0.021%	2P/S+	DOUGLAS
Bae 125 (H25C) / Hawker 1000	125-900	HS25/B	281	85	61	51	70	72	16	636	D	27400	23350	25375	12053.13	6026.5625	99,116,883	1.138%		
Short 360, SD3-40		SH36		1	1	2	2	60		66	S	27100	26500	26800	12730	12730	10,285,714	0.118%	2T/S+	SHORT BRO
SAAB 340		SF34					1	17	4	2	D	27275	26500	26837.5	12771.66	6395.7813	3,740,959	0.043%	2T/S+	SAAB
Falcon 20/100, Mystere 20/200, Gardien (HU-20)		FA20	309	274	358	522	560	803	289	3125	D	28600	26734	27227	12932.83	6456.4125	487,072,99	5.592%	2J/S+	BREGUET
Dassault Falcon 20	20-	DA20	86	80	114	49	100	83	17	529	D	28600	27324	27990	12926.25	6647.525	82,441,658	0.947%		
Grumman	Gulfstream-G	GULF	153	32	1	2				188	D	33600	30400	32000	16200	7600	29,288,701	0.336%		
750 Citation X		CT50	123	198	174	176	388	387	177	1623	D	35700	31800	33750	16031.25	8016.625	252,935,06	2.904%		
Dassault Mercure 100	10-	DA01	7	8					15		D	35600	32220	34010	16154.75	8077.375	2,337,6623	0.027%	2J/S+	CESSNA
GAC 159-C, Gulfstream 1		G159	5	5	2	6	11	3	4	38	D	36000	34235	35142.5	16592.89	8346.3438	5,922,077.9	0.068%		
F-16 Fighting Falcon, Herz, Barak, Brakheet	900-	F16	1	3	3	1	3	8	1	20	S	37500	33750	35625	16221.88	16921.875	3,116,883.1	0.036%	2T/S+	AEROSPACE
JetStar	JETSTAR-	JSTA	236	2						238	D	38940	35046	36993	17571.68	8785.8375	37,090,909	0.420%	1J/L	DYNAMICS
Lockheed Jetstar C140		L329	56	21	3	3	1	1	85		DT	38940	35046	36993	17571.68	8785.8375	37,090,909	0.420%		LOCKHEED
Dassault Falcon 50		DA50	18	3	8	4	21	4	2	60	D	38800	35715	37257.5	17697.31	8848.6583	9,350,6484	0.107%		
DHC8 Dash 8		DH8	2						2		D	41100	40000	40550	19261.25	9630.625	0,311,6883	0.004%		
F-27, FH-227, C-31		F27	6			1	3	14	24		D	43500	43000	43250	20640.75	10271.875	3,740,959	0.043%	2T/L	INDUSTRIES
Dassault Falcon 900 Mystere	900-	DA90	75	6	5	7	14	43	49	199	D	45500	42000	43750	20781.25	10390.625	31,072,987	0.336%		
DHC-7 Dash 7 (O-5, EO-5)		DH7							2		D	47000	42300	44500	21208.75	10604.375	0,311,6883	0.004%		
SA-226TB, SA-227TT Merin 3, Fairchild 300	FH-227	SW3	196	274	320	427	462	398	142	2219	D	45500	45000	45250	21493.75	10746.875	345,81818	3.971%	2T/S+	INDUSTRIES
EMB-145, ERL-145, R-99		E145							4		D	48500	42549	46524.5	21624.14	10812.069	0,623,3766	0.007%	2J/L	EMBRAER
C-46 Commando (CW-20)		C46	2			1	2				S	48000	48800	47400	22515	22515	0,158,8442	0.002%	2P/L	WRIGHT
Canadair Regional Jet		CARJ	87	2					89		D	61000	47000	49000	23275	11637.5	13,87013	0.159%		
CL-600/Challenger 699/601/604 (CC-144)	Challenger(CL)	CL600/65	1518	162	157	206	174	267	165	2559	D	61250	47000	49125	23334.38	11667.188	403,48052	4.633%		
S-3, ES-3, US-3 Viking (L-394)		S3						1	1		S	62540	47286	49913	23708.68	23708.675	0,158,8442	0.002%	2J/L	LOCKHEED
Canadair Regional Jet 100		T38	2	3	1	6	1	6	19		D	63000	51300	60000	23750	11875	2,861,039	0.034%		(CR1)
Conquest 640		CV64	2		2				4		D	67000	57000	64150	28721.25	12850.625	0,623,3766	0.007%		
C-2 Greyhound		C2							2	2	S	67500	51750	54625	25846.88	25846.875	0,311,6883	0.004%	2T/L	AEROSPACE
Conquest CV-580		CV58				1			1		S	63000	56700	59850	28428.75	28428.75	0,158,8442	0.002%		
P-2D to H, SP-2, P2V Neptune (L-)		P2				1			1		S	63000	56700	59850	28428.75	28428.75	0,158,8442	0.002%	2P/L	LOCKHEED
FA-18, CF-188, EF-18, C-15, hornet		F18	8	4	3	7	1	7	2	32	S	66000	59400	62700	29782.5	29782.5	4,987,013	0.057%	2J/L	DOUGLAS
G-1159A/C Gulfstream 3/SRA, 300, 400 C-20 G-1		GLF4/3	46	105	324	344	394	651	247	2171	D	69700	58500	64100	30447.5	15223.75	338,33766	3.885%	2J/L	AEROSPACE
G-1159, G-1159B Gulfstream II/2B/25P, C- Gulfstream-G		GLF2/G	111	234	242	276	334	269	124	1590	D	69700	58500	64100	30447.5	15223.75	247,79221	2.845%	2J/L	AEROSPACE
G-1159D Gulfstream 5/500/550, C-37		GLF5	3	5	50	46	79	45	37	265	D	69700	58500	64100	30447.5	15223.75	41,288701	0.474%	2J/L	AEROSPACE
F-15 Eagle, Baz, Akai, R&am		F15							1		S	68000	61200	64600	30685	30685	0,158,8442	0.002%	2J/L	DOUGLAS
F-28, Fellowship		F28					2	1		3	D	73000	64000	69500	32537.5	16268.75	0,467,5325	0.005%	2J/L	FOKKER BV
F-14 Tomcat		F14		1	1	1	1	2	5		S	72900	65610	69255	32896.13	32896.125	0,779,2288	0.009%	2J/L	AEROSPACE
Gulfstream		G4	18	9	6	5	2	7	2	49	D	74600	67140	70870	33665.25	16831.625	7,636,3536	0.088%		
Bae 146	146-100	BA46	55	107	102	98	81	89	32	564	D	84000	77500	80750	38356.25	19175.125	87,896104	1.009%	4P/L	DOUGLAS
DC-9/B, Liftmaster		DC9							2	4	D	104000	85200	95100	45172.5	22585.25	0,623,3766	0.007%		
BAC-111 One-Eleven		BA11	32	9	3		8	3	2	57	D	104500	94050	99275	47155.63	23577.813	8,883,1169	0.102%	2J/L	AEROSPACE
L-188 Electra		L188					24	25	2	53	D	116000	95650	105825	50266.88	25135.438	8,2597403	0.095%	4T/L	LOCKHEED

Figure C2 – Aircraft Traffic Summary – 10,830 < Loads ≤ 50,267 lbs

Aircraft Model			Model - Series										Type Designator	1998 Ops	1999 Ops	2000 Ops	2001 Ops	2002 Ops	2003 Ops	2004 Jan-May	Total Ops Jan 1998 to May 2004	Gear Config.	Max Takeoff Weight (lbs)	Max Landing Weight (lbs)	Avg. Load (MTOW + MLW)/2	Load/Rear Gear Assembly	Load/Tire	Avg Ops/FY	% of traffic > 10,000 lb	Number & Type of Engines / Weight Class	Additional Comments		
DC9-	Douglas DC-9/C-9	DC9-	DC9	19	20	30	162	15	9	2	257	D	114000	102000	108000	51300	26550	40,051,948	0.460%											2/JL	BOEING		
	737-100 (Survaller, CT-43, VC-9B)		737A	4								4	115400	103860	109630	52074.25	26037.125	0.6233766	0.007%											2/JL	DOUGLAS		
	DC-9-30 (C-9, VC-9, Nightingale, Skytrain 2)		DC93									7	117000	105000	111000	52725	26362.5	5,7662338	0.066%											2/JL	DOUGLAS		
	737-500		737B	8								7	121000	108900	114950	54601.25	27300.625	12,165844	0.140%											2/JL	DOUGLAS		
	737-300		737B	3	4	7	5	2		1	19		D	133500	120150	128625	60241.88	30120.938	1,2467532	0.014%											2/JL	BOEING	
MD-80	P-3, CP-140 Orion, Aurora, Arcturus, L-85-		P3								2	D	135000	121500	128250	60918.75	30459.375	0.6233766	0.004%											4/JL	LOCKHEED		
	737-300		737S								2	D	138500	124650	131575	62498.13	31249.063	0.3116883	0.007%														
	McDonald Douglas 80		MD80	2	1	3	51	92	79	33	261	D	140000	128000	134000	63650	31825	40,675325	0.467%											2/JL	DOUGLAS		
	MD-81		MD81								8	D	140000	128000	134000	63650	31825	1,2467532	0.014%											2/JL	DOUGLAS		
	MD-82		MD82	2							21	D	149500	130000	139750	66381.25	33190.625	3,2727273	0.038%											2/JL	DOUGLAS		
DC-9 Skytrain ?	MD-88		MD88								2	D	149500	130000	139750	66381.25	33190.625	0.3116883	0.004%											2/JL	DOUGLAS		
	C9		C9	69	19	14	3			105		D	149500	134550	142025	67461.88	33720.938	16,363636	0.188%											4/JL	LOCKHEED		
	C-130 Hercules, Spectre, L100, 182, 282, 382		C130	30	3	17	20	5	10	5	90	DT	155000	139500	147250	71131.25	35565.625	3,5844166	0.161%											2/JL	DOUGLAS		
	MD-83		MD83	4							23	D	160000	139500	149750	71131.25	35565.625	3,5844166	0.041%											2/JL	DOUGLAS		
	A-320		A320									D	162040	142195	152117.5	72255.81	36127.906	0.3116883	0.004%										2/JL	AIRBUS			
	727 Stage 3 (-100 or -200)		727Q	12	46	31	31	30	10	1	161	D	169000	142500	155750	73981.25	36990.625	25,090909	0.288%											3/JL	BOEING		
	Boeing 727		727	21	35	23	6			1	86	D	169000	142500	155750	73981.25	36990.625	13,402597	0.154%											3/JL	BOEING		
	727-200		727	2	43	18	9	1	4		77	D	169000	142500	155750	73981.25	36990.625	12	0.138%											3/JL	BOEING		
	727-100 (C-22)		727	4	10	3	6	2		25		D	169000	142500	155750	73981.25	36990.625	3,9961039	0.045%											3/JL	BOEING		
	767-200		767	1									D	164800	148320	156660	74366	37183	0.1558442	0.002%										2/JL	BOEING		
737-700, BBJ, C-40		737	5	4	4	4	13	11	18	59	D	174200	146300	160250	76118.75	38069.375	9,1948052	0.106%											2/JL	BOEING			
737-800, BBJ2	737-BBJ	737B								12		D	174200	146300	160250	76118.75	38069.375	1,8701299	0.021%											2/JL	BOEING		
757-200 (C-32)		757								3		DT	255000	210000	232500	110437.5	55716.875	0.4675325	0.005%										2/JL	BOEING			
A-310 (CC-150 Polaris)		A310								1		DT	330693	271169	300931	142942.2	6735.556	0.1558442	0.002%										2/JH	AIRBUS			
C-97	DC-8		DC8							2		DT	325000	292500	308750	146656.3	36664.063	0.3116883	0.004%											2/JH	BOEING		
	DC-8-60		DC86							29		DT	355000	275000	315000	149625	37406.25	4,5194805	0.052%											4/JH	DOUGLAS		
	C-141 Starlifter (L-300)		C141									DT	316600	316100	316350	150266.3	37566.563	0.1558442	0.002%										4/JH	LOCKHEED			
	C-135B/C/E/K Strolighter (EC-135, NKC-)		C135									DT	323100	316100	319600	151810	37952.5	0.1558442	0.002%										4/JH	BOEING			
	767-300		767		2					3		DT	380000	300000	340000	161500	40375	0.4675325	0.005%										2/JH	BOEING			
	DC-10 (KC-10 Extender, KDC-10, MD-10)		DC10	5	12	18				36		DT	690000	411000	500500	23737.5	59434.375	5,6103896	0.064%										3/JH	DOUGLAS			
	C-17 Globemaster 3		C17	1								DT	685000	526900	555750	263981.3	65995.313	0.1558442	0.002%										4/JH	BOEING			
	MD-11		MD11	6	18	49				73		DT	602555	542300	572427.3	271902.9	67975.736	11,376623	0.131%										3/JH	DOUGLAS			
	747SP		747S	7						7		DT	700000	450000	575000	273125	68281.25	1,9090091	0.013%										4/JH	BOEING			
	777-200		777							1		TRIDEIM	750000	487000	618500	293787.5	48964.583	0.1558442	0.002%										2/JH	BOEING			
777		777							1		TRIDEIM	750000	487000	618500	293787.5	48964.583	0.1558442	0.002%										2/JH	BOEING				
747		747	3						3		DT	750000	675000	712500	338437.5	84609.375	0.4675325	0.005%										4/JH	BOEING				
747-200 (E-4, VC-25)		747							1		DT	833000	530000	731500	347462.5	86865.625	0.1558442	0.002%										4/JH	BOEING				
747-400 (International winglets)		7474							1		DT	850000	530000	740000	351500	87875	0.1558442	0.002%										4/JH	BOEING				
Fort Worth Meacham		7474							55985									8709.3506	Total														

Figure C3 – Aircraft Traffic Summary – 50,267 < Loads ≤ 351,500 lbs

Appendix D – Modeling and Conversion of Heavy Load Group

Section 6.5 briefly examined the process of modeling heavier aircraft passes experienced by Runway 16/34 into load quantities capable of testing under SDD operations. Load Groups #1, #2, and #3 were within the loading limits of equipment. Load Groups #4, #5, and #6 were beyond the loading capability of the equipment and required the development of a conversion process. This process was presented in Section 6.5. Representative aircraft were determined for the three load groups requiring conversion into equivalent load applications at the equipment loading limit. Representative aircraft were selected based on three criteria: predominance of occurrence of the selected aircraft, a similar loading per single rear gear configuration to that of the normalized load for the load group, and the same gear configuration as the majority of the aircraft applications observed (see Table D1).

Table D1 – Load Group Data and Equivalent Aircraft

Load Group	Normalized Load (lbs)	Predominant Gear Config.	Number of Applications	Equiv. Aircraft	Load Per Rear Gear Config. (lbs)
#4	64,065	Dual	1,087	B-727	73,981
#5	147,322	Dual Tandem	31	DC-8	149,625
#6	265,203	Dual Tandem	97	MD-11	271,902

Using the same finite element analysis set up, as described in Appendix B, stress-induced by each representative aircraft was determined for all three heavy load groups:

- B-727 produced a tensile stress of 0.146026 ksi
- DC-8 produced a tensile stress of 0.131538 ksi
- MD-11 produced a tensile stress of 0.180073 ksi

Following induced stress determination, these stress values were used to determine the equivalent number of applications of the highest equipment-capable load group, Load Group #3 at 31.6 kips. The following computations were completed for all three heavy load groups. Boeing 727 is presented as an example of the steps taken for equivalent application determination. Results for this loading along with the other two load groups and respective aircraft are presented in Table D2.

- Determine maximum number of applications (N_f) for a B-727

- - Using the fatigue equation for concrete

$$\log N_f = 17.61 - 17.61 \left(\frac{\sigma_c}{S_c} \right)$$

$$\log N_f = 17.61 - 17.61 \left(\frac{146.026 \text{ psi}}{650 \text{ psi}} \right)$$

$$N_f = 4.506 \times 10^{13}$$

- - Using the PCA method

If $\frac{\sigma}{S_c} \leq 0.45$, then applications unlimited

$$\frac{146.026 \text{ psi}}{650 \text{ psi}} = 0.2247$$

- Determine maximum number of applications (N_f) for Load Group #3 at 31.6 kips

- - Using the fatigue equation for concrete

$$\log N_f = 17.61 - 17.61 \left(\frac{\sigma_c}{S_c} \right)$$

$$\log N_f = 17.61 - 17.61 \left(\frac{125.919 \text{ psi}}{650 \text{ psi}} \right)$$

$$N_f = 1.580 \times 10^{14}$$

- Use results from fatigue equation for concrete and Miner's hypothesis

$$\frac{n_{Group\#3}}{N_{f_{Group\#3}}} = \frac{n_{B-727}}{N_{f_{B-727}}}$$

$$\frac{n_{Group\#3}}{1.580 \times 10^{14}} = \frac{1087}{4.506 \times 10^{13}}$$

$$n_{Group\#3} = 3,811$$

A summary of the results from this process for all three heavy load groups is presented in Table D2. The resulting data required the original applications for Load Group #3 be increased by 6,699 applications. The computation process above enabled equivalent load determination for loads which extended beyond the capability of the SDD. This process enabled all traffic expected on Runway 16/34 to be represented within the traffic model used in the SDD SAP testing application. This process is a simple approximation to enable an equivalent loading scenario on the pavement. It is based on the postulation that a certain higher number of applications of a lesser load causes the equivalent damage of a lesser number of applications of a higher load.

Table D2 – Load Group Data and Equivalent Aircraft

Load Group	Number of Applications	Equiv. Aircraft	Number of Applications (Load Group #3 – 31.6 kips)
#4	1,087	B-727	3,811
#5	31	DC-8	44
#6	97	MD-11	2,844

Total Applications = 6,699

Appendix E – Sample Induced-Stress Comparison Between Load Frame and Actual Aircraft Footprint

In an effort to further solidify the processes and assumptions employed in conducting this research, a direct comparison was made between stress induced by an actual aircraft footprint and the same aircraft loads transmitted by use of the two-wheel load frame. By conducting a comparison analysis, the use of the rear gear configuration load for a given aircraft on the same load frame footprint, irrespective of the variation of actual aircraft gear footprint, can be proved a legitimate assumption. The following analysis supports this assumption.

To begin the analysis, a suitable aircraft was selected. The British Aerospace (BAe) 146 is regional jet airliner which has had a significant amount of operations at Meacham Airport, over the 6.5 years of traffic history. This aircraft has a dual-wheel landing gear configuration and comprises just over 1% of the operations at Meacham Airport. Its load per rear gear assembly is approximately 38.4 kips, placing it among the aircraft repetitions modeled by Load Group #3, as described in Section 6.4. Figure E1 is a typical picture of the BAe 146.



Figure E1 – BAe 146 – Regional Jet Airliner

Finite element analysis tools were used to estimate the stress induced by an actual BAe 146 pass on a pavement system of the same construction as Runway 16/34. FEAFAA is a program developed by the FAA Airport Technology Research & Development Branch to provide a stand-alone three-dimensional finite element analysis of multiple-slab rigid airport pavements and overlays. It is capable of placing individual aircraft landing gear loads on a defined pavement system and computing accurate pavement responses, including stresses, strains, and deflections. FEAFAA utilizes the three-dimensional finite element programs (NIKE3D and INGRID) developed by the United States Department of Energy, Lawrence Livermore National Laboratory. FEAFAA enabled selection of the BAe 146 to determine response on a pavement system, mirroring that of Runway 16/34 (as specified in Appendix B).

In order to determine an equivalent response through the use of the load frame incorporated into the SDD SAP testing, the program EverFE was employed. A two-wheel load footprint with the same dimensions and orientation as the load frame pads was defined in the program. The load selected was equivalent to a single rear gear of the BAe 146, distributed equally among the two-wheel footprint (approximately 20 kips on each pad). Once again, this loading scenario was placed on a pavement system, mirroring that of Runway 16/34. Load frame dimension, orientation, and pavement system constraints were used as specified in Appendix B. Both analysis using FEAFAA and EverFE were conducted producing comparable data, supporting the assumptions made on the loading scenarios within this report. The two values for tensile stress induced differed by less than 4%. This is a difference well within acceptable limits, and could be attributed to differing finite element modules in each program. Finite element analysis is only as accurate as the number and location of analysis points selected. Table E1 summarizes the results of the finite element analysis.

Table E1 – Stress Induced by BAe 146 and Equivalent Two-Wheel Load Frame

Load Configuration	Program Used	Stress Induced (psi)
BAe 146 rear gear	FEAFAA	163.1
Two-Wheel Load Frame	EverFE	157.2

Appendix F – Determining Deflection from Accelerometer Voltage Output

Both the rolling sensors used in the RDD deflection testing and the stationary accelerometers used in the SDD SAP testing required the same process of data transformation to obtain deflection from a voltage output. The steps below outline the process of determining deflection.

1) Given a sample wavelength amplitude in volts – define as “X” volts

2) Translate “X” volts to acceleration due to gravity (g)

$$calibration \approx 1 \frac{volt}{g}$$

therefore “X” volts = “X” g

3) Determine deflection in terms of acceleration (a) and angular frequency (ω)

$$a = \omega^2 \cdot d$$

$$d = \frac{a}{\omega^2}$$

4) Define acceleration (a) and angular frequency (ω), where $f = 20$ Hz

$$a = "X" g \cdot \frac{32.2 \frac{ft}{s^2}}{g} \cdot \frac{12 in}{1 ft} \cdot \frac{1000 mil}{1 in} = 386400 \cdot "X" \frac{mil}{s^2}$$

$$\omega = 2\pi f = 2\pi \cdot 20 Hz = 125.66 \frac{rad}{s}$$

$$\omega^2 = \left(125.66 \frac{rad}{s} \right)^2 = 15791.36704 \frac{rad^2}{s^2}$$

5) Solve for deflection (d)

$$d = \frac{386,400 \cdot "X" \frac{mil}{s^2}}{15791.36704 \frac{rad^2}{s^2}} = 24.46906585 \cdot "X" \text{ mils}$$

Use of the above conversion factor, determined in Step 5), enabled transformation of voltage amplitude (volts) into a dynamic deflection reading (mils).

Appendix G – Longitudinal Profiles from RDD Testing 5-8 July 2004

The following Figures G1, G2, and G3 show RDD deflection profiles of two respective paving lanes of Runway 16/34. Deflection response of the six lanes shows similar patterns and trends. General high and low deflections follow similar trends across all six lanes. Variations in trends can be attributed to varying subgrade conditions and localized areas of distress, including cracking. Deflection response of Lane 6 is missing the last 400 feet of deflection data, as seen in Figure G3. Missing data is a result of field complications and loss of data.

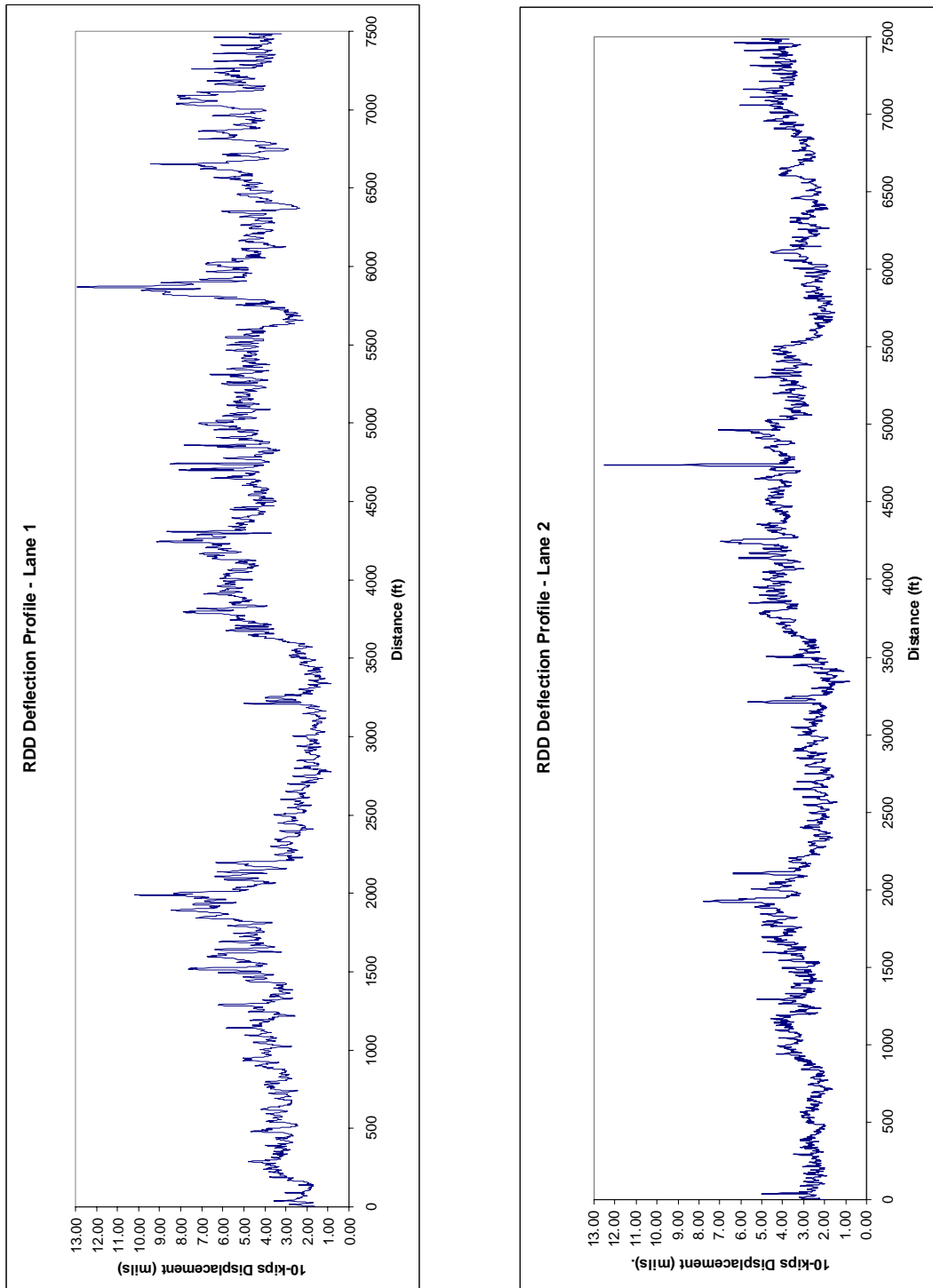


Figure G1 – RDD Deflection Profiles – Lanes 1 and 2

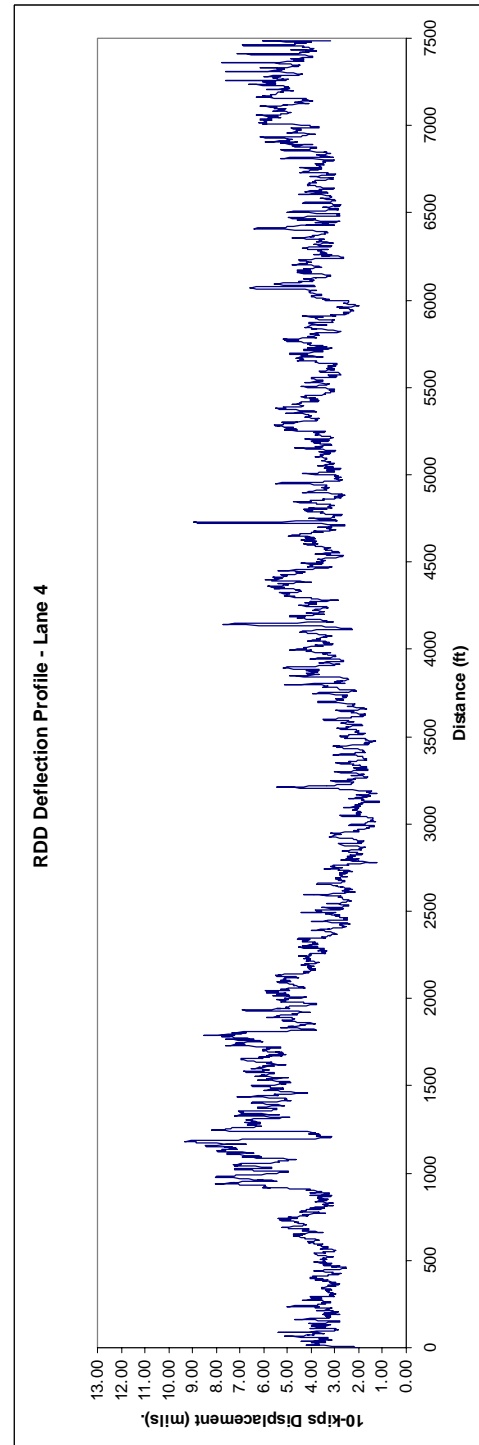
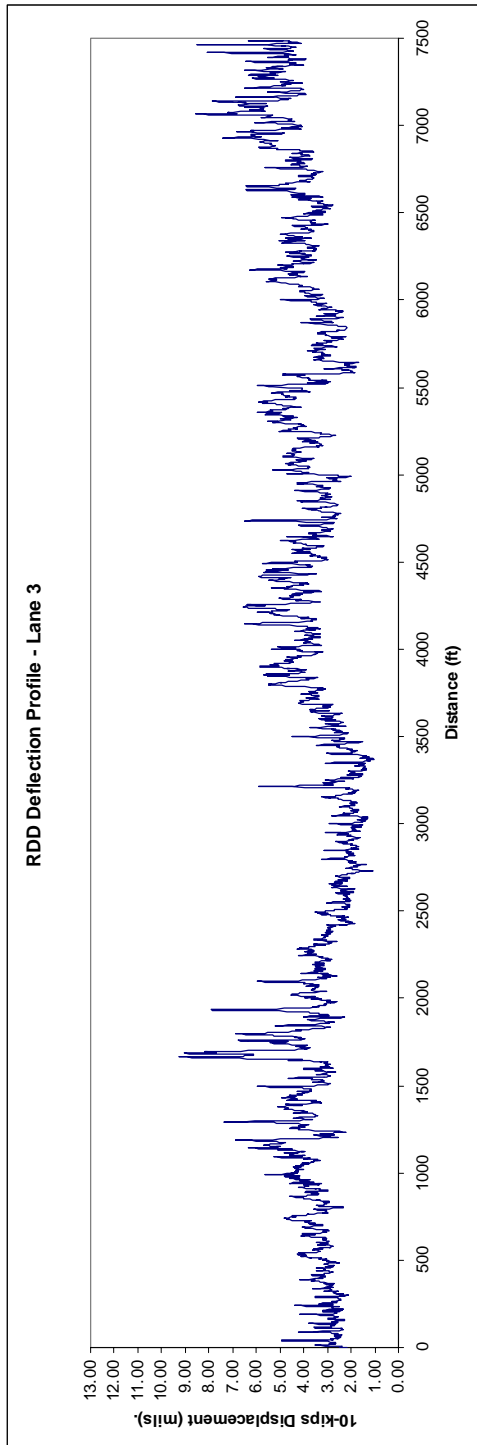


Figure G2 – RDD Deflection Profiles – Lanes 3 and 4

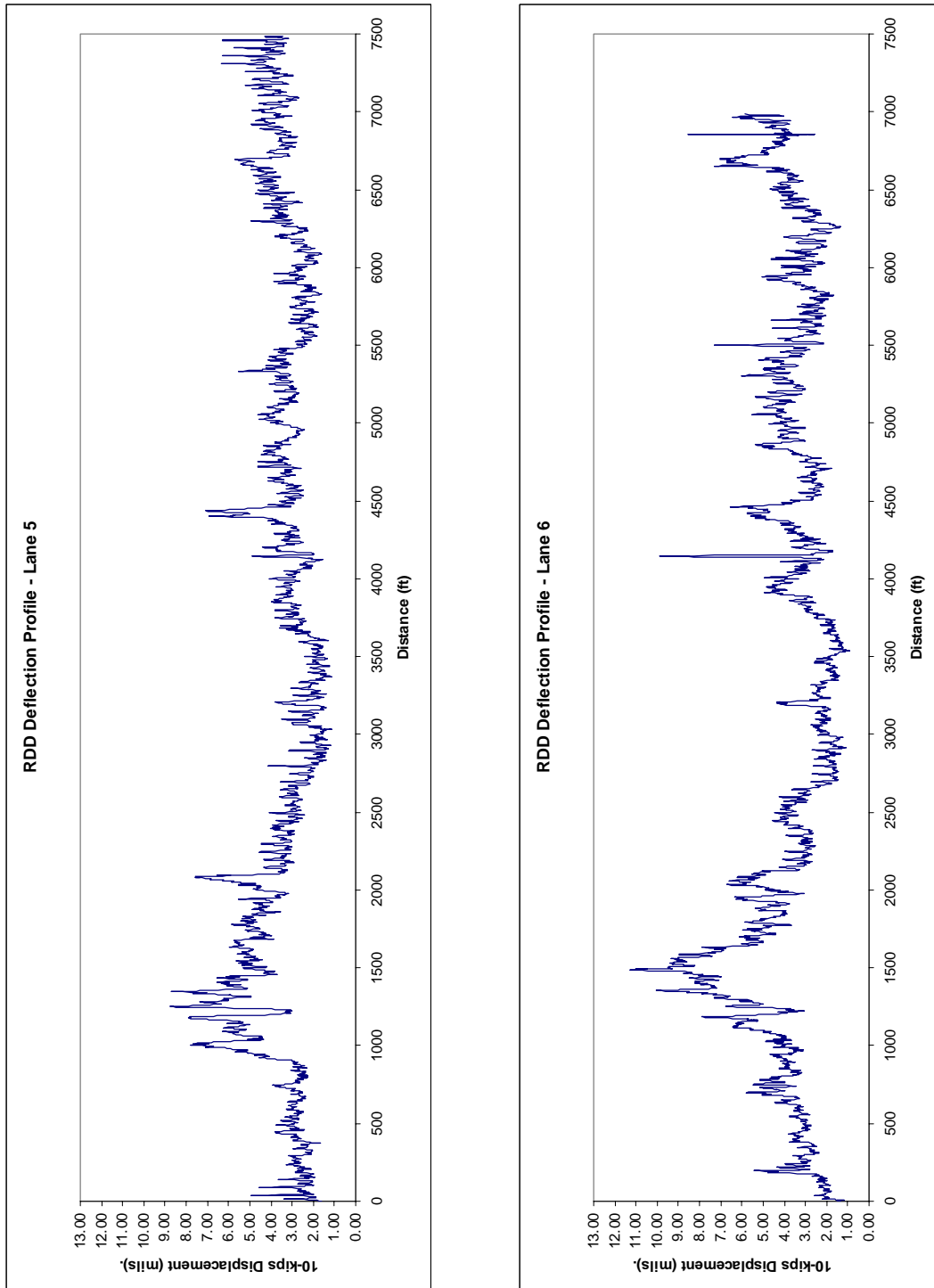


Figure G3 – RDD Deflection Profiles – Lanes 5 and 6

Appendix H – Sample Raw Data from SDD SAP Testing

The following figures provide the reader with a sample of the raw data received by the data acquisition system, during field testing. This data was transformed in accordance with Appendix F. The raw data includes two samples of load cell output and two samples of accelerometer outputs. Figure H1 illustrates the first five-year increment of load cell readings. The three-tiered loading is apparent along with the relative length of testing between the three different levels. It is important to reiterate the sampling rate of 200 samples per second, since figures are given in terms of number of sample points.

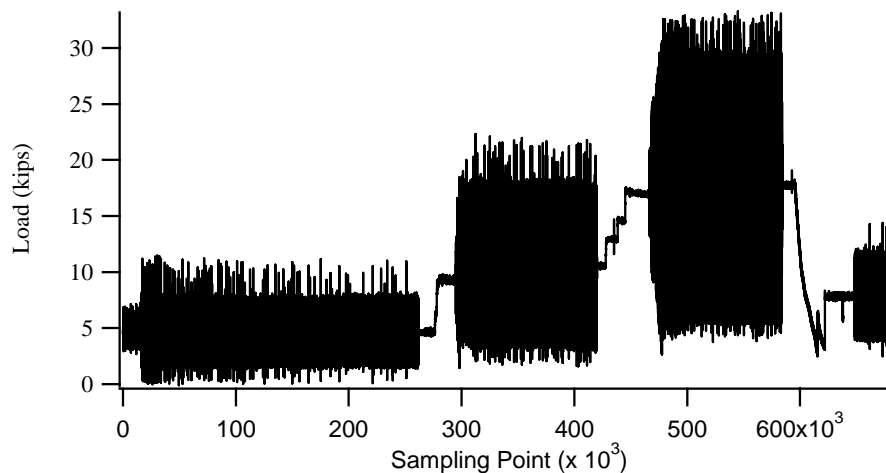


Figure H1 – Load Cell Output for First Five-Year Increment at Taxiway A6 Edge

The oscillation of the load cell output is difficult to perceive, due to the scale of the x-axis in Figure H1. Figure H2 improves the resolution of the load cell output by scaling down the x-axis, examining the data output over a 50-second period. This 50-second period falls within the first load group, as shown by the peak load of approximately 7.1 kips.

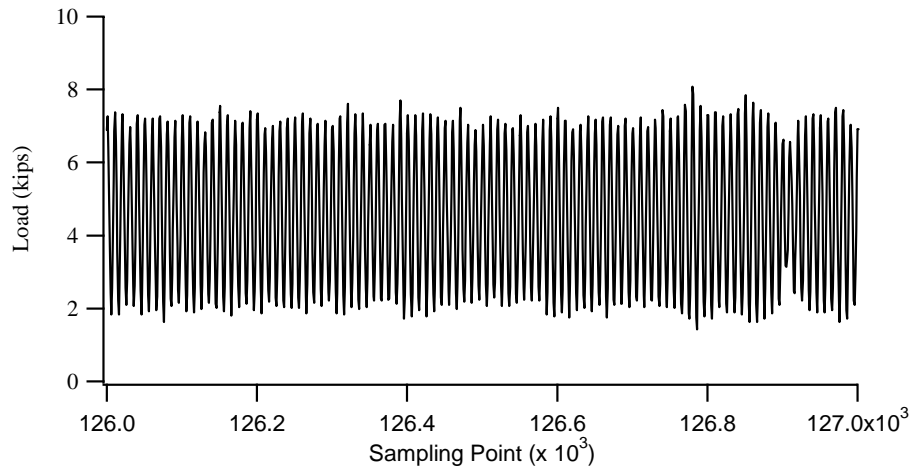


Figure H2 – Sample Load Cell Output for 50-Second Period at Taxiway A6 Edge

Figure H3 illustrates the first five-year increment of accelerometer #1 for the same edge loading scenario at Taxiway A6. Once again, the three-tiered loading is apparent along with the relative length of testing between the three different levels. Figure H3 shows the accelerometer readings for the same period of time as the load cell output in Figure H1.

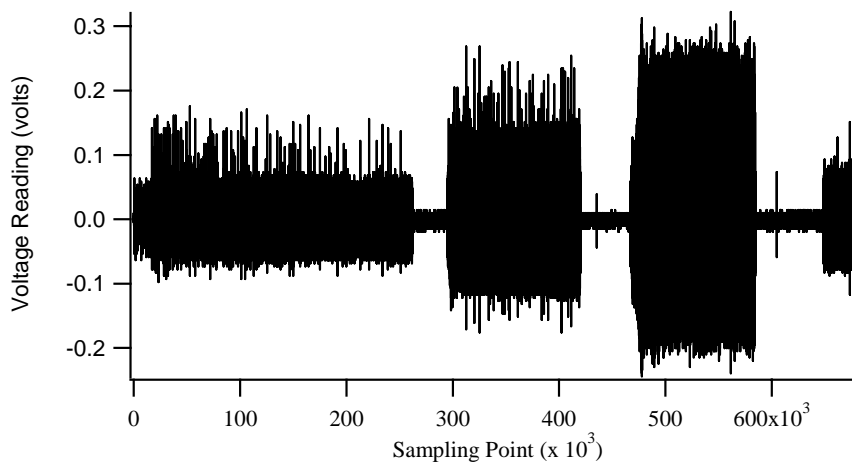


Figure H3 – Accelerometer Readings for the First Five-Year Increment at Taxiway A6 Edge

As with Figure H1, the oscillation of the load cell output is difficult to perceive, due to the scale of the x-axis in Figure H3. Figure H4 improves the resolution of the accelerometer reading by scaling down the x-axis, examining the data output over a 50-second period. This 50-second period falls within the first load group, and mirrors the same period as the one used in Figure H2.

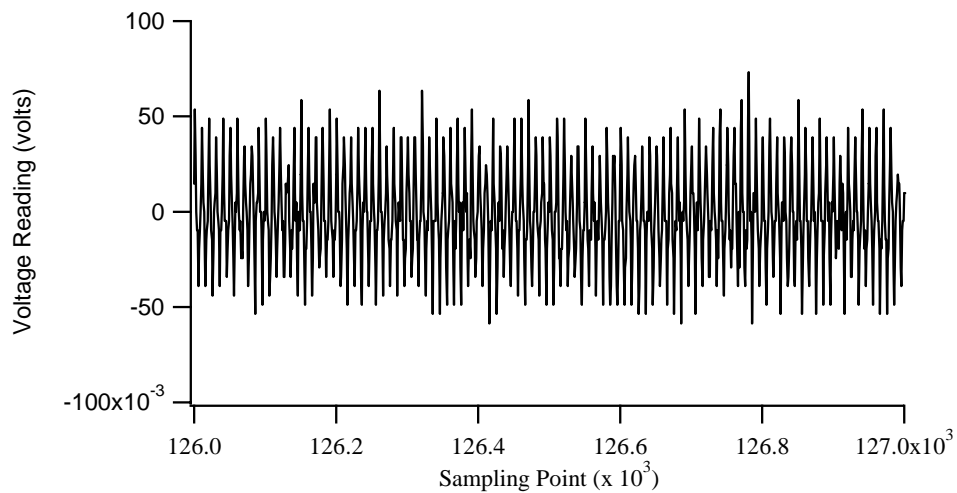


Figure H4 – Sample Accelerometer Reading Over 50-Second Period at Taxiway A6 Edge

Appendix I – Data Reduction and Summary for Each Test Point

In this Appendix, a data summary is presented for each point. Figure I1 through I36 presents the reduced raw data in tabular form. Data is arranged in five-year load periods (one per page) and load levels (major row groupings). Data includes: start/stop time, total applications, peak-to-peak readings for load cell and all three accelerometers, measured deflections, and normalized deflections. Once again, data from load cell and accelerometers were sampled over the entire load level, taking average values for five sample areas and over the entire period. Standard deviation and variance was computed for the load and deflection measurements. The highlighted rows designate the average of the load and deflection readings, and the average reading for the entire test period for a given load level. Due to the extent of the data record, spreadsheet was reduced in size and split into two parts for viewing of a five-year load period for a given location.

Point #1														
A6 Edge														
1-5 Years														
File "B"														
Goal	Start (s)	Stop (s)		Start (s)	Apps.	Load Peak	Valley	Accelerometer #1 Peak	Valley	Adj. Pk.	Adj. Vly	Defl.(mils)	Norm. Defl. (mils/pl)	
20,600 app. (1330 s) @ 7.1 kips	65	1310	100s intervals	285	4000	7.34	1.78	0.64	-0.65	1.14	-1.16	2.29	0.31	
Test Time		1225.0		485	8000	7.26	1.88	0.69	-0.68	1.23	-1.21	2.44	0.34	
Total Apps./Period		24500		685	12000	7.32	1.88	0.77	-0.71	1.37	-1.26	2.63	0.36	
Total Apps./Overall		24500		885	16000	7.36	1.86	0.78	-0.67	1.39	-1.19	2.58	0.35	
				1085	20000	7.40	1.86	0.76	-0.66	1.35	-1.17	2.52	0.34	
					Avg Load	7.34			Avg			2.49	0.34	
					σ	0.05			σ			0.13	0.02	
					Variance	0.00			Variance			0.02	0.00	
						7.36	1.83		0.73	-0.67	1.30	-1.19	2.49	0.34
					Avg Reading for Entire Test Period									
Goal	Start (s)	Stop (s)		Start (s)	Apps.	Load Peak	Valley	Accelerometer #1 Peak	Valley	Adj. Pk.	Adj. Vly	Defl.(mils)	Norm. Defl. (mils/pl)	
12,100 app. (605 s) @ 15.9 kips	1485	2100	100s intervals	1500	24800	17.16	4.00	2.51	-1.90	4.46	-3.38	7.84	0.46	
Test Time		615.0		1600	26800	17.44	3.56	2.46	-2.13	4.37	-3.79	8.16	0.47	
Total Apps./Period		12300		1700	28800	17.40	3.60	2.43	-2.19	4.32	-3.89	8.21	0.47	
Total Apps./Overall		36800		1800	30800	17.39	3.69	2.46	-2.22	4.37	-3.95	8.32	0.48	
				1900	32800	17.45	3.56	2.50	-2.23	4.45	-3.96	8.41	0.48	
					Avg Load	17.37			Avg			8.19	0.47	
					σ	0.12			σ			0.22	0.01	
					Variance	0.01			Variance			0.05	0.00	
						17.32	3.65		2.45	-2.12	4.36	-3.77	8.13	0.47
					Avg Reading for Entire Test Period									
Goal	Start (s)	Stop (s)		Start (s)	Apps.	Load Peak	Valley	Accelerometer #1 Peak	Valley	Adj. Pk.	Adj. Vly	Defl.(mils)	Norm. Defl. (mils/pl)	
10,400 app. (520 s) @ 31.6 kips	2400	2920	50s intervals	2450	37800	28.86	5.97	3.96	-3.98	7.04	-7.08	14.12	0.49	
Test Time		520.0		2550	39800	28.73	6.03	3.85	-3.97	6.85	-7.06	13.90	0.48	
Total Apps./Period		10400		2650	41800	28.59	6.05	3.79	-3.99	6.74	-7.09	13.83	0.48	
Total Apps./Overall		47200		2750	43800	28.60	6.10	3.74	-3.94	6.65	-7.01	13.66	0.48	
				2850	45800	28.52	6.14	3.64	-3.94	6.47	-7.01	13.48	0.47	
					Avg Load	28.66			Avg			13.80	0.48	
					σ	0.14			σ			0.24	0.01	
					Variance	0.02			Variance			0.06	0.00	
						28.64	6.14		3.79	-3.95	6.74	-7.02	13.76	0.48
					Avg Reading for Entire Test Period									



Accelerometer #2							Accelerometer #3						
Peak	Valley	Adj. Pk.	Adj. Vly	Defl.(mils)	Norm. Defl. (mils/pl)	LT _{us} (%)	Peak	Valley	Defl.(mils)	Norm. Defl. (mils/pl)	LT _{us} (%)		
		0.00	0.00	0.00	0.00	0.00		0.35	-0.37	0.72	0.10		
0.67	-0.47	1.19	-0.84	2.03	0.28	83.21	0.37	-0.37	0.74	0.10			
0.59	-0.48	1.05	-0.85	1.90	0.26	72.30	0.40	-0.36	0.76	0.10			
0.60	-0.49	1.07	-0.87	1.94	0.26	75.17	0.43	-0.37	0.80	0.11			
0.62	-0.50	1.10	-0.89	1.99	0.27	78.67	0.41	-0.35	0.76	0.10			
	Avg			1.57	0.21	63.05		Avg	0.76	0.10			
	σ			0.88	0.01			σ	0.03	0.00			
	Variance			0.77	0.00			Variance	0.00	0.00			
0.62	-0.47	1.10	-0.84	1.94	0.26		0.40	-0.36	0.76	0.10			
Accelerometer #2							Accelerometer #3						
Peak	Valley	Adj. Pk.	Adj. Vly	Defl.(mils)	Norm. Defl. (mils/pl)	LT _{us} (%)	Peak	Valley	Defl.(mils)	Norm. Defl. (mils/pl)	LT _{us} (%)		
2.04	-1.35	3.63	-2.40	6.03	0.35	76.87	1.46	-0.94	2.40	0.14			
1.98	-1.47	3.52	-2.61	6.13	0.35	75.16	1.42	-1.01	2.43	0.14			
1.93	-1.47	3.43	-2.61	6.05	0.35	73.59	1.36	-1.02	2.38	0.14			
1.94	-1.49	3.45	-2.65	6.10	0.35	73.29	1.37	-1.02	2.39	0.14			
1.98	-1.50	3.52	-2.67	6.19	0.35	73.57	1.39	-1.02	2.41	0.14			
	Avg			6.10	0.35	74.47		Avg	2.40	0.14			
	σ			0.07	0.00			σ	0.02	0.00			
	Variance			0.00	0.00			Variance	0.00	0.00			
1.96	-1.46	3.48	-2.60	6.08	0.35		1.39	-1.00	2.39	0.14			
Accelerometer #2							Accelerometer #3						
Peak	Valley	Adj. Pk.	Adj. Vly	Defl.(mils)	Norm. Defl. (mils/pl)	LT _{us} (%)	Peak	Valley	Defl.(mils)	Norm. Defl. (mils/pl)	LT _{us} (%)		
3.13	-2.73	5.57	-4.85	10.42	0.38	73.80	2.28	-1.85	4.13	0.15			
3.24	-2.72	5.76	-4.84	10.60	0.37	76.21	2.33	-1.87	4.20	0.15			
3.21	-2.73	5.71	-4.85	10.56	0.37	76.35	2.32	-1.88	4.20	0.15			
3.29	-2.71	5.85	-4.82	10.67	0.37	76.13	2.35	-1.86	4.21	0.15			
3.20	-2.70	5.69	-4.80	10.49	0.37	77.84	2.36	-1.85	4.21	0.15			
	Avg			10.55	0.37	76.44		Avg	4.19	0.15			
	σ			0.19	0.00			σ	0.03	0.00			
	Variance			0.01	0.00			Variance	0.00	0.00			
3.21	-2.71	5.71	-4.82	10.53	0.37		2.32	-1.86	4.18	0.15			
Average LT						71.32							

Figure I1 – Data Summary for Taxiway A6 – Edge Load Point – Years 1-5

6-10 Years File "B1"													
Goal	Start (s)	Stop (s)	Start (s)	Apps.	Load Peak	Valley	Accelerometer #1 Peak	Valley	Adj. Pk.	Adj. Vly.	Defl.(mils)	Norm. Defl. (mils/pl)	
26,600 app. (1330 s)	10	1160	100s intervals	50	48000	11.37	4.31	1.17	-1.14	2.08	-2.03	4.11	0.36
@ 7.1 kips	Test Time	1150.0		250	52000	11.28	4.45	1.16	-1.14	2.06	-2.03	4.09	0.36
	Additional - from B	180.0		500	57000	11.43	4.29	1.12	-1.13	1.99	-2.01	4.00	0.35
	Total Apps./Period	26600		750	62000	11.39	4.40	1.12	-1.12	1.99	-1.99	3.98	0.35
	Total Apps./Overall	73800		1000	67000	11.31	4.45	1.16	-1.21	2.06	-2.15	4.21	0.37
					Avg Load	11.36			Avg		4.08	0.36	
					σ	0.06			σ		0.09	0.01	
					Variance	0.00			Variance		0.01	0.00	
					Avg Reading for Entire Test Period	11.36	4.38	1.15	-1.15	2.04	-2.04	4.09	0.36
				Additional - from B	11.32	4.32							
Goal	Start (s)	Stop (s)	Start (s)	Apps.	Load Peak	Valley	Accelerometer #1 Peak	Valley	Adj. Pk.	Adj. Vly.	Defl.(mils)	Norm. Defl. (mils/pl)	
12,100 app. (605 s)	1380	1990	100s intervals	1400	74200	16.11	3.02	2.35	-3.11	4.18	-5.53	9.71	0.60
@ 15.9 kips	Test Time	610.0		1500	76200	16.20	2.87	2.44	-3.15	4.34	-5.60	9.94	0.61
	Total Apps./Period	12200		1600	78200	16.17	2.92	2.56	-3.25	4.55	-5.78	10.33	0.64
		86000		1700	80200	16.19	2.90	2.56	-3.33	4.55	-5.92	10.47	0.65
				1800	82200	16.15	3.00	2.71	-3.26	4.82	-5.80	10.61	0.66
					Avg Load	16.16			Avg		10.21	0.63	
					σ	0.04			σ		0.38	0.02	
					Variance	0.00			Variance		0.14	0.00	
					Avg Reading for Entire Test Period	16.15	2.97	2.53	-3.15	4.50	-5.60	10.10	0.63
Goal	Start (s)	Stop (s)	Start (s)	Apps.	Load Peak	Valley	Accelerometer #1 Peak	Valley	Adj. Pk.	Adj. Vly.	Defl.(mils)	Norm. Defl. (mils/pl)	
10,400 app. (520 s)	2150	2610	50s intervals	2200	87000	30.70	6.91	4.23	-4.30	7.52	-7.47	14.99	0.48
@ 31.6 kips	Test Time	520.0		2300	89000	30.56	6.92	4.28	-4.23	7.61	-7.52	15.13	0.50
	Total Apps./Period	10400		2400	91000	30.59	6.94	4.34	-4.22	7.72	-7.50	15.22	0.50
		96400		2500	93000	30.56	6.94	4.57	-4.19	8.13	-7.45	15.58	0.51
				2600	95000	30.51	6.95	4.48	-4.23	7.97	-7.52	15.49	0.51
					Avg Load	30.58			Avg		15.28	0.50	
					σ	0.07			σ		0.25	0.01	
					Variance	0.01			Variance		0.06	0.00	
					Avg Reading for Entire Test Period	30.61	6.92	4.37	-4.23	7.77	-7.52	15.29	0.50



Accelerometer #2							Accelerometer #3				
Peak	Valley	Adj. Pk.	Adj. Vly.	Defl.(mils)	Norm. Defl. (mils/pl)	LT _{avg} (%)	Peak	Valley	Defl.(mils)	Norm. Defl. (mils/pl)	
0.81	-0.73	1.44	-1.30	2.74	0.24	66.67	0.55	-0.52	1.07	0.09	
0.80	-0.74	1.42	-1.32	2.74	0.24	66.96	0.53	-0.50	1.03	0.09	
0.85	-0.78	1.51	-1.39	2.90	0.25	72.44	0.58	-0.53	1.11	0.10	
0.80	-0.74	1.42	-1.32	2.74	0.24	68.75	0.54	-0.50	1.04	0.09	
0.83	-0.77	1.48	-1.37	2.84	0.25	67.51	0.54	-0.52	1.06	0.09	
				Avg	2.79	0.25	0.54		Avg	1.06	0.09
				σ	0.08	0.01			σ	0.03	0.00
				Variance	0.01	0.00			Variance	0.00	0.00
0.81	-0.75	1.44	-1.33	2.77	0.24		0.55	-0.51	1.06	0.09	

Accelerometer #2							Accelerometer #3				
Peak	Valley	Adj. Pk.	Adj. Vly.	Defl.(mils)	Norm. Defl. (mils/pl)	LT _{avg} (%)	Peak	Valley	Defl.(mils)	Norm. Defl. (mils/pl)	
1.73	-1.69	3.08	-3.00	6.08	0.38	62.64	1.18	-1.10	2.28	0.14	
1.79	-1.73	3.18	-3.08	6.26	0.39	62.97	1.23	-1.13	2.36	0.15	
1.80	-1.73	3.20	-3.08	6.26	0.39	60.76	1.20	-1.12	2.32	0.14	
1.77	-1.77	3.15	-3.15	6.29	0.39	60.10	1.17	-1.13	2.30	0.14	
1.91	-1.74	3.40	-3.09	6.49	0.40	61.14	1.26	-1.10	2.36	0.15	
				Avg	6.28	0.39	1.18		Avg	2.32	0.14
				σ	0.15	0.01			σ	0.04	0.00
				Variance	0.02	0.00			Variance	0.00	0.00
1.81	-1.72	3.22	-3.06	6.28	0.39		1.21	-1.11	2.32	0.14	

Accelerometer #2							Accelerometer #3				
Peak	Valley	Adj. Pk.	Adj. Vly.	Defl.(mils)	Norm. Defl. (mils/pl)	LT _{avg} (%)	Peak	Valley	Defl.(mils)	Norm. Defl. (mils/pl)	
3.85	-2.64	6.85	-4.69	11.54	0.38	76.99	2.74	-1.77	4.51	0.15	
3.83	-2.62	6.81	-4.66	11.47	0.38	75.79	2.75	-1.75	4.50	0.15	
3.84	-2.63	6.83	-4.68	11.50	0.38	75.58	2.73	-1.75	4.48	0.15	
3.87	-2.65	6.88	-4.71	11.59	0.38	74.43	2.71	-1.76	4.47	0.15	
3.82	-2.65	6.79	-4.71	11.50	0.38	74.28	2.66	-1.77	4.43	0.15	
				Avg	11.52	0.38	2.72		Avg	4.48	0.15
				σ	0.05	0.00			σ	0.03	0.00
				Variance	0.00	0.00			Variance	0.00	0.00
3.84	-2.65	6.83	-4.71	11.54	0.38		2.72	-1.76	4.48	0.15	
Average LT						68.44					

Figure I2 – Data Summary for Taxiway A6 – Edge Load Point – Years 6-10

11-15 Years File "B1"													
Goal	Start (s)	Stop (s)		Start (s)	Apps.	Load Peak	Valley	Accelerometer #1 Peak	Valley	Adj. Pk.	Adj. Vly	Defl.(mils)	Norm. Defl. (mils/pl)
26,600 app. (1330 s) @ 7.1 kips	2860	4199	50s intervals	3000	99200	10.80	4.18	1.21	-1.34	2.15	-2.38	4.53	0.42
Test Time	1339.0			3200	103200	10.83	4.15	1.22	-1.42	2.17	-2.52	4.69	0.43
Total Apps./Period	26780			3450	108200	10.84	4.15	1.17	-1.38	2.08	-2.45	4.53	0.42
Total Apps./Overall	123180			3700	113200	10.84	4.25	1.20	-1.32	2.13	-2.35	4.48	0.41
				3950	118200	10.82	4.20	1.16	-1.32	2.06	-2.35	4.41	0.41
						Avg Load	10.83			Avg		4.53	0.42
						σ	0.02			σ		0.10	0.01
						Variance	0.00			Variance		0.01	0.00
Avg Reading for Entire Test Period						10.83	4.20	1.19	-1.35	2.12	-2.40	4.52	0.42

Goal	Start (s)	Stop (s)		Start (s)	Apps.	Load Peak	Valley	Accelerometer #1 Peak	Valley	Adj. Pk.	Adj. Vly	Defl.(mils)	Norm. Defl. (mils/pl)
12,100 app. (605 s) @ 15.9 kips	4310	4905	50s intervals	4350	123980	16.12	2.73	2.63	-3.37	4.68	-5.99	10.67	0.66
Test Time	595.0			4450	125980	16.37	2.92	2.66	-3.40	4.73	-6.05	10.77	0.66
Total Apps./Period	11900			4550	127980	16.39	2.95	2.58	-3.44	4.59	-6.12	10.70	0.65
Total Apps./Overall	135080			4650	128180	16.33	2.99	2.65	-3.49	4.71	-6.21	10.92	0.67
				4750	131980	16.30	2.86	2.70	-3.49	4.80	-6.21	11.01	0.68
						Avg Load	16.30			Avg		10.81	0.66
						σ	0.11			σ		0.14	0.01
						Variance	0.01			Variance		0.02	0.00
Avg Reading for Entire Test Period						16.27	2.94	2.65	-3.42	4.71	-6.08	10.79	0.66

Goal	Start (s)	Stop (s)		Start (s)	Apps.	Load Peak	Valley	Accelerometer #1 Peak	Valley	Adj. Pk.	Adj. Vly	Defl.(mils)	Norm. Defl. (mils/pl)
10,400 app. (520 s) @ 31.6 kips	5040	5540	50s intervals	5050	135280	30.26	6.29	4.79	-5.36	8.52	-9.53	18.05	0.60
Test Time	500.0			5150	137280	29.84	6.54	4.58	-5.16	8.14	-9.17	17.32	0.58
Total Apps./Period	10000			5250	139280	29.82	6.52	4.56	-5.16	8.11	-9.17	17.28	0.58
Total Apps./Overall	145080			5350	141280	29.83	6.53	4.47	-5.28	7.95	-9.39	17.34	0.58
				5450	143280	29.90	6.39	4.48	-5.54	7.97	-9.85	17.82	0.60
						Avg Load	29.93			Avg		17.56	0.59
						σ	0.19			σ		0.35	0.01
						Variance	0.03			Variance		0.12	0.00
Avg Reading for Entire Test Period						29.96	6.41	4.55	-5.26	8.09	-9.35	17.44	0.58



Accelerometer #2							
Peak	Valley	Adj. Pk.	Adj. Vly	Defl.(mils)	Norm. Defl. (mils/pl)	LT _{US} (%)	
0.81	-0.74	1.44	-1.32	2.76	0.26	60.76	
0.83	-0.76	1.48	-1.35	2.83	0.26	60.23	
0.82	-0.79	1.46	-1.40	2.86	0.26	63.14	
0.80	-0.79	1.42	-1.40	2.83	0.26	63.10	
0.80	-0.75	1.42	-1.33	2.76	0.25	62.50	
				Avg	2.81	0.26	61.93
				σ	0.05	0.00	
				Variance	0.00	0.00	
0.81	-0.76	1.44	-1.35	2.79	0.26		

Accelerometer #2							
Peak	Valley	Adj. Pk.	Adj. Vly	Defl.(mils)	Norm. Defl. (mils/pl)	LT _{US} (%)	
1.96	-1.69	3.48	-3.00	6.49	0.40	60.83	
2.01	-1.72	3.57	-3.06	6.63	0.41	61.55	
2.12	-1.71	3.77	-3.04	6.81	0.42	63.62	
2.08	-1.74	3.70	-3.09	6.79	0.42	62.21	
2.09	-1.76	3.72	-3.13	6.85	0.42	62.20	
				Avg	6.71	0.41	62.08
				σ	0.15	0.01	
				Variance	0.02	0.00	
2.05	-1.72	3.64	-3.06	6.70	0.41		

Accelerometer #2							
Peak	Valley	Adj. Pk.	Adj. Vly	Defl.(mils)	Norm. Defl. (mils/pl)	LT _{US} (%)	
4.00	-3.02	7.11	-5.37	12.48	0.41	69.16	
3.92	-2.93	6.97	-5.21	12.18	0.41	70.33	
3.95	-2.93	7.02	-5.21	12.23	0.41	70.78	
3.99	-2.98	7.09	-5.30	12.39	0.42	71.49	
4.06	-3.00	7.22	-5.33	12.55	0.42	70.46	
				Avg	12.37	0.41	70.43
				σ	0.16	0.00	
				Variance	0.03	0.00	
3.96	-2.96	7.04	-5.25	12.30	0.41		

Accelerometer #3							
Peak	Valley	Defl.(mils)	Norm. Defl. (mils/pl)				
0.54	-0.26	1.03	0.10				
0.54	-0.50	1.04	0.10				
0.54	-0.50	1.04	0.10				
0.52	-0.48	1.00	0.09				
0.52	-0.48	1.01	0.09				
		Avg	1.02	0.09			
		σ	0.02	0.00			
		Variance	0.00	0.00			
0.53	-0.49	1.02	0.09				

Accelerometer #3							
Peak	Valley	Defl.(mils)	Norm. Defl. (mils/pl)				
1.41	-1.07	2.48	0.15				
1.44	-1.08	2.52	0.16				
1.50	-1.08	2.58	0.16				
1.49	-1.08	2.57	0.16				
1.50	-1.10	2.60	0.16				
		Avg	2.55	0.16			
		σ	0.05	0.00			
		Variance	0.00	0.00			
1.46	-1.08	2.54	0.16				

Accelerometer #3							
Peak	Valley	Defl.(mils)	Norm. Defl. (mils/pl)				
2.85	-1.96	4.81	0.16				
2.75	-1.91	4.66	0.16				
2.75	-1.89	4.64	0.16				
2.77	-1.92	4.69	0.16				
2.83	-1.92	4.75	0.16				
		Avg	4.71	0.16			
		σ	0.07	0.00			
		Variance	0.00	0.00			
2.77	-1.91	4.68	0.16				

Figure I3 – Data Summary for Taxiway A6 – Edge Load Point – Years 11-15

16-20 Years File "B1 & B2"									
Goal	Start (s)	Stop (s)	Start (s)	Apps.	Load Peak	Valley	Accelerometer #1 Peak	Valley	Adj. Pk.
28,500 app. (1330 s) @ 7.1 kips	6205	7035	50s intervals	8000 155180	10.27	3.98	1.63	-1.75	2.34
Test Time	1340.0			6200 155180	10.34	3.98	1.37	-1.76	2.44
Total Apps/Period	26800			6450 160180	10.22	4.10	1.25	-1.57	2.22
Total Apps/Overall	171890			6700 165180	10.35	3.99	1.38	-1.70	2.45
				6950 170180	10.29	4.18	1.31	-1.64	2.33
				Avg Load	10.29		Avg		5.44
				Variance	0.05		Variance		0.34
					0.00				0.12
				Avg Reading for Entire Test Period	10.30	4.07	1.32	-1.63	2.35
									-2.90
									5.25
									% Inc
									55.64
Goal	Start (s)	Stop (s)	Start (s)	Apps.	Load Peak	Valley	Accelerometer #1 Peak	Valley	Adj. Pk.
12,100 app. (805 s) @ 15.9 kips	7170	7550	50s intervals	7200 172480	16.84	4.52	2.56	-3.35	4.55
Test Time	480.0			7300 174480	17.04	4.60	2.30	-3.28	4.09
Total Apps/Period	9600			7350 175480	16.97	4.65	2.29	-3.15	4.07
Total Apps/Overall	181480			7400 176480	16.94	4.61	2.40	-3.21	4.27
				7500 178480	16.99	4.64	2.68	-3.49	4.77
				Avg Load	16.96		Avg		10.20
				Variance	0.07		Variance		0.52
					0.01				0.27
				Avg Reading for Entire Test Period	16.95	4.64	2.47	-3.31	4.39
									-5.89
									10.28
									% Inc
									27.60
Goal	Start (s)	Stop (s)	Start (s)	Apps.	Load Peak	Valley	Accelerometer #1 Peak	Valley	Adj. Pk.
10,400 app. (520 s) @ 31.6 kips	7500	8075	50s intervals	7800 181480	29.97	4.33	4.46	-6.96	7.33
Test Time	175.0			8000 183480	30.24	4.24	5.00	-7.08	8.89
				50 184000	30.18	4.23	4.67	-7.51	8.30
Additional - from B2	24	294		150 186000	29.71	4.67	4.62	-7.28	8.21
Test Time	270.0			200 187000	29.70	4.72	4.50	-7.19	8.00
				Avg Load	29.96		Avg		21.68
				Variance	0.25		Variance		0.53
					0.06				0.28
					30.11	4.31	4.67	-7.04	8.30
				Avg Reading for Entire Test Period	29.83	4.56	4.58	-7.30	8.14
									-12.52
									20.82
									21.12
									% Inc
									46.18



Accelerometer #2							
Peak	Valley	Adj. Pk.	Adj. Vly	Defl.(mils)	Norm. Defl. (mils/pl)	LT use (%)	
0.88	-0.82	1.56	-1.46	3.02	0.29	51.05	
0.92	-0.85	1.64	-1.51	3.15	0.30	56.55	
0.88	-0.84	1.56	-1.49	3.06	0.30	60.99	
0.90	-0.84	1.60	-1.49	3.09	0.30	56.49	
0.87	-0.80	1.55	-1.42	2.97	0.29	56.61	
Avg				3.06	0.30	56.17	
Variance				0.07	0.01		
				0.00	0.00		
0.88	-0.82	1.56	-1.46	3.02	0.29		

Accelerometer #3							
Peak	Valley	Defl.(mils)	Norm. Defl. (mils/pl)				
0.60	-0.52	1.12	0.11				
0.63	-0.53	1.16	0.11				
0.59	-0.52	1.11	0.11				
0.61	-0.53	1.14	0.11				
0.59	-0.50	1.09	0.11				
Avg		1.12	0.11				
Variance		0.03	0.00				
		0.00	0.00				
0.60	-0.52	1.12	0.11				

Accelerometer #2							
Peak	Valley	Adj. Pk.	Adj. Vly	Defl.(mils)	Norm. Defl. (mils/pl)	LT use (%)	
1.92	-1.77	3.41	-3.15	6.56	0.39	62.65	
1.91	-1.77	3.40	-3.15	6.54	0.38	65.95	
1.87	-1.74	3.32	-3.09	6.42	0.38	66.36	
1.91	-1.75	3.40	-3.11	6.51	0.38	65.24	
1.98	-1.80	3.52	-3.20	6.72	0.40	61.26	
Avg				6.55	0.39	64.20	
Variance				0.11	0.01		
				0.01	0.00		
1.93	-1.77	3.43	-3.15	6.58	0.39		

Accelerometer #3							
Peak	Valley	Defl.(mils)	Norm. Defl. (mils/pl)				
1.36	-1.13	2.49	0.15				
1.37	-1.10	2.47	0.14				
1.33	-1.08	2.41	0.14				
1.35	-1.08	2.43	0.14				
1.38	-1.09	2.47	0.15				
Avg		2.45	0.14				
Variance		0.03	0.00				
		0.00	0.00				
1.36	-1.09	2.45	0.14				

Accelerometer #2							
Peak	Valley	Adj. Pk.	Adj. Vly	Defl.(mils)	Norm. Defl. (mils/pl)	LT use (%)	
4.02	-3.76	7.15	-6.69	13.83	0.48	68.01	
4.55	-3.87	8.09	-6.88	14.97	0.50	69.70	
4.13	-4.02	7.34	-7.15	14.49	0.48	66.91	
3.91	-3.89	6.95	-6.92	13.87	0.47	65.55	
4.02	-3.91	7.15	-6.95	14.10	0.47	67.94	
Avg				14.25	0.48	67.60	
Variance				0.48	0.01		
				0.23	0.00		
4.22	-3.83	7.50	-6.81	14.31	0.48		
4.02	-3.95	7.15	-7.02	14.17	0.48		
Average LT						62.65	

Accelerometer #3							
Peak	Valley	Defl.(mils)	Norm. Defl. (mils/pl)				
3.11	-2.43	5.54	0.18				
3.49	-2.49	5.98	0.20				
3.11	-2.50	5.71	0.19				
2.96	-2.51	5.47	0.18				
3.01	-2.51	5.52	0.19				
Avg		5.64	0.19				
Variance		0.21	0.01				
		0.04	0.00				
3.27	-2.46	5.73	0.19				
3.04	-2.54	5.58	0.19				

Figure I4 – Data Summary for Taxiway A6 – Edge Load Point – Years 16-20

Point #2 A6 Corner

1-5 Years File "C1"

Goal	Start (s)	Stop (s)	Start (s)	Apps.	Load	Valley	Accelerometer #1	Peak	Valley	Defl.(mils)
26,600 app. (1330 s)	50	1400.0	50 sec intervals	100	1000	9.99	3.94	2.04	-2.38	4.42
@ 7.1 kips	Test Time	1350.0	300	5000	9.89	4.02	1.95	-2.17	4.12	
Total Apps/Period		27000	550	10000	9.94	4.08	1.91	-2.06	3.97	
Total Apps/Overall		27000	800	15000	9.96	4.04	1.96	-2.10	4.06	
			1050	20000	10.95	3.01	2.80	-3.74	6.54	
					Avg Load	10.15		Avg	4.62	
					σ	0.45		σ	1.09	
					Variance	0.20		Variance	1.18	
					Avg Reading for Entire Test Period	10.21	3.77	1.96	-2.18	4.14

Goal	Start (s)	Stop (s)	Start (s)	Apps.	Load	Valley	Accelerometer #1	Peak	Valley	Defl.(mils)
12,100 app. (605 s)	1545	2152.0	50 sec intervals	1600	28100	15.88	3.17	4.21	-6.73	10.94
@ 15.9 kips	Test Time	607.0	1700	30100	16.05	3.22	4.18	-6.87	11.05	
Total Apps/Period		12140	1800	32100	16.01	3.27	4.10	-6.76	10.86	
Total Apps/Overall		39140	1900	34100	15.97	2.82	4.10	-6.65	10.75	
			2000	36100	16.05	3.23	4.13	-6.78	10.91	
					Avg Load	15.99		Avg	10.90	
					σ	0.07		σ	0.11	
					Variance	0.01		Variance	0.01	
					Avg Reading for Entire Test Period	15.96	3.23	4.14	-6.70	10.84

Goal	Start (s)	Stop (s)	Start (s)	Apps.	Load	Valley	Accelerometer #1	Peak	Valley	Defl.(mils)
10,400 app. (520 s)	2440	2961.0	50 sec intervals	2500	40340	29.82	4.64	7.17	-12.90	20.07
@ 31.6 kips	Test Time	521.0	2600	42340	29.96	4.87	7.27	-12.86	20.13	
Total Apps/Period		10420	2700	44340	29.94	4.82	7.30	-12.99	20.29	
Total Apps/Overall		49560	2800	46340	29.92	4.81	7.56	-13.38	20.94	
			2900	48340	29.79	4.97	7.54	-13.24	20.78	
					Avg Load	29.89		Avg	20.44	
					σ	0.08		σ	0.39	
					Variance	0.01		Variance	0.16	
					Avg Reading for Entire Test Period	29.85	4.79	7.34	-13.05	20.39



Accelerometer #2					Accelerometer #3			
Peak	Valley	Defl.(mils)	Norm. Defl. (mils/pl)	LT _{US} (%)	Peak	Valley	Defl.(mils)	Norm. Defl. (mils/pl)
1.37	-1.26	2.63	0.26	59.50	1.03	-0.93	1.96	0.20
1.32	-1.21	2.53	0.26	61.41	0.99	-0.90	1.89	0.19
1.27	-1.18	2.45	0.25	61.71	0.96	-0.86	1.82	0.18
1.29	-1.17	2.46	0.25	60.59	0.97	-0.86	1.83	0.18
1.77	-1.90	3.67	0.34	66.12	1.34	-1.42	2.76	0.25
Avg	2.78	0.27	60.09		Avg	2.05	0.20	
σ	0.60	0.04			σ	0.40	0.03	
Variance	0.36	0.00			Variance	0.16	0.00	
1.31	-1.21	2.52	0.25		1.08	-1.01	2.09	0.20

Accelerometer #2					Accelerometer #3			
Peak	Valley	Defl.(mils)	Norm. Defl. (mils/pl)	LT _{US} (%)	Peak	Valley	Defl.(mils)	Norm. Defl. (mils/pl)
2.94	-3.83	6.77	0.43	61.88	2.23	-2.95	5.18	0.33
3.02	-3.97	6.99	0.44	63.26	2.26	-3.06	5.32	0.33
2.98	-3.96	6.94	0.43	63.90	2.26	-3.07	5.33	0.33
2.93	-3.94	6.87	0.43	63.91	2.24	-3.05	5.29	0.33
3.01	-4.01	7.02	0.44	64.34	2.72	-3.12	5.84	0.36
Avg	6.92	0.43	63.46		Avg	5.39	0.34	
σ	0.10	0.00			σ	0.26	0.02	
Variance	0.01	0.00			Variance	0.07	0.00	
2.97	-3.89	6.86	0.43		2.25	-3.01	5.26	0.33

Accelerometer #2					Accelerometer #3			
Peak	Valley	Defl.(mils)	Norm. Defl. (mils/pl)	LT _{US} (%)	Peak	Valley	Defl.(mils)	Norm. Defl. (mils/pl)
5.21	-8.09	13.30	0.45	66.27	3.95	-6.29	10.24	0.34
5.28	-8.11	13.39	0.45	66.52	4.03	-6.32	10.35	0.35
5.27	-8.19	13.46	0.45	66.34	4.02	-6.37	10.39	0.35
5.38	-8.43	13.81	0.46	65.95	4.09	-6.55	10.64	0.36
5.35	-8.39	13.74	0.46	66.12	4.07	-6.92	10.99	0.37
Avg	13.54	0.45	66.24		Avg	10.52	0.35	
σ	0.22	0.01			σ	0.30	0.01	
Variance	0.05	0.00			Variance	0.09	0.00	
5.27	-8.22	13.49	0.45		4.01	-6.89	10.90	0.37
Average LT				63.26				

Figure I5 – Data Summary for Taxiway A6 – Corner Load Point – Years 1-5

6-10 Years

File "C1"

Goal	Start (s)	Stop (s)
26,600 app. (1330 s)	3129	4466.0
@ 7.1 kips	Test Time	1337.0
	Total Apps./Period	26740
	Total Apps./Overall	76300

Start (s)	Apps.
50 sec intervals	3200 50980
	3400 54980
	3600 58980
	3800 62980
	4000 66980

Load	Valley
Peak	
11.18	5.41
11.18	5.24
11.20	5.41
11.29	5.34
11.27	5.34
Avg Load	11.22
σ	0.05
Variance	0.00
	11.25 5.37

Accelerometer #1	Defl.(mils)
Peak	Valley
1.98	-2.42
1.88	-2.31
1.83	-2.21
1.90	-2.29
1.85	-2.17
Avg	4.17
σ	0.15
Variance	0.02
	1.87 -2.26 4.13

Avg Reading for Entire Test Period

Goal	Start (s)	Stop (s)
12,100 app. (605 s)	4585	5188.0
@ 15.9 kips	Test Time	603.0
	Total Apps./Period	12060
	Total Apps./Overall	88360

Start (s)	Apps.
50 sec intervals	4600 76600
	4700 78600
	4800 80600
	4900 82600
	5000 84600

Load	Valley
Peak	
16.85	2.89
17.09	3.05
17.08	3.09
17.10	3.10
17.13	3.06
Avg Load	17.05
σ	0.11
Variance	0.01
	17.07 3.03

Accelerometer #1	Defl.(mils)
Peak	Valley
5.28	-7.37
5.08	-7.42
4.96	-7.38
4.82	-7.27
4.73	-7.35
Avg	12.33
σ	0.25
Variance	0.06
	4.89 -7.40 12.29

Avg Reading for Entire Test Period

Goal	Start (s)	Stop (s)
10,400 app. (520 s)	5290	5817.0
@ 31.6 kips	Test Time	527.0
	Total Apps./Period	10540
	Total Apps./Overall	98900

Start (s)	Apps.
50 sec intervals	5350 89560
	5450 91560
	5550 93560
	5650 95560
	5750 97560

Load	Valley
Peak	
30.42	5.18
30.54	5.41
30.58	5.34
30.84	5.25
31.47	5.16
Avg Load	30.77
σ	0.42
Variance	0.18
	30.75 5.17

Accelerometer #1	Defl.(mils)
Peak	Valley
7.86	-12.01
7.81	-11.71
7.92	-11.92
7.98	-12.19
7.89	-12.67
Avg	19.99
σ	0.39
Variance	0.15
	7.91 -12.17 20.08

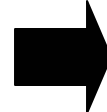
Avg Reading for Entire Test Period



Accelerometer #2	Peak	Valley	Defl.(mils)	Norm. Defl. (mils/pi)	LT _{US} (%)	Accelerometer #3	Peak	Valley	Defl.(mils)	Norm. Defl. (mils/pi)
	1.28	-1.46	2.74	0.25	62.27		0.97	-1.10	2.07	0.19
	1.23	-1.42	2.65	0.24	63.25		0.93	-1.07	2.00	0.18
	1.22	-1.41	2.63	0.23	65.10		0.92	-1.05	1.97	0.18
	1.24	-1.44	2.68	0.24	63.96		0.95	-1.09	2.04	0.18
	1.22	-1.38	2.60	0.23	64.68		0.93	-1.06	1.99	0.18
	Avg	2.64	0.24	63.34			Avg	2.01	0.18	
	σ	0.03	0.01				σ	0.04	0.00	
	Variance	0.00	0.00				Variance	0.00	0.00	
	1.23	-1.40	2.63	0.23			0.93	-1.07	2.00	0.18
Accelerometer #2	Peak	Valley	Defl.(mils)	Norm. Defl. (mils/pi)	LT _{US} (%)	Accelerometer #3	Peak	Valley	Defl.(mils)	Norm. Defl. (mils/pi)
	3.76	-4.21	7.97	0.47	63.00		2.87	-3.29	6.16	0.37
	3.67	-4.27	7.94	0.46	63.52		2.85	-3.32	6.17	0.36
	3.57	-4.24	7.81	0.46	63.29		2.79	-3.30	6.09	0.36
	3.46	-4.18	7.64	0.45	63.19		2.71	-3.21	5.92	0.35
	3.38	-4.22	7.60	0.44	62.91		2.66	-3.29	5.95	0.35
	Avg	7.79	0.46	63.19			Avg	6.06	0.36	
	σ	0.17	0.01				σ	0.12	0.01	
	Variance	0.03	0.00				Variance	0.01	0.00	
	3.51	-4.24	7.75	0.45			2.73	-3.31	6.04	0.35
Accelerometer #2	Peak	Valley	Defl.(mils)	Norm. Defl. (mils/pi)	LT _{US} (%)	Accelerometer #3	Peak	Valley	Defl.(mils)	Norm. Defl. (mils/pi)
	5.77	-8.07	13.84	0.45	69.65		4.46	-6.24	10.70	0.35
	5.69	-7.86	13.55	0.44	69.42		4.43	-6.07	10.50	0.34
	5.77	-7.96	13.73	0.45	69.20		4.40	-6.16	10.56	0.35
	5.89	-8.00	13.89	0.45	68.86		4.53	-6.19	10.72	0.35
	6.07	-8.20	14.27	0.45	69.41		4.81	-6.34	11.15	0.35
	Avg	13.86	0.45	69.31			Avg	10.73	0.35	
	σ	0.27	0.00				σ	0.25	0.00	
	Variance	0.07	0.00				Variance	0.06	0.00	
	5.85	-8.06	13.91	0.45			4.52	-6.23	10.75	0.35
Average LT					65.28					

Figure I6 – Data Summary for Taxiway A6 – Corner Load Point – Years 6-10

11-15 Years File "C1"									
Goal	Start (s)	Stop (s)	Start (s)	Apps.	Load Peak	Valley	Accelerometer #1 Peak	Valley	Defl.(mils)
26,600 app. (1330 s)	5900	7241.0	50 sec intervals	6000 100900	11.31	4.63	2.43	-2.95	5.38
@ 7.1 kips	Test Time	1341.0		6200 104900	11.43	4.56	2.40	-2.98	5.38
	Total Apps./Period	26820		6400 108900	11.44	4.67	2.35	-2.86	5.21
	Total Apps./Overall	125720		6600 112900	11.57	4.57	2.38	-2.95	5.33
				6800 116900	11.54	4.61	2.34	-2.86	5.20
				Avg Load	11.46			Avg	5.30
				σ	0.10			σ	0.09
				Variance	0.01			Variance	0.01
				Avg Reading for Entire Test Period	11.48	4.59		2.36	-2.89 5.25
Goal	Start (s)	Stop (s)	Start (s)	Apps.	Load Peak	Valley	Accelerometer #1 Peak	Valley	Defl.(mils)
12,100 app. (605 s)	7312	7932.0	50 sec intervals	7400 127480	15.70	3.50	3.77	-5.28	9.05
@ 15.9 kips	Test Time	620.0		7500 129480	15.85	3.50	3.76	-5.34	9.10
	Total Apps./Period	12400		7600 131480	15.86	3.51	3.78	-5.42	9.20
	Total Apps./Overall	138120		7700 133480	15.93	3.48	3.73	-5.42	9.15
				7800 135480	15.85	3.40	3.81	-5.35	9.16
				Avg Load	15.84			Avg	9.13
				σ	0.06			σ	0.06
				Variance	0.01			Variance	0.00
				Avg Reading for Entire Test Period	16.02	4.19		4.01	-5.62 9.63
Goal	Start (s)	Stop (s)	Start (s)	Apps.	Load Peak	Valley	Accelerometer #1 Peak	Valley	Defl.(mils)
10,400 app. (520 s)	8075	8596.0	50 sec intervals	8100 138620	30.08	4.15	9.17	-12.37	21.54
@ 31.6 kips	Test Time	521.0		8200 140620	30.09	4.12	9.19	-12.49	21.68
	Total Apps./Period	10420		8300 142620	30.17	4.12	9.09	-15.66	24.65
	Total Apps./Overall	148540		8400 144620	30.13	4.17	8.44	-12.54	20.98
				8500 146620	30.30	4.00	8.68	-12.57	21.25
				Avg Load	30.15			Avg	22.02
				σ	0.09			σ	1.49
				Variance	0.01			Variance	2.23
				Avg Reading for Entire Test Period	30.15	4.07		9.01	-12.57 21.58



Accelerometer #2						Accelerometer #3			
Peak	Valley	Defl.(mils)	Norm. Defl. (mils/pl)	LT _{US} (%)		Peak	Valley	Defl.(mils)	Norm. Defl. (mils/pl)
1.57	-1.77	3.34	0.30	62.08		1.20	-1.36	2.56	0.23
1.55	-1.81	3.36	0.29	62.45		1.19	-1.37	2.56	0.22
1.49	-1.70	3.19	0.28	61.23		1.13	-1.31	2.44	0.21
1.54	-1.76	3.30	0.29	61.89		1.18	-1.36	2.54	0.22
1.54	-1.75	3.29	0.29	63.27		1.17	-1.34	2.51	0.22
	Avg	3.29	0.29	61.98			Avg	2.52	0.22
	σ	0.07	0.01				σ	0.05	0.01
	Variance	0.00	0.00				Variance	0.00	0.00
1.54	-1.75	3.29	0.29			1.17	-1.34	2.51	0.22
Accelerometer #2						Accelerometer #3			
Peak	Valley	Defl.(mils)	Norm. Defl. (mils/pl)	LT _{US} (%)		Peak	Valley	Defl.(mils)	Norm. Defl. (mils/pl)
2.60	-3.24	5.84	0.37	64.53		2.01	-2.48	4.49	0.29
2.60	-3.27	5.87	0.37	64.51		2.01	-2.50	4.51	0.28
2.62	-3.30	5.92	0.37	64.35		2.01	-2.52	4.53	0.29
2.56	-3.27	5.83	0.37	63.72		1.98	-2.52	4.50	0.28
2.58	-3.26	5.84	0.37	63.76		1.93	-2.48	4.41	0.28
	Avg	5.86	0.37	64.17			Avg	4.49	0.28
	σ	0.04	0.00				σ	0.05	0.00
	Variance	0.00	0.00				Variance	0.00	0.00
2.78	-3.41	6.19	0.39			2.13	-2.62	4.75	0.30
Accelerometer #2						Accelerometer #3			
Peak	Valley	Defl.(mils)	Norm. Defl. (mils/pl)	LT _{US} (%)		Peak	Valley	Defl.(mils)	Norm. Defl. (mils/pl)
7.15	-7.95	15.10	0.50	70.10		5.51	-6.12	11.83	0.39
7.13	-8.01	15.14	0.50	69.83		5.48	-6.19	11.67	0.39
6.90	-8.05	14.95	0.50	60.65		5.37	-6.22	11.59	0.38
6.59	-8.03	14.62	0.49	69.69		5.11	-6.21	11.32	0.38
6.45	-8.22	14.67	0.48	69.04		5.05	-6.34	11.39	0.38
	Avg	14.90	0.49	67.65			Avg	11.52	0.38
	σ	0.24	0.01				σ	0.16	0.01
	Variance	0.06	0.00				Variance	0.02	0.00
6.81	-8.03	14.84	0.49			5.27	-6.20	11.47	0.38
Average LT				64.60					

Figure I7 – Data Summary for Taxiway A6 – Corner Load Point – Years 11-15

16-20 Years			File "C2"																														
Goal	Start (s)	Stop (s)	Start (s)	Apps.	Load Peak	Valley	Accelerometer #1 Peak	Valley	Defl.(mils)																								
26,600 app. (1330 s) @ 7.1 kips	518	1858.0	50 sec intervals	600 150180	7.13	1.94	2.13	-2.53	4.66																								
Test Time	1340.0			800 154180	7.10	1.95	2.09	-2.43	4.52																								
Total Apps./Period	26800			1100 160180	7.31	1.80	2.16	-2.49	4.65																								
Total Apps./Overall	175340			1400 166180	7.28	1.86	2.14	-2.41	4.55																								
				1600 170180	7.36	1.36	2.21	-2.40	4.61																								
					Avg Load	7.24		Avg	4.60																								
					σ	0.11		σ	0.06																								
					Variance	0.01		Variance	0.00																								
						7.24	1.85		2.14	-2.43	4.57																						
									% inc																								
Avg Reading for Entire Test Period																																	
Goal	Start (s)	Stop (s)	Start (s)	Apps.	Load Peak	Valley	Accelerometer #1 Peak	Valley	Defl.(mils)																								
12,100 app. (605 s) @ 15.9 kips	2020	2640.0	50 sec intervals	2100 176940	16.15	3.50	4.67	-6.01	10.68																								
Test Time	620.0			2200 178940	16.16	3.50	4.49	-6.01	10.50																								
Total Apps./Period	12400			2300 180940	16.12	3.51	4.35	-5.96	10.31																								
Total Apps./Overall	187740			2400 182940	16.14	3.48	4.26	-6.00	10.26																								
				2500 184940	16.13	3.40	4.19	-6.08	10.27																								
					Avg Load	16.14		Avg	10.40																								
					σ	0.02		σ	0.18																								
					Variance	0.00		Variance	0.03																								
						16.17	3.42		4.43	-6.07	10.50																						
									% inc																								
Avg Reading for Entire Test Period																																	
Goal	Start (s)	Stop (s)	Start (s)	Apps.	Load Peak	Valley	Accelerometer #1 Peak	Valley	Defl.(mils)																								
10,400 app. (520 s) @ 31.6 kips	2775	3303.0	50 sec intervals	2800 188240	30.73	3.21	9.91	-14.60	24.51																								
Test Time	528.0			2900 190240	31.01	3.53	10.31	-14.96	25.27																								
Total Apps./Period	10560			3000 192240	30.97	3.59	10.30	-14.91	25.21																								
Total Apps./Overall	198300			3100 194240	30.82	3.67	10.21	-14.83	25.04																								
				3200 196240	32.74	3.36	10.93	-15.29	26.22																								
					Avg Load	31.25		Avg	25.25																								
					σ	0.84		σ	0.62																								
					Variance	0.70		Variance	0.38																								
						31.31	3.46		10.35	-14.92	25.27																						
									% inc																								

Accelerometer #2					Accelerometer #3				
Peak	Valley	Defl.(mils)	Norm. Defl. (mils/pl)	LT us (%)	Peak	Valley	Defl.(mils)	Norm. Defl. (mils/pl)	
1.23	-1.45	2.68	0.38	57.51	0.92	-1.12	2.04	0.29	
1.22	-1.38	2.60	0.37	57.52	0.90	-1.06	1.96	0.28	
1.28	-1.40	2.68	0.37	57.63	0.96	-1.08	2.04	0.28	
1.28	-1.33	2.61	0.36	57.36	0.96	-1.01	1.97	0.27	
1.30	-1.30	2.60	0.35	56.40	0.99	-1.02	2.01	0.27	
	Avg	2.62	0.36	57.04		Avg	2.00	0.28	
	σ	0.04	0.01			σ	0.04	0.01	
	Variance	0.00	0.00			Variance	0.00	0.00	
1.27	-1.36	2.63	0.36		0.95	-1.05	2.00	0.28	

Accelerometer #2					Accelerometer #3				
Peak	Valley	Defl.(mils)	Norm. Defl. (mils/pl)	LT us (%)	Peak	Valley	Defl.(mils)	Norm. Defl. (mils/pl)	
3.29	-3.65	6.94	0.43	64.98	2.54	-2.80	5.34	0.33	
3.16	-3.66	6.82	0.42	64.95	2.46	-2.81	5.27	0.33	
3.04	-3.63	6.67	0.41	64.69	2.35	-2.80	5.15	0.32	
2.94	-3.63	6.57	0.41	64.04	2.28	-2.78	5.06	0.31	
2.89	-3.65	6.54	0.41	63.68	2.22	-2.79	5.01	0.31	
	Avg	6.71	0.42	64.48		Avg	5.17	0.32	
	σ	0.17	0.01			σ	0.14	0.01	
	Variance	0.03	0.00			Variance	0.02	0.00	
3.07	-3.66	6.73	0.42		2.37	-2.81	5.18	0.32	

Accelerometer #2					Accelerometer #3					
Peak	Valley	Defl.(mils)	Norm. Defl. (mils/pl)	LT us (%)	Peak	Valley	Defl.(mils)	Norm. Defl. (mils/pl)		
7.04	-9.21	16.25	0.53	66.30	5.23	-7.06	12.29	0.40		
7.47	-9.64	17.11	0.55	67.71	5.47	-7.29	12.76	0.41		
7.47	-9.94	17.41	0.56	69.06	Errors in Accelerometer Readings					
7.36	-10.10	17.46	0.57	69.73		Avg	12.53	0.40		
8.25	-9.99	18.24	0.56	69.57		σ	0.33	0.01		
	Avg	17.29	0.55	68.49		Variance	0.11	0.00		
	σ	0.72	0.01				5.38	-7.18	12.56	0.40
	Variance	0.51	0.00							
4.22	-3.83	8.05	0.26							

Average LT63.33

Figure I8 – Data Summary for Taxiway A6 – Corner Load Point – Years 16-20

Point #3		A6 Center	
1-5 Years		File "D1"	
Goal	Start (s)	Stop (s)	
26,600 app. (1330 s)	273	1613.0	
@ 7.1 kips	Test Time	1340.0	
	Total Apps./Period	26800	
	Total Apps./Overall	26800	
	Start (s)	Apps.	
50 sec intervals	300	540	
	500	4540	
	800	10540	
	1100	16540	
	1300	20540	
	Load	Valley	
	Peak	Valley	
	7.00	1.81	
	7.13	1.64	
	7.18	1.62	
	7.28	1.59	
	7.31	1.58	
	Avg Load	7.18	
	σ	0.12	
	Variance	0.02	
	Avg Reading for Entire Test Period	7.22	1.61
	Accelerometer #1	Peak	Valley
	Peak	Valley	Defl.(mils)
	1.36	-1.44	2.80
	1.36	-1.43	2.79
	1.27	-1.31	2.58
	1.31	-1.32	2.63
	1.31	-1.32	2.63
	Avg	2.69	
	σ	0.10	
	Variance	0.01	
	Avg Reading for Entire Test Period	1.33	-1.36
	2.69		
Goal	Start (s)	Stop (s)	
12,100 app. (605 s)	1725	2331.0	
@ 15.9 kips	Test Time	606.0	
	Total Apps./Period	12120	
	Total Apps./Overall	38920	
	Start (s)	Apps.	
50 sec intervals	1800	28300	
	1900	30300	
	2000	32300	
	2100	34300	
	2200	36300	
	Load	Valley	
	Peak	Valley	
	16.43	3.18	
	16.33	3.11	
	16.37	3.02	
	16.30	3.11	
	16.40	3.02	
	Avg Load	16.37	
	σ	0.05	
	Variance	0.00	
	Avg Reading for Entire Test Period	16.36	3.09
	Accelerometer #1	Peak	Valley
	Peak	Valley	Defl.(mils)
	2.55	-3.54	6.09
	2.56	-3.53	6.09
	2.61	-3.60	6.21
	2.57	-3.53	6.10
	2.61	-3.58	6.19
	Avg	6.14	
	σ	0.06	
	Variance	0.00	
	Avg Reading for Entire Test Period	2.58	-3.55
	6.13		
Goal	Start (s)	Stop (s)	
10,400 app. (520 s)	2429	2959.0	
@ 31.6 kips	Test Time	530.0	
	Total Apps./Period	10600	
	Total Apps./Overall	49520	
	Start (s)	Apps.	
50 sec intervals	2500	40340	
	2600	42340	
	2700	44340	
	2800	46340	
	2900	48340	
	Load	Valley	
	Peak	Valley	
	31.12	3.49	
	31.13	3.65	
	31.11	3.66	
	31.08	3.63	
	31.09	3.60	
	Avg Load	31.11	
	σ	0.02	
	Variance	0.00	
	Avg Reading for Entire Test Period	31.08	3.57
	Accelerometer #1	Peak	Valley
	Peak	Valley	Defl.(mils)
	5.56	-6.96	12.52
	5.55	-7.02	12.57
	5.42	-7.05	12.47
	5.19	-7.10	12.29
	5.06	-7.08	12.14
	Avg	12.40	
	σ	0.18	
	Variance	0.03	
	Avg Reading for Entire Test Period	5.32	-7.01
	12.33		



Accelerometer #2				
Peak	Valley	Defl.(mils)	Norm. Defl. (mils/pl)	LT _{us} (%)
1.26	-1.20	2.46	0.35	87.88
1.29	-1.19	2.48	0.35	88.89
1.26	-1.27	2.53	0.35	98.06
1.27	-1.31	2.58	0.35	98.10
1.25	-1.27	2.52	0.34	95.82
	Avg	2.53	0.35	94.10
	σ	0.04	0.00	
	Variance	0.00	0.00	
1.28	-1.28	2.56	0.35	
Accelerometer #3				
Peak	Valley	Defl.(mils)	Norm. Defl. (mils/pl)	
1.17	-1.08	2.25	0.32	
1.24	-1.21	2.45	0.34	
1.20	-1.18	2.38	0.33	
1.22	-1.21	2.43	0.33	
1.16	-1.18	2.34	0.32	
	Avg	2.37	0.33	
	σ	0.08	0.01	
	Variance	0.01	0.00	
1.22	-1.19	2.41	0.33	
Accelerometer #2				
Peak	Valley	Defl.(mils)	Norm. Defl. (mils/pl)	LT _{us} (%)
2.34	-3.37	5.71	0.35	93.76
2.37	-3.36	5.73	0.35	94.09
2.43	-3.40	5.83	0.36	93.88
2.41	-3.34	5.75	0.35	94.26
2.48	-3.37	5.85	0.36	94.51
	Avg	5.77	0.35	94.10
	σ	0.06	0.00	
	Variance	0.00	0.00	
2.40	-3.37	5.77	0.35	
Accelerometer #3				
Peak	Valley	Defl.(mils)	Norm. Defl. (mils/pl)	
2.06	-3.15	5.21	0.32	
2.09	-3.15	5.24	0.32	
2.15	-3.18	5.33	0.33	
2.17	-3.10	5.27	0.32	
2.23	-3.13	5.36	0.33	
	Avg	5.28	0.32	
	σ	0.06	0.00	
	Variance	0.00	0.00	
2.13	-3.13	5.26	0.32	
Accelerometer #2				
Peak	Valley	Defl.(mils)	Norm. Defl. (mils/pl)	LT _{us} (%)
4.61	-6.44	11.05	0.36	88.26
4.89	-6.50	11.39	0.37	90.61
5.07	-6.55	11.62	0.37	93.18
5.03	-6.61	11.64	0.37	94.71
4.85	-6.58	11.43	0.37	94.15
	Avg	11.43	0.37	92.16
	σ	0.24	0.01	
	Variance	0.06	0.00	
4.83	-6.51	11.34	0.36	
Accelerometer #3				
Peak	Valley	Defl.(mils)	Norm. Defl. (mils/pl)	
3.89	-5.92	9.81	0.32	
3.93	-5.97	9.90	0.32	
4.00	-6.06	10.06	0.32	
4.00	-6.11	10.11	0.33	
4.12	-6.09	10.21	0.33	
	Avg	10.02	0.32	
	σ	0.16	0.01	
	Variance	0.03	0.00	
3.97	-6.00	9.97	0.32	
Average LT				
				93.45

Figure I9 – Data Summary for Taxiway A6 – Center Load Point – Years 1-5

6-10 Years			File "D1"																
Goal	Start (s)	Stop (s)	Start (s)	Apps.	Load Peak	Valley	Accelerometer #1 Peak	Valley	Defl.(mils)										
26,600 app. (1330 s) @ 7.1 kips	3147	4482.0	50 sec intervals	3200 50580	7.71	1.85	1.74	-1.48	3.22										
Test Time	1335.0			3400 54580	7.70	1.82	1.69	-1.49	3.18										
Total Apps./Period	26700			3700 60580	7.67	1.67	1.76	-1.46	3.22										
Total Apps./Overall	76220			4000 66580	7.71	1.73	1.73	-1.45	3.18										
				4200 70580	7.71	1.78	1.68	-1.50	3.18										
				Avg Load	7.70		Avg		3.20										
				σ	0.02		σ		0.02										
				Variance	0.00		Variance		0.00										
Avg Reading for Entire Test Period					7.69	1.76	1.72	-1.49	3.21										
Goal	Start (s)	Stop (s)	Start (s)	Apps.	Load Peak	Valley	Accelerometer #1 Peak	Valley	Defl.(mils)										
12,100 app. (605 s) @ 15.9 kips	4600	5205.0	50 sec intervals	4700 78220	16.53	3.35	2.84	-3.69	6.53										
Test Time	605.0			4800 80220	16.47	3.27	2.88	-3.69	6.57										
Total Apps./Period	12100			4900 82220	16.44	3.29	2.96	-3.73	6.69										
Total Apps./Overall	88320			5000 84220	16.40	3.35	3.00	-3.73	6.73										
				5100 86220	16.47	3.26	3.15	-3.78	6.93										
				Avg Load	16.46		Avg		6.69										
				σ	0.05		σ		0.16										
				Variance	0.00		Variance		0.02										
Avg Reading for Entire Test Period					16.52	3.35	3.01	-3.75	6.76										
Goal	Start (s)	Stop (s)	Start (s)	Apps.	Load Peak	Valley	Accelerometer #1 Peak	Valley	Defl.(mils)										
10,400 app. (520 s) @ 31.6 kips	5315	5836.0	50 sec intervals	5350 89020	30.44	5.18	4.36	-6.57	10.93										
Test Time	521.0			5450 91020	30.26	5.41	4.35	-6.66	11.01										
Total Apps./Period	10420			5550 93020	30.20	5.34	4.77	-6.74	11.51										
Total Apps./Overall	98740			5650 95020	30.16	5.25	4.67	-6.85	11.52										
				5750 97020	29.76	5.16	4.77	-6.74	11.51										
				Avg Load	30.16		Avg		11.30										
				σ	0.25		σ		0.30										
				Variance	0.06		Variance		0.09										
Avg Reading for Entire Test Period					30.20	3.73	4.55	-6.75	11.30										

Accelerometer #2					Accelerometer #3				
Peak	Valley	Defl.(mils)	Norm. Defl. (mils/pl)	LT _{us} (%)	Peak	Valley	Defl.(mils)	Norm. Defl. (mils/pl)	
1.60	-1.40	3.00	0.39	93.17	1.49	-1.26	2.75	0.36	
1.56	-1.41	2.97	0.39	93.40	1.45	-1.29	2.74	0.36	
1.64	-1.40	3.04	0.40	94.41	1.51	-1.29	2.80	0.37	
1.58	-1.37	2.95	0.38	92.77	1.48	-1.26	2.74	0.36	
1.55	-1.40	2.95	0.38	92.77	1.42	-1.27	2.69	0.35	
Avg		2.98	0.39	93.16	Avg		2.74	0.36	
σ		0.04	0.01		σ		0.04	0.01	
Variance		0.00	0.00		Variance		0.00	0.00	
1.59	-1.40	2.99	0.39		1.47	-1.26	2.73	0.36	
Accelerometer #2					Accelerometer #3				
Peak	Valley	Defl.(mils)	Norm. Defl. (mils/pl)	LT _{us} (%)	Peak	Valley	Defl.(mils)	Norm. Defl. (mils/pl)	
2.56	-3.42	5.98	0.36	91.58	2.28	-3.11	5.39	0.33	
2.63	-3.43	6.06	0.37	92.24	2.34	-3.09	5.43	0.33	
2.73	-3.46	6.19	0.38	92.53	2.42	-3.12	5.54	0.34	
2.75	-3.44	6.19	0.38	91.98	2.45	-3.08	5.53	0.34	
2.90	-3.50	6.40	0.39	92.35	2.60	-3.16	5.76	0.35	
Avg		6.16	0.37	92.14	Avg		5.53	0.34	
σ		0.16	0.01		σ		0.14	0.01	
Variance		0.03	0.00		Variance		0.02	0.00	
2.75	-3.74	6.49	0.39		2.45	-3.14	5.59	0.34	
Accelerometer #2					Accelerometer #3				
Peak	Valley	Defl.(mils)	Norm. Defl. (mils/pl)	LT _{us} (%)	Peak	Valley	Defl.(mils)	Norm. Defl. (mils/pl)	
3.92	-6.07	9.99	0.33	91.40	3.59	-5.50	9.09	0.30	
3.88	-6.15	10.03	0.33	91.13	3.63	-5.57	9.20	0.30	
3.99	-6.23	10.22	0.34	88.79	3.62	-5.64	9.26	0.31	
4.27	-6.32	10.59	0.35	91.93	3.80	-5.71	9.51	0.32	
4.36	-6.20	10.56	0.35	91.75	3.87	-5.61	9.48	0.32	
Avg		10.28	0.34	90.99	Avg		9.31	0.31	
σ		0.28	0.01		σ		0.18	0.01	
Variance		0.08	0.00		Variance		0.03	0.00	
4.13	-6.22	10.35	0.34		3.74	-5.63	9.37	0.31	
Average LT				92.10					

Figure I10 – Data Summary for Taxiway A6 – Center Load Point – Years 6-10

11-15 Years			File "D2"																	
Goal	Start (s)	Stop (s)	Start (s)	Apps.	Load	Peak	Valley	Accelerometer #1	Peak	Valley	Defl.(mils)	Peak	Valley	Defl.(mils)	Peak	Valley	Defl.(mils)			
26,600 app. (1330 s)	133	1521.0	50 sec intervals	200	100080	7.52	2.23	1.50	-1.26	2.76	1.42	-1.18	2.60	1.59	-1.28	2.87	1.58	-1.36	2.94	
@ 7.1 kips	Test Time	1388.0		400	104080	7.51	2.33	1.50	-1.26	2.76	1.42	-1.18	2.60	1.59	-1.28	2.87	1.58	-1.36	2.94	
	Total Apps./Period	27760		700	110080	7.61	2.25	1.50	-1.26	2.76	1.42	-1.18	2.60	1.59	-1.28	2.87	1.58	-1.36	2.94	
	Total Apps./Overall	126500		1000	116080	7.71	2.17	1.50	-1.31	2.81	1.42	-1.18	2.60	1.59	-1.28	2.87	1.58	-1.36	2.94	
				1200	120080	7.67	2.22	1.50	-1.31	2.81	1.42	-1.18	2.60	1.59	-1.28	2.87	1.58	-1.36	2.94	
						Avg Load	7.60		Avg	2.80										
						σ	0.09		σ	0.13										
						Variance	0.01		Variance	0.02										
							7.61	2.24		1.52	-1.27	2.79								
						Avg Reading for Entire Test Period														
Goal	Start (s)	Stop (s)	Start (s)	Apps.	Load	Peak	Valley	Accelerometer #1	Peak	Valley	Defl.(mils)	Peak	Valley	Defl.(mils)	Peak	Valley	Defl.(mils)			
12,100 app. (605 s)	1595	2207.0	50 sec intervals	1650	127600	16.15	3.51	3.17	-3.78	6.95	3.26	-3.81	7.07	3.15	-3.80	6.95	3.26	-3.81	7.07	
@ 15.9 kips	Test Time	612.0		1750	129600	16.14	3.50	3.26	-3.81	7.07	3.15	-3.80	6.95	3.15	-3.80	6.95	3.26	-3.81	7.07	
	Total Apps./Period	12240		1850	131600	16.15	3.51	3.15	-3.80	6.95	3.15	-3.80	6.95	3.15	-3.80	6.95	3.26	-3.81	7.07	
	Total Apps./Overall	138740		1950	133600	16.17	3.48	3.20	-3.79	6.99	3.15	-3.80	6.95	3.15	-3.80	6.95	3.26	-3.81	7.07	
				2050	135600	16.24	3.40	3.18	-3.82	7.00	3.15	-3.80	6.95	3.15	-3.80	6.95	3.26	-3.81	7.07	
						Avg Load	16.17		Avg	6.99										
						σ	0.04		σ	0.05										
						Variance	0.00		Variance	0.00										
							16.18	3.33		3.18	-3.80	6.98								
						Avg Reading for Entire Test Period														
Goal	Start (s)	Stop (s)	Start (s)	Apps.	Load	Peak	Valley	Accelerometer #1	Peak	Valley	Defl.(mils)	Peak	Valley	Defl.(mils)	Peak	Valley	Defl.(mils)			
10,400 app. (520 s)	2396	2916.0	50 sec intervals	2450	139820	30.77	4.15	4.68	-7.21	11.89	4.92	-6.89	11.81	5.12	-6.79	11.91	5.03	-6.87	11.90	
@ 31.6 kips	Test Time	520.0		2550	141820	30.36	4.12	4.92	-6.89	11.81	5.12	-6.79	11.91	5.12	-6.79	11.91	5.03	-6.87	11.90	
	Total Apps./Period	10400		2650	143820	30.29	4.12	5.12	-6.79	11.91	5.12	-6.79	11.91	5.12	-6.79	11.91	5.03	-6.87	11.90	
	Total Apps./Overall	149140		2750	145820	30.34	4.17	5.03	-6.87	11.90	5.12	-6.79	11.91	5.12	-6.79	11.91	5.03	-6.87	11.90	
				2850	147820	30.34	4.00	4.73	-6.81	11.54	5.12	-6.79	11.91	5.12	-6.79	11.91	5.03	-6.87	11.90	
						Avg Load	30.42		Avg	11.81										
						σ	0.20		σ	0.16										
						Variance	0.04		Variance	0.02										
							30.41	5.07		4.86	-6.91	11.77								
						Avg Reading for Entire Test Period														



Accelerometer #2					Accelerometer #3				
Peak	Valley	Defl.(mils)	Norm. Defl. (mils/pl)	LT _{US} (%)	Peak	Valley	Defl.(mils)	Norm. Defl. (mils/pl)	LT _{US} (%)
1.40	-1.16	2.56	0.34	92.68	1.33	-1.07	2.40	0.32	92.32
1.33	-1.12	2.45	0.33	94.23	1.27	-1.03	2.30	0.31	94.23
1.45	-1.20	2.65	0.35	92.33	1.38	-1.10	2.48	0.33	92.33
1.46	-1.28	2.74	0.36	93.20	1.36	-1.19	2.55	0.33	93.20
1.41	-1.23	2.64	0.34	93.95	1.28	-1.11	2.39	0.31	93.95
	Avg	2.62	0.34	93.71		Avg	2.42	0.32	93.71
	σ	0.12	0.01			σ	0.10	0.01	
	Variance	0.01	0.00			Variance	0.01	0.00	
1.41	-1.20	2.61	0.34		1.31	-1.10	2.41	0.32	
Accelerometer #2					Accelerometer #3				
Peak	Valley	Defl.(mils)	Norm. Defl. (mils/pl)	LT _{US} (%)	Peak	Valley	Defl.(mils)	Norm. Defl. (mils/pl)	LT _{US} (%)
2.91	-3.51	6.42	0.40	92.37	2.62	-3.17	5.79	0.36	92.37
2.93	-3.50	6.43	0.40	90.95	2.64	-3.19	5.83	0.36	90.95
2.86	-3.50	6.36	0.39	91.51	2.59	-3.22	5.81	0.36	91.51
2.84	-3.49	6.33	0.39	90.56	2.62	-3.21	5.83	0.36	90.56
2.83	-3.52	6.35	0.39	90.71	2.58	-3.25	5.83	0.36	90.71
	Avg	6.38	0.39	91.22		Avg	5.82	0.36	91.22
	σ	0.04	0.00			σ	0.02	0.00	
	Variance	0.00	0.00			Variance	0.00	0.00	
2.86	-3.50	6.36	0.39		2.59	-3.21	5.80	0.36	
Accelerometer #2					Accelerometer #3				
Peak	Valley	Defl.(mils)	Norm. Defl. (mils/pl)	LT _{US} (%)	Peak	Valley	Defl.(mils)	Norm. Defl. (mils/pl)	LT _{US} (%)
4.09	-6.55	10.64	0.35	89.49	3.73	-5.95	9.68	0.31	89.49
3.88	-6.25	10.13	0.33	85.77	3.42	-5.66	9.08	0.30	85.77
3.99	-6.17	10.16	0.34	85.31	3.28	-5.53	8.81	0.29	85.31
4.30	-6.25	10.55	0.35	88.66	3.29	-5.70	8.99	0.30	88.66
4.30	-6.20	10.50	0.35	90.99	3.34	-5.69	9.03	0.30	90.99
	Avg	10.40	0.34	88.03		Avg	9.12	0.30	88.03
	σ	0.23	0.01			σ	0.33	0.01	
	Variance	0.06	0.00			Variance	0.11	0.00	
4.08	-6.20	10.28	0.34		3.45	-5.71	9.16	0.30	
Average LT				90.98					

Figure I11 – Data Summary for Taxiway A6 – Center Load Point – Years 11-15

Point #4

South Run-Up Center

1-5 Years

File "E1"

Goal	Start (s)	Stop (s)	Start (s)	Apps.	Load Peak	Valley	Accelerometer #1 Peak	Valley	Defl.(mils)		
26,600 app. (1330 s)	25	1425.0	50 sec intervals	200	3500	7.54	1.64	1.22	-1.22	2.44	
@ 7.1 kips	Test Time	1400.0		400	7500	7.62	1.62	1.28	-1.26	2.54	
Total Apps./Period		28000		700	13500	7.56	1.63	1.26	-1.23	2.49	
Total Apps./Overall		28000		1000	19500	7.56	1.66	1.17	-1.22	2.39	
				1200	23500	7.60	1.63	1.20	-1.23	2.43	
						Avg Load	7.58		Avg	2.46	
						σ	0.03		σ	0.06	
						Variance	0.00		Variance	0.00	
						Avg Reading for Entire Test Period	7.50	1.70	1.19	-1.20	2.39

Goal	Start (s)	Stop (s)	Start (s)	Apps.	Load Peak	Valley	Accelerometer #1 Peak	Valley	Defl.(mils)		
12,100 app. (605 s)	1550	2178.0	50 sec intervals	1600	29000	14.83	3.18	2.03	-2.44	4.47	
@ 15.9 kips	Test Time	628.0		1700	31000	14.82	3.11	2.03	-2.39	4.42	
Total Apps./Period		12560		1800	33000	14.82	3.02	2.00	-2.39	4.39	
Total Apps./Overall		40560		1900	35000	14.77	3.11	1.99	-2.31	4.30	
				2000	37000	14.82	3.02	2.02	-2.37	4.39	
						Avg Load	14.81		Avg	4.39	
						σ	0.02		σ	0.06	
						Variance	0.00		Variance	0.00	
						Avg Reading for Entire Test Period	14.83	4.46	2.02	-2.37	4.39

Goal	Start (s)	Stop (s)	Start (s)	Apps.	Load Peak	Valley	Accelerometer #1 Peak	Valley	Defl.(mils)		
10,400 app. (520 s)	2320	2835.0	50 sec intervals	2350	41160	31.12	3.49	6.16	-7.85	14.01	
@ 31.6 kips	Test Time	515.0		2450	43160	31.08	3.65	6.23	-7.29	13.52	
Total Apps./Period		10300		2550	45160	30.98	3.66	6.07	-6.93	13.00	
Total Apps./Overall		50860		2650	47160	30.22	3.63	5.45	-6.75	12.20	
				2750	49160	30.30	3.60	5.55	-6.83	12.38	
						Avg Load	30.74		Avg	13.02	
						σ	0.44		σ	0.76	
						Variance	0.20		Variance	0.58	
						Avg Reading for Entire Test Period	30.61	3.71	5.84	-7.07	12.91



Accelerometer #2	Peak	Valley	Defl.(mils)	Norm. Defl. (mils/pi)	LT _{avg} (%)
	1.10	-1.17	2.27	0.30	93.03
	1.13	-1.21	2.34	0.31	92.13
	1.13	-1.18	2.31	0.31	92.77
	1.07	-1.17	2.24	0.30	93.72
	1.09	-1.18	2.27	0.30	93.42
	Avg		2.29	0.30	93.17
	σ		0.04	0.00	
	Variance		0.00	0.00	
	1.07	-1.15	2.22	0.30	

Accelerometer #2	Peak	Valley	Defl.(mils)	Norm. Defl. (mils/pi)	LT _{avg} (%)
	1.90	-2.33	4.23	0.29	94.63
	1.89	-2.30	4.19	0.28	94.80
	1.86	-2.30	4.16	0.28	94.76
	1.85	-2.22	4.07	0.28	94.65
	1.88	-2.27	4.15	0.28	94.53
	Avg		4.16	0.28	94.67
	σ		0.06	0.00	
	Variance		0.00	0.00	
	1.88	-2.27	4.15	0.28	

Accelerometer #2	Peak	Valley	Defl.(mils)	Norm. Defl. (mils/pi)	LT _{avg} (%)
	5.74	-7.62	13.36	0.43	95.36
	5.84	-7.31	13.15	0.42	97.26
	5.68	-6.89	12.57	0.41	96.69
	4.99	-6.36	11.35	0.38	93.03
	5.01	-6.44	11.45	0.38	92.49
	Avg		12.38	0.40	95.04
	σ		0.94	0.02	
	Variance		0.88	0.00	
	5.39	-6.84	12.23	0.40	
	Average LT 94.29				

Accelerometer #3	Peak	Valley	Defl.(mils)	Norm. Defl. (mils/pi)
	0.96	-1.01	1.97	0.26
	0.98	-1.02	2.00	0.26
	0.97	-0.99	1.96	0.26
	0.96	-0.99	1.95	0.26
	0.95	-0.99	1.94	0.26
	Avg		1.96	0.26
	σ		0.02	0.00
	Variance		0.00	0.00
	0.94	-0.99	1.93	0.26

Accelerometer #3	Peak	Valley	Defl.(mils)	Norm. Defl. (mils/pi)
	1.65	-1.96	3.61	0.24
	1.64	-1.93	3.57	0.24
	1.62	-1.93	3.55	0.24
	1.61	-1.88	3.49	0.24
	1.63	-1.92	3.55	0.24
	Avg		3.55	0.24
	σ		0.04	0.00
	Variance		0.00	0.00
	1.63	-1.92	3.55	0.24

Accelerometer #3	Peak	Valley	Defl.(mils)	Norm. Defl. (mils/pi)
	4.88	-6.23	11.11	0.36
	4.97	-6.35	11.32	0.36
	4.88	-6.01	10.89	0.35
	4.29	-5.25	9.54	0.32
	4.29	-5.29	9.58	0.32
	Avg		10.49	0.34
	σ		0.86	0.02
	Variance		0.74	0.00
	4.61	-5.75	10.36	0.34

Figure I13 – Data Summary for South Run-Up – Center Load Point – Years 1-5

11-15 Years

File "E2"

Goal	Start (s)	Stop (s)	Start (s)	Apps.	Load Peak	Valley	Accelerometer #1 Peak	Valley	Defl.(mils)
26,600 app. (1330 s)	133	1521.0	200	101440	7.32	1.99	1.12	-1.22	2.34
@ 7.1 kips			400	105440	7.34	1.99	1.13	-1.23	2.36
Test Time	1388.0		700	111440	7.38	1.94	1.13	-1.25	2.38
Total Apps./Period	27760		1000	117440	7.40	1.96	1.12	-1.23	2.35
Total Apps./Overall	127860		1200	121440	7.44	1.92	1.11	-1.24	2.35
					Avg Load	7.38		Avg	2.36
					σ	0.05		σ	0.02
					Variance	0.00		Variance	0.00
Avg Reading for Entire Test Period					7.34	1.99	1.10	-1.22	2.32

Goal	Start (s)	Stop (s)	Start (s)	Apps.	Load Peak	Valley	Accelerometer #1 Peak	Valley	Defl.(mils)
12,100 app. (605 s)	1550	2164.0	1600	128860	15.56	3.97	2.32	-2.87	5.19
@ 15.9 kips			1700	130860	15.50	3.94	2.35	-2.86	5.21
Test Time	614.0		1800	132860	15.56	3.90	2.33	-2.85	5.18
Total Apps./Period	12280		1900	134860	15.55	3.93	2.33	-2.84	5.17
Total Apps./Overall	140140		2000	136860	15.60	3.85	2.34	-2.86	5.20
					Avg Load	15.55		Avg	5.19
					σ	0.04		σ	0.02
					Variance	0.00		Variance	0.00
Avg Reading for Entire Test Period					15.56	3.93	2.33	-2.84	5.17

Goal	Start (s)	Stop (s)	Start (s)	Apps.	Load Peak	Valley	Accelerometer #1 Peak	Valley	Defl.(mils)
10,400 app. (520 s)	2320	2830.0	2350	140740	30.44	3.33	5.82	-7.08	12.90
@ 31.6 kips			2450	142740	29.89	3.81	5.40	-6.66	12.06
Test Time	510.0		2550	144740	29.89	3.82	5.34	-6.45	11.79
Total Apps./Period	10200		2650	146740	29.82	3.81	5.33	-6.35	11.68
Total Apps./Overall	150340		2750	148740	29.89	3.83	5.36	-6.31	11.67
					Avg Load	29.99		Avg	12.02
					σ	0.26		σ	0.52
					Variance	0.07		Variance	0.27
Avg Reading for Entire Test Period					29.98	3.71	5.46	-6.58	12.04



Accelerometer #2					Accelerometer #3				
Peak	Valley	Defl.(mils)	Norm. Defl. (mils/pi)	LT _{US} (%)	Peak	Valley	Defl.(mils)	Norm. Defl. (mils/pi)	LT _{US} (%)
1.00	-1.17	2.17	0.30	92.74	0.85	-0.98	1.83	0.25	0.25
1.01	-1.18	2.19	0.30	92.80	0.86	-0.98	1.84	0.25	0.25
1.01	-1.20	2.21	0.30	92.86	0.86	-0.99	1.85	0.25	0.25
1.01	-1.18	2.19	0.30	93.19	0.86	-0.99	1.85	0.25	0.25
1.02	-1.19	2.21	0.30	94.04	0.87	-0.99	1.86	0.25	0.25
Avg	2.20	0.30	93.38		Avg	1.85	0.25		
σ	0.01	0.00			σ	0.01	0.00		
Variance	0.00	0.00			Variance	0.00	0.00		
0.99	-1.16	2.15	0.29		0.84	-0.97	1.81	0.25	0.25

Accelerometer #2					Accelerometer #3				
Peak	Valley	Defl.(mils)	Norm. Defl. (mils/pi)	LT _{US} (%)	Peak	Valley	Defl.(mils)	Norm. Defl. (mils/pi)	LT _{US} (%)
2.15	-2.71	4.86	0.31	93.64	1.86	-2.23	4.09	0.26	0.26
2.18	-2.72	4.90	0.32	94.05	1.86	-2.25	4.11	0.27	0.27
2.16	-2.72	4.88	0.31	94.21	1.85	-2.26	4.11	0.26	0.26
2.16	-2.71	4.87	0.31	94.20	1.85	-2.25	4.10	0.26	0.26
2.17	-2.72	4.89	0.31	94.04	1.86	-2.26	4.12	0.26	0.26
Avg	4.88	0.31	94.03		Avg	4.11	0.26		
σ	0.02	0.00			σ	0.01	0.00		
Variance	0.00	0.00			Variance	0.00	0.00		
2.86	-3.50	6.36	0.41		1.85	-2.25	4.10	0.26	0.26

Accelerometer #2					Accelerometer #3				
Peak	Valley	Defl.(mils)	Norm. Defl. (mils/pi)	LT _{US} (%)	Peak	Valley	Defl.(mils)	Norm. Defl. (mils/pi)	LT _{US} (%)
5.44	-6.92	12.36	0.41	95.87	4.58	-5.64	10.22	0.34	0.34
5.07	-6.56	11.63	0.39	96.43	4.33	-5.44	9.77	0.33	0.33
5.00	-6.39	11.39	0.38	96.61	4.31	-5.37	9.68	0.32	0.32
5.00	-6.27	11.27	0.38	96.49	4.27	-5.31	9.58	0.32	0.32
5.00	-6.09	11.09	0.37	95.03	4.29	-5.14	9.43	0.32	0.32
Avg	11.55	0.39	96.07		Avg	9.74	0.32		
σ	0.49	0.01			σ	0.30	0.01		
Variance	0.24	0.00			Variance	0.09	0.00		
5.11	-6.45	11.56	0.39		4.36	-5.39	9.75	0.33	0.33
Average LT				94.49					

Figure I15 – Data Summary for South Run-Up – Center Load Point – Years 11-15

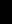
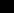
16-20 Years			File "E2"															
Goal	Start (s)	Stop (s)	Start (s)	Apps.	Load	Peak	Valley	Accelerometer #1	Peak	Valley	Defl.(mils)	Peak	Valley	Defl.(mils)	Peak	Valley	Defl.(mils)	Peak
26,600 app. (1330 s)	2960	4305.0	50 sec intervals	3100	153140	7.31	1.95	1.11	-1.21	2.32	2.32	1.11	-1.21	2.32	1.11	-1.21	2.32	1.11
@ 7.1 kips	Test Time	1345.0		3300	157140	7.39	1.88	1.15	-1.24	2.39	2.39	1.15	-1.24	2.39	1.15	-1.24	2.39	1.15
	Total Apps./Period	26900		3600	163140	7.40	1.89	1.13	-1.25	2.38	2.38	1.13	-1.25	2.38	1.13	-1.25	2.38	1.13
	Total Apps./Overall	177240		3900	169140	7.41	1.88	1.13	-1.25	2.38	2.38	1.13	-1.25	2.38	1.13	-1.25	2.38	1.13
				4100	173140	7.44	1.86	1.12	-1.26	2.38	2.38	1.12	-1.26	2.38	1.12	-1.26	2.38	1.12
						Avg Load	7.39		Avg	2.37	2.37		Avg	2.37		Avg	2.37	2.37
						σ	0.05		σ	0.03	0.03		σ	0.03		σ	0.03	0.03
						Variance	0.00		Variance	0.00	0.00		Variance	0.00		Variance	0.00	0.00
						Avg Reading for Entire Test Period	7.38	1.90		1.13	-1.24	2.37		1.13	-1.24	2.37		1.13
											% inc							
Goal	Start (s)	Stop (s)	Start (s)	Apps.	Load	Peak	Valley	Accelerometer #1	Peak	Valley	Defl.(mils)	Peak	Valley	Defl.(mils)	Peak	Valley	Defl.(mils)	Peak
12,100 app. (605 s)	4397	5007.0	50 sec intervals	4450	178300	16.62	3.55	2.63	-3.23	5.86	5.86	2.63	-3.23	5.86	2.63	-3.23	5.86	2.63
@ 15.9 kips	Test Time	610.0		4550	180300	16.59	3.50	2.60	-3.17	5.77	5.77	2.60	-3.17	5.77	2.60	-3.17	5.77	2.60
	Total Apps./Period	12200		4650	182300	16.67	3.57	2.64	-3.23	5.87	5.87	2.64	-3.23	5.87	2.64	-3.23	5.87	2.64
	Total Apps./Overall	189440		4750	184300	16.62	3.47	2.62	-3.21	5.83	5.83	2.62	-3.21	5.83	2.62	-3.21	5.83	2.62
				4850	186300	16.57	3.58	2.62	-3.16	5.78	5.78	2.62	-3.16	5.78	2.62	-3.16	5.78	2.62
						Avg Load	16.61		Avg	5.82	5.82		Avg	5.82		Avg	5.82	5.82
						σ	0.04		σ	0.05	0.05		σ	0.05		σ	0.05	0.05
						Variance	0.00		Variance	0.00	0.00		Variance	0.00		Variance	0.00	0.00
						Avg Reading for Entire Test Period	16.59	3.31		2.62	-3.19	5.81		2.62	-3.19	5.81		2.62
											% inc							
Goal	Start (s)	Stop (s)	Start (s)	Apps.	Load	Peak	Valley	Accelerometer #1	Peak	Valley	Defl.(mils)	Peak	Valley	Defl.(mils)	Peak	Valley	Defl.(mils)	Peak
10,400 app. (520 s)	5115	5635.0	50 sec intervals	5150	190140	29.89	3.13	5.82	-6.46	12.28	12.28	5.82	-6.46	12.28	5.82	-6.46	12.28	5.82
@ 31.6 kips	Test Time	520.0		5250	192140	29.98	4.17	5.27	-6.42	11.69	11.69	5.27	-6.42	11.69	5.27	-6.42	11.69	5.27
	Total Apps./Period	10400		5350	194140	29.97	4.20	5.35	-6.56	11.91	11.91	5.35	-6.56	11.91	5.35	-6.56	11.91	5.35
	Total Apps./Overall	199840		5450	196140	29.90	4.35	5.35	-6.58	11.93	11.93	5.35	-6.58	11.93	5.35	-6.58	11.93	5.35
				5550	198140	29.97	4.29	5.44	-6.73	12.17	12.17	5.44	-6.73	12.17	5.44	-6.73	12.17	5.44
						Avg Load	29.94		Avg	12.00	12.00		Avg	12.00		Avg	12.00	12.00
						σ	0.04		σ	0.23	0.23		σ	0.23		σ	0.23	0.23
						Variance	0.00		Variance	0.05	0.05		Variance	0.05		Variance	0.05	0.05
						Avg Reading for Entire Test Period	30.18	4.04		5.36	-6.49	11.85		5.36	-6.49	11.85		5.36
											% inc							



Accelerometer #2					Accelerometer #3				
Peak	Valley	Defl.(mils)	Norm. Defl. (mils/pi)	LT _{US} (%)	Peak	Valley	Defl.(mils)	Norm. Defl. (mils/pi)	LT _{US} (%)
0.99	-1.16	2.15	0.29	92.67	0.85	-0.96	1.81	0.25	0.25
1.02	-1.20	2.22	0.30	92.89	0.86	-0.98	1.84	0.25	0.25
1.02	-1.19	2.21	0.30	92.86	0.88	-0.98	1.86	0.25	0.25
1.02	-1.19	2.21	0.30	92.86	0.88	-0.99	1.87	0.25	0.25
1.02	-1.21	2.23	0.30	93.70	0.87	-0.99	1.86	0.25	0.25
	Avg	2.22	0.30	93.57		Avg	1.85	0.25	0.25
	σ	0.01	0.00			σ	0.02	0.00	0.00
	Variance	0.00	0.00			Variance	0.00	0.00	0.00
1.01	-1.18	2.19	0.30		0.87	-0.98	1.85	0.25	0.25
Accelerometer #2					Accelerometer #3				
Peak	Valley	Defl.(mils)	Norm. Defl. (mils/pi)	LT _{US} (%)	Peak	Valley	Defl.(mils)	Norm. Defl. (mils/pi)	LT _{US} (%)
2.44	-3.08	5.52	0.33	94.20	2.09	-2.55	4.64	0.28	0.28
2.42	-3.03	5.45	0.33	94.45	2.08	-2.53	4.61	0.28	0.28
2.44	-3.09	5.53	0.33	94.21	2.10	-2.58	4.68	0.28	0.28
2.43	-3.06	5.49	0.33	94.17	2.07	-2.55	4.62	0.28	0.28
2.42	-3.01	5.43	0.33	93.94	2.08	-2.51	4.59	0.28	0.28
	Avg	5.48	0.33	94.19		Avg	4.63	0.28	0.28
	σ	0.04	0.00			σ	0.03	0.00	0.00
	Variance	0.00	0.00			Variance	0.00	0.00	0.00
2.43	-3.04	5.47	0.33		2.08	-2.53	4.61	0.28	0.28
Accelerometer #2					Accelerometer #3				
Peak	Valley	Defl.(mils)	Norm. Defl. (mils/pi)	LT _{US} (%)	Peak	Valley	Defl.(mils)	Norm. Defl. (mils/pi)	LT _{US} (%)
5.41	-6.28	11.69	0.39	95.20	4.59	-5.35	9.94	0.33	0.33
4.90	-6.15	11.05	0.37	94.53	4.16	-5.04	9.20	0.31	0.31
4.91	-6.23	11.14	0.37	93.53	4.16	-5.04	9.20	0.31	0.31
4.88	-6.23	11.11	0.37	93.13	4.12	-5.06	9.18	0.31	0.31
4.95	-6.34	11.29	0.38	92.77	4.14	-5.16	9.30	0.31	0.31
	Avg	11.26	0.38	93.83		Avg	9.36	0.31	0.31
	σ	0.26	0.01			σ	0.33	0.01	0.01
	Variance	0.07	0.00			Variance	0.11	0.00	0.00
4.94	-6.19	11.13	0.37		4.18	-5.08	9.26	0.31	0.31
Average LT				93.86					

Figure I16 – Data Summary for South Run-Up – Center Load Point – Years 16-20

South Run-Up Corner



211

6-10 Years

File "F2"

Goal	Start (s)	Stop (s)
26,600 app. (1330 s)	2865	4196.0
@ 7.1 kips	Test Time	1331.0
	Total Apps./Period	26620
	Total Apps./Overall	71960

Start (s)	Apps.
3000	48040
3200	52040
3500	58040
3800	64040
4000	68040

Load	Peak	Valley
	7.03	2.28
	7.05	2.26
	7.20	2.23
	7.15	2.22
	7.17	2.22
Avg Load	7.12	
σ	0.08	
Variance	0.01	
	7.13	2.24

Accelerometer #1	Peak	Valley	Defl.(mils)
	1.82	-2.39	4.21
	1.78	-2.40	4.18
	1.72	-2.39	4.11
	1.78	-2.39	4.17
	1.78	-2.40	4.18
Avg			4.17
σ			0.04
Variance			0.00
	1.76	-2.39	4.15

Avg Reading for Entire Test Period

Goal	Start (s)	Stop (s)
12,100 app. (605 s)	4320	4926.0
@ 15.9 kips	Test Time	606.0
	Total Apps./Period	12120
	Total Apps./Overall	84080

Start (s)	Apps.
4400	73560
4500	75560
4600	77560
4700	79560
4800	81560

Load	Peak	Valley
	15.91	3.35
	15.99	3.27
	15.93	3.29
	15.79	3.35
	15.81	3.26
Avg Load	15.89	
σ	0.08	
Variance	0.01	
	15.87	3.82

Accelerometer #1	Peak	Valley	Defl.(mils)
	3.45	-5.33	8.78
	3.57	-5.53	9.10
	3.51	-5.54	9.05
	3.46	-5.47	8.93
	3.46	-5.47	8.93
Avg			8.96
σ			0.12
Variance			0.02
	3.49	-5.46	8.95

Avg Reading for Entire Test Period

Goal	Start (s)	Stop (s)
10,400 app. (520 s)	5120	5626.0
@ 31.6 kips	Test Time	506.0
	Total Apps./Period	10120
	Total Apps./Overall	94200

Start (s)	Apps.
5150	84680
5250	86680
5350	88680
5450	90680
5550	92680

Load	Peak	Valley
	31.05	4.64
	31.34	4.79
	31.47	4.75
	31.46	4.75
	31.40	4.80
Avg Load	31.34	
σ	0.17	
Variance	0.03	
	31.30	4.71

Accelerometer #1	Peak	Valley	Defl.(mils)
	8.25	-12.33	20.58
	8.08	-11.30	19.38
	8.15	-11.20	19.35
	8.11	-11.29	19.40
	8.07	-11.71	19.78
Avg			19.70
σ			0.52
Variance			0.27
	8.11	-11.54	19.65

Avg Reading for Entire Test Period



Accelerometer #2					Accelerometer #3				
Peak	Valley	Defl.(mils)	Norm. Defl. (mils/pi)	LT _{US} (%)	Peak	Valley	Defl.(mils)	Norm. Defl. (mils/pi)	
1.34	-1.55	2.89	0.41	68.65	1.53	-1.85	3.38	0.48	
1.41	-1.61	3.02	0.43	72.25	1.09	-1.31	2.40	0.34	
1.35	-1.59	2.94	0.41	71.53	1.08	-1.29	2.37	0.33	
1.29	-1.57	2.86	0.40	68.59	1.03	-1.27	2.30	0.32	
1.34	-1.57	2.91	0.41	69.62	1.03	-1.27	2.30	0.32	
Avg		2.93	0.41	70.32	Avg		2.55	0.36	
σ		0.07	0.01		σ		0.47	0.07	
Variance		0.00	0.00		Variance		0.22	0.00	
1.32	-1.56	2.88	0.40		1.09	-1.32	2.41	0.34	
Accelerometer #2					Accelerometer #3				
Peak	Valley	Defl.(mils)	Norm. Defl. (mils/pi)	LT _{US} (%)	Peak	Valley	Defl.(mils)	Norm. Defl. (mils/pi)	
2.88	-3.92	6.80	0.43	77.45	2.36	-3.23	5.59	0.35	
2.96	-4.06	7.02	0.44	77.14	2.40	-3.33	5.73	0.36	
2.92	-3.89	6.81	0.43	75.25	2.37	-3.21	5.58	0.35	
2.86	-3.72	6.58	0.42	73.68	2.32	-3.03	5.35	0.34	
2.85	-3.69	6.54	0.41	73.24	2.30	-2.99	5.29	0.33	
Avg		6.75	0.42	75.35	Avg		5.51	0.35	
σ		0.19	0.01		σ		0.18	0.01	
Variance		0.04	0.00		Variance		0.03	0.00	
2.88	-3.85	6.73	0.42		2.34	-3.15	5.49	0.35	
Accelerometer #2					Accelerometer #3				
Peak	Valley	Defl.(mils)	Norm. Defl. (mils/pi)	LT _{US} (%)	Peak	Valley	Defl.(mils)	Norm. Defl. (mils/pi)	
6.74	-9.57	16.31	0.53	79.25	5.42	-7.51	12.93	0.42	
6.69	-9.94	16.63	0.53	85.81	5.49	-7.48	12.97	0.41	
6.78	-9.49	16.27	0.52	84.08	5.53	-7.55	13.08	0.42	
6.79	-9.30	16.09	0.51	82.94	5.55	-7.49	13.04	0.41	
6.75	-9.07	15.82	0.50	79.98	5.51	-7.50	13.01	0.41	
Avg		16.22	0.52	82.36	Avg		13.01	0.41	
σ		0.30	0.01		σ		0.06	0.00	
Variance		0.09	0.00		Variance		0.00	0.00	
6.73	-9.34	16.07	0.51		5.49	-7.48	12.97	0.41	
Average LT				76.01					

Figure I18 – Data Summary for South Run-Up – Corner Load Point – Years 6-10

11-15 Years File "F3"												
Goal			Start (s)	Stop (s)	Start (s)		Apps.	Load		Accelerometer #1		
Peak	Valley	Defl.(mils)										
26,600 app. (1330 s)	54	1389.0	50 sec intervals	200	97120			7.08	2.13	1.73	-2.32	4.05
@ 7.1 kips	Test Time	1335.0		400	101120			7.23	2.12	1.72	-2.36	4.08
	Total Apps./Period	26700		700	107120			7.26	2.07	1.70	-2.44	4.14
	Total Apps./Overall	120900		1000	113120			7.25	2.12	1.71	-2.30	4.01
				1200	117120			7.28	2.05	1.71	-2.33	4.04
						Avg Load	7.22			Avg	4.06	
						σ	0.08			σ	0.05	
						Variance	0.01			Variance	0.00	
			Avg Reading for Entire Test Period				7.21	2.05		1.72	-2.36	4.08
Goal			Start (s)	Stop (s)	Start (s)		Apps.	Load		Accelerometer #1		
Peak	Valley	Defl.(mils)										
12,100 app. (605 s)	1495	2100.0	50 sec intervals	1600	123000			16.57	3.23	3.97	-5.87	9.84
@ 15.9 kips	Test Time	605.0		1700	125000			16.58	3.21	4.00	-6.01	10.01
	Total Apps./Period	12100		1800	127000			16.59	3.15	4.00	-6.08	10.08
	Total Apps./Overall	133000		1900	129000			16.60	3.17	4.02	-6.09	10.11
				2000	131000			16.70	3.10	4.00	-6.10	10.10
						Avg Load	16.61			Avg	10.03	
						σ	0.05			σ	0.11	
						Variance	0.00			Variance	0.01	
			Avg Reading for Entire Test Period				16.56	3.17		3.98	-5.97	9.95
Goal			Start (s)	Stop (s)	Start (s)		Apps.	Load		Accelerometer #1		
Peak	Valley	Defl.(mils)										
10,400 app. (520 s)	2220	2740.0	50 sec intervals	2250	133600			30.68	3.97	8.11	-11.49	19.60
@ 31.6 kips	Test Time	520.0		2350	135600			30.80	4.64	7.93	-10.95	18.88
	Total Apps./Period	10400		2450	137600			30.21	5.27	7.38	-10.45	17.83
	Total Apps./Overall	143400		2550	139600			30.07	5.36	7.38	-10.64	18.02
				2650	141600			30.02	5.34	7.36	-10.87	18.23
						Avg Load	30.36			Avg	18.51	
						σ	0.36			σ	0.73	
						Variance	0.13			Variance	0.53	
			Avg Reading for Entire Test Period				30.27	4.96		7.57	-10.76	18.33



Accelerometer #2					Accelerometer #3				
Peak	Valley	Defl.(mils)	Norm. Defl. (mils/pl)	LT _{US} (%)	Peak	Valley	Defl.(mils)	Norm. Defl. (mils/pl)	LT _{US} (%)
1.32	-1.46	2.78	0.39	68.64	1.04	-1.20	2.24	0.32	
1.32	-1.46	2.78	0.38	68.14	1.07	-1.20	2.27	0.31	
1.28	-1.49	2.77	0.38	66.98	1.04	-1.21	2.25	0.31	
1.28	-1.43	2.71	0.37	67.58	1.03	-1.17	2.20	0.30	
1.29	-1.43	2.72	0.37	67.33	1.04	-1.18	2.22	0.30	
	Avg	2.75	0.38	67.56		Avg	2.24	0.31	
	σ	0.04	0.01			σ	0.03	0.01	
	Variance	0.00	0.00			Variance	0.00	0.00	
1.30	-1.46	2.76	0.38		1.04	-1.19	2.23	0.31	
Accelerometer #2					Accelerometer #3				
Peak	Valley	Defl.(mils)	Norm. Defl. (mils/pl)	LT _{US} (%)	Peak	Valley	Defl.(mils)	Norm. Defl. (mils/pl)	LT _{US} (%)
3.15	-4.01	7.16	0.43	72.76	2.56	-3.34	5.90	0.36	
3.14	-3.98	7.12	0.43	71.13	2.54	-3.29	5.83	0.35	
3.10	-3.98	7.08	0.43	70.24	2.55	-3.23	5.78	0.35	
3.10	-4.00	7.10	0.43	70.23	2.52	-3.22	5.74	0.35	
3.09	-4.07	7.16	0.43	70.89	2.53	-3.27	5.80	0.35	
	Avg	7.12	0.43	71.04		Avg	5.81	0.35	
	σ	0.04	0.00			σ	0.06	0.00	
	Variance	0.00	0.00			Variance	0.00	0.00	
2.83	-3.49	6.32	0.38		2.54	-3.27	5.81	0.35	
Accelerometer #2					Accelerometer #3				
Peak	Valley	Defl.(mils)	Norm. Defl. (mils/pl)	LT _{US} (%)	Peak	Valley	Defl.(mils)	Norm. Defl. (mils/pl)	LT _{US} (%)
6.65	-9.13	15.78	0.51	80.51	5.34	-7.29	12.83	0.41	
6.56	-8.85	15.41	0.50	81.62	5.32	-7.18	12.50	0.41	
5.30	-6.63	11.93	0.39	66.91	5.11	-6.69	11.80	0.39	
6.01	-7.68	13.69	0.46	75.97	5.01	-6.46	11.47	0.38	
5.85	-7.59	13.44	0.45	73.72	4.95	-6.24	11.19	0.37	
	Avg	14.05	0.46	75.90		Avg	11.92	0.39	
	σ	1.57	0.05			σ	0.63	0.02	
	Variance	2.46	0.00			Variance	0.40	0.00	
6.10	-8.00	14.10	0.47		5.12	-6.71	11.83	0.39	
Average LT				71.50					

Figure I19 – Data Summary for South Run-Up – Corner Load Point – Years 11-15

16-20 Years			File "F3"	
Goal	Start (s)	Stop (s)	Start (s)	Apps.
26,600 app. (1330 s) @ 7.1 kips	2874	4214.0	3000	145920
Test Time	1340.0		3200	149920
Total Apps./Period	26800		3500	155920
Total Apps./Overall	170200		3800	161920
			4000	165920
50 sec intervals			Load	
			Peak	Valley
			7.24	1.99
			7.32	1.93
			7.26	1.96
			7.25	1.94
			7.30	1.92
			Avg Load	7.27
			σ	0.03
			Variance	0.00
Avg Reading for Entire Test Period			7.28	1.94
			Accelerometer #1	
			Peak	Valley
			1.69	-2.23
			1.70	-2.28
			1.65	-2.23
			1.63	-2.20
			1.65	-2.18
			Avg	3.89
			σ	0.06
			Variance	0.00
			1.67	-2.23
			% inc	
Goal	Start (s)	Stop (s)	Start (s)	Apps.
12,100 app. (605 s) @ 15.9 kips	4326	4930.0	4400	171700
Test Time	605.0		4500	173700
Total Apps./Period	12100		4600	175700
Total Apps./Overall	182300		4700	177700
			4800	179700
50 sec intervals			Load	
			Peak	Valley
			16.15	3.55
			16.13	3.50
			16.10	3.57
			16.06	3.47
			16.06	3.58
			Avg Load	16.10
			σ	0.04
			Variance	0.00
Avg Reading for Entire Test Period			16.05	3.74
			Accelerometer #1	
			Peak	Valley
			3.40	-4.90
			3.39	-4.93
			3.40	-4.96
			3.37	-4.99
			3.39	-4.97
			Avg	8.34
			σ	0.03
			Variance	0.00
			3.37	-4.92
			% inc	
Goal	Start (s)	Stop (s)	Start (s)	Apps.
10,400 app. (520 s) @ 31.6 kips	5025	5540.0	5050	182800
Test Time	515.0		5150	184800
Total Apps./Period	10300		5250	186800
Total Apps./Overall	192600		5350	188800
			5450	190800
50 sec intervals			Load	
			Peak	Valley
			30.64	3.13
			30.90	4.17
			31.03	4.20
			30.96	4.35
			30.89	4.29
			Avg Load	30.88
			σ	0.15
			Variance	0.02
Avg Reading for Entire Test Period			30.82	4.24
			Accelerometer #1	
			Peak	Valley
			8.21	-12.01
			8.23	-11.64
			8.22	-11.05
			8.10	-10.48
			8.08	-10.23
			Avg	19.25
			σ	0.82
			Variance	0.66
			8.11	-10.93
			% inc	

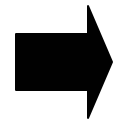


Accelerometer #2					Accelerometer #3				
Peak	Valley	Defl.(mils)	Norm. Defl. (mils/pi)	LT _{US} (%)	Peak	Valley	Defl.(mils)	Norm. Defl. (mils/pi)	
1.27	-1.41	2.68	0.37	68.37	1.03	-1.15	2.18	0.30	
1.31	-1.44	2.75	0.38	69.10	1.05	-1.18	2.23	0.30	
1.26	-1.39	2.65	0.37	68.30	1.03	-1.13	2.16	0.30	
1.25	-1.39	2.64	0.36	68.93	1.03	-1.12	2.15	0.30	
1.28	-1.39	2.67	0.37	69.71	1.04	-1.13	2.17	0.30	
Avg	2.68	0.37	68.87		Avg	2.18	0.30		
σ	0.05	0.00			σ	0.03	0.00		
Variance	0.00	0.00			Variance	0.00	0.00		
1.28	-1.41	2.69	0.37		1.03	-1.15	2.18	0.30	
Accelerometer #2					Accelerometer #3				
Peak	Valley	Defl.(mils)	Norm. Defl. (mils/pi)	LT _{US} (%)	Peak	Valley	Defl.(mils)	Norm. Defl. (mils/pi)	
2.75	-3.46	6.21	0.38	74.82	2.26	-2.84	5.10	0.32	
2.58	-3.13	5.71	0.35	68.63	2.24	-2.77	5.01	0.31	
2.74	-3.34	6.08	0.38	72.73	2.22	-2.74	4.96	0.31	
2.71	-3.32	6.03	0.38	72.13	2.19	-2.70	4.89	0.30	
2.74	-3.32	6.06	0.38	72.49	2.22	-2.69	4.91	0.31	
Avg	6.02	0.37	72.16		Avg	4.97	0.31		
σ	0.19	0.01			σ	0.08	0.00		
Variance	0.03	0.00			Variance	0.01	0.00		
2.70	-3.32	6.02	0.38		2.21	-2.75	4.96	0.31	
Accelerometer #2					Accelerometer #3				
Peak	Valley	Defl.(mils)	Norm. Defl. (mils/pi)	LT _{US} (%)	Peak	Valley	Defl.(mils)	Norm. Defl. (mils/pi)	
4.42	-8.89	9.31	0.30	46.04	5.32	-6.76	12.08	0.39	
6.31	-8.35	14.66	0.47	73.78	5.28	-6.91	12.19	0.39	
6.50	-8.54	15.04	0.48	78.05	5.28	-6.98	12.26	0.40	
6.58	-8.63	15.21	0.49	81.86	5.25	-7.02	12.27	0.40	
6.48	-8.12	14.60	0.47	79.74	5.26	-6.99	12.25	0.40	
Avg	13.76	0.45	71.50		Avg	12.21	0.40		
σ	2.50	0.08			σ	0.08	0.00		
Variance	6.26	0.01			Variance	0.01	0.00		
6.22	-7.87	14.09	0.46		5.25	-6.90	12.15	0.39	
Average LT				70.84					

Figure I20 – Data Summary for South Run-Up – Corner Load Point – Years 16-20

Point #6 South Run-Up Edge

1-5 Years File "G1"									
Goal	Start (s)	Stop (s)	Start (s)	Apps.	Load Peak	Valley	Accelerometer #1 Peak	Valley	Defl.(mils)
26,600 app. (1330 s) @ 7.1 kips	470	1798.0	50 sec intervals	600 2600	7.14 1.56		1.50	-1.67	3.17
	Test Time	1328.0		800 6600	7.20 1.63		1.51	-1.71	3.22
	Total Apps./Period	26560		1100 12600	7.19 1.58		1.52	-1.71	3.23
	Total Apps./Overall	26560		1400 18600	7.19 1.50		1.55	-1.70	3.25
				1600 22600	7.18 1.55		1.51	-1.69	3.20
					Avg Load	7.18		Avg	3.21
					σ	0.02		σ	0.03
					Variance	0.00		Variance	0.00
					Avg Reading for Entire Test Period	7.18 1.60		1.50 -1.68	3.18
Goal	Start (s)	Stop (s)	Start (s)	Apps.	Load Peak	Valley	Accelerometer #1 Peak	Valley	Defl.(mils)
12,100 app. (605 s) @ 15.9 kips	1875	2487.0	50 sec intervals	1950 28060	15.91 3.27		3.10	-4.06	7.16
	Test Time	612.0		2050 30060	15.88 3.30		3.10	-4.08	7.18
	Total Apps./Period	12240		2150 32060	15.88 3.36		3.07	-4.08	7.15
	Total Apps./Overall	38800		2250 34060	15.85 3.39		3.07	-4.10	7.17
				2350 36060	15.77 3.42		3.03	-4.11	7.14
					Avg Load	15.86		Avg	7.16
					σ	0.05		σ	0.02
					Variance	0.00		Variance	0.00
					Avg Reading for Entire Test Period	15.87 3.33		3.08 -4.09	7.17
Goal	Start (s)	Stop (s)	Start (s)	Apps.	Load Peak	Valley	Accelerometer #1 Peak	Valley	Defl.(mils)
10,400 app. (520 s) @ 31.6 kips	2670	3190.0	50 sec intervals	2700 39400	30.07 2.56		7.92	-10.03	17.95
	Test Time	520.0		2800 41400	30.04 2.54		8.01	-10.06	18.07
	Total Apps./Period	10400		2900 43400	29.92 2.62		8.00	-9.79	17.79
	Total Apps./Overall	49200		3000 45400	29.78 2.68		7.89	-9.54	17.43
				3100 47400	29.66 2.77		7.75	-9.47	17.22
					Avg Load	29.89		Avg	17.69
					σ	0.17		σ	0.36
					Variance	0.03		Variance	0.13
					Avg Reading for Entire Test Period	29.80 2.76		7.82 -9.65	17.47



Accelerometer #2					Accelerometer #3			
Peak	Valley	Defl.(mils)	Norm. Defl. (mils/pi)	LT _{US} (%)	Peak	Valley	Defl.(mils)	Norm. Defl. (mils/pi)
1.23	-1.31	2.54	0.36	80.73	0.98	-1.07	2.05	0.29
1.26	-1.34	2.60	0.36	80.75	1.00	-1.10	2.10	0.29
1.25	-1.34	2.59	0.36	80.19	1.01	-1.09	2.10	0.29
1.24	-1.34	2.58	0.36	79.38	1.01	-1.08	2.09	0.29
1.23	-1.32	2.55	0.36	79.69	0.98	-1.08	2.06	0.29
	Avg	2.58	0.36	80.27		Avg	2.08	0.29
	σ	0.02	0.00			σ	0.02	0.00
	Variance	0.00	0.00			Variance	0.00	0.00
1.22	-1.32	2.54	0.35		0.99	-1.08	2.07	0.29
Accelerometer #2					Accelerometer #3			
Peak	Valley	Defl.(mils)	Norm. Defl. (mils/pi)	LT _{US} (%)	Peak	Valley	Defl.(mils)	Norm. Defl. (mils/pi)
2.63	-3.22	5.85	0.37	81.70	1.65	-1.96	3.61	0.23
2.64	-3.21	5.85	0.37	81.48	1.64	-1.93	3.57	0.22
2.63	-3.17	5.80	0.37	81.12	1.62	-1.93	3.55	0.22
2.63	-3.17	5.80	0.37	80.89	1.61	-1.88	3.49	0.22
2.59	-3.19	5.78	0.37	80.95	1.63	-1.92	3.55	0.22
	Avg	5.82	0.37	81.23		Avg	3.55	0.22
	σ	0.03	0.00			σ	0.04	0.00
	Variance	0.00	0.00			Variance	0.00	0.00
2.62	-3.20	5.82	0.37		1.63	-1.92	3.55	0.22
Accelerometer #2					Accelerometer #3			
Peak	Valley	Defl.(mils)	Norm. Defl. (mils/pi)	LT _{US} (%)	Peak	Valley	Defl.(mils)	Norm. Defl. (mils/pi)
6.41	-8.16	14.57	0.48	81.17	5.12	-6.49	11.61	0.39
6.57	-8.33	14.90	0.50	82.46	5.22	-6.65	11.87	0.40
6.62	-8.43	15.05	0.50	84.60	5.24	-6.74	11.98	0.40
6.60	-8.45	15.05	0.51	86.35	5.21	-6.83	12.04	0.40
6.55	-8.15	14.70	0.50	85.37	5.22	-6.73	11.95	0.40
	Avg	14.85	0.50	83.96		Avg	11.89	0.40
	σ	0.21	0.01			σ	0.17	0.01
	Variance	0.05	0.00			Variance	0.03	0.00
6.49	-8.19	14.68	0.49		5.16	-6.61	11.77	0.39
Average LT				81.82				

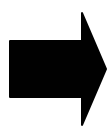


Figure I21 – Data Summary for South Run-Up – Edge Load Point – Years 1-5

6-10 Years			File "G1"	
Goal	Start (s)	Stop (s)	Start (s)	Apps.
26,600 app. (1330 s) @ 7.1 kips	3290	4625.0	3400	51400
Test Time	1335.0		3600	55400
Total Apps./Period	26700		3900	61400
Total Apps./Overall	75900		4200	67400
			4400	71400
50 sec intervals			Load	
			Peak	Valley
			7.39	1.50
			7.49	1.41
			7.55	1.43
			7.55	1.43
			7.60	1.42
			Avg Load	7.52
			σ	0.08
			Variance	0.01
Avg Reading for Entire Test Period			7.49	1.50
			Accelerometer #1	
			Peak	Valley
			1.70	-1.98
			1.75	-2.10
			1.77	-2.08
			1.75	-2.05
			1.77	-2.09
			Avg	3.81
			σ	0.08
			Variance	0.01
			1.71	-2.01
			3.72	
Goal	Start (s)	Stop (s)	Start (s)	Apps.
12,100 app. (605 s) @ 15.9 kips	4695	5300.0	4800	78000
Test Time	605.0		4900	80000
Total Apps./Period	12100		5000	82000
Total Apps./Overall	88000		5100	84000
			5200	86000
50 sec intervals			Load	
			Peak	Valley
			15.74	3.37
			15.67	3.40
			15.71	3.37
			15.73	3.32
			15.66	3.40
			Avg Load	15.70
			σ	0.04
			Variance	0.00
Avg Reading for Entire Test Period			15.68	3.40
			Accelerometer #1	
			Peak	Valley
			3.25	-4.30
			3.23	-4.21
			3.28	-4.21
			3.29	-4.23
			3.26	-4.19
			Avg	7.49
			σ	0.05
			Variance	0.00
			3.24	-4.22
			7.46	
Goal	Start (s)	Stop (s)	Start (s)	Apps.
10,400 app. (520 s) @ 31.6 kips	5421	5941.0	5450	88580
Test Time	520.0		5550	90580
Total Apps./Period	10400		5650	92580
Total Apps./Overall	98400		5750	94580
			5850	96580
50 sec intervals			Load	
			Peak	Valley
			29.89	2.97
			29.79	3.19
			29.65	3.32
			29.64	3.33
			29.42	3.40
			Avg Load	29.68
			σ	0.18
			Variance	0.03
Avg Reading for Entire Test Period			29.65	3.25
			Accelerometer #1	
			Peak	Valley
			7.44	-9.80
			7.43	-9.92
			7.44	-9.89
			7.42	-9.77
			7.32	-9.47
			Avg	17.18
			σ	0.23
			Variance	0.05
			7.39	-9.73
			17.12	



Accelerometer #2					Accelerometer #3				
Peak	Valley	Defl.(mils)	Norm. Defl. (mils/pi)	LT _{US} (%)	Peak	Valley	Defl.(mils)	Norm. Defl. (mils/pi)	
1.35	-1.50	2.85	0.39	77.45	1.10	-1.23	2.33	0.32	
1.40	-1.58	2.98	0.40	77.40	1.12	-1.29	2.41	0.32	
1.45	-1.57	3.02	0.40	78.44	1.15	-1.28	2.43	0.32	
1.42	-1.55	2.97	0.39	78.16	1.15	-1.26	2.41	0.32	
1.42	-1.58	3.00	0.39	77.72	1.15	-1.28	2.43	0.32	
Avg		2.99	0.40	78.58	Avg		2.40	0.32	
σ		0.02	0.01		σ		0.04	0.00	
Variance		0.00	0.00		Variance		0.00	0.00	
1.38	-1.52	2.90	0.39		1.11	-1.24	2.35	0.31	
Accelerometer #2					Accelerometer #3				
Peak	Valley	Defl.(mils)	Norm. Defl. (mils/pi)	LT _{US} (%)	Peak	Valley	Defl.(mils)	Norm. Defl. (mils/pi)	
2.67	-3.38	6.05	0.38	80.13	2.19	-2.73	4.92	0.31	
2.63	-3.32	5.95	0.38	79.97	2.15	-2.70	4.85	0.31	
2.68	-3.33	6.01	0.38	80.24	2.18	-2.71	4.89	0.31	
2.70	-3.35	6.05	0.38	80.45	2.17	-2.74	4.91	0.31	
2.68	-3.29	5.97	0.38	80.13	2.17	-2.69	4.86	0.31	
Avg		6.01	0.38	80.19	Avg		4.89	0.31	
σ		0.05	0.00		σ		0.03	0.00	
Variance		0.00	0.00		Variance		0.00	0.00	
2.26	-3.32	5.58	0.36		2.17	-2.70	4.87	0.31	
Accelerometer #2					Accelerometer #3				
Peak	Valley	Defl.(mils)	Norm. Defl. (mils/pi)	LT _{US} (%)	Peak	Valley	Defl.(mils)	Norm. Defl. (mils/pi)	
5.99	-7.81	13.60	0.46	78.89	4.97	-6.14	11.11	0.37	
5.81	-7.75	13.56	0.46	78.16	4.83	-6.20	11.03	0.37	
5.87	-7.80	13.67	0.46	78.88	4.83	-6.23	11.06	0.37	
5.93	-7.85	13.78	0.46	80.16	4.89	-6.28	11.17	0.38	
5.94	-7.91	13.85	0.47	82.49	4.80	-6.32	11.12	0.38	
Avg		13.69	0.46	79.70	Avg		11.10	0.37	
σ		0.12	0.01		σ		0.05	0.00	
Variance		0.01	0.00		Variance		0.00	0.00	
5.90	-7.77	13.67	0.46		4.85	-6.23	11.08	0.37	
Average LT				79.49					

Figure I22 – Data Summary for South Run-Up – Edge Load Point – Years 6-10

16-20 Years			File "G3"	
Goal	Start (s)	Stop (s)	Start (s)	Apps.
26,600 app. (1330 s) @ 7.1 kips	1373	2623.0	1400	147740
Test Time	1250.0		1600	151740
Total Apps./Period	25000		1900	157740
Total Apps./Overall	172200		2200	163740
			2400	167740
50 sec intervals			Load	
			Peak	Valley
			7.26	1.77
			7.48	1.72
			7.57	1.67
			7.55	1.81
			7.61	1.74
			Avg Load	7.49
			σ	0.14
			Variance	0.02
Avg Reading for Entire Test Period			7.50	1.80
			Accelerometer #1	
			Peak	Valley
			1.62	-1.87
			1.66	-1.99
			1.68	-1.97
			1.66	-1.98
			1.71	-2.00
			Avg	3.63
			σ	0.08
			Variance	0.01
			1.63	-1.90
			% inc	
Goal	Start (s)	Stop (s)	Start (s)	Apps.
12,100 app. (605 s) @ 15.9 kips	2675	3285.0	2750	173700
Test Time	610.0		2850	175700
Total Apps./Period	12200		2950	177700
Total Apps./Overall	184400		3050	179700
			3150	181700
50 sec intervals			Load	
			Peak	Valley
			16.11	2.82
			16.08	2.87
			16.07	2.87
			16.07	2.92
			16.07	2.87
			Avg Load	16.08
			σ	0.02
			Variance	0.00
Avg Reading for Entire Test Period			16.03	2.97
			Accelerometer #1	
			Peak	Valley
			3.61	-4.78
			3.61	-4.65
			3.58	-4.62
			3.55	-4.59
			3.53	-4.66
			Avg	8.24
			σ	0.10
			Variance	0.01
			3.54	-4.61
			% inc	
Goal	Start (s)	Stop (s)	Start (s)	Apps.
10,400 app. (520 s) @ 31.6 kips	3368	3892.0	3400	185040
Test Time	524.0		3500	187040
Total Apps./Period	10480		3600	189040
Total Apps./Overall	194880		3700	191040
			3800	193040
50 sec intervals			Load	
			Peak	Valley
			29.83	2.76
			30.04	2.80
			31.85	2.15
			31.72	2.18
			31.60	2.17
			Avg Load	31.01
			σ	0.99
			Variance	0.97
Avg Reading for Entire Test Period			30.94	2.55
			Accelerometer #1	
			Peak	Valley
			7.85	-10.33
			7.81	-10.50
			8.26	-11.42
			8.20	-11.42
			8.09	-11.10
			Avg	19.00
			σ	0.71
			Variance	0.51
			7.93	-10.81
			% inc	



Accelerometer #2					Accelerometer #3				
Peak	Valley	Defl.(mils)	Norm. Defl. (mils/pl)	LT _{US} (%)	Peak	Valley	Defl.(mils)	Norm. Defl. (mils/pl)	LT _{US} (%)
1.26	-1.41	2.67	0.37	76.50	1.00	-1.15	2.15	0.30	0.30
1.34	-1.49	2.83	0.38	77.53	1.05	-1.21	2.26	0.30	0.30
1.36	-1.47	2.83	0.37	77.53	1.10	-0.20	1.30	0.17	0.17
1.29	-1.47	2.76	0.37	75.82	1.06	-1.19	2.25	0.30	0.30
1.32	-1.50	2.82	0.37	76.01	1.05	-1.22	2.27	0.30	0.30
Avg	2.81	0.37	77.45		Avg	2.05	0.27		
σ	0.03	0.01			σ	0.42	0.06		
Variance	0.00	0.00			Variance	0.18	0.00		
1.29	-1.42	2.71	0.36		1.05	-1.19	2.24	0.30	0.30
Accelerometer #2					Accelerometer #3				
Peak	Valley	Defl.(mils)	Norm. Defl. (mils/pl)	LT _{US} (%)	Peak	Valley	Defl.(mils)	Norm. Defl. (mils/pl)	LT _{US} (%)
2.84	-3.74	6.58	0.41	78.43	2.31	-3.00	5.31	0.33	0.33
2.86	-3.69	6.55	0.41	79.30	2.31	-2.99	5.30	0.33	0.33
2.90	-3.69	6.59	0.41	80.37	2.33	-3.01	5.34	0.33	0.33
2.91	-3.62	6.53	0.41	80.22	2.35	-2.97	5.32	0.33	0.33
2.91	-3.62	6.53	0.41	79.73	2.34	-2.96	5.30	0.33	0.33
Avg	6.56	0.41	79.60		Avg	5.31	0.33		
σ	0.03	0.00			σ	0.02	0.00		
Variance	0.00	0.00			Variance	0.00	0.00		
2.86	-3.60	6.46	0.40		2.31	-2.93	5.24	0.33	0.33
Accelerometer #2					Accelerometer #3				
Peak	Valley	Defl.(mils)	Norm. Defl. (mils/pl)	LT _{US} (%)	Peak	Valley	Defl.(mils)	Norm. Defl. (mils/pl)	LT _{US} (%)
5.99	-7.99	13.98	0.47	76.90	4.88	-6.40	11.28	0.38	0.38
6.12	-8.29	14.41	0.48	78.70	4.97	-6.61	11.58	0.39	0.39
6.67	-8.81	15.48	0.49	78.66	5.54	-6.94	12.48	0.39	0.39
6.67	-8.99	15.66	0.49	79.82	5.48	-7.09	12.57	0.40	0.40
6.65	-9.07	15.72	0.50	81.92	5.44	-7.17	12.61	0.40	0.40
Avg	15.05	0.49	79.23		Avg	12.10	0.39		
σ	0.80	0.01			σ	0.63	0.01		
Variance	0.64	0.00			Variance	0.39	0.00		
6.34	-8.54	14.88	0.48		5.18	-6.77	11.95	0.39	0.39
Average LT				78.76					

Figure I24 – Data Summary for South Run-Up – Edge Load Point – Years 16-20

Point #7 North Run-Up Center

1-5 Years

File "H1"

Goal	Start (s)	Stop (s)
26,600 app. (1330 s)	22	1392.0
@ 7.1 kips	Test Time	1370.0
	Total Apps./Period	27400
	Total Apps./Overall	27400

Start (s)	Apps.
50 sec intervals	200 3560
	400 7560
	700 13560
	1000 19560
	1200 23560

Load	Peak	Valley
	8.25	1.28
	8.18	1.31
	8.25	1.27
	8.19	1.28
	8.06	1.37
Avg Load	8.19	
σ	0.08	
Variance	0.01	
	8.20	1.29

Accelerometer #1	Peak	Valley	Defl.(mils)
	0.54	-0.51	1.05
	0.55	-0.53	1.08
	0.59	-0.59	1.18
	0.51	-0.54	1.05
	0.48	-0.49	0.97
Avg	0.54	-0.54	1.01
σ			0.08
Variance			0.01

Avg Reading for Entire Test Period

Goal	Start (s)	Stop (s)
12,100 app. (605 s)	1471	2079.0
@ 15.9 kips	Test Time	608.0
	Total Apps./Period	12160
	Total Apps./Overall	39560

Start (s)	Apps.
50 sec intervals	1550 28980
	1650 30980
	1750 32980
	1850 34980
	1950 36980

Load	Peak	Valley
	16.35	5.32
	16.45	5.50
	16.53	5.51
	16.59	5.46
	16.56	5.48
Avg Load	16.50	
σ	0.10	
Variance	0.01	
	16.48	5.40

Accelerometer #1	Peak	Valley	Defl.(mils)
	0.92	-1.14	2.06
	0.93	-1.14	2.07
	0.93	-1.17	2.10
	0.95	-1.14	2.09
	0.91	-1.10	2.01
Avg	0.93	-1.13	2.00
σ			0.04
Variance			0.00

Avg Reading for Entire Test Period

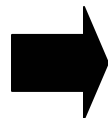
Goal	Start (s)	Stop (s)
10,400 app. (520 s)	2135	2655.0
@ 31.6 kips	Test Time	520.0
	Total Apps./Period	10400
	Total Apps./Overall	49960

Start (s)	Apps.
50 sec intervals	2175 40360
	2275 42360
	2375 44360
	2475 46360
	2575 48360

Load	Peak	Valley
	32.70	2.56
	31.76	2.54
	31.81	2.62
	31.74	2.68
	31.74	2.77
Avg Load	31.95	
σ	0.42	
Variance	0.18	
	31.66	5.90

Accelerometer #1	Peak	Valley	Defl.(mils)
	2.14	-2.58	4.72
	2.02	-2.40	4.42
	2.01	-2.39	4.40
	2.00	-2.36	4.36
	2.00	-2.35	4.35
Avg	1.99	-2.36	4.35
σ			0.15
Variance			0.02

Avg Reading for Entire Test Period



Accelerometer #2				
Peak	Valley	Defl.(mils)	Norm. Defl. (mils/pl)	LT _{US} (%)
0.47	-0.46	0.93	0.11	88.57
0.31	-0.32	0.63	0.08	58.33
0.39	-0.40	0.79	0.10	66.95
0.39	-0.42	0.81	0.10	77.14
0.42	-0.44	0.86	0.11	86.66
	Avg	0.77	0.09	72.47
	σ	0.10	0.01	
	Variance	0.01	0.00	
0.39	-0.40	0.79	0.10	

Accelerometer #3				
Peak	Valley	Defl.(mils)	Norm. Defl. (mils/pl)	
0.42	-0.43	0.85	0.10	
0.42	-0.43	0.85	0.10	
0.47	-0.48	0.95	0.12	
0.43	-0.47	0.90	0.11	
0.39	-0.43	0.82	0.10	
	Avg	0.87	0.11	
	σ	0.05	0.01	
	Variance	0.00	0.00	
0.43	-0.45	0.88	0.11	

Accelerometer #2				
Peak	Valley	Defl.(mils)	Norm. Defl. (mils/pl)	LT _{US} (%)
0.66	-0.79	1.45	0.09	70.39
0.82	-1.00	1.82	0.11	87.92
0.82	-1.02	1.84	0.11	87.62
0.83	-1.03	1.86	0.11	89.00
0.82	-0.98	1.80	0.11	89.55
	Avg	1.75	0.11	84.90
	σ	0.17	0.01	
	Variance	0.03	0.00	
0.78	-0.95	1.73	0.10	

Accelerometer #3				
Peak	Valley	Defl.(mils)	Norm. Defl. (mils/pl)	
0.72	-0.90	1.62	0.10	
0.73	-0.91	1.64	0.10	
0.73	-0.93	1.66	0.10	
0.76	-0.94	1.70	0.10	
0.75	-0.92	1.67	0.10	
	Avg	1.66	0.10	
	σ	0.03	0.00	
	Variance	0.00	0.00	
0.74	-0.92	1.66	0.10	

Accelerometer #2				
Peak	Valley	Defl.(mils)	Norm. Defl. (mils/pl)	LT _{US} (%)
1.87	-2.28	4.15	0.13	87.92
1.77	-2.11	3.88	0.12	87.78
1.76	-2.11	3.87	0.12	87.95
1.75	-2.08	3.83	0.12	87.84
1.75	-2.07	3.82	0.12	87.82
	Avg	3.91	0.12	87.87
	σ	0.14	0.00	
	Variance	0.02	0.00	
1.74	-2.08	3.82	0.12	
Average LT				81.74

Accelerometer #3				
Peak	Valley	Defl.(mils)	Norm. Defl. (mils/pl)	
1.68	-2.06	3.74	0.11	
1.58	-1.92	3.50	0.11	
1.57	-1.91	3.48	0.11	
1.56	-1.89	3.45	0.11	
1.56	-1.87	3.43	0.11	
	Avg	3.52	0.11	
	σ	0.13	0.00	
	Variance	0.02	0.00	
1.55	-1.89	3.44	0.11	

Figure I25 – Data Summary for North Run-Up – Center Load Point – Years 1-5

6-10 Years

File "H1"

Goal	Start (s)	Stop (s)
26,600 app. (1330 s)	2737	4032.0
@ 7.1 kips	Test Time	1295.0
	Total Apps./Period	25900
	Total Apps./Overall	75860

Start (s)	Apps.
2900	53220
3100	57220
3400	63220
3700	69220
3900	73220

Load	Valley
Peak	
7.79	2.55
7.78	2.55
7.85	2.49
7.93	2.44
7.89	2.45
Avg Load	7.85
σ	0.06
Variance	0.00
	7.78 2.51

Accelerometer #1	Defl.(mils)
Peak	Valley
0.42	-0.35
0.43	-0.36
0.44	-0.36
0.41	-0.36
0.39	-0.34
Avg	0.77
σ	0.03
Variance	0.00
	0.42 -0.35 0.77

Avg Reading for Entire Test Period

Goal	Start (s)	Stop (s)
12,100 app. (605 s)	4110	4725.0
@ 15.9 kips	Test Time	615.0
	Total Apps./Period	12300
	Total Apps./Overall	88160

Start (s)	Apps.
4200	77660
4300	79660
4400	81660
4500	83660
4600	85660

Load	Valley
Peak	
16.30	4.44
16.37	4.53
16.30	4.56
16.35	4.47
16.34	4.49
Avg Load	16.33
σ	0.03
Variance	0.00
	16.29 4.45

Accelerometer #1	Defl.(mils)
Peak	Valley
1.05	-1.06
1.05	-1.08
1.06	-1.11
1.07	-1.13
1.08	-1.17
Avg	2.17
σ	0.06
Variance	0.00
	1.06 -1.11 2.17

Avg Reading for Entire Test Period

Goal	Start (s)	Stop (s)
10,400 app. (520 s)	4861	5381.0
@ 31.6 kips	Test Time	520.0
	Total Apps./Period	10400
	Total Apps./Overall	98560

Start (s)	Apps.
4900	88940
5000	90940
5100	92940
5200	94940
5300	96940

Load	Valley
Peak	
31.60	5.17
32.02	5.99
32.00	6.00
32.12	5.93
32.06	5.96
Avg Load	31.96
σ	0.21
Variance	0.04
	31.63 6.02

Accelerometer #1	Defl.(mils)
Peak	Valley
1.93	-2.47
2.04	-2.36
2.05	-2.36
2.05	-2.39
2.03	-2.37
Avg	4.41
σ	0.02
Variance	0.00
	1.98 -2.33 4.31

Avg Reading for Entire Test Period



Accelerometer #2					Accelerometer #3				
Peak	Valley	Defl.(mils)	Norm. Defl. (mils/pi)	LT _{US} (%)	Peak	Valley	Defl.(mils)	Norm. Defl. (mils/pi)	
0.37	-0.31	0.68	0.09	88.31	0.33	-0.28	0.61	0.08	
0.39	-0.32	0.71	0.09	89.87	0.34	-0.30	0.64	0.08	
0.39	-0.33	0.72	0.09	90.00	0.35	-0.31	0.66	0.08	
0.37	-0.32	0.69	0.09	89.61	0.34	-0.30	0.64	0.08	
0.35	-0.30	0.65	0.08	89.04	0.33	-0.29	0.62	0.08	
Avg		0.69	0.09	89.70	Avg		0.63	0.08	
σ		0.03	0.00		σ		0.02	0.00	
Variance		0.00	0.00		Variance		0.00	0.00	
0.37	-0.32	0.69	0.09		0.34	-0.30	0.64	0.08	

Accelerometer #2					Accelerometer #3				
Peak	Valley	Defl.(mils)	Norm. Defl. (mils/pi)	LT _{US} (%)	Peak	Valley	Defl.(mils)	Norm. Defl. (mils/pi)	
0.91	-0.92	1.83	0.11	86.73	0.80	-0.83	1.63	0.10	
0.92	-0.94	1.86	0.11	87.32	0.80	-0.84	1.64	0.10	
0.93	-0.96	1.89	0.12	87.10	0.82	-0.86	1.68	0.10	
0.94	-0.98	1.92	0.12	87.27	0.82	-0.88	1.70	0.10	
0.95	-1.03	1.98	0.12	88.00	0.84	-0.91	1.75	0.11	
Avg		1.90	0.12	87.29	Avg		1.68	0.10	
σ		0.06	0.00		σ		0.05	0.00	
Variance		0.00	0.00		Variance		0.00	0.00	
0.93	-0.97	1.90	0.12		0.82	-0.87	1.69	0.10	

Accelerometer #2					Accelerometer #3				
Peak	Valley	Defl.(mils)	Norm. Defl. (mils/pi)	LT _{US} (%)	Peak	Valley	Defl.(mils)	Norm. Defl. (mils/pi)	
1.70	-2.17	3.87	0.12	87.95	1.52	-1.93	3.45	0.11	
1.76	-2.07	3.83	0.12	87.05	1.54	-1.87	3.41	0.11	
1.77	-2.07	3.84	0.12	87.07	1.55	-1.87	3.42	0.11	
1.79	-2.10	3.89	0.12	87.61	1.59	-1.89	3.48	0.11	
1.78	-2.08	3.86	0.12	87.73	1.59	-1.87	3.46	0.11	
Avg		3.86	0.12	87.48	Avg		3.44	0.11	
σ		0.02	0.00		σ		0.03	0.00	
Variance		0.00	0.00		Variance		0.00	0.00	
1.72	-2.05	3.77	0.12		1.52	-1.85	3.37	0.11	
Average LT					88.16				

Figure I26 – Data Summary for North Run-Up – Center Load Point – Years 6-10

11-15 Years

File "H2"

Goal	Start (s)	Stop (s)	Start (s)	Apps.	Load Peak	Valley	Accelerometer #1 Peak	Valley	Defl.(mils)	
26,600 app. (1330 s)	107	1442.0	50 sec intervals	300	102420	7.49	1.62	0.42	-0.33	0.75
@ 7.1 kips	Test Time	1335.0		500	106420	7.51	1.70	0.45	-0.35	0.80
Total Apps./Period	26700			800	112420	7.54	1.63	0.45	-0.36	0.81
Total Apps./Overall	125260			1100	118420	7.59	1.63	0.45	-0.37	0.82
				1300	122420	7.62	1.63	0.43	-0.36	0.79
					Avg Load	7.55		Avg	0.79	
					σ	0.05		σ	0.03	
					Variance	0.00		Variance	0.00	
					Avg Reading for Entire Test Period	7.54	2.10	0.44	-0.35	0.79

Goal	Start (s)	Stop (s)	Start (s)	Apps.	Load Peak	Valley	Accelerometer #1 Peak	Valley	Defl.(mils)	
12,100 app. (605 s)	1520	2125.0	50 sec intervals	1600	126860	16.45	4.57	1.05	-1.11	2.16
@ 15.9 kips	Test Time	605.0		1700	128860	16.52	4.68	1.04	-1.12	2.16
Total Apps./Period	12100			1800	130860	16.50	4.69	1.03	-1.13	2.16
Total Apps./Overall	137360			1900	132860	16.49	4.67	1.01	-1.13	2.14
				2000	134860	16.44	4.64	0.99	-1.15	2.14
					Avg Load	16.48		Avg	2.15	
					σ	0.03		σ	0.01	
					Variance	0.00		Variance	0.00	
					Avg Reading for Entire Test Period	16.49	4.56	1.03	-1.13	2.16

Goal	Start (s)	Stop (s)	Start (s)	Apps.	Load Peak	Valley	Accelerometer #1 Peak	Valley	Defl.(mils)	
10,400 app. (520 s)	2215	2725.0	50 sec intervals	2250	138060	30.26	5.08	1.78	-2.33	4.11
@ 31.6 kips	Test Time	510.0		2350	140060	31.82	5.05	2.16	-2.37	4.53
Total Apps./Period	10200			2450	142060	31.91	5.17	2.11	-2.36	4.47
Total Apps./Overall	147560			2550	144060	31.85	5.34	2.11	-2.36	4.47
				2650	146060	31.89	5.20	2.03	-2.37	4.40
					Avg Load	31.55		Avg	4.40	
					σ	0.72		σ	0.17	
					Variance	0.52		Variance	0.03	
					Avg Reading for Entire Test Period	31.29	5.40	2.01	-2.31	4.32



Accelerometer #2					Accelerometer #3			
Peak	Valley	Defl.(mils)	Norm. Defl. (mils/pl)	LT _{US} (%)	Peak	Valley	Defl.(mils)	Norm. Defl. (mils/pl)
0.38	-0.29	0.67	0.09	89.33	0.33	-0.27	0.60	0.08
0.39	-0.31	0.70	0.09	87.50	0.34	-0.28	0.62	0.08
0.40	-0.32	0.72	0.10	88.89	0.35	-0.30	0.65	0.09
0.40	-0.32	0.72	0.09	87.80	0.36	-0.30	0.66	0.09
0.38	-0.32	0.70	0.09	88.61	0.35	-0.30	0.65	0.09
	Avg	0.71	0.09	89.42		Avg	0.64	0.08
	σ	0.01	0.00			σ	0.03	0.00
	Variance	0.00	0.00			Variance	0.00	0.00
0.39	-0.31	0.70	0.09		0.35	-0.29	0.64	0.08
Accelerometer #2					Accelerometer #3			
Peak	Valley	Defl.(mils)	Norm. Defl. (mils/pl)	LT _{US} (%)	Peak	Valley	Defl.(mils)	Norm. Defl. (mils/pl)
0.92	-0.96	1.88	0.11	87.04	0.81	-0.86	1.67	0.10
0.90	-0.97	1.87	0.11	86.57	0.80	-0.86	1.66	0.10
0.90	-0.98	1.88	0.11	87.04	0.80	-0.88	1.68	0.10
0.90	-0.99	1.89	0.11	88.32	0.79	-0.89	1.68	0.10
0.88	-1.01	1.89	0.11	88.32	0.78	-0.90	1.68	0.10
	Avg	1.88	0.11	87.45		Avg	1.67	0.10
	σ	0.01	0.00			σ	0.01	0.00
	Variance	0.00	0.00			Variance	0.00	0.00
0.90	-0.99	1.89	0.11		0.79	-0.88	1.67	0.10
Accelerometer #2					Accelerometer #3			
Peak	Valley	Defl.(mils)	Norm. Defl. (mils/pl)	LT _{US} (%)	Peak	Valley	Defl.(mils)	Norm. Defl. (mils/pl)
1.54	-2.04	3.58	0.12	87.10	1.36	-1.83	3.19	0.11
1.88	-2.08	3.96	0.12	87.42	1.64	-1.86	3.50	0.11
1.86	-2.07	3.93	0.12	87.92	1.65	-1.86	3.51	0.11
1.85	-2.06	3.91	0.12	87.47	1.66	-1.85	3.51	0.11
1.78	-2.07	3.85	0.12	87.50	1.60	-1.86	3.46	0.11
	Avg	3.85	0.12	87.49		Avg	3.43	0.11
	σ	0.15	0.00			σ	0.14	0.00
	Variance	0.02	0.00			Variance	0.02	0.00
1.75	-2.02	3.77	0.12		1.56	-1.81	3.37	0.11
Average LT				88.12				

Figure I27 – Data Summary for North Run-Up – Center Load Point – Years 11-15

16-20 Years File "H2"									
Goal	Start (s)	Stop (s)	Start (s)	Apps.	Load Peak	Valley	Accelerometer #1 Peak	Valley	Defl.(mils)
26,600 app. (1330 s) @ 7.1 kips	2805	4150.0	50 sec intervals	3000 151460	7.59	2.15	0.43	-0.35	0.78
				3200 155460	7.60	2.18	0.44	-0.35	0.79
				3500 161460	7.56	2.16	0.43	-0.36	0.79
				3800 167460	7.51	2.15	0.41	-0.35	0.76
				4000 171460	7.52	2.14	0.39	-0.34	0.73
					Avg Load	7.56		Avg	0.77
					σ	0.04		σ	0.03
					Variance	0.00		Variance	0.00
						7.52	2.14	0.42	-0.35
									% inc
Goal	Start (s)	Stop (s)	Start (s)	Apps.	Load Peak	Valley	Accelerometer #1 Peak	Valley	Defl.(mils)
12,100 app. (605 s) @ 15.9 kips	4230	4848.0	50 sec intervals	4300 175860	16.83	3.11	1.15	-1.19	2.34
				4400 177860	16.86	3.15	1.12	-1.20	2.32
				4500 179860	16.85	3.12	1.14	-1.21	2.35
				4600 181860	16.75	3.21	1.12	-1.20	2.32
				4700 183860	16.79	3.12	1.11	-1.22	2.33
					Avg Load	16.82		Avg	2.33
					σ	0.05		σ	0.01
					Variance	0.00		Variance	0.00
						16.78	3.14	1.13	-1.20
									% inc
Goal	Start (s)	Stop (s)	Start (s)	Apps.	Load Peak	Valley	Accelerometer #1 Peak	Valley	Defl.(mils)
10,400 app. (520 s) @ 31.6 kips	4945	5450.0	50 sec intervals	4975 187420	31.67	2.76	2.10	-2.49	4.59
				5075 189420	31.05	4.06	2.09	-2.31	4.40
				5175 191420	31.07	4.08	2.07	-2.32	4.39
				5275 193420	31.13	4.19	2.10	-2.31	4.41
				5375 195420	31.21	4.13	2.07	-2.34	4.41
					Avg Load	31.23		Avg	4.44
					σ	0.26		σ	0.08
					Variance	0.07		Variance	0.01
						31.04	3.98	2.06	-2.33
									% inc

Accelerometer #2				
Peak	Valley	Defl.(mils)	Norm. Defl. (mils/pi)	LT us (%)
0.36	-0.31	0.67	0.09	85.90
0.38	-0.31	0.69	0.09	87.34
0.37	-0.31	0.68	0.09	86.08
0.37	-0.31	0.68	0.09	89.47
0.35	-0.30	0.65	0.09	89.04
		Avg	0.68	87.66
		σ	0.02	0.00
		Variance	0.00	0.00
0.37	-0.31	0.68	0.09	

Accelerometer #3				
Peak	Valley	Defl.(mils)	Norm. Defl. (mils/pi)	
0.33	-0.28	0.61	0.08	0.08
0.35	-0.29	0.64	0.08	0.08
0.34	-0.29	0.63	0.08	0.08
0.33	-0.29	0.62	0.08	0.08
0.32	-0.28	0.60	0.08	0.08
		Avg	0.62	0.08
		σ	0.02	0.00
		Variance	0.00	0.00
0.33	-0.28	0.61	0.08	0.08

Accelerometer #2				
Peak	Valley	Defl.(mils)	Norm. Defl. (mils/pi)	LT us (%)
1.00	-1.04	2.04	0.12	87.18
0.99	-1.06	2.05	0.12	88.36
0.99	-1.06	2.05	0.12	87.23
0.98	-1.05	2.03	0.12	87.50
0.97	-1.07	2.04	0.12	87.55
		Avg	2.04	87.56
		σ	0.01	0.00
		Variance	0.00	0.00
0.99	-1.05	2.04	0.12	

Accelerometer #3				
Peak	Valley	Defl.(mils)	Norm. Defl. (mils/pi)	
0.87	-0.94	1.81	0.11	0.11
0.87	-0.95	1.82	0.11	0.11
0.87	-0.94	1.81	0.11	0.11
0.86	-0.94	1.80	0.11	0.11
0.85	-0.96	1.81	0.11	0.11
		Avg	1.81	0.11
		σ	0.01	0.00
		Variance	0.00	0.00
0.86	-0.94	1.80	0.11	0.11

Accelerometer #2				
Peak	Valley	Defl.(mils)	Norm. Defl. (mils/pi)	LT us (%)
1.82	-2.17	3.99	0.13	86.93
1.79	-2.03	3.82	0.12	86.62
1.79	-2.03	3.82	0.12	87.02
1.83	-2.02	3.85	0.12	87.30
1.81	-2.04	3.85	0.12	87.30
		Avg	3.87	87.07
		σ	0.07	0.00
		Variance	0.01	0.00
1.79	-2.04	3.83	0.12	

Accelerometer #3				
Peak	Valley	Defl.(mils)	Norm. Defl. (mils/pi)	
1.61	-1.94	3.55	0.11	0.11
1.55	-1.82	3.37	0.11	0.11
1.57	-1.83	3.40	0.11	0.11
1.61	-1.81	3.42	0.11	0.11
1.62	-1.83	3.45	0.11	0.11
		Avg	3.44	0.11
		σ	0.07	0.00
		Variance	0.00	0.00
1.57	-1.83	3.40	0.11	0.11

Average LT87.43

Figure I28 – Data Summary for North Run-Up – Center Load Point – Years 16-20

Point #8 North Run-Up Edge

1-5 Years File "J1"									
Goal	Start (s)	Stop (s)	Start (s)	Apps.	Load Peak	Valley	Accelerometer #1 Peak	Valley	Defl.(mils)
26,600 app. (1330 s) @ 7.1 kips	74	1524.0	50 sec intervals	200 2520 400 6520 700 12520 1000 18520 1200 22520	8.01 1.69 7.96 1.83 7.81 1.78 7.79 1.78 7.75 1.80		0.73 -0.67 1.40 0.66 -0.64 1.30 0.58 -0.60 1.18 0.59 -0.59 1.18 0.59 -0.58 1.17		
Test Time		1450.0			Avg Load	7.84	Avg	1.25	
Total Apps./Period		29000			σ	0.10	σ	0.10	
Total Apps./Overall		29000			Variance	0.01	Variance	0.01	
Avg Reading for Entire Test Period						7.83 1.75		0.61 -0.60 1.21	
Goal	Start (s)	Stop (s)	Start (s)	Apps.	Load Peak	Valley	Accelerometer #1 Peak	Valley	Defl.(mils)
12,100 app. (605 s) @ 15.9 kips	1625	2238.0	50 sec intervals	1700 30500 1800 32500 1900 34500 2000 36500 2100 38500	16.43 5.21 16.37 5.26 16.40 5.21 16.37 5.21 16.41 5.41		1.23 -1.44 2.67 1.21 -1.44 2.65 1.23 -1.48 2.71 1.21 -1.47 2.68 1.20 -1.48 2.68		
Test Time		613.0			Avg Load	16.40	Avg	2.68	
Total Apps./Period		12260			σ	0.03	σ	0.02	
Total Apps./Overall		41260			Variance	0.00	Variance	0.00	
Avg Reading for Entire Test Period						16.43 5.14		1.22 -1.47 2.69	
Goal	Start (s)	Stop (s)	Start (s)	Apps.	Load Peak	Valley	Accelerometer #1 Peak	Valley	Defl.(mils)
10,400 app. (520 s) @ 31.6 kips	2297	2817.0	50 sec intervals	2350 42320 2450 44320 2550 46320 2650 48320 2750 50320	31.07 5.71 32.03 4.37 31.98 4.33 31.88 4.29 31.83 4.34		2.89 -3.15 6.04 3.04 -3.58 6.62 3.07 -3.57 6.64 3.10 -3.57 6.67 3.10 -3.55 6.65		
Test Time		520.0			Avg Load	31.76	Avg	6.52	
Total Apps./Period		10400			σ	0.39	σ	0.27	
Total Apps./Overall		51660			Variance	0.15	Variance	0.07	
Avg Reading for Entire Test Period						31.52 4.88		3.01 -3.41 6.42	



Accelerometer #2					Accelerometer #3				
Peak	Valley	Defl.(mils)	Norm. Defl. (mils/pl)	LT _{US} (%)	Peak	Valley	Defl.(mils)	Norm. Defl. (mils/pl)	
0.51	-0.48	0.99	0.12	70.71	0.38	-0.39	0.77	0.10	
0.48	-0.46	0.94	0.12	72.31	0.36	-0.36	0.72	0.09	
0.42	-0.44	0.86	0.11	72.88	0.32	-0.36	0.68	0.09	
0.42	-0.43	0.85	0.11	72.03	0.32	-0.35	0.67	0.09	
0.41	-0.42	0.83	0.11	70.94	0.31	-0.34	0.65	0.08	
Avg		0.87	0.11	69.82	Avg		0.70	0.09	
σ		0.05	0.01		σ		0.05	0.00	
Variance		0.00	0.00		Variance		0.00	0.00	
0.43	-0.44	0.87	0.11		0.33	-0.36	0.69	0.09	
Accelerometer #2					Accelerometer #3				
Peak	Valley	Defl.(mils)	Norm. Defl. (mils/pl)	LT _{US} (%)	Peak	Valley	Defl.(mils)	Norm. Defl. (mils/pl)	
0.88	-1.03	1.91	0.12	71.54	0.65	-0.80	1.45	0.09	
0.87	-1.03	1.90	0.12	71.70	0.65	-0.79	1.44	0.09	
0.89	-1.05	1.94	0.12	71.59	0.66	-0.80	1.46	0.09	
0.87	-1.06	1.93	0.12	72.01	0.65	-0.80	1.45	0.09	
0.87	-1.08	1.95	0.12	72.76	0.66	-0.82	1.48	0.09	
Avg		1.93	0.12	71.92	Avg		1.46	0.09	
σ		0.02	0.00		σ		0.02	0.00	
Variance		0.00	0.00		Variance		0.00	0.00	
0.88	-1.06	1.94	0.12		0.66	-0.81	1.47	0.09	
Accelerometer #2					Accelerometer #3				
Peak	Valley	Defl.(mils)	Norm. Defl. (mils/pl)	LT _{US} (%)	Peak	Valley	Defl.(mils)	Norm. Defl. (mils/pl)	
2.19	-2.28	4.47	0.14	74.01	1.66	-1.78	3.44	0.11	
2.15	-2.62	4.77	0.15	72.05	1.56	-2.04	3.60	0.11	
2.19	-2.62	4.81	0.15	72.44	1.59	-2.04	3.63	0.11	
2.23	-2.62	4.85	0.15	72.71	1.63	-2.04	3.67	0.12	
2.25	-2.61	4.86	0.15	73.08	1.64	-2.04	3.68	0.12	
Avg		4.75	0.15	72.84	Avg		3.60	0.11	
σ		0.16	0.00		σ		0.10	0.00	
Variance		0.03	0.00		Variance		0.01	0.00	
2.18	-2.49	4.67	0.15		1.61	-1.95	3.56	0.11	
Average LT					71.53				

Figure I29 – Data Summary for North Run-Up – Edge Load Point – Years 1-5

6-10 Years

File "J1"

Goal	Start (s)	Stop (s)
26,600 app. (1330 s)	2947	4282.0
@ 7.1 kips	Test Time	1335.0
	Total Apps./Period	26700
	Total Apps./Overall	78360

Start (s)	Apps.
3100	54720
3300	58720
3600	64720
3900	70720
4100	74720

Load	Peak	Valley
	8.14	2.44
	8.18	2.39
	8.32	2.31
	8.44	2.18
	8.52	2.19
Avg Load	8.32	
σ	0.16	
Variance	0.03	
	8.31	2.29

Accelerometer #1	Peak	Valley	Defl.(mils)
	0.65	-0.68	1.33
	0.66	-0.67	1.33
	0.70	-0.66	1.36
	0.72	-0.71	1.43
	0.69	-0.69	1.38
Avg	1.37		
σ	0.04		
Variance	0.00		
	0.69	-0.69	1.38

Avg Reading for Entire Test Period

Goal	Start (s)	Stop (s)
12,100 app. (605 s)	4350	4955.0
@ 15.9 kips	Test Time	605.0
	Total Apps./Period	12100
	Total Apps./Overall	90460

Start (s)	Apps.
4400	79360
4500	81360
4600	83360
4700	85360
4800	87360

Load	Peak	Valley
	16.55	3.03
	16.65	3.24
	16.65	3.37
	16.65	3.32
	16.67	3.39
	16.66	3.38
Avg Load	16.64	
σ	0.05	
Variance	0.00	
	16.63	3.28

Accelerometer #1	Peak	Valley	Defl.(mils)
	1.57	-1.72	3.29
	1.55	-1.72	3.27
	1.56	-1.71	3.27
	1.53	-1.74	3.27
	1.53	-1.73	3.26
Avg	3.27		
σ	0.01		
Variance	0.00		
	1.54	-1.72	3.26

Avg Reading for Entire Test Period

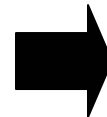
Goal	Start (s)	Stop (s)
10,400 app. (520 s)	5020	5540.0
@ 31.6 kips	Test Time	520.0
	Total Apps./Period	10400
	Total Apps./Overall	100860

Start (s)	Apps.
5050	91060
5150	93060
5250	95060
5350	97060
5450	99060

Load	Peak	Valley
	31.61	4.69
	31.85	4.18
	31.77	4.04
	31.79	4.06
	31.70	4.06
Avg Load	31.74	
σ	0.09	
Variance	0.01	
	31.75	4.26

Accelerometer #1	Peak	Valley	Defl.(mils)
	2.95	-3.38	6.33
	3.09	-3.56	6.65
	3.17	-3.58	6.75
	3.18	-3.53	6.71
	3.21	-3.52	6.73
Avg	6.63		
σ	0.17		
Variance	0.03		
	3.12	-3.49	6.61

Avg Reading for Entire Test Period



Accelerometer #2				
Peak	Valley	Defl.(mils)	Norm. Defl. (mils/pi)	LT _{US} (%)
0.46	-0.49	0.95	0.12	71.43
0.47	-0.49	0.96	0.12	72.18
0.50	-0.48	0.98	0.12	72.06
0.52	-0.51	1.03	0.12	72.03
0.50	-0.51	1.01	0.12	73.19
Avg		1.00	0.12	72.84
σ		0.03	0.00	
Variance		0.00	0.00	
0.49	-0.50	0.99	0.12	
Accelerometer #3				
Peak	Valley	Defl.(mils)	Norm. Defl. (mils/pi)	
0.34	-0.38	0.72	0.09	
0.35	-0.39	0.74	0.09	
0.37	-0.38	0.75	0.09	
0.39	-0.39	0.78	0.09	
0.38	-0.41	0.79	0.09	
Avg		0.76	0.09	
σ		0.03	0.00	
Variance		0.00	0.00	
0.37	-0.39	0.76	0.09	
Accelerometer #2				
Peak	Valley	Defl.(mils)	Norm. Defl. (mils/pi)	LT _{US} (%)
1.13	-1.24	2.37	0.14	72.04
1.11	-1.23	2.34	0.14	71.56
1.12	-1.22	2.34	0.14	71.56
1.10	-1.22	2.32	0.14	70.95
1.11	-1.23	2.34	0.14	71.78
Avg		2.34	0.14	71.58
σ		0.02	0.00	
Variance		0.00	0.00	
1.11	-1.23	2.34	0.14	
Accelerometer #3				
Peak	Valley	Defl.(mils)	Norm. Defl. (mils/pi)	
0.83	-0.96	1.79	0.11	
0.83	-0.95	1.78	0.11	
0.84	-0.94	1.78	0.11	
0.83	-0.94	1.77	0.11	
0.83	-0.95	1.78	0.11	
Avg		1.78	0.11	
σ		0.01	0.00	
Variance		0.00	0.00	
0.83	-0.94	1.77	0.11	
Accelerometer #2				
Peak	Valley	Defl.(mils)	Norm. Defl. (mils/pi)	LT _{US} (%)
2.12	-2.44	4.56	0.14	72.04
2.15	-2.57	4.72	0.15	70.98
2.20	-2.59	4.79	0.15	70.96
2.23	-2.56	4.79	0.15	71.39
2.27	-2.55	4.82	0.15	71.62
Avg		4.74	0.15	71.39
σ		0.11	0.00	
Variance		0.01	0.00	
2.19	-2.53	4.72	0.15	
Average LT				71.94
Accelerometer #3				
Peak	Valley	Defl.(mils)	Norm. Defl. (mils/pi)	
1.61	-1.90	3.51	0.11	
1.56	-1.99	3.55	0.11	
1.59	-2.01	3.60	0.11	
1.63	-2.00	3.63	0.11	
1.66	-2.00	3.66	0.12	
Avg		3.59	0.11	
σ		0.06	0.00	
Variance		0.00	0.00	
1.61	-1.97	3.58	0.11	

Figure I30 – Data Summary for North Run-Up – Edge Load Point – Years 6-10

11-15 Years File "J2"									
Goal	Start (s)	Stop (s)	Start (s)	Apps.	Load Peak	Valley	Accelerometer #1 Peak	Valley	Defl.(mils)
26,600 app. (1330 s)	78	1413.0	50 sec intervals	200 103300	8.18	2.45	0.67	-0.67	1.34
@ 7.1 kips	Test Time	1335.0		400 107300	8.16	2.46	0.64	-0.67	1.31
	Total Apps./Period	26700		700 113300	8.20	2.44	0.62	-0.67	1.29
	Total Apps./Overall	127560		1000 119300	8.19	2.45	0.62	-0.66	1.28
				1200 123300	8.25	2.41	0.63	-0.68	1.31
				Avg Load	8.20		Avg	1.31	
				σ	0.03		σ	0.02	
				Variance	0.00		Variance	0.00	
				Avg Reading for Entire Test Period	8.17	2.43	0.63	-0.66	1.29
Goal	Start (s)	Stop (s)	Start (s)	Apps.	Load Peak	Valley	Accelerometer #1 Peak	Valley	Defl.(mils)
12,100 app. (605 s)	1500	2200.0	50 sec intervals	1600 129560	16.65	3.51	1.46	-1.67	3.13
@ 15.9 kips	Test Time	700.0		1700 131560	16.60	3.58	1.43	-1.65	3.08
	Total Apps./Period	14000		1800 133560	16.55	3.60	1.42	-1.65	3.07
	Total Apps./Overall	141560		1900 135560	16.57	3.59	1.40	-1.65	3.05
				2000 137560	16.51	3.62	1.40	-1.64	3.04
				Avg Load	16.58		Avg	3.07	
				σ	0.05		σ	0.04	
				Variance	0.00		Variance	0.00	
				Avg Reading for Entire Test Period	16.56	3.56	1.42	-1.65	3.07
Goal	Start (s)	Stop (s)	Start (s)	Apps.	Load Peak	Valley	Accelerometer #1 Peak	Valley	Defl.(mils)
10,400 app. (520 s)	2340	2845.0	50 sec intervals	2375 142260	30.67	1.63	3.64	-3.70	7.34
@ 31.6 kips	Test Time	505.0		2475 144260	30.85	1.48	3.77	-3.75	7.52
	Total Apps./Period	10100		2575 146260	30.71	1.71	3.73	-3.75	7.48
	Total Apps./Overall	151660		2675 148260	33.16	1.15	3.86	-3.83	7.69
				2775 150260	33.30	1.19	3.91	-3.94	7.85
				Avg Load	31.74		Avg	7.58	
				σ	1.36		σ	0.20	
				Variance	1.86		Variance	0.04	
				Avg Reading for Entire Test Period	31.64	1.61	3.73	-3.76	7.49



Accelerometer #2					Accelerometer #3				
Peak	Valley	Defl.(mils)	Norm. Defl. (mils/pl)	LT us (%)	Peak	Valley	Defl.(mils)	Norm. Defl. (mils/pl)	
0.48	-0.49	0.97	0.12	72.39	0.33	-0.27	0.60	0.07	
0.46	-0.49	0.95	0.12	72.52	0.34	-0.28	0.62	0.08	
0.45	-0.49	0.94	0.11	72.87	0.35	-0.30	0.65	0.08	
0.42	-0.48	0.90	0.11	70.31	0.36	-0.30	0.66	0.08	
0.44	-0.49	0.93	0.11	70.99	0.35	-0.30	0.65	0.08	
	Avg	0.93	0.11	71.21		Avg	0.64	0.08	
	σ	0.02	0.00			σ	0.03	0.00	
	Variance	0.00	0.00			Variance	0.00	0.00	
0.45	-0.48	0.93	0.11		0.35	-0.29	0.64	0.08	
Accelerometer #2					Accelerometer #3				
Peak	Valley	Defl.(mils)	Norm. Defl. (mils/pl)	LT us (%)	Peak	Valley	Defl.(mils)	Norm. Defl. (mils/pl)	
1.03	-1.18	2.21	0.13	70.45	0.78	-0.94	1.72	0.10	
1.01	-1.17	2.18	0.13	70.78	0.76	-0.91	1.67	0.10	
1.00	-1.16	2.16	0.13	70.36	0.76	-0.93	1.69	0.10	
0.99	-1.16	2.15	0.13	70.49	0.75	-0.91	1.66	0.10	
0.98	-1.16	2.14	0.13	70.39	0.74	-0.91	1.65	0.10	
	Avg	2.17	0.13	70.49		Avg	1.68	0.10	
	σ	0.03	0.00			σ	0.03	0.00	
	Variance	0.00	0.00			Variance	0.00	0.00	
1.00	-1.17	2.17	0.13		0.76	-0.92	1.68	0.10	
Accelerometer #2					Accelerometer #3				
Peak	Valley	Defl.(mils)	Norm. Defl. (mils/pl)	LT us (%)	Peak	Valley	Defl.(mils)	Norm. Defl. (mils/pl)	
2.42	-2.57	4.99	0.16	67.98	1.79	-2.01	3.80	0.12	
2.50	-2.61	5.11	0.17	67.95	1.83	-2.02	3.85	0.12	
2.46	-2.60	5.06	0.16	67.65	1.78	-2.01	3.79	0.12	
2.53	-2.67	5.20	0.16	67.62	1.92	-2.15	4.07	0.12	
2.56	-2.70	5.26	0.16	67.01	1.90	-2.14	4.04	0.12	
	Avg	5.12	0.16	67.63		Avg	3.91	0.12	
	σ	0.11	0.00			σ	0.13	0.00	
	Variance	0.01	0.00			Variance	0.02	0.00	
2.46	-2.61	5.07	0.16		1.82	-2.05	3.87	0.12	
Average LT				69.78					

Figure I31 – Data Summary for North Run-Up – Edge Load Point – Years 11-15

16-20 Years

File "J2"

Goal	Start (s)	Stop (s)
26,600 app. (1330 s)	2923	4258.0
@ 7.1 kips	Test Time	1335.0
	Total Apps./Period	26700
	Total Apps./Overall	178360

Start (s)	Apps.
50 sec intervals	3100 155200
	3300 159200
	3600 165200
	3900 171200
	4100 175200

Load	Valley
Peak	
	8.18 2.42
	8.21 2.42
	8.20 2.46
	8.28 2.38
	8.29 2.36
Avg Load	8.23
σ	0.05
Variance	0.00
	8.21 2.41

Accelerometer #1	Valley	Defl.(mils)
Peak		
	0.64	-0.64 1.28
	0.64	-0.63 1.27
	0.62	-0.62 1.24
	0.65	-0.64 1.29
	0.63	-0.66 1.29
Avg		1.27
σ		0.02
Variance		0.00
	0.64	-0.64 1.28

Avg Reading for Entire Test Period

% Inc

Goal	Start (s)	Stop (s)
12,100 app. (605 s)	4320	4925.0
@ 15.9 kips	Test Time	605.0
	Total Apps./Period	12100
	Total Apps./Overall	190460

Start (s)	Apps.
50 sec intervals	4400 179960
	4500 181960
	4600 183960
	4700 185960
	4800 187960

Load	Valley
Peak	
	16.68 3.60
	16.66 3.67
	16.64 3.72
	16.61 3.72
	16.71 3.65
Avg Load	16.66
σ	0.04
Variance	0.00
	16.62 3.61

Accelerometer #1	Valley	Defl.(mils)
Peak		
	1.43	-1.65 3.08
	1.38	-1.62 3.00
	1.40	-1.60 3.00
	1.36	-1.62 2.98
	1.42	-1.61 3.03
Avg		3.02
σ		0.04
Variance		0.00
	1.40	-1.62 3.02

Avg Reading for Entire Test Period

% Inc

Goal	Start (s)	Stop (s)
10,400 app. (520 s)	5005	5525.0
@ 31.6 kips	Test Time	520.0
	Total Apps./Period	10400
	Total Apps./Overall	200860

Start (s)	Apps.
50 sec intervals	5050 191360
	5150 193360
	5250 195360
	5350 197360
	5450 199360

Load	Valley
Peak	
	32.41 1.76
	31.55 2.45
	31.71 2.25
	31.66 2.23
	31.61 2.25
Avg Load	31.79
σ	0.35
Variance	0.12
	31.57 2.32

Accelerometer #1	Valley	Defl.(mils)
Peak		
	3.63	-3.80 7.43
	3.32	-3.65 6.97
	3.42	-3.71 7.13
	3.39	-3.71 7.10
	3.42	-3.68 7.10
Avg		7.15
σ		0.17
Variance		0.03
	3.39	-3.66 7.05

Avg Reading for Entire Test Period

% Inc

Accelerometer #2					Accelerometer #3				
Peak	Valley	Defl.(mils)	Norm. Defl. (mils/pt)	$L7_{US}(\%)$	Peak	Valley	Defl.(mils)	Norm. Defl. (mils/pt)	
0.44	-0.46	0.90	0.11	70.31	0.33	-0.38	0.71	0.09	
0.45	-0.45	0.90	0.11	70.87	0.34	-0.37	0.71	0.09	
0.43	-0.44	0.87	0.11	70.16	0.33	-0.37	0.70	0.09	
0.44	-0.46	0.90	0.11	69.77	0.34	-0.39	0.73	0.09	
0.44	-0.48	0.92	0.11	71.32	0.34	-0.40	0.74	0.09	
	Avg	0.90	0.11	70.45		Avg	0.72	0.09	
	σ	0.02	0.00			σ	0.02	0.00	
	Variance	0.00	0.00			Variance	0.00	0.00	
0.44	-0.46	0.90	0.11		0.34	-0.38	0.72	0.09	

Accelerometer #2					Accelerometer #3				
Peak	Valley	Defl.(mils)	Norm. Defl. (mils/pt)	$L7_{US}(\%)$	Peak	Valley	Defl.(mils)	Norm. Defl. (mils/pt)	
0.99	-1.14	2.13	0.13	69.16	0.75	-0.91	1.66	0.10	
0.95	-1.13	2.08	0.12	69.33	0.73	-0.90	1.63	0.10	
0.97	-1.11	2.08	0.13	69.33	0.75	-0.89	1.64	0.10	
0.93	-1.11	2.04	0.12	68.46	0.72	-0.89	1.61	0.10	
0.97	-1.14	2.11	0.13	69.64	0.75	-0.91	1.66	0.10	
	Avg	2.09	0.13	69.18		Avg	1.64	0.10	
	σ	0.03	0.00			σ	0.02	0.00	
	Variance	0.00	0.00			Variance	0.00	0.00	
0.96	-1.13	2.09	0.13		0.74	-0.90	1.64	0.10	

Accelerometer #2					Accelerometer #3				
Peak	Valley	Defl.(mils)	Norm. Defl. (mils/pt)	$L7_{US}(\%)$	Peak	Valley	Defl.(mils)	Norm. Defl. (mils/pt)	
2.41	-2.59	5.00	0.15	67.29	1.80	-2.06	3.86	0.12	
2.23	-2.50	4.73	0.15	67.86	1.67	-2.00	3.67	0.12	
2.30	-2.55	4.85	0.15	68.02	1.72	-2.04	3.76	0.12	
2.31	-2.57	4.88	0.15	68.73	1.73	-2.06	3.79	0.12	
2.33	-2.58	4.91	0.16	69.15	1.75	-2.06	3.81	0.12	
	Avg	4.87	0.15	68.21		Avg	3.78	0.12	
	σ	0.10	0.00			σ	0.07	0.00	
	Variance	0.01	0.00			Variance	0.00	0.00	
2.29	-2.52	4.81	0.15		1.71	-2.02	3.73	0.12	

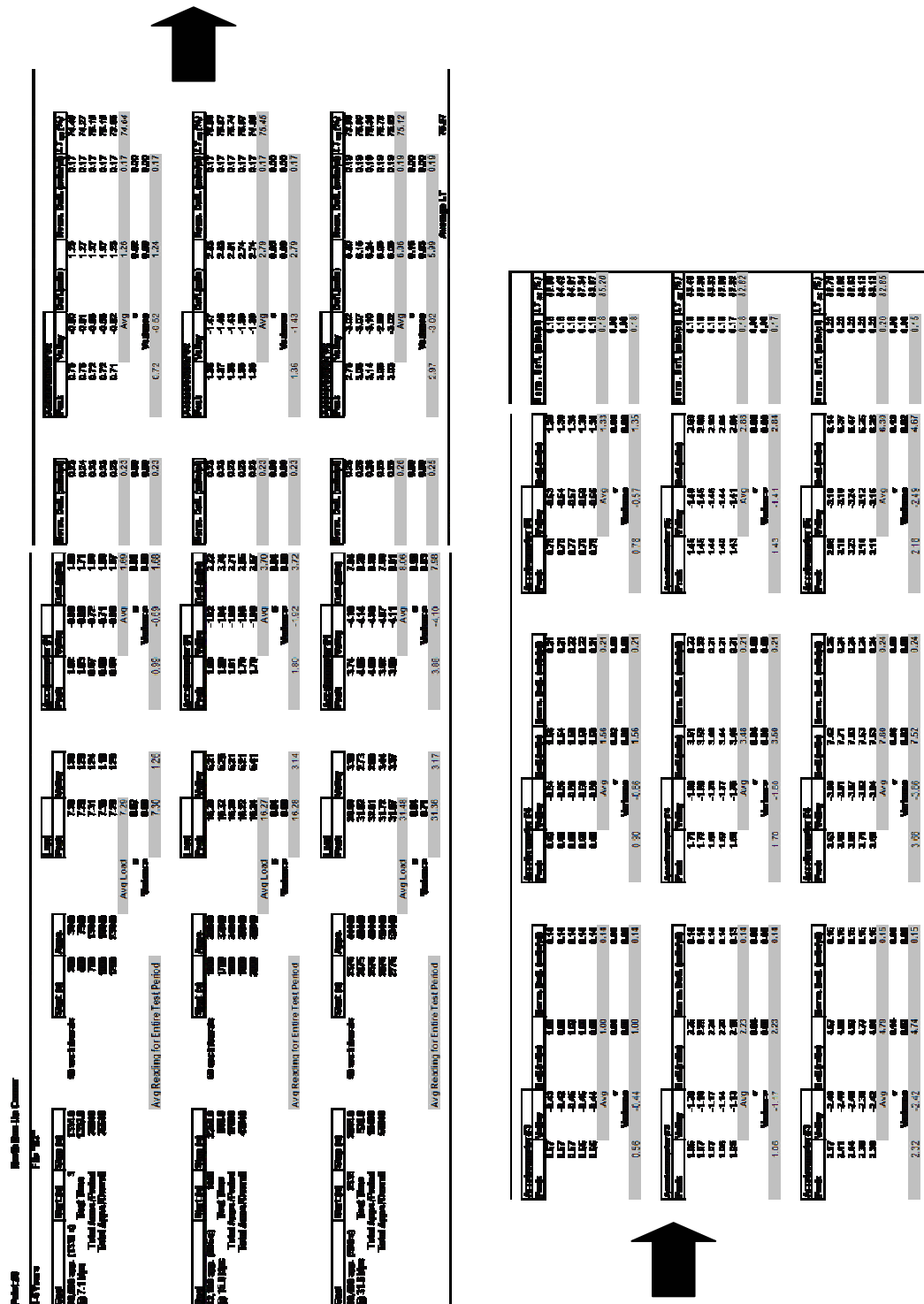


Figure I33 – Data Summary for North Run-Up – Corner Load Point – Years 1-5

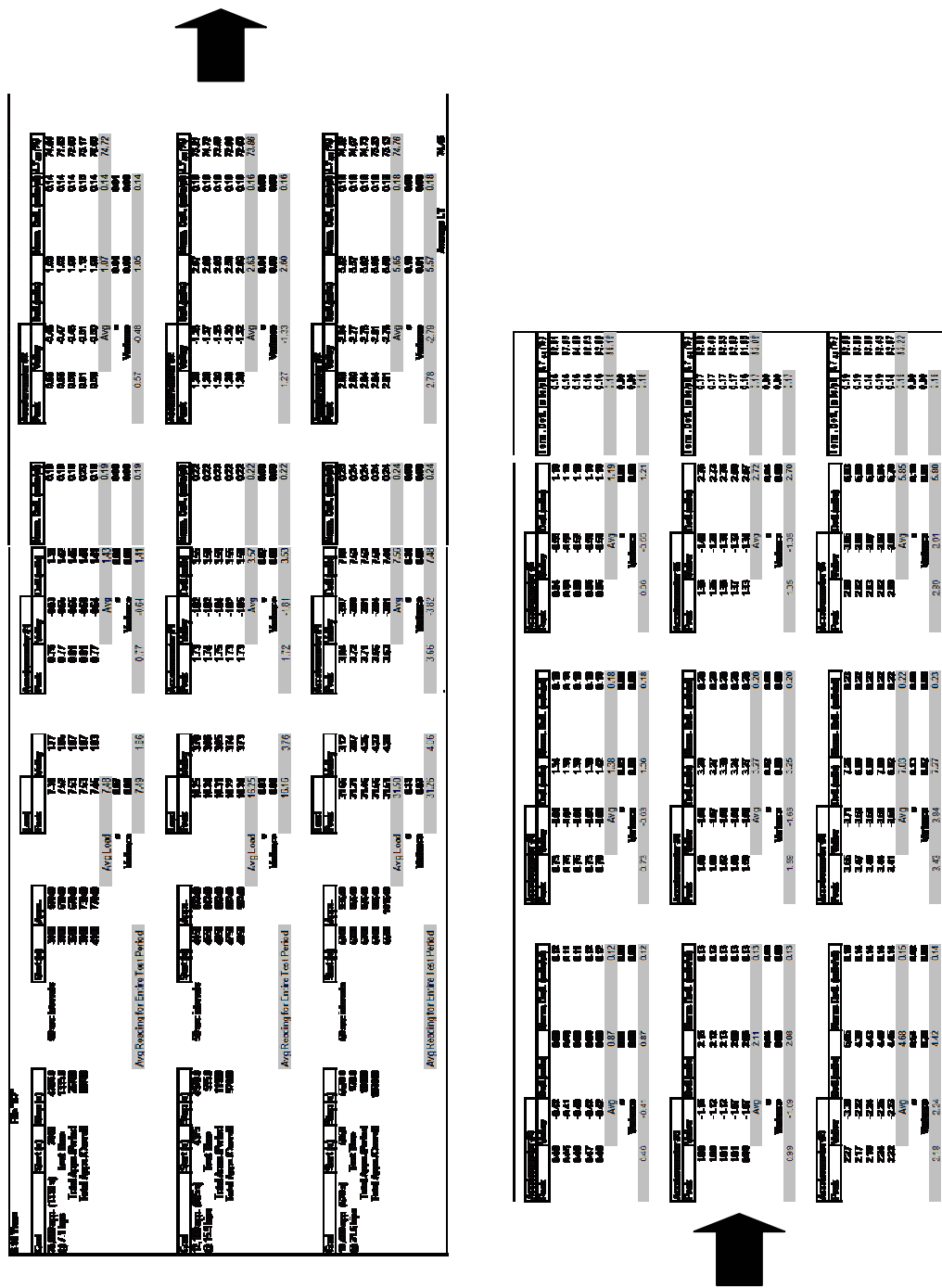


Figure I34 – Data Summary for North Run-Up – Corner Load Point – Years 6-10

[illegible]

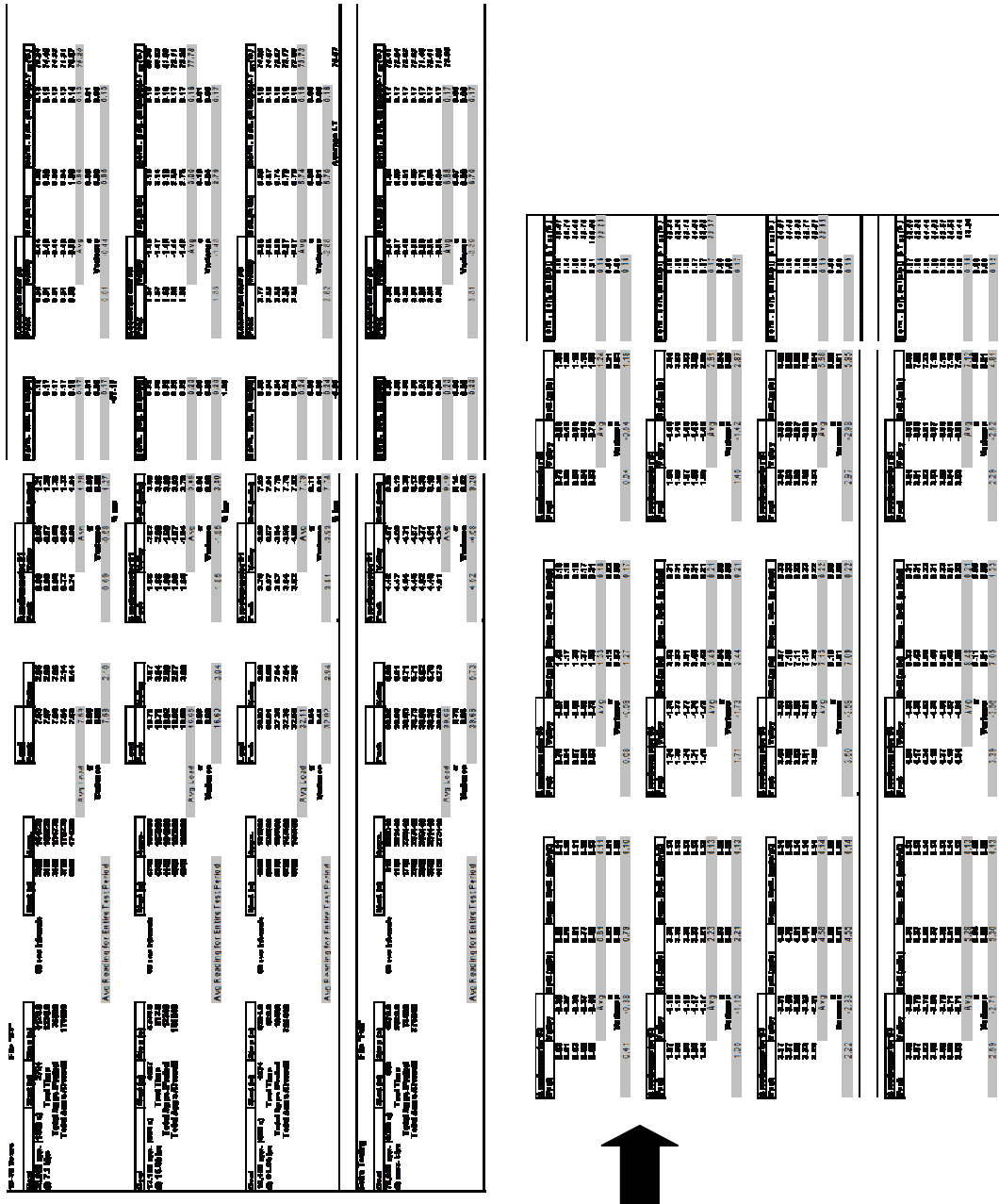


Figure I35 – Data Summary for North Run-Up – Corner Load Point – Years 16-20

Appendix J – Data Adjustment for Taxiway A6 Edge Loading Scenario

Due to the difference in distance of the first accelerometer from the load frame for the Taxiway A6 edge loading scenario, an adjustment had to be made to bring the data for the edge loading in line with the relationship between deflection at the center and corner loading scenarios. To determine this relationship, the slope of the line determined by plotting deflection versus load was listed for each of the three different locations. A percentage difference, among the three different loading scenarios at each location, was determined to compare center, edge, and corner loading. Table J1 illustrates the slope values of each line and the relationship at each location. As highlighted in Table J1, the edge loading scenario at Taxiway A6 does not fall in line with the expected trend of increasing slope for the order center, edge, and corner loading.

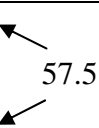
Table J1 – Relationship of Slope Values for Deflection Versus Load

	Taxiway A6 (Slope)	Slope (%)	Center Slope (%)	South Run-Up (Slope)	Slope (%)	% Increase	North Run-Up (Slope)	Slope (%)	% Increase
Center	0.3933			0.3880			0.1357		
Edge	0.3284	?	57.5	0.5539	70.0	63.9	0.2076	65.8	57.5
Corner	0.6837	?		0.6070	91.3		0.2359	88.0	

In order to determine and adjustment factor for the slope of the edge loading scenario at Taxiway A6, it is important to determine trends to interpolate values for the unknown values highlighted in Table J1. The percentage of the “edge slope” over the “corner slope” produced similar values at the two known test locations at the

South and North Run-Up. An average of the two known values (91.3%, 88.0%) was determined as 89.7%. This percentage was applied to the corner loading at Taxiway A6, giving a slope value of 0.61 for the edge scenario. The same process was then repeated for “center slope” over the “edge slope.” Again, similar values were produced at the two known test locations at the South and North Run-Up. An average of the two known values (70.0%, 65.8%) was determined as 67.9%. This percentage was applied to the center loading at Taxiway A6, giving a slope/slope value of 0.58 for the edge scenario. This value was then averaged with the first interpolation to produce a slope value of 0.60 for the edge at Taxiway A6. All calculations are summarized in Table J2. This crude interpolation process produced data which coincides with observed trends. As seen from the center slope over corner slope percentages presented in Table J1, the order of highest to lowest percentage was South Run-Up followed by similar values at Taxiway A6 and the North Run-Up. This order held true for values calculated, with percentage values highlighted in Table J2 exhibiting the same sequence from highest to lowest percentages.

Table J2 – Interpolated Values for Taxiway A6

	Taxiway A6 (Slope)	Slope (%) Slope	Center Slope (%) Corner Slope
Center	0.3933		
Edge	<u>0.60</u>	<u>65.6</u>	
Corner	0.6837	<u>87.8</u>	

Due to the nature of interpolation, the slope value for the edge loading scenario was left in limited significant figures. Using the value determine (0.60) and the original value (0.3284). A scaling factor was determined by dividing the

determined value by the original value. An approximate scaling factor of 1.8 was then used to scale the existing data for the edge loading scenario at Taxiway A6.

Appendix K – Normalized Deflection with Applications – Taxiway A6 and North Run-Up

Figures K1 through K6 show the relationship of normalized deflection with number of load applications for the Taxiway A6 and North Run-Up. These figures combined with Figures 9.11 through 9.13 from Section 9.2.2 complete the presentation of the aforementioned relationship.

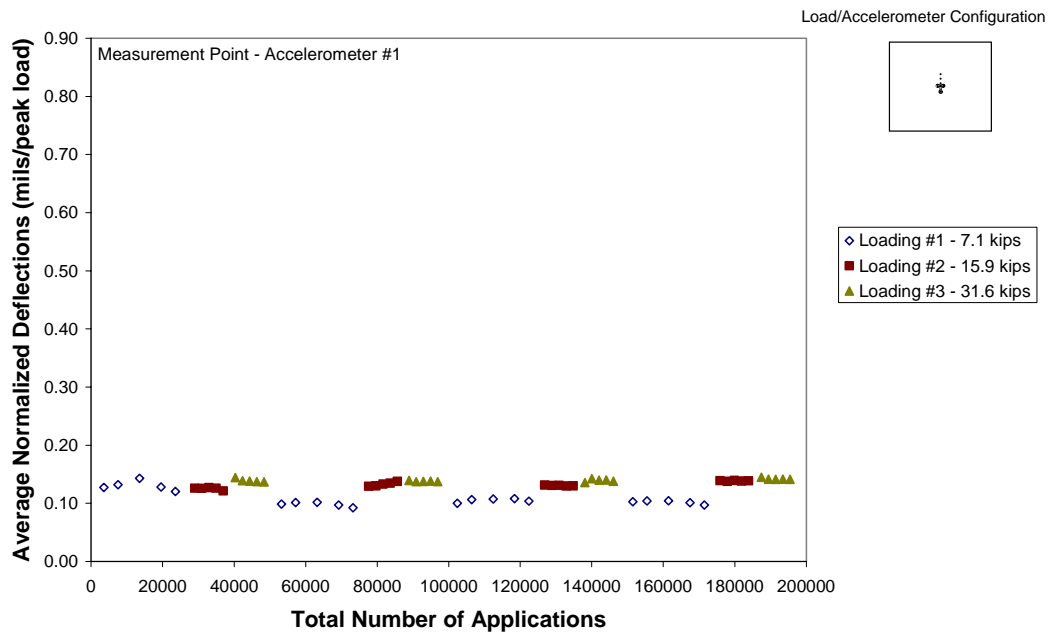


Figure K1 – Variation of Average Normalized Deflections with Number of Load Applications: North Run-Up – Center Load Point

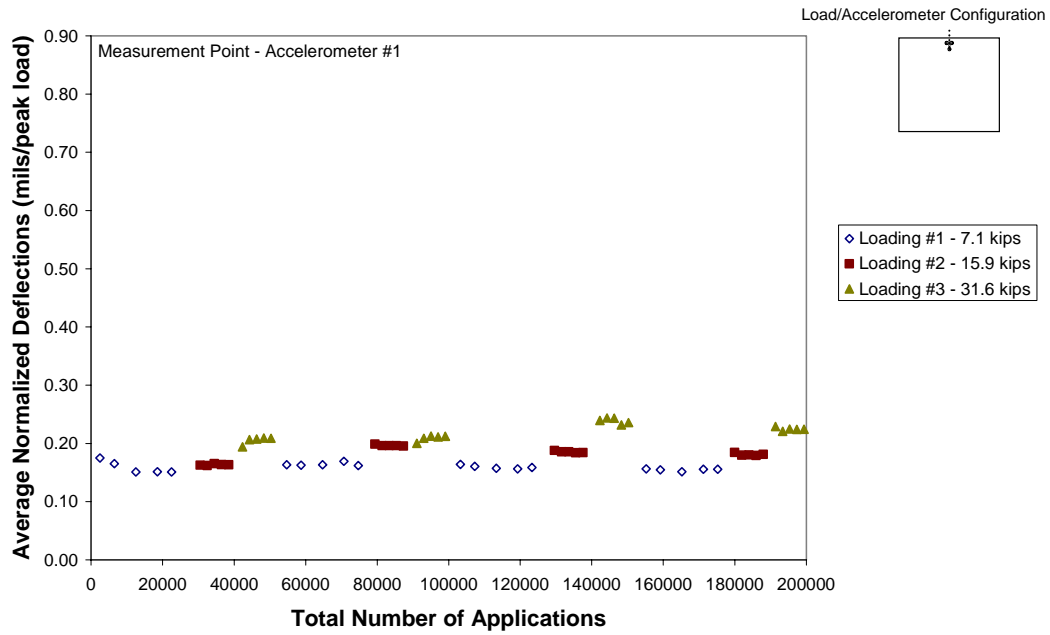


Figure K2 – Variation of Average Normalized Deflections with Number of Load Applications: North Run-Up – Edge Load Point

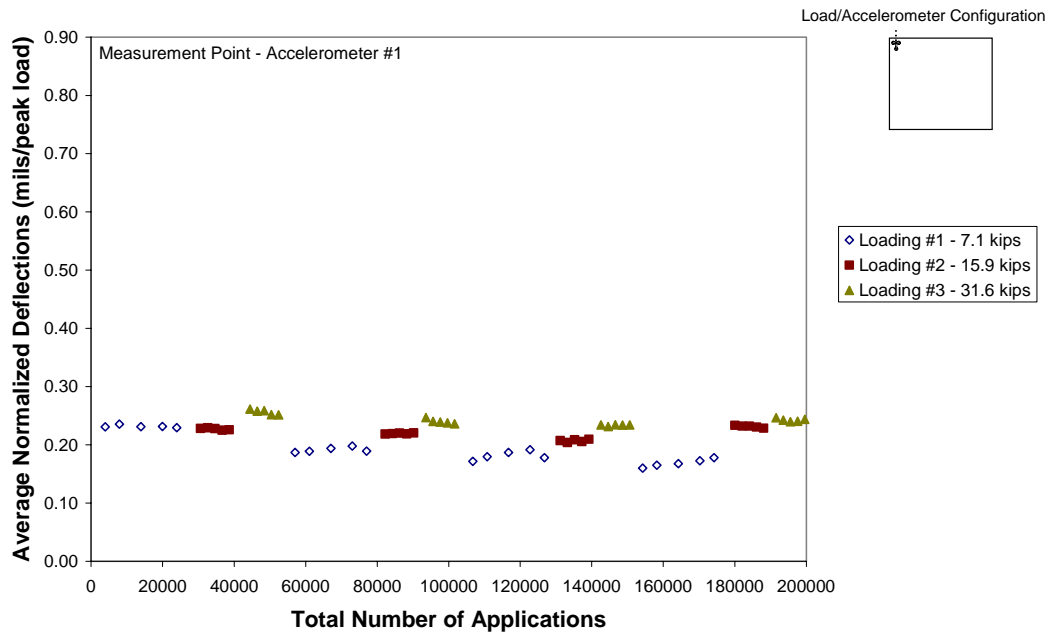


Figure K3 – Variation of Average Normalized Deflections with Number of Load Applications: North Run-Up – Corner Load Point

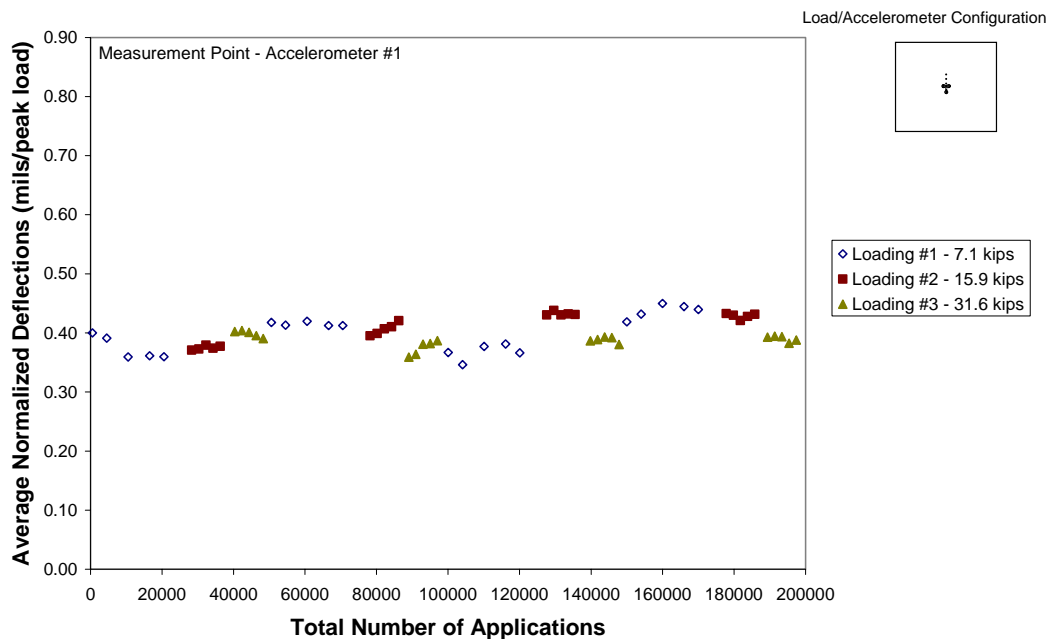


Figure K4 – Variation of Average Normalized Deflections with Number of Load Applications: Taxiway A6 – Center Load Point

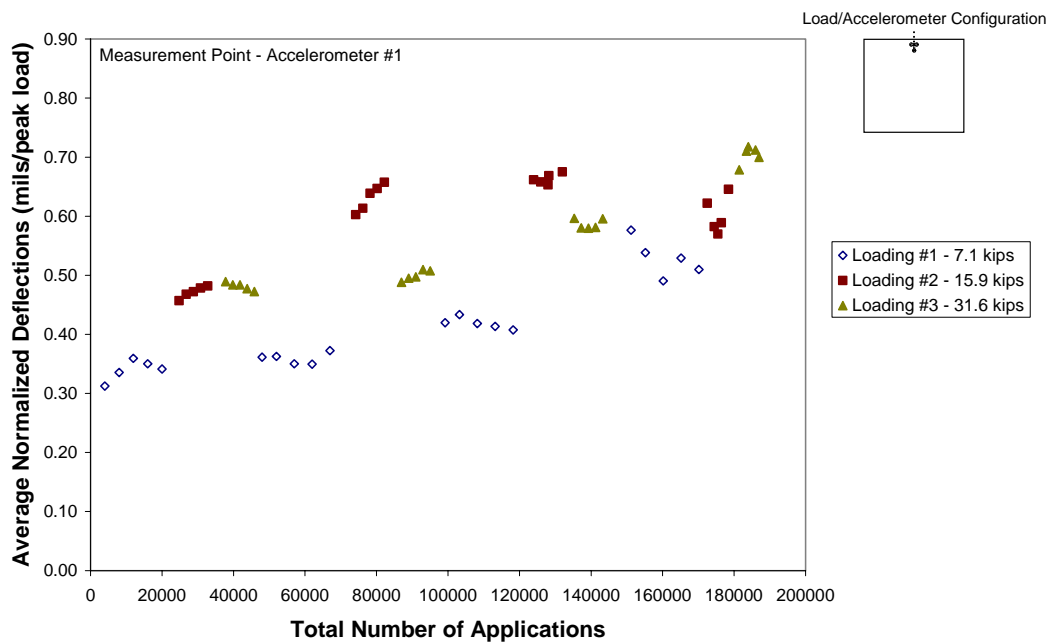


Figure K5 – Variation of Average Normalized Deflections with Number of Load Applications: Taxiway A6 – Edge Load Point

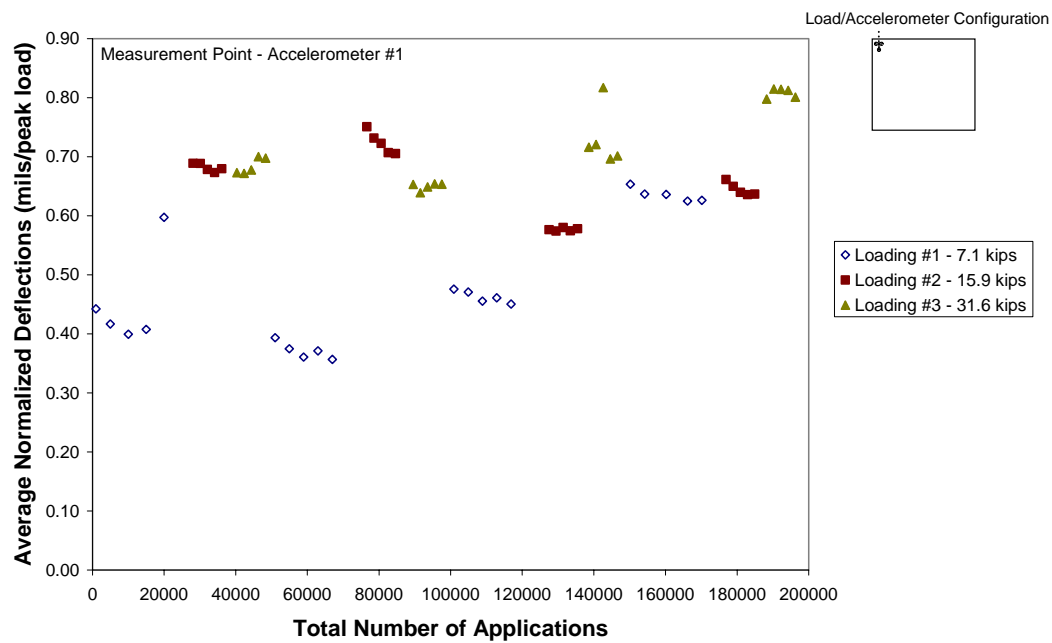


Figure K6 – Variation of Average Normalized Deflections with Number of Load Applications: Taxiway A6 – Corner Load Point

Appendix L – PCASE Computer Program

Pavement-Transportation Computer Assisted Structural Engineering (PCASE) is a robust program developed as a tri-service effort of the United States Army, Air Force, and Navy. The program is a computer-based design and evaluation tool, which includes rigid and flexible airfield and road design (both conventional and layered elastic methodologies), as well as railroad planning and design.

In using this computer program to forecast allowable passes, two modules were employed, the traffic module and the evaluation module. Prior to evaluating the pavement system, specific traffic had to be selected. Three aircraft were selected to represent the three load levels tested during the 20-year equivalent loading cycle. The following three aircraft were selected, since their reported weights coincided with range of representation of each respective load level (or load group).

- Load Group #1 – BAe Jetstream MK3 11,481 lbs
- Load Group #2 – DHC Dash 7 33,000 lbs
- Load Group #3 – BAe 146-100 61,994 lbs

Once the Traffic Module was established, a file was retrieved in the Evaluation Module and the parameters (layer type, material type, modulus of subgrade reaction, and flexural strength) of the runway were established in the Layer Manager. Upon completion of layer selection, the analysis was run. In addition to assessing allowable passes for the three representative load groups, a large-scale aircraft (Boeing 747-400) was selected to replicate loads, which were not directly tested on the pavement at Meacham Airport. Results were summarized and included in Chapter 10 in Table 10.2.

References

- AirNav, LLC. (viewed May 2004), *FAA Information on Forth Worth Meacham International Airport*, <http://www.airnav.com/airport/KFTW>.
- Barnes, V.E. (1972), *Geologic Atlas of Texas, Dallas Sheet*, Bureau of Economic Geology, University of Texas at Austin.
- Bay, J.A. (1997), "Development of a Rolling Dynamic Deflectometer for Continuous Deflection Testing of Pavements," PhD Dissertation, The University of Texas at Austin.
- Bay J.A., Stokoe, K.H. (1998), "Development of a Rolling Dynamic Deflectometer for Continuous Deflection Testing in Pavements," *Project Summary Report 1422-3F*, Center for Transportation Research, University of Texas at Austin.
- Bay J.A., Stokoe, K.H. (2000), "Continuous Profiling for Flexible and Rigid Highway and Airport Pavements with the Rolling Dynamic Deflectometer," *ASTM STP 1375, Nondestructive Testing of Pavements and Backcalculation of Moduli*, American Society for Testing of Materials, pp.429-443.
- Bay, J.A., Stokoe, K.H., McNerney, M.T., Sorasump, S., Van Vleet, D.A., and Rozycki, D.K. (2000), "Evaluating Runway Pavements at Seattle-Tacoma International Airport – Continuous Deflection Profiles Measured with the Rolling Dynamic Deflectometer," *Transportation Research Record 1716, Paper No. 00-1305*, TRB, Washington D.C., pp. 1-9.
- Carter & Burgess, Inc. (CBI). (1972), *Plans for Construction of Airfield Improvements – As Constructed*, Fort Worth Municipal Airport, Meacham Field, FAA Project No. 7-48-0085-01, Forth Worth, Texas.
- Chul, S., Lee, J.L.K., Fowler, D.W., and Stokoe, K.H. (2004) "Super-Accelerated Pavement Testing on Full-Scale Concrete Slabs," *Submitted for Transportation Research Board 84th Annual Meeting*, Committee AFD40, Full-Scale and Accelerated Pavement Testing, Washington, D.C.
- Coetzee, N.F., Nokes, W., Monismith, C., Metcalf, J.B. and Mahoney, J. (1999), "Full-Scale/Accelerated Pavement Testing: Current Status and Future Directions," *A2B52: Task Force on Full-Scale Accelerated Pavement Testing – Millennium Paper*, Transportation Research Board, Washington D.C.

- Darter, M.I., and Barenberg, E.J. (1977), *Design of Zero-Maintenance Plain Jointed Concrete Pavement*, Report No. FHWA-RD-77-111, Vol. 1, FHWA, Washington D.C.
- Davids, William (2004), *EverFE: Software for the 3D Finite Element Analysis of Jointed Plain Concrete*, University of Maine, <http://www.civil.umaine.edu/EverFE>.
- Dong, M. and Hayhoe, G.F. (2002), "Analysis of Falling Weight Deflectometer Tests at Denver International Airport," *Proc., 2002 Federal Aviation Administration Airport Technology Transfer Conference*, Atlantic City, NJ.
- Dynatest International (viewed September 2004), *Heavy Vehicle Simulator (Mark IV)*, <http://www.dynatest.com/hardware/hvs/htm>.
- Fabre, C., Balay, J.M. and Mazars, A. (2004), "A380 Pavement Experimental Programme/Rigid Phase," *Proc., 2004 FAA Worldwide Airport Technology Transfer Conference*, April, Atlantic City, NJ.
- Federal Aviation Association (FAA). (2000), *2000 FAA National Aviation Research Plan (NARP)*, U.S. Department of Federal Aviation.
- FAA (2004), *Fort Worth Meacham International Airport Traffic Data – January 1998 – May 2004*.
- FAA (2004(1)), *2004 FAA National Aviation Research Plan (NARP)*, U.S. Department of Federal Aviation.
- FAA (2004(2)), *Advisory Circular (AC) 150/5320-6D Change 3, Chapter 3. Pavement Design, Section I. Design Considerations*, Airports Publications Library, Washington D.C.
- Federal Highway Administration (FHWA). (2002), *Highway Statistics 2002*, Section V, United States Department of Transportation (USDOT), Washington, D.C.
- FHWA. (view October 2004), Long Term Pavement Performance (LTPP) Program *General Presentation*, USDOT, <http://www.tfhr.gov/pavement/ltp/ltp.htm>.
- Fort Worth Meacham International Airport (FTW) (viewed June 2004), *Meacham History*, <http://www.meacham.com/history.htm>.

- Hall, J. (1999), "Rolling Wheel Deflectometer," *Eyes on ERES*, Vol. 6, No. 3, Summer, pp.1-3.
- Hazard Mitigation Action Planning (HAZMAP). (2003), *Expansive and Plastic Soils*, North Central Texas Council of Governments (NCTCOG), Department of Environmental Resources.
- Herr, W.J., Hall, J.W., White, T.D. and Johnson, W. (1995), "Continuous Deflection Basin Measurement and Backcalculation Under a Rolling Wheel Load Using Laser Scanning Technology," *Proc., 2005 ASCE Transportation Congress*, San Diego, CA, October, pp. 600-611.
- Highway Research Board (HRB). (1962), *The AASHO Road Test*, HRB Special Report 61.
- Hildebrand, G., Rasmussen, S., and Andrés R. (1999), "Development of a Laser Based High Speed Deflecto-graph. Nondestructive Testing of Pavements and Backcalculation of Moduli," *ASTM STP 1375*, American Society for Testing and Materials.
- Huang, Y. H. (2004), *Pavement Analysis and Design*, 2nd ed., Pearson Prentice Hall, Upper Saddle River, NJ.
- Hugo, F. and Epps-Martin, A.L. (2004), "Significant Findings from Full-Scale Accelerated Pavement Testing," *NCHRP Synthesis of Highway Practice 325*, Transportation Research Board, Washington D.C.
- Joel, R. (2004), "Minimum Requirements to Widen Existing 150-Foot Wide Runways for Airbus A380 Operations," *Engineering Brief No. 65*, FAA, Office of Airport Safety and Standards, Airport Engineering Division, Washington, D.C.
- Kestler, M.A. and Nam S.I. (1999), "Reducing Damage to Low Volume Asphalt-Surfaced Roads, and Improving Local Economies: Update on Variable Tie Pressure Project," *Proc., 10th International Conference on Cold Regions Engineering*, Lincoln, NH, August 16-19, pp 461-471.
- Lee, J.L., Turner, D.J., Oshinski, E., Stokoe, K.H., Bay, J.A., and Rasmussen, R.O. (2003), "Continuous Structural Evaluation of Airport Pavements with the Rolling Dynamic Deflectometer," *Proc., ASCE Airfield Pavements Specialty Conference*, Las Vegas, NV, September 21- 24, pp. 348-363.

- Malvar, L.J. and Cline, G. (2001), "Detecting Voids Under Asphalt and Concrete Pavements," Naval Facilities Engineering Service Center, Port Hueneme, CA.
- Metcalf, J.B. (1996), "Application of Full-Scale Accelerated Pavement Testing," *NCHRP Synthesis of Highway Practice 235*, Transportation Research Board, Washington D.C.
- Metcalf, J.B. (2001), "ALT Around the World," *Proc., Workshop on Accelerated Load Testing of Pavements*, European Cooperation in the Field of Scientific and Technical Research (COST) 347 – Pavement Research and Accelerated Load Testing Facilities, June 27, Koln, Germany.
- Miller, J.S. and Bellinger W.Y. (2002), *Distress Identification Manual for the Long-Term Pavement Performance Program*, Pub. No. FHWA-RD-03-031, USDOT, FHWA, June, Washington D.C.
- Miner, M.A. (1945), "Cumulative Damage in Fatigue," *Transactions of ASME*, Vol. 67, pp. A159-A194.
- Nam, B. (2005), "Continuous Deflection Profiling at Forth Worth Meacham International Airport," Master's Thesis *in progress*, The University of Texas at Austin.
- Packard, R.G., and Tayabji, S.D. (1985), "New PCA Thickness Design Procedure for Concrete Highway and Street Pavements," *Proc., Third International Conference on Concrete Pavement Design and Rehabilitation*, Purdue University, pp. 235-236.
- Portland Cement Association (PCA). (viewed August 2004), *Airport Pavements*, http://www.cement.org/pavements/pv_cp_airports.asp.
- Saeed, A. and Hall, J.W. (2003), "Accelerated Pavement Testing: Data Guidelines," *NCHRP Report 512*, Transportation Research Board, Washington D.C. pp. 1-6, 36-38.
- Stokoe II, K.H., Bay, J.A., Rosenbald, B.L., Murphy, M.R., Fults K.W. and Chen, D. (2004), "Super-accelerated Testing of Flexible Pavement with Stationary Dynamic Deflectometer," *Transportation Research Record*, Issue 1716, TRB, Washington D.C.
- Texas Department of Transportation (TxDOT). (2001), "Review of Preliminary Engineering Report, October 3, 2001," *Meacham International Airport – Runway 16L-34R Rehabilitation*. Aviation Division.

TxDOT. (2004), *Aerial Photograph of Fort Worth Meacham International Airport*. Aviation Division.

United States Army Corps of Engineers Cold Regions Research and Engineering Laboratory (USACE CRREL). (1997), "Heavy Vehicle Simulator Condenses Pavement-Testing Time," *Engineer Update*, May, Hanover, New Hampshire.

Vita

John Bertram Lantz was born in State College, Pennsylvania. He attended Dulaney High School in Timonium, Maryland, and graduated in June 1993. In August 1993, he enrolled in the University of Delaware in Newark, Delaware, where the degree of Bachelor of Science in Civil Engineering was conferred in June 1997. At that same time, he was commissioned an officer in the United States Air Force. Over the next six years he served as a Civil Engineers (CE) officer in the Air Force. His assignments have included positions in base level engineering, deployable construction engineering (RED HORSE), and regional and combat support engineering at Dover AFB, Delaware, Osan AB, Republic of Korea, and Aviano AB, Italy, respectively. In December 2002, he was selected for the Air Force Civilian Institute Program, and in August 2003 he entered The Graduate School at The University of Texas at Austin.

This dissertation was typed by the author.